UNIVERSIDADE FEDERAL DO RIO GRANDE DO SUL
INSTITUTO DE GEOCIÊNCIAS
PROGRAMA DE PÓS-GRADUAÇÃO EM GEOCIÊNCIAS

ESTRATIGRAFIA, SEDIMENTOLOGIA, PETROLOGIA E GEOQUÍMICA DO GRUPO PORT AU PORT (CAMBRIANO) EM TERRA NOVA (NEWFOUNDLAND), CANADÁ

Rosalia Barili da Cunha

ORIENTADOR – Prof. Dr. Luiz Fernando De Ros
CO-ORIENTADORA – Profª. Drª. Karin Goldberg

Porto Alegre - 2019

UNIVERSIDADE FEDERAL DO RIO GRANDE DO SUL
INSTITUTO DE GEOCIÊNCIAS
PROGRAMA DE PÓS-GRADUAÇÃO EM GEOCIÊNCIAS

ESTRATIGRAFIA, SEDIMENTOLOGIA, PETROLOGIA E GEOQUÍMICA DO GRUPO PORT AU PORT (CAMBRIANO) EM TERRA NOVA (NEWFOUNDLAND), CANADÁ

Rosalia Barili da Cunha

ORIENTADOR – Prof. Dr. Luiz Fernando De Ros
CO-ORIENTADORA – Prof. Drª. Karin Goldberg

BANCA EXAMINADORA
Prof. Drª. Marcela Marques Vieira - UFRN
Prof. Drª. Valesca Brasil Lemos - UFRGS
Prof. Dr. Francisco Manoel Wohnrath Tognoli - Unisinos

Tese de Doutorado apresentada como requisito parcial para a obtenção do Título de Doutor em Ciências.

Porto Alegre – 2019

Cunha, Rosalia Barili da
Estratigrafia, sedimentologia, petrologia e geoquímica do Grupo Port au Port (Cambriano) em Terra Nova (Newfoundland), Canadá. / Rosalia Barili da Cunha. -- 2019.
168 f.
Orientador: Luiz Fernando De Ros.

Coorientador: Karin Goldberg.

Tese (Doutorado) -- Universidade Federal do Rio Grande do Sul, Instituto de Geociências, Programa de Pós-Graduação em Geociências, Porto Alegre, BR-RS, 2019.

1. Carbonato. 2. Grupo Port au Port. 3. Cambriano. 4. Diagênese. 5. Estratigrafia química. I. De Ros, Luiz Fernando, orient. II. Goldberg, Karin, coorient. III. Título.

DEDICATÓRIA

Para minha mãe, Maria Barili.

"– Who is that on the trenches by your side?
– And does it matter?
– More than the war itself."

Ernest Hemingway

AGRADECIMENTOS

À Shell Brasil pelo suporte através do projeto “Sistemas Sedimentares BG05: UoA-UFRGS-SWB”, enquadrado no regulamento de incentivo aos projetos de pesquisa, desenvolvimento e inovação da Agência Nacional do Petróleo (ANP).

Ao PPGGEO e à UFRGS, pelo ensino público, gratuito e de qualidade.

Aos colegas do IPR/PUCRS, grupo que me acolheu e ao qual possuo um sentimento de pertencimento sem precedentes.

Aos colegas e amigos da estratigrafia, os que ainda estão por lá e os que já estão em outras peleias, pelo companheirismo e suporte.

À Profª. Drª Karin Goldbenrg, por ter me acolhido no início, me acompanhando mesmo de longe.

Ao Prof. Dr. Luiz Fernando De Ros, que me recebeu como “espólio” da Karin, me orientando no doutorado e no trabalho.

À Profª. Drª. Joyce Neilson, que deu origem ao projeto de pesquisa e acompanhou a evolução dos trabalhos desde sempre.

Aos amigos, que mesmo de longe acompanharam a loucura.

À minha mãezinha, Maria, que nunca me deixou desistir.

RESUMO

O Grupo Port au Port é uma sequência mista, que marca a transição entre o Cambriano Médio, predominantemente siliciclástico, e o Cambriano Superior dominantemente carbonático. Está situado na porção oeste da Ilha de Newfoundand (Terra Nova), no Canadá. Esta sequência é correlacionada ao grande banco carbonático norte americano que se formou no entorno e sobre o paleocontinente Laurentia durante a evolução do Oceano Iapetus. O grupo compreende rochas híbridas, carbonáticas e siliciclásticas, cujo empilhamento não apresenta uma sequência diagnóstica, mas que pode ser dividido em três grandes ciclos de raseamento correlacionáveis com outras unidades. O limite entre os ciclos superiores coincide com o limite entre as sequencias Sauk II / III. O grupo Port au Port possui um arcabouço estratigráfico bem conhecido, mas a falta de dados geoquímicos e isotópicos, bem como alguns pontos passíveis de revisão, permitem novas interpretações sobre esta sucessão carbonática. Anteriormente interpretadas como gretas de contração, agora são indicadas como gretas de sinérese, que associadas a fauna marinha e inexistência de feições de exposição subaérea nos afloramentos visitados, evidenciam condições de deposição predominantemente em ambiente de inframaré. O processo de eodiagênese marinha freática, como a micritização auxiliou na manutenção da estrutura das partículas e a formação de franjas fibrosas, ocorreu em um ambiente freático marinho. A calcita é o componente eodiagenético mais abundante, associada a zona eodiagenética freática meterórica, mas também ocorre dolomita microcristalina, de zona de mistura, sendo observada também dissolução relacionada a fluídos insaturados. Com o avanço do soterramento e implementação da mesodiagênese, a dolomitização se intensifica, sendo observada presença de dolomita blocosa e em sela. Os eventos orogenéticos que dão origem aos Apalaches são responsáveis pelo soerguimento da bacia e exposição destas rochas. Apesar de magnitude e espessura reduzidas, a ocorrência da excursão positiva de carbono relacionada a transição Sauk II / III foi confirmada, e evidencia uma assinatura isotópica local superimposta, relacionada a condições de plataforma mais rasa e gradiente isotópico, similares à Bacia Amadeus, na Austrália. Os dados de estratigrafia química revelam valores de Mn/Sr >2 (0,53 – 33,31), que se relacionam com a intensa dolomitização. As razões de $^{87}Sr/^{86}Sr$ apresentam valores dentro do esperado para o Cambriano Médio/Superior (~0,7093-0,7095), com exceção do valores observados nas camadas da excursão positiva de carbono que atingem valores ~0.7089, sendo relacionados ao evento de regressão que deu origem ao SPICE. Os resultados geoquímicos indicam teores variáveis de Mg e de Ca ao longo do grupo, com razões Mg/Ca entre 0,03 e 0,6. As concentrações de estrôncio variam entre 54 e 466 ppm nas análises por FRX, mas atingem valores de até 2000ppm nas análises por Microssonda eletrônica. Altas concentrações de estrôncio associadas à presença de franjas fibrosas e dissolução/substituição preferencial em partículas biminerálicas pode ser um indicativo da mineralogia original destas rochas, sendo necessário estudos complementares

ABSTRACT

The Port au Port Group is a mixed siliciclastic/carbonate sequence that marks the transition between Middle and Upper Cambrian, situated in the western Newfoundland, Canada. This sequence is correlated to the Great North American Carbonate Bank formed during the evolution of the Iapetus Ocean in the surroundings of Laurentia. The group comprises hybrid, carbonate and siliciclastic rocks, whose stratigraphic stacking does not have a clear arrangement, but can be divided into three major Grand Cycles, correlated with other units across Laurentia. The transition between the two upper Grand Cycles coincides with the Sauk II / III sequence boundary. The Port au Port Group has a well-known stratigraphy framework. However, there is a lack of chemostratigraphy data and few stratigraphic interpretations liable to be reviewed. Previous dissecation cracks are now interpreted as syneresis cracks, and the lack of exposure features associated to marine fauna evidences prevailing subtidal conditions, interpreted before as intertidal environment. Petrographic analysis showed that early eodiagenesis occurs within marine phreatic conditions evidenced by micritization and fibrous fringes. Calcite is the most abundant eodiagenetic constituent, occurring in different cement types, related to phreatic meteoric zone. Microcrystalline dolomite and dissolution occur as a result of the eodiagenetic process within mixing phreatic zones. The process of mesodiagenesis starts with burial progression, and dolomitization intensifies, forming blocky and saddle dolomite. The orogenic events that originated Appalachians are also responsible for basin uplift and rock exposure, which telogianenetic products includes calcification of previous dolomites, dissolution and oxidation. The occurrence of SPICE in Port au Port Group has lower magnitude and thickness than expected for the global measured excursion and, although a subtidal environment, this local superimposed signature may reflect a shallower shelf position, similar to shallower portion of Amadeus Basin in Australia. The chemostratigraphic data reveals Mn/Sr ratios > 2 for Felix Cove section (0.53-17) and March Point section (0.38-33.31), corroborating the extensive diagenetic influence. However, the $^{87}Sr/^{86}Sr$ results are the expected range to Middle/Upper Cambrian (~0.7093-0.7095), with exception of those layers related to the SPICE (~0.7089), and therefore linked to the regression event, which exposed older carbonate Cambrian rocks. The Mg and Ca concentrations are variable throughout the group, with Mg / Ca ratios between 0.03 and 0.6. Strontium concentrations range from 54 up to 466 ppm in FRX results, but reach values up to 2000ppm in Electron Probe results. High strontium concentrations associated with the presence of fibrous fringes and preferential dissolution / replacement in bimineralic particles may be indicative of the original mineralogy of these rocks, requiring further studies.

SUMÁRIO

PREÂMBULO

ESTRUTURA DESTA TESE:

Esta tese de doutorado está estruturada em artigos submetidos e/ou aceitos e/ou publicados em periódicos classificados nos estratos Qualis-CAPES GEOCIÊNCIAS A1, A2, B1 ou B2. A sua organização compreende as seguintes partes:

PARTE I: Texto Integrador, compreendendo introdução com formulação do problema de investigação, os objetivos da pesquisa, o estado da arte do tema da pesquisa, os materiais e métodos utilizados, o contexto geológico da área/objeto de estudo, um resumo dos principais resultados obtidos no estudo e das interpretações desenvolvidas, discussão integradora dos resultados, conclusões e referências bibliográficas.

PARTE II: Corpo Principal da Tese, constituído por três artigos científicos, sendo o doutorando o primeiro autor, relacionados diretamente ao tema central da Tese, submetidos ou publicados em periódicos classificados nos estratos Qualis-CAPES GEOCIÊNCIAS A1, A2, B1 ou B2, escritos durante o desenvolvimento de seu Curso de Doutorado. Cada artigo ainda não publicado deverá ser precedido pela carta de aceite ou de recebimento do Editor da revista científica.

PARTE III: Anexos, compreendendo: tabelas, cálculos, gráficos (figuras, diagramas, mapas, seções) e fotografias, os quais devem ser referidos no Texto Integrador, identificados por letras maiúsculas, consecutivas, e pelos respectivos títulos. Também poderão ser inseridos nos Anexos resumos, artigos publicados em eventos e outros artigos em que o doutorando seja primeiro autor ou coautor, produzidos durante o Curso de Doutorado.

PARTE I

INTRODUÇÃO

OBJETO DE ESTUDO

O objeto de estudos desta Tese de Doutoramento compreende a sequência carbonática cambriana contemplada pelo Grupo Port au Port em Terra Nova (Newfoundland), Canadá. O projeto foi originalmente proposto juntamente com pesquisadores da Universidade de Aberdeen, uma vez que se iniciou como um projeto para dupla titulação.

ÁREA DE ESTUDO

O estudo foi desenvolvido na Península de Port au Port, Terra Nova (Newfoundland), Canadá (Figura 1). O trabalho de campo foi realizado entre os anos de 2016 e de 2017, totalizando 4 semanas, em duas áreas com bons afloramentos. Os levantamentos estratigráficos e a amostragem foram realizados durante o trabalho de campo em 2016, e um breve retorno para conferência de alguns pontos foi feito em 2017.

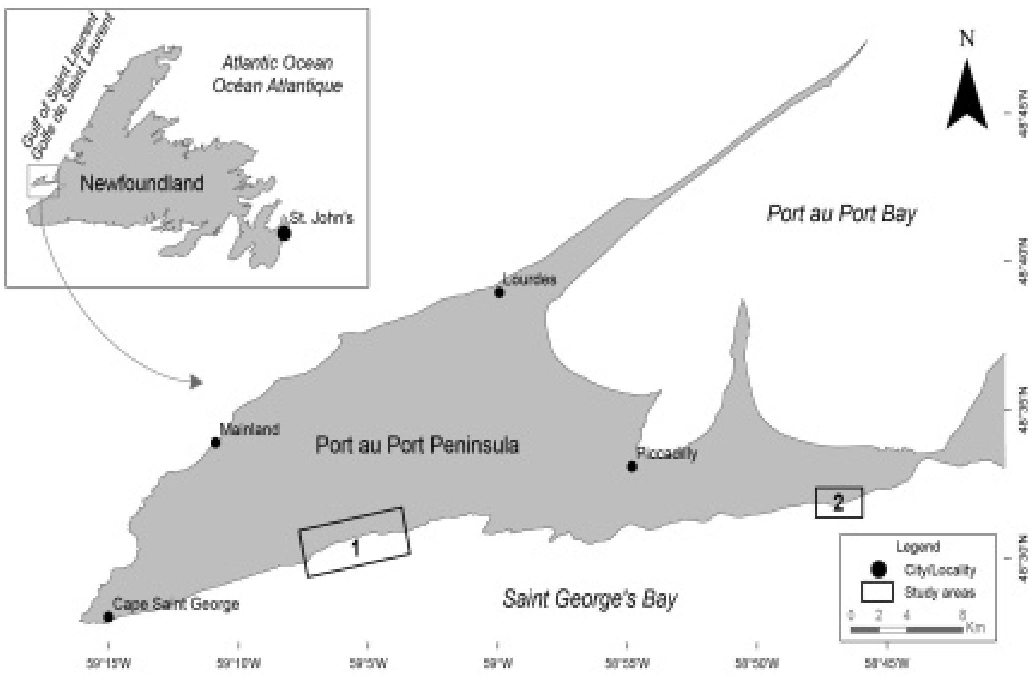

Figura 1. Mapa de localização da área de estudo em Newfoundland nas localidades de March Point (1) e Felix Cove (2).

ESTADO DA ARTE

GRUPO PORT AU PORT

Estudos abrangentes, relacionados à estratigrafia e petrografia da península de Newfoundland foram feitos por Chow (1985), Chow & James (1987b, 1987a) e Cowan & James (1993). Chow (1985) sumarizou os trabalhos anteriores sobre o Grupo Port au Port na península de mesmo nome, na porção Oeste de Newfoundland até 1985. Segundo essa autora, os primeiros trabalhos na península datam do período entre 1861 e 1863 publicados por Logan (1863, *apud* Chow, 1985). Schuchert & Dunbar (1934) integraram este primeiro trabalho a um estudo estratigráfico da porção oeste de Newfoundland, citando pela primeira vez a Formação March Point e relacionando esta como pertencente ao Cambriano Superior. Lochman (1938, *apud* Chow, 1985) subdivide a Formação March Point, através de dados bioestratigráficos coletados por Schuchert & Dunbar (1934), na Formação March Point, com idade estimada no Cambriano Médio, e Formação Petit Jardin, com idade estimada no Cambriano Superior.

Ainda de acordo com Chow (1985), os mapeamentos subsequentes da região não tiveram grandes contribuições na definição cronoestratigráfica do grupo e de sua correlação com as demais áreas aflorantes (e.g. Betz, 1939; Troelsen, 1947; Walthier, 1949; Lilly, 1961; Lock, 1969). Estudos sobre a bioestratigrafia do grupo reconheceram novas exposições de estratos Cambrianos em Newfoundland. Kindle e Whittington 1965) e Whittington e Kindle (1963, 1969) reconheceram que muitos dos níveis anteriormente indicados por Schuchert & Dunbar (1934) como pertencentes ao Cambriano Tardio seriam na verdade de idade Cambriana Média. Levesque (1977) sumarizou os trabalhos sobre a plataforma autóctone Cambro-Ordoviciana, publicados entre 1934 e 1977, reconhecendo pela primeira vez a ciclicidade entre os pacotes sedimentares, bem como feições de alta energia na sequência Cambriana Média e Superior. O autor confirmou a divisão estratigráfica que, na área da península de Port au Port, inclui a Formação March Point sobreposta pela Formação Petit Jardin.

Em relação aos estudos sobre sedimentologia e evolução diagenética do grupo, Chow (1985) cita Smit (1971) e Swett & Smit (1972), que reconheceram a predominância de sedimentos de ambientes de inframaré e de supramaré, propondo uma evolução diagenética baseada nos carbonatos oolíticos. A sequência proposta por estes autores incluiu: (1) recristalização; (2) primeira fase de dolomitização; (3) silicificação; (4) calcitização; e (5) segunda fase de dolomitização. A comparação desta sequência com seções correlatas na Escócia e na Groenlândia sugerem similaridades deposicionais e diagenéticas (Chow 1985). Adicionalmente, Chow (1985) e Chow & James (1987a) fazem um estudo mais detalhado sobre os aspectos diagenéticos do grupo. Os trabalhos incluíram aspectos sobre a cimentação e a formação de *hardgrounds*, origem e diagênese dos oólitos, origem e diagênese dos carbonatos finamente intercalados com *mudstones* e folhelhos (*parted* ou *ribbon limestones*), a dolomitização, a evolução diagenética e os primeiros resultados de isótopos estáveis. Chow (1985) e Chow & James (1987a) ainda fazem menção à mineralogia original dos oólitos e à possível resposta desta em função da evolução diagenética do grupo

Incorporando as divisões propostas por Levesque (1977), Chow (1985) faz uma revisão estratigráfica detalhada, abrangendo aspectos sedimentológicos e bioestratigráficos compreendendo toda região do Oeste de Newfoundland, e propondo inclusive o nome atual do grupo. Segundo a autora, o Grupo Port au Port possui seções bem expostas ao longo de toda costa oeste de Newfoundland, desde o Sul na Península Port au Port, até a costa de Saint Barbe ao Norte. O Grupo Port au Port é composto por uma sequência de carbonatos finamente intercalados com *mudstones*, folhelhos e dolomitos argiláceos; camadas grossas de *grainstones* oolíticos e *packstones/grainstones* bioclásticos e dolomitos laminados. Depósitos microbiais aparecem localmente na sequência como estromatólitos e trombolitos, assim como *rudstones* de intraclastos “achatados” (*flat pebble conglomerate*). Atualmente, a divisão do Grupo Port au Port compreende as formações March Point, Petit Jardin, e Berry Head. As descrições de cada seção tipo como propostas por Chow (1985) são sumarizadas com mais detalhe na Parte III - Anexo A.

Em trabalhos mais recentes, Saltzman *et al.*,(2004) reporta a ocorrência de uma excursão positiva de carbono do Steptoeano (SPICE), cuja ocorrência em diversas partes do mundo é amplamente reconhecida (e.g. Neilson *et al., 2016;* Saltzman *et al.,* 2000, 2004, 2011; Saltzman *et al*., 1998), na localidade de Felix Cove, Península Port au Port, na seção tipo do Membro Felix (Formação Petit Jardin). Esta excursão positiva também é relacionada com a possível ocorrência de um mar aragonítico (Neilson *et al*., 2016).

CONTEXTO GEOLÓGICO

ORÓGENO APALACHIANO

O Orógeno Apalachiano inclui diversas regiões do leste do Canadá como Newfoundland, Nova Scotia, New Bruswick, Prince Edward Island e a parte sul de Quebec ao longo do Rio Sant Laurence. Este Orógeno compreende uma área de 500,000km², com sua porção mais larga (600 km) localizado na fronteira entre Canadá e Estados Unidos da América, em New Bruswick e Nova Scotia (Figura 2). Entretanto, uma grande área, onde não existe exposição das rochas e estruturas que compõe este Orógeno, está presente também ao longo do golfo de Saint Laurence e submersa no limite com o Oceano Atlântico. A ilha de Newfoundland, onde está situada a área de estudo, é a terminação mais ao norte do Orógeno Apalachiano na América do Norte (Williams, 1976).

Os Apalaches foram formados em três eventos orogênicos distintos. A Orogenia Tacônica (ca. 440 Ma) é reconhecida como o primeiro grande evento tectônico, seguida pela orogenia Acadiana (Siluriano-Devoniano); ambas afetando toda a região. Localmente, apenas em Newfoundland, a Zona tectono-estratigráfica Humber também apresenta deformação Alleghaniana. Os dois primeiros eventos são quase coincidentes ao longo da margem ocidental enquanto a frente estrutural Alleghaniana é errática, cortando estruturas mais antigas (Williams, 1995).

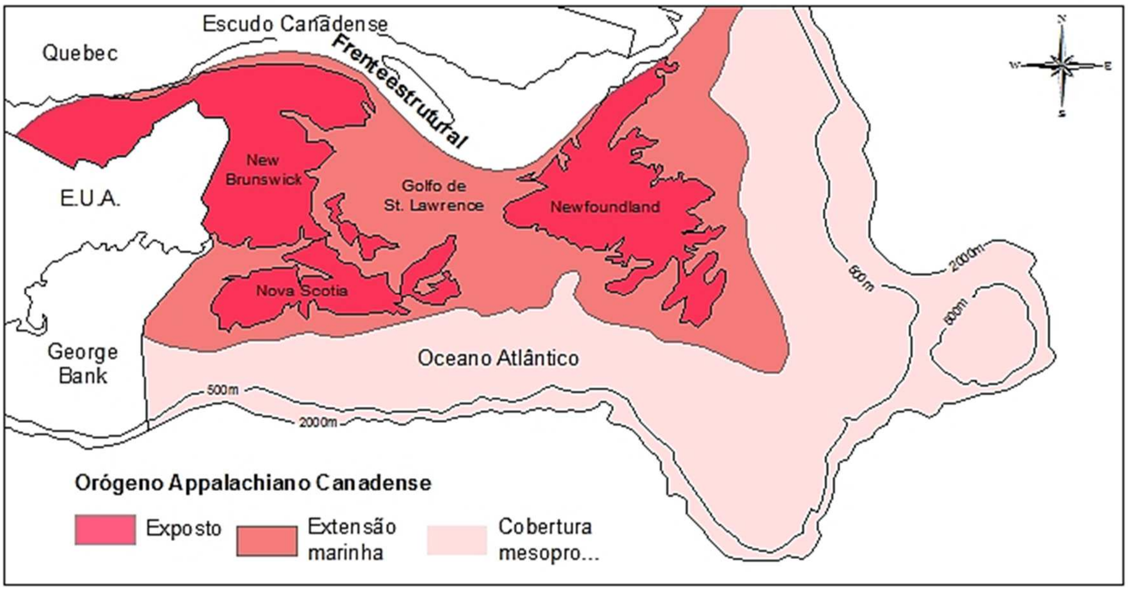

Figura 2. Extensão do Orógeno Apalachiano na América do Norte.

COMPARTIMENTAÇÃO TECTONO-ESTRATIGRÁFICA

Os Apalaches são dividos em 4 zonas tectono-estratigráficas: Humber, Dunnage, Gander, Avalon e Meguma (Figura 3). De acordo com o modelo do Ciclo de Wilson, a Zona Humber apresenta o registro da abertura e fechamento de uma margem passiva do tipo Atlântico, relacionada à antiga margem continental oriental da América do Norte, enquanto partes da Zona Dunnage apresentam vestígios do Oceano Iapetus, com sequências vulcânicas e melanges construídas sobre o assoalho oceânico. As zonas Gander, Avalon e Meguma são amostras de elementos tectônicos que estariam posicionados na margem oposta do oceano (Williams, 1995).

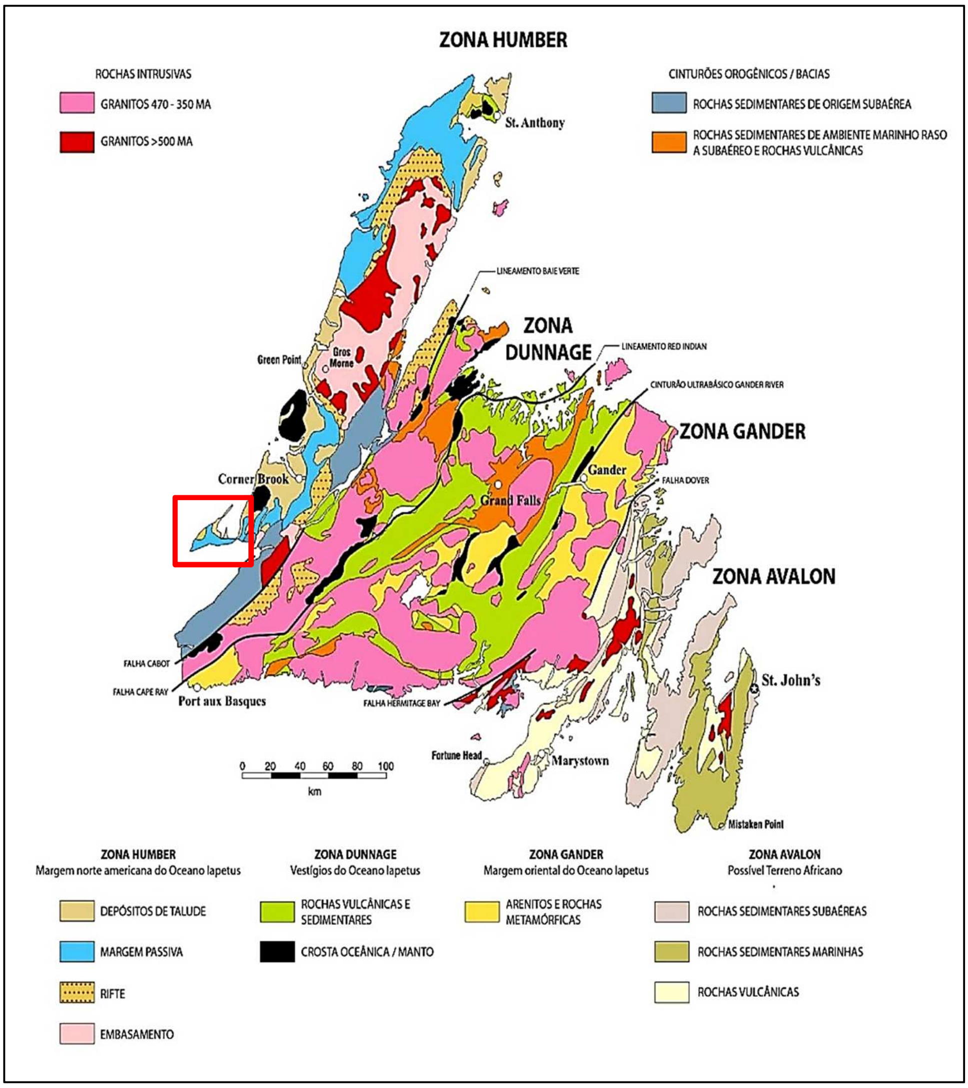

Figura 3. Mapa geológico de Newfoundland mostrando a divisão tectono-estratigráfica. A localização da Península de Port au Port é indicada pelo retângulo vermelho. Fonte: Serviço Geológico de Newfoundland e Labrador.

ZONA HUMBER

Segundo Williams (1995) esta zona tectono-estratigráfica é subdividida em parte interna e parte externa, sendo que esta divisão é baseada em estilos estruturais e metamórficos. Na parte externa o embasamento cristalino é composto por rochas pré-cambrianas da Província Greenviliana do Escudo Canadense. O embasamento é cortado por diques de rochas máficas e é sobreposto por arcóseos e derrames de rochas máficas localizados. A unidade basal é recoberta por folhelhos e quartzitos cambrianos, seguidos por uma sequência carbonáticas que vai desde o Cambriano até o Ordoviciano, que por sua vez é capeada por uma unidade de folhelhos seguidos por melanges. A deformação desta zona aumenta de oeste para o leste, tornando as relações estruturais e estratigráficas menos claras na parte interna da Zona Humber, onde as rochas são predominantemente xistos psamíticos e pelíticos, com presença de mármores e clorita xistos.

Quanto ao estilo estrutural, a parte externa é relacionada a um cinturão de empurrão e dobramento de uma bacia *foreland*. No Oeste de Newfoundland rochas deformadas e metamorfisadas da parte interna da Zona Humber são empurradas sobre as rochas da parte externa, menos deformadas e menos metamorfizadas. A margem oeste da Zona Humber é definida pelo limite da deformação Apalachiana enquanto a margem leste é um "degrau estrutural" marcado por ofiolitos que separam xistos polideformados da parte interna da Zona Humber das sequências vulcânicas menos deformadas da Zona Dunnage (Williams, 1995).

PLATAFORMA CARBONÁTICA

A história da plataforma carbonática ocidental de Newfoundland, de acordo com Williams (1995). As quatro fases de desenvolvimento, são apresentadas na Figura 4 e brevemente descritas a seguir:

Fase 1 – Pré-Plataforma (Proterozóico superior – Cambriano) - Sedimentos terrígenos e carbonatos formam uma plataforma estreita sobre o embasamento rifteado, na forma de uma sequência *onlap-offlap* pronunciada, cujo controle primário é tectônico.

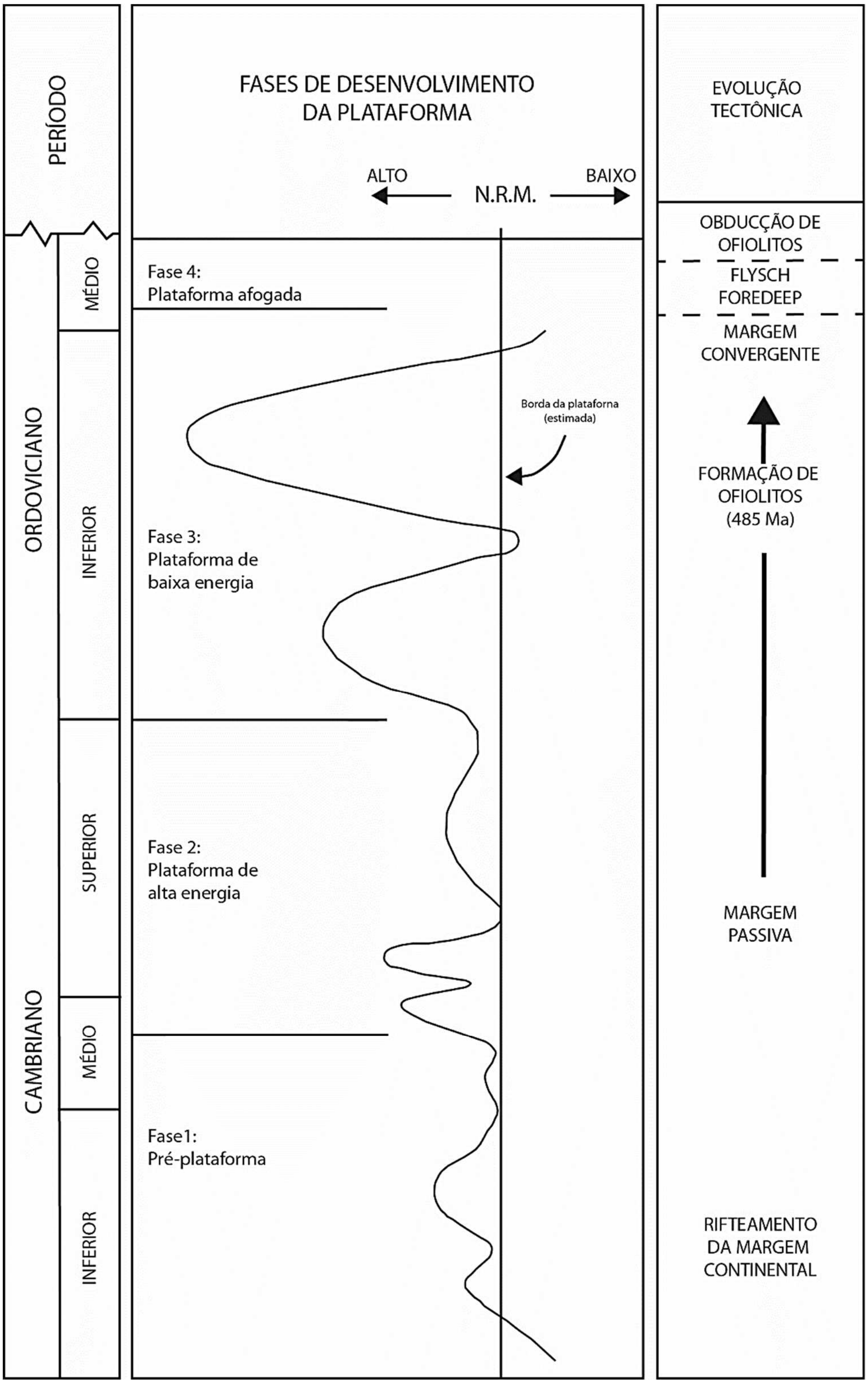

Figura 4 Síntese do desenvolvimento da plataforma carbonática Cambro-Ordoviciana, indicando as fases reconhecidas. Modificado de Williams (1995).

Fase 2 – Plataforma de alta energia (Cambriano médio a superior) - Evolução para uma plataforma carbonática com menos de 200 km de largura recoberta por sedimentos terrígenos e carbonáticos (com menos constituintes bióticos em relação à fase anterior) e com banco, de areia e de oólitos/pelóides na margem da plataforma (Figura 5). O controle primário desta fase é tectônico, mas torna-se um controle eustático durante a evolução da plataforma.

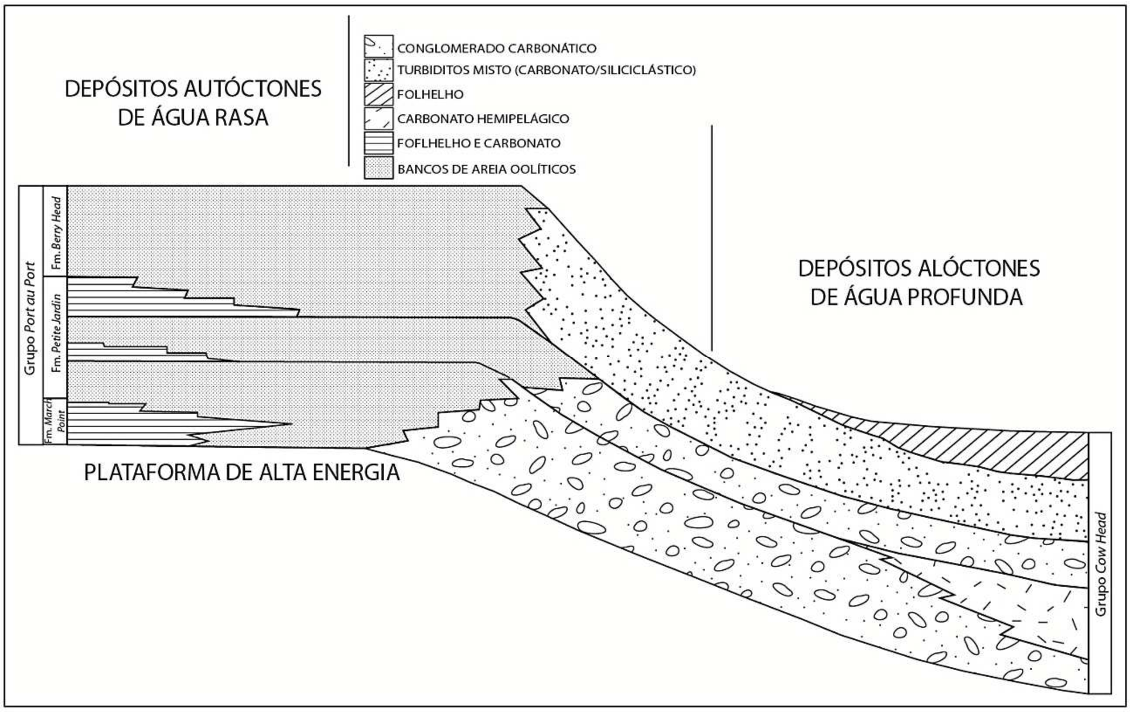

Figura 5 Seção esquemática da Fase 2: plataforma de alta energia contemporânea aos sedimentos de água profunda. Modificado de Williams (1995).

Fase 3 – Plataforma de baixa energia (Ordoviciano inferior a médio) - evolução para uma plataforma larga, com mais de 500 km e onlap geral; deposição carbonática absoluta, com fauna diversa e acumulação na borda da plataforma; controle primário eustático.

Fase 4 – Plataforma “afogada” (Ordoviciano médio a superior) - Colapso e soterramento da plataforma; deposição de carbonatos seguida por correntes de turbidez (*Flysch*) (Figura 6); controle primário tectônico.

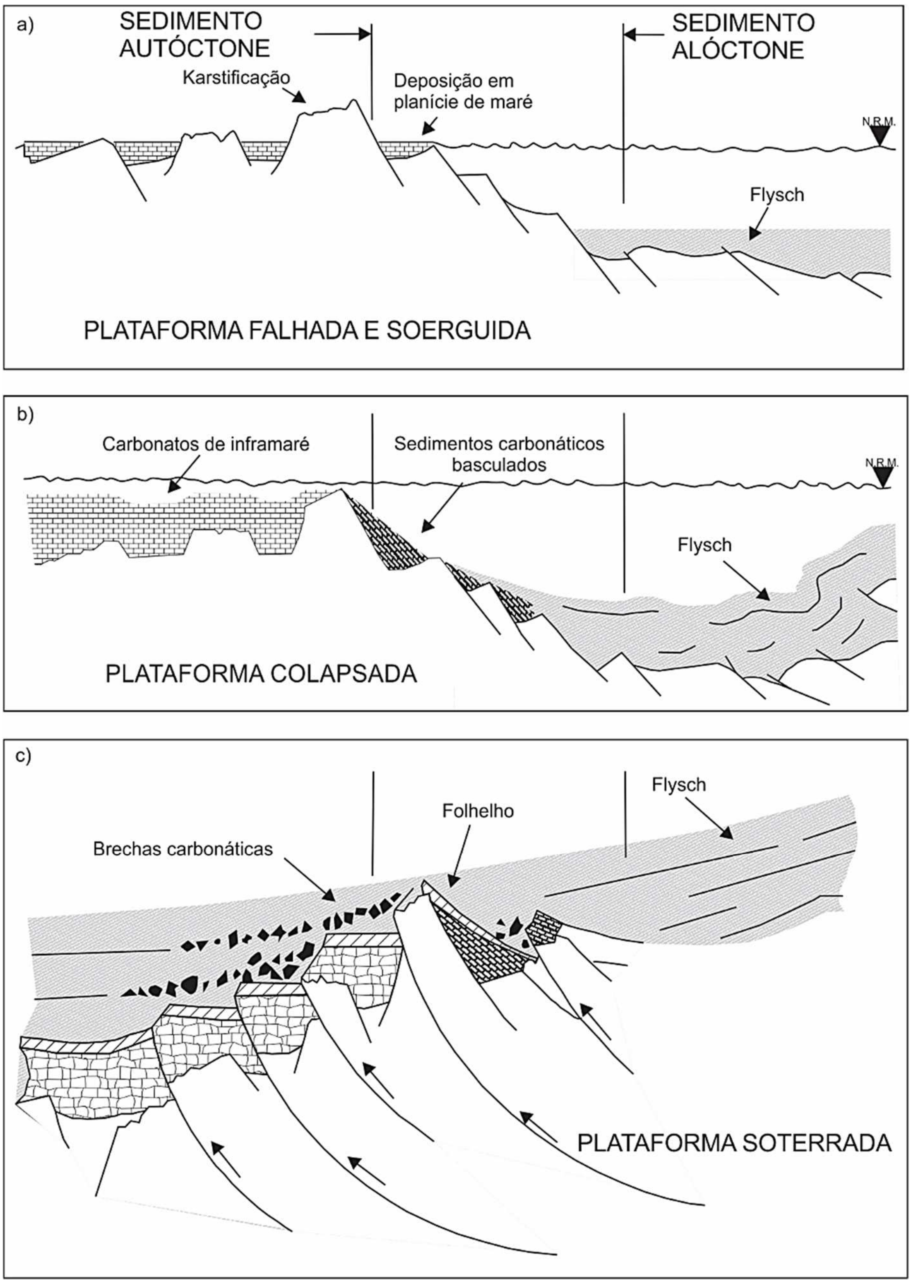

Figura 6 Diagramas interpretativos ilustrando a evolução da plataforma carbonática durante o final da fase 4: a) desenvolvimento de uma bacia tipo foreland no leste, soerguimento, falhamento e karstificação no oeste. B) cavalgamento e deformação da bacia foreland no Leste, afogamento e rápida subsidência da plataforma falhada no oeste; c) cavalgamento e transporte de estratos no leste, subsidência para níveis profundos abaixo do nível de sedimentação de carbonatos, cavalgamento e colapso de escarpas formando conglomerados, soterramento por Flysch. Modificado de Williams (1995).

GRANDE BANCO CARBONÁTICO NORTE AMERICANO

O grande banco carbonático americano refere-se a um sistema misto, carbonático/siliciclástico, formado sobre e no entorno do cráton Laurentia durante a Megasequência Sauk. Esta sequência ocorreu desde o Cambriano ao Ordoviciano Médio, compreendendo uma das maiores plataformas dominadas por carbonatos do Fanerozóico. A megasequência de Sauk apresenta vários de metros de espessura, sendo variável ao longo do cráton devido a diferenças paleogeográficas ao longo do sistema. Apesar disto, a sequência, que consiste em litofácies e fauna distintas, é amplamente reconhecida em toda Laurentia (Fritz *et al.,* 2012).

O paleocontinente Laurentia apresentava uma margem continental irregular em sua paleoface sul/sudoeste, com saliências e reentrâncias. Na porção oriental Canadá estas margens correspondem ao promontório de Saint Laurence, principalmente porção oeste da ilha de Newfoundland, e da reentrância de Quebec, desde a Ilha Anticosti até a fronteira dom os Estados Unidos da América (Allen, 2009; Thomas, 1977, 1991) (Figura 7). Esta grande endentação na costa teve grande impacto na formação do sistema carbonático na região, controlando as fácies e arquitetura de fácies da sucessão (Lavoie *et al.,* 2012).

A formação deste extenso sistema carbonático no Canadá ocorre em ambiente marinho raso, com predominância de fácies de alta energia como grainstone oolíticos, e recorrência de recifes microbiais com predominância de trombolitos. A sucessão consiste de ciclos transgressivo-regressivos de larga escala nomeados como "*Cambrian Grand Cycles*". Apesar do período Cambriano ser um momento de transgressão contínua do nível do mar, a transição Cambro-Ordoviciana se dá após um período de mar baixo (*LST*). Esta transição deu origem a uma grande discordância no sul de Quebec e em Ontário. Entretanto, em Newfoundland, para o mesmo período são identificadas fácies regressivas no último grande ciclo Cambriano, sem evidências de exposição subaérea (Lavoie *et al.,* 2012). Em Newfoundland, o Grande Banco Carbonático Norte Americano é representado por depósitos de baixa a alta energia do Grupo Port au Port.

Figura 7 Configuração do Paleocontinente Laurentia durante o Cambriano Inferior (~516Ma). Parte dos estados Norte Americanos e do Canadá estão indicados, assim como as paleolatitudes e o paleonorte geográfico. A posição de Newfoundland, Canadá, é indicada pela seta vermelha.

GRUPO PORT AU PORT

O Grupo Port au Port faz parte da sequência autóctone Cambro-Ordoviciana que constitui a Zona Humber em Newfoundland (Williams, 1976, 1979). Apresenta espessura total entre 450 e 500m e compreende a transição entre as sequencias Sauk II a Sauk III (James *et al.,* 1989; Lavoie *et al.,* 2012). As formações que compõe este grupo, em ordem ascendente, são: March Point, Petit Jardin, e Berry Head (Chow, 1985) (Figura 8). Estas formações são interpretadas como depósitos marinhos rasos da parte externa desta plataforma carbonática estável do paleocontinente Laurentia, que bordejou o Oceano Iapetus. Estes depósitos mistos (siliciclástico/carbonático) marcam a transição gradual entre a deposição siliciclástica do Cambriano Médio ao Superior e a sedimentação carbonática no Ordoviciano Inferior durante a evolução desta plataforma (Chow; James, 1987a). Os membros Campbells e Felix, da Formação Petit Jardin, e a Formação Berry Head são compostos por *grainstones* oolíticos e *mudstones*, interpretados como complexos de bancos oolíticos (Chow 1985). A Formação *March Point* e os membros *Cape Ann*, *Big Cove* e *Man O'War*, da Formação *Petit Jardin*, consistem em *mudstones* e dolomitos argilosos, interpretados como depósitos de planície de maré. Ciclos de raseamento ascendente depositados em planícies de maré são facilmente identificados em todo o grupo, e como mencionado anteriormente, são referidos como *Grande Cycles* correlacionáveis através do grande banco carbonático Norte Americano (Chow & James, 1987a; Fritz *et al*., 2012; Lavoie *et al.,* 2012) (Figura 9).

Estes grandes ciclos consistem em um semiciclo inferior com carbonatos e folhelhos, e um semiciclo superior com carbonatos oolíticos e mudstones. Cada grande ciclo pode ser interpretado como a deposição de complexos de bancos carbonáticos oolíticos, de borda de plataforma associados à planície de maré adjacente e seus depósitos lamosos envolvendo os seguintes processos: (1) uma rápida transgressão que inunda a plataforma e resulta na formação de planícies de maré lamosas; (2) Desenvolvimento gradual de complexos de bancos carbonáticos oolíticos que avançam sobre as planícies de maré, acompanhando o declínio de sedimentos siliciclásticos e a desaceleração da transgressão. O empilhamento destas camadas, entretanto, não teria uma boa predição uma vez que seriam gerados pela migração dos bancos oolíticos em resposta à variação da lâmina d'água em função da variação das marés ou de tempestades. As variações de terceira ordem no espaço de acomodação seriam responsáveis por pelas mudanças nas tendências dos grandes ciclos apresentados. A comparação entre estes grandes ciclos com os observados na Grande Bacia Norte-americana (*Great American Basin*), de mesma idade, indica um mecanismo eustático envolvendo variações na taxa de subida do nível do mar (Chow & James, 1987a).

.

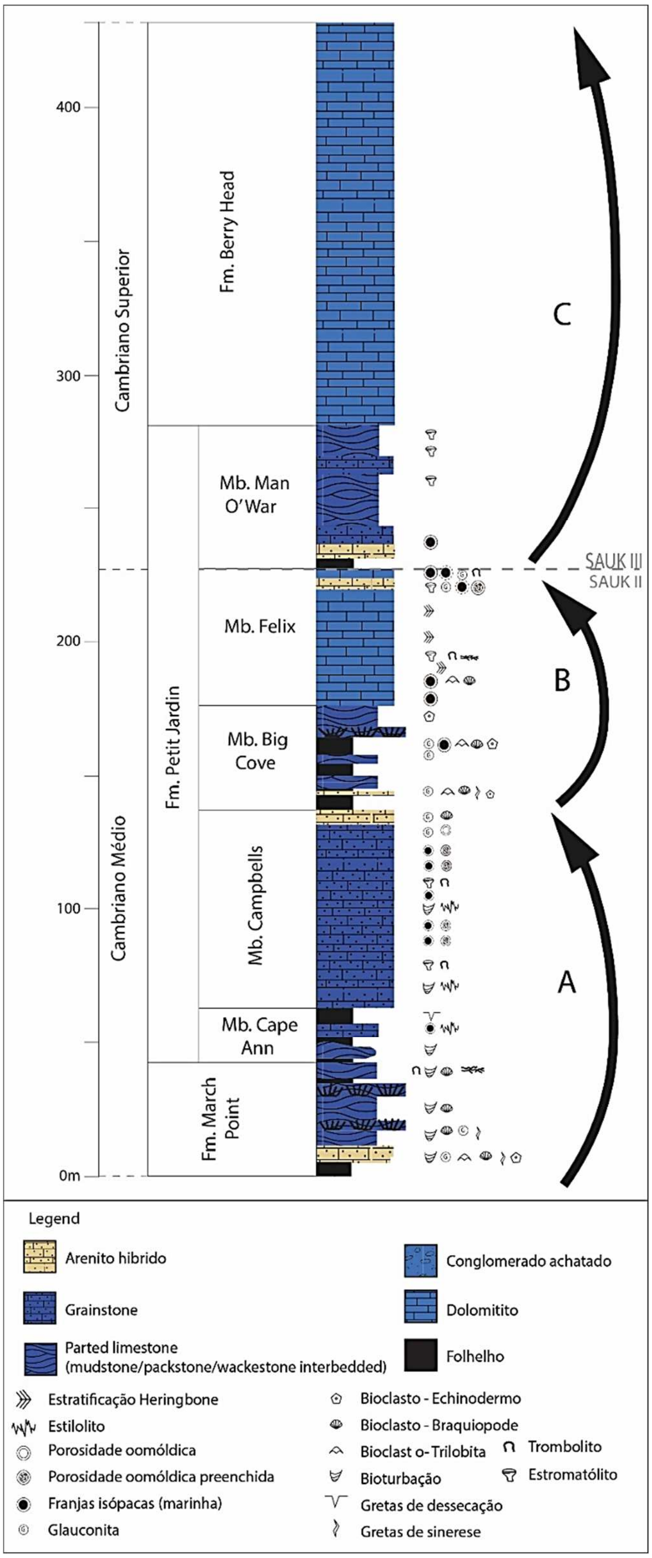

Figura 8 Coluna estratigráfica condensada do Cambriano médio a superior de Newfoundland, mostrando a plataforma mista com seus três grandes ciclos (A, B e C) (Barili *et al.,* 2018 adaptado de Chow & James, 1987b)

A transição entre as sequencias Sauk II e Sauk III é marcada por uma excursão positiva de carbono de até +5‰ relacionada a um evento de regressão, observado em diferentes graus de magnitude em toda Laurentia e em outras localidades como Austrália, China, Cazaquistão, Sultanato de Omã e Sibéria (Kouchinsky *et al*., 2008; Neilson *et al*., 2016; Saltzman *et al*., 2000, 2004; Schmid *et al*., 2018; Woods *et al*., 2011). Esta excursão, nomeada SPICE devido a sua ocorrência no Steptoeano, ocorre na transição entre as formações Felix e Man O'War no Grupo Port au Port. Além de estar relacionada com um momento de redução do nível relativo do mar, esta excursão positiva de carbono além também estaria associada a condições marinhas de composição aragonítica (Neilson *et al*., 2016).

OBJETIVOS

Apesar de abrangentes, os estudos anteriores datam da década de 1980/90, e não apresentam dados de estratigrafia química, tendo limitada informação sobre isótopos estáveis. O objetivo geral deste projeto de doutoramento foi, portanto, de revisitar a estratigrafia do Grupo Port au Port na porção oeste de Newfoundland, relacionando os dados isotópicos e geoquímicos aos processos deposicionais e diagenéticos.

Os objetivos específicos deste projeto incluíram:

- Revisão da estratigrafia do Grupo Port au Port, com indicação de lacunas ou de pontos passíveis de correção relacionadas ao ambiente deposicional sugerido em estudos anteriores.
- Confirmação da existência da excursão positiva de carbono nos afloramentos estudados, com investigação da assinatura isotópica de carbono identificada na região e a relação desta com as demais ocorrências.
- Comparação dos resultados geoquímicos e dados estratigráficos, correlacionando com as tendências esperadas para a transição Cambriano Médio a Superior.

- Estudo petrográfico para identificação de ambientes diagenéticos que afetaram a sequência e, onde possível, sua correlação com os ambientes deposicionais e a evolução estratigráfica.
- Interpretação tentativa da mineralogia original dos carbonatos com base no hábito dos minerais e em análises geoquímicas.

METODOLOGIAS

O processo de coleta das amostras ocorreu em dois períodos de campo, entre 2016 e 2017, totalizando 30 dias. O levantamento sedimentológico / estratigráfico foi executado numa escala de 1:50, com coleta de amostras das fácies diagnósticas, mas também em intervalos regulares quando em fácies continuas.

As metodologias aplicadas para o desenvolvimento do projeto incluíram análises sedimentológicas e estratigráficas, análises petrográficas, análises de isótopos estáveis de C e O e das razões de estrôncio ($^{87}Sr/^{86}Sr$), análises de elétrons retroespalhados e de catodoluminescência por microscopia eletrônica de varredura, análises geoquímicas por fluorescência de raios-X e por microssonda eletrônica. O detalhamento de cada método empregado é feito nos artigos apresentados no corpo principal da tese.

RESULTADOS

ANÁLISE ESTRATIGRÁFICA

Foram identificadas 8 fácies agrupadas em 4 associações de fácies que compreendem o intervalo inframaré a intermarés, apresentadas na tabela de fácies no Anexo A. Os resultados do levantamento sedimentológico / estratigráfico integrados à análise de fácies é apresentado no Anexo B como o perfil estratigráfico interpretado.

PETROGRAFIA

O estudo petrográfico incluiu amostras de arenitos híbridos, rochas carbonáticas e arenitos quartzosos. O registro fotomicrográfico dos principais constituintes primários e diagenéticos são apresentados no Anexo C.

Os grainstones oolíticos apresentam partículas com estrutura radial e concêntrica, frequentemente afetados por micritização, que auxiliou na preservação destas feições. As partículas apresentam hábitos variados, podendo ocorrer envelopes concêntricos sobre a estrutura radial, estrutura radial apenas, ou estrutura radial no envelope mais externo da partícula. Também são frequentes partículas biminerálicas, descritas em trabalhos anteriores (e.g. Chow, 1985), evidenciadas pela dissolução de alguns envelopes e preservação de outros, que mantém seu habito original, e posterior precipitação de calcita e/ou dolomita. Ocorre ainda partículas totalmente dissolvidas e preenchidas por calcita, posteriormente dolomitizada, evidenciada pela formação de franjas circundando os poros oomóldicos. Pelóides carbonáticos são frequentemente micritizados e ocorrem associados a intraclastos microbiais. Oncóides apresentam dissolução similar aos oólitos biminerálicos, com preenchimento por dolomita. Bioclastos também apresentam micritização, sendo trilobitas e crinóides os mais frequentes. Também ocorrem fragmentos de braquiópodes, e conchas inteiras são observadas no campo.

Intraclastos carbonáticos ocorrem com diversas texturas, abrangendo *mudstones*, *grainstones*, arenitos híbridos e depósitos microbiais. Intraclastos formados pelo retrabalhamento de *mudstones* dão origem a *flat pebble conglomerates*, mas também ocorrem compactados a pseudomatrix. Os intraclastos formados a partir do retrabalhamento de grainstones apresentam uma mistura de oólitos, pelóides e bioclastos. Já os intraclastos formados a partir do retrabalhamento de arenitos híbridos apresentam pelóides de glauconita e grãos de quartzo. Grãos de quartzo e de feldspatos nos arenitos híbridos são de tamanho areia fina a muito fina, e angulares. O quartzo geralmente é monocristalino, ocasionalmente policristalino, e o microclínio é o feldspato mais abundante. Pelóides de glauconita ocorrem parcialmente calcitizados/dolomitizados, ou compactados a pseudomatriz.

Os produtos da diagênese incluem processos eo-, meso- e telodiagenéticos. A micritização e a formação de franjas fibrosas são frequentes, e relacionadas com processos eodiagenéticos marinhos. A calcita é o constituinte eodiagenético mais frequentes, e ocorre como franjas prismáticas radiais cimentando partículas e recobrindo as franjas fibrosas. Calcita ocorre ainda como cimento do tipo mosaico preenchendo porosidade oomóldica e fraturas, preenchendo e deslocando partículas associadas à porosidade vugular, como crescimento sintaxial sobre equinodermas, e microcristalina substituindo partículas carbonáticas e pelóides de glauconita. Adicionalmente ocorre calcita ferrosa de forma subordinada como cimentos prismático radial e em mosaico.

A dolomita ocorre inicialmente com hábito microcristalino, substituindo partículas e franjas fibrosas, preservando mesmo que parcialmente, a estrutura dos aloquímicos. Já a dolomita blocosa ocorre substituindo partículas e pseudomatrix, bem como o cimento calcítico, podendo ocorrer ainda precipitada diretamente como cimento. Pode, ainda, preencher porosidade vugular e móldica ou ser concentrada ao longo de estilolitos. Dolomita em sela ocorre substituindo cimentos calcíticos e porosidade gerada pela dissolução de calcita e dolomita blocosa.

Crescimentos descontínuos de quartzo e feldspato são observados nas camadas de rochas híbridas e siliciclásticas. Ocasional quartzo blocoso preenche porosidade interpartícula e substitui calcita em arenitos híbridos. Pirita parcialmente oxidada ocorre com hábitos microcristalino, macrocristalino, framboidal e blocosa, substituindo partículas carbonáticas e matéria orgânica. Óxidos e hidróxidos de ferro, assim como a pirita, substituem dolomita e preenchem porosidade móldica e intercristalina.

ISÓTOPOS ESTÁVEIS DE C E O E RAZÕES ^{87}SR/^{86}SR

Os resultados das análises de isótopos estáveis e as razões $^{87}Sr/^{86}Sr$ são apresentados nas tabelas 2 e 3 (Anexo D), e sumarizadas nas figuras 9 e 10. Os resultados de $\delta\ ^{13}C_{carb}$ evidenciam a excursão positiva de carbono em ambos os afloramentos. Para $\delta\ ^{13}C_{carb}$ os valores variam entre -2 e +2‰ para a seção de Felix Cove e entre -4 e +1,8‰ para a seção de March Point. Em ambos os afloramentos a excursão positiva ocorre na transição entre as formações Felix e Man O'War. Esta excursão positiva de carbono também foi observada nos resultados $\delta^{13}C_{org}$ que variaram entre -28 e -23‰ e -30 e -21‰ para Felix Cove e March Point respectivamente. Entretanto, a excursão inicia um pouco abaixo na estratigrafia, compreendida apenas na Formação Felix. Já os resultados de $\delta^{18}O_{carb}$ são bem variáveis, ficando entre -9 e -3 para os dois aforamentos, sendo que em Felix Cove este isótopo apresenta tendências similares ao $\delta^{13}C_{carb}$, e em ambos afloramentos ocorrem excursões positivas simultâneas à observada para o carbono. Os resultados de isótopos de estrôncio apresentam valores dentro do esperado para o Cambriano Médio/Superior, variando entre 0,7093 e 0,7096. Entretanto, para as camadas coincidentes com a excursão positiva de carbono as razões $^{87}Sr/^{86}Sr$ apresentam valores reduzidos a 0,7089, retornando a valores entre 0,7095 nas camadas sobrepostas.

GEOQUÍMICA DE ELEMENTOS MAIORES

Os resultados das análises por fluorescência de raios X (FRX) são apresentados nas tabelas 2 e 3 (Anexo D), e sumarizados nas figuras 11 e 12. Os dados indicam concentrações variáveis dos elementos, com cálcio geralmente maior que 20% e magnésio variando entre 0 e 15%, sendo que os maiores teores ocorrem a partir do Membro Big Cove. As razões Mg/Ca consequentemente, são também variáveis, ficando predominantemente entre 0 e 0,5 entre a Formação March Point e o Membro Big Cove, e entre 0,5 e 0,6 a partir do Membro Big Cove. Concentrações mais elevadas de alumínio e sílica ocorrem ao longo do grupo, sendo relacionadas às camadas de arenitos híbridos, arenitos siliciclásticos ou folhelhos. As razões Mn/Sr apresentam valores elevados para parte das análises, variando entre 0,67 e 29,12 na seção de March Point e entre 0,53 e 17 na seção de Felix Cove. Já as razões Sr/Ca permanecem abaixo de 0,0001 para todas as amostras.

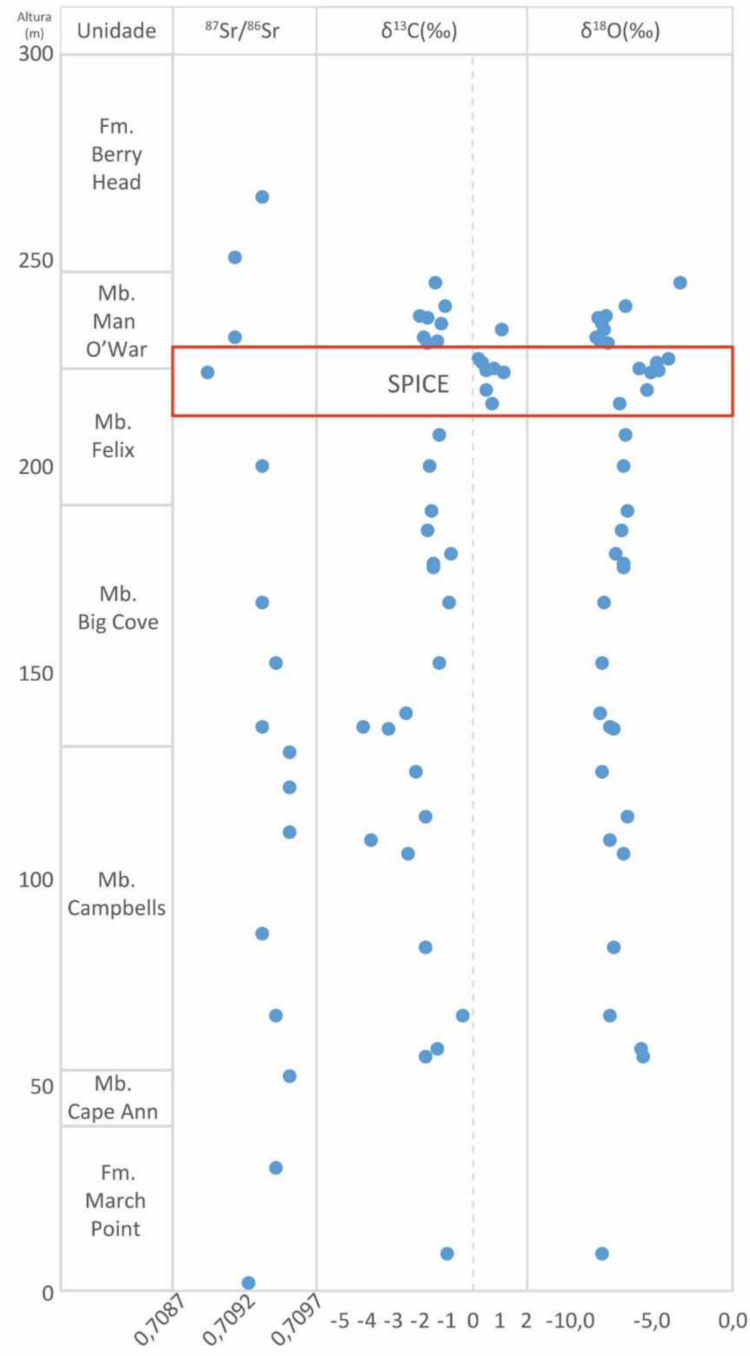

Figura 9 Resultados de isótopos estáveis e de razões de estrôncio para o Grupo Port au Port no afloramento de March Point.

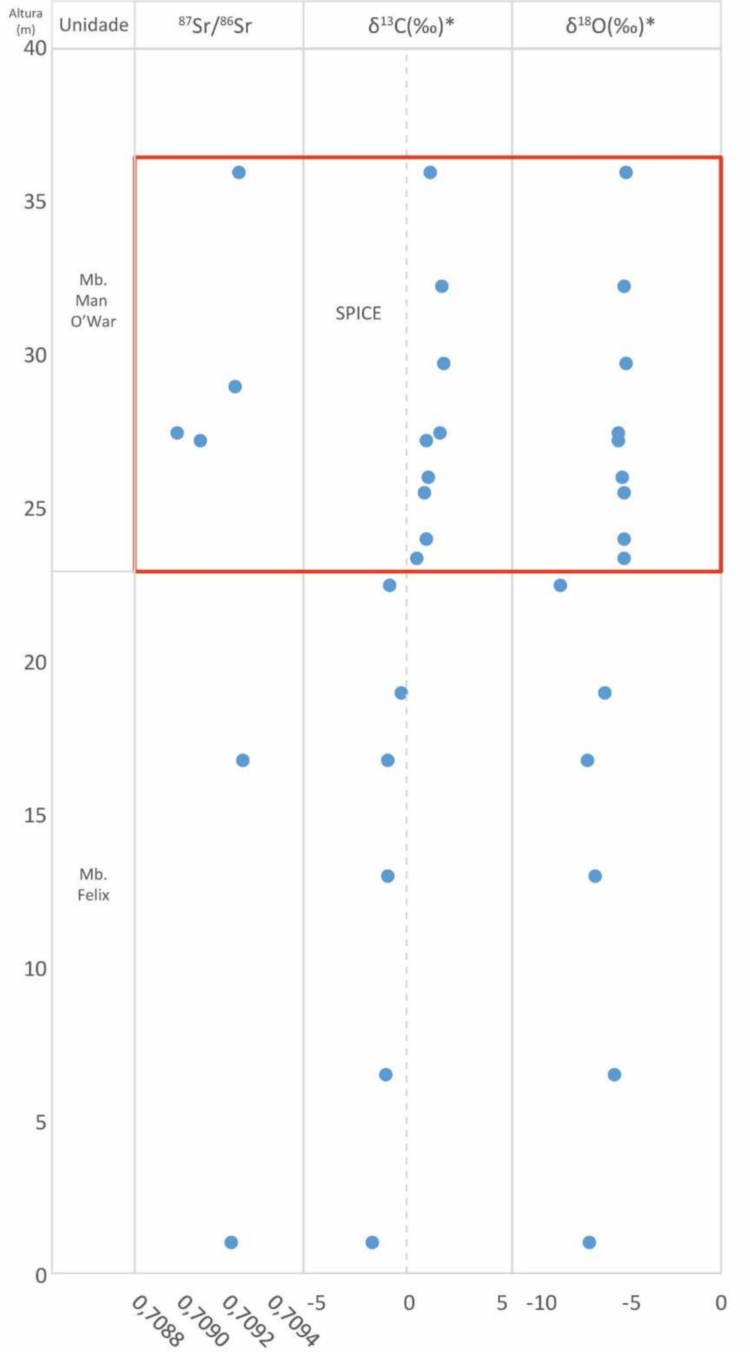

Figura 10 Resultados de isótopos estáveis e de razões de estrôncio para o Grupo Port au Port no afloramento de Felix Cove.

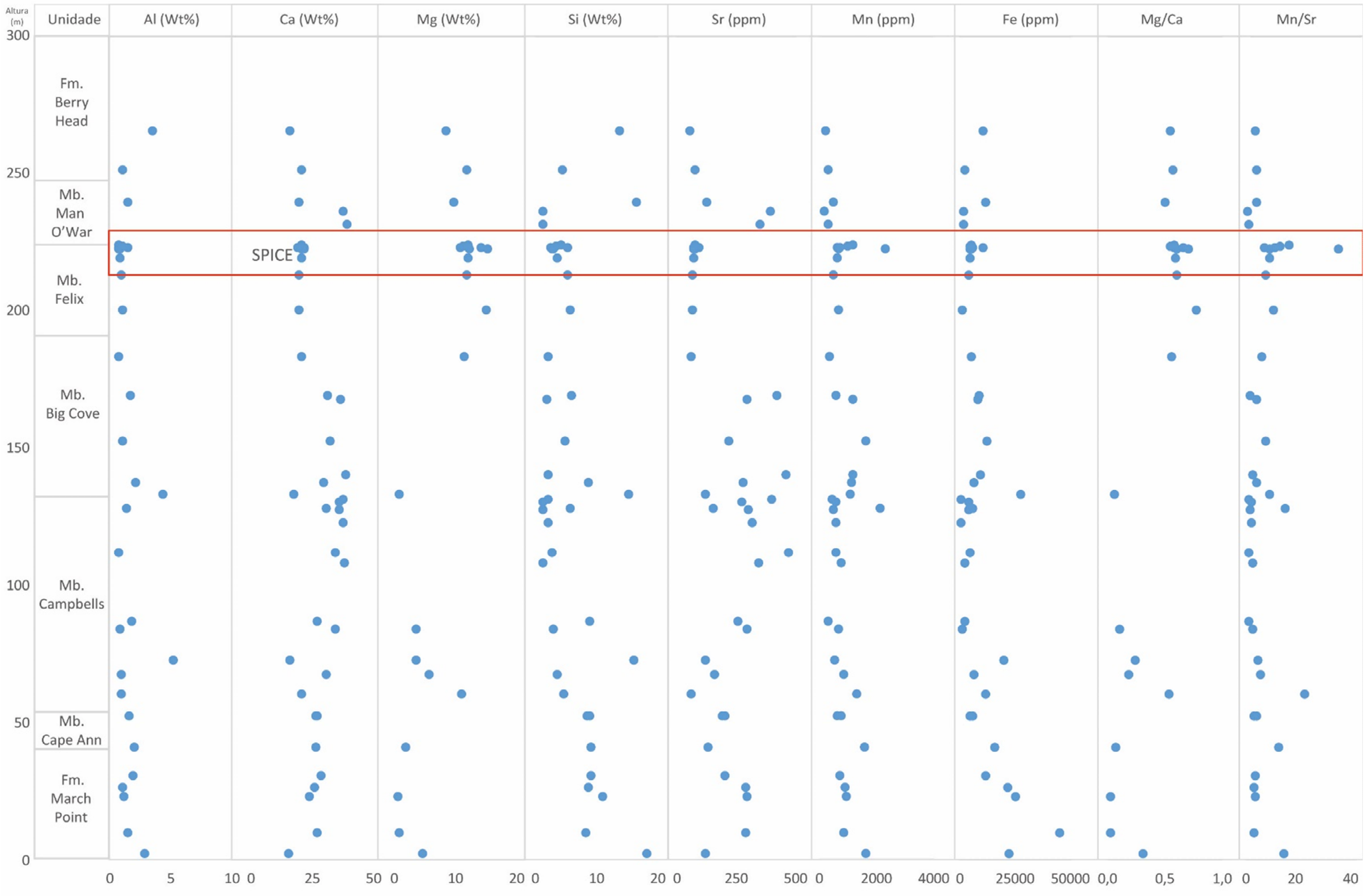

Figura 11 Resultados geoquímicos para o Grupo Port au Port no afloramento de Felix Cove.

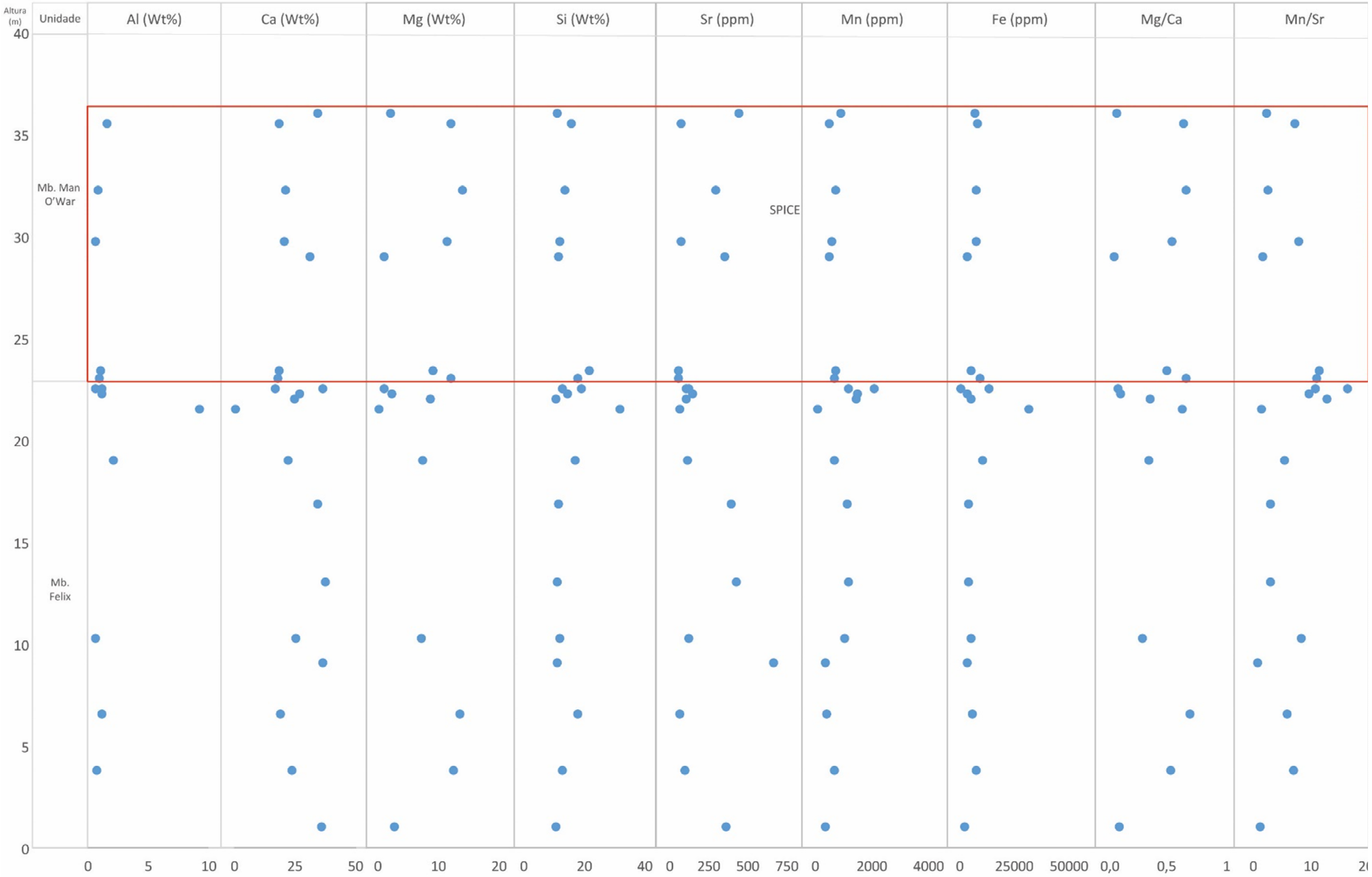

Figura 12 Resultados geoquímicos para o Grupo Port au Port no afloramento de Felix Cove.

DISCUSSÃO

A literatura sobre o Grupo Por au Port compreende trabalhos anteriores abrangentes, que contemplam a estratigrafia e diagênese do grupo (e.g. Chow, 1985; Chow & James, 1987a, 1987b, 1992; Cowan & James, 1993). Entretanto, os trabalhos datam da década de 1980/90, não havendo um maior detalhamento geoquímico e isotópico.

Esta unidade de idade cambriana é descrita como depósitos de ambiente marinho raso dominado por marés. Os ciclos observados são correlacionáveis com os grande ciclos cambrianos presentes em todo o banco carbonático Norte Americano (Chow, 1985; Chow & James, 1987a; Lavoie *et al*., 2012). Apesar dessa correlação, Newfoundland apresenta paleogeografia ligeiramente diferente, estando em uma porção reentrante da costa (Figura 7), o que influencia no padrão deposicional da região (Lavoie *et al*., 2012).

Em relação à estratigrafia, estudos anteriores (e.g. Chow, 1985; Chow & James, 1987a) argumentam sobre a ocorrência de exposição subaérea, utilizada como parâmetro indicativo de uma zona intermarés. Entretanto, durante o levantamento estratigráfico realizado, as feições anteriormente descritas como gretas de contração relacionadas a dessecação, foram reinterpretadas como gretas subaquáticas geradas por sinerese. Estas gretas apresentam origens diversas, podendo estar relacionadas com variação na salinidade ou ação de ondas, entre outros. A forma das gretas é usada como indicativo: linhas retas, polígonos pequenos em planta, e formatos anastamosados e em V quando em corte transversal à camada (McMahon *et al*., 2017). Outra evidência da origem subaquática das gretas é a ocorrência de bioturbação e de bioclastos exclusivamente marinhos, até mesmo como conchas inteiras, associada aos estratos onde estas feições são observadas. Desta forma, a interpretação anterior de zona intermarés pode ser indicada agora como uma zona de inframaré. Assim, a sequência deposicional do grupo passa a ser dominantemente inframaré, com possível associação com condição intermarés apenas quando da ocorrência de depósitos microbiais do tipo esteiras.

Em relação à estratigrafia química, o afloramento de Felix Cove foi incluído nas ocorrências do SPICE por Saltzman *et al*. (2004). Esta ocorrência foi corroborada pelos isótopos de carbono inorgânico e orgânico aqui apresentados. Entretanto, a magnitude da excursão não atinge valores indicados para a excursão em outras localidades (e.g. +5‰, Saltzman *et al*., 2000, 2004). Assim como em March Point, os dados de $\delta^{13}C_{inorg}$ mostram excursões que atingem no máximo +2‰. Além disso, a influência diagenética sobre os valores isotópicos destas rochas de ca. 500Ma não deve ser descartada. Entretanto, valores de menor magnitude para o SPICE são relacionado com um gradiente isotópico na plataforma, indicando áreas mais rasas (Schmid *et al*., 2018). Assim, apesar de menor magnitude, a excursão está presente em ambos os afloramentos visitados, indicando a prevalência de uma assinatura isotópica local.

As razões de estrôncio também apresentam valores dentro do esperado para o Cambriano Médio/Superior (~0.709, Montañez *et al*., 1996, 2000; Peters & Gaines, 2012), apesar de uma anomalia que coincide com os estratos onde se observa o SPICE. Nestas camadas as razões $^{87}Sr/^{86}Sr$ aparecem reduzidas à 0,7089. Este valor estaria evidenciando a influência da diagênese sobre a razão isotópica, uma vez que na Formação Felix os carbonatos estão fortemente dolomitizados, sendo corroborada pelas análises geoquímicas, cuja razão Mn/Sr é predominantemente >2 (Stein *et al*., 1999). Entretanto, os demais valores de $^{87}Sr/^{86}Sr$ se mantém na variação esperada para o período, mesmo em camadas totalmente dolomitizadas. Ademais, processos diagenéticos levam as razões para valores maiores (Knoll, 2000). Portanto, esta mudança brusca na tendência isotópica está relacionada com a regressão que deu origem à excursão positiva de carbono, cuja progradação da linha de costa permitiu o intemperismo das partes mais rasas da plataforma, influenciando assim na assinatura isotópica.

Os processos diagenéticos que afetaram a sucessão carbonática incluem micritização e formação de franjas fibrosas, nos estágios iniciais da diagênese em um ambiente inframaré. A micritização ocorre em resposta à mineralogia original das partículas, e sua consequente instabilidade, sendo neomorfizadas por calcita microcristalina e mantendo seu habito original (Flügel, 1982). As franjas fibrosas lembram franjas de constituição aragonítica ou de calcita magnesiana, podendo ser relacionadas com a composição da água do mar em que estas partículas se formaram (Chow, 1985; Flügel, 1982; Tucker, 1985, 1992). A micritização está relacionada com o ambiente marinho freático estagnante, e as franjas fibrosas com o ativo (James & Choquette, 1983; Longman, 1980; Tucker, 1993). Já as fases de dissolução, neomorfismo, e preenchimento de porosidade por calcita ocorreram na zona de diagênese meteórica freática, onde fluidos insaturados lixiviaram as partículas mais instáveis e propiciam a formação de calcita não-magnesiana (Longman, 1980; Morad *et al*., 2012). A formação de cimentos prismático-radiais, mosaico e crescimento sintaxiais sobre equinodermos está relacionado a este ambiente diagenético. A dolomita, quando relacionada com processos eodiagenéticos (Longman, 1980), pode também estar atrelada à uma mistura de águas meteórica e marinha (Longman 1980; Morad *et al.,* 2012; Tucker 1993).

A intensidade das mesodiagênese foi relativamente limitada pela volumosa cimentação eodiagenética. Os processos mesodiagenéticos incluem limitada compactação mecânica e química, cimentação por dolomita blocosa e em sela, e por calcita grossa. Soerguimento e exposição relacionados à orogênese promoveram a substituição da dolomita por calcita e óxidos de ferro.

As diferentes trajetórias de evolução diagenética, que variam de acordo com os tipos e proporções de constituintes primários, evidenciam uma relação com o ambiente deposicional e evolução com o soterramento relativamente simples. Após a deposição, com baixa taxa deposicional, os processos eodiagenéticos marinhos e meteóricos se intensificaram. Com a progressão do soterramento, foram seguidos por limitada mesodiagênese, e finalmente pelo soerguimento e exposição, relacionados aos eventos orogênicos que deram origem aos Apalaches (Williams, 1979, 1995).

Apesar das intensas modificações diagenéticas, a composição dos constituintes primários e eodiagenéticos marinhos são comumente bem identificáveis. A ocorrência de franjas fibrosas, relacionada à diagênese precoce marinha, é indicado na literatura como um indício de mineralogia originalmente aragonítica ou calcítica de alto magnésio (e.g. (Chow & James, 1987b; Flügel, 1982; Tucker, 1993, 2001; Tucker & Wright, 1990). Adicionalmente, são identificadas partículas biminerálicas (Chow, 1985; Chow & James, 1987b), identificada pela dissolução, recristalização ou dolomitização preferencial de alguns envelopes dos oólitos, enquanto outros permanecem inalterados. De maneira similar, é possível identificar camadas, onde foi gerada porosidade oomóldica pela dissolução completa de partículas com mineralogia instável (HMC/aragonita), enquanto as partículas micritizadas e de composição calcítica com baixo teor de magnésio sequer afetando.

Outras evidências de uma mineralogia originalmente aragonítica/HMC são a ocorrência de microdolomita e de altas concentrações de estrôncio nos carbonatos (Dickson, 2014; Lohman & Meyers, 1977; Longman, 1980; Neilson *et al*., 2016), ambas presentes nas amostras do Grupo Port au Port. Dadas as evidências e apesar da intensa diagênese, a mineralogia primária das rochas do grupo indica uma composição marinha rica em magnésio, fato corroborado pela excursão positiva de carbono (SPICE) que é relacionada à um período de mares aragoníticos. Entretanto, estudos mais detalhados, abrangendo populações amostrais maiores, serão necessários para definir os processos que geraram as partículas bimineralícas, e a relação destas com a composição marinha.

CONCLUSÕES

A evolução do Grupo Port au Port, assim como de outras sequências carbonáticas antigas, é desafiadora por que essas passaram por eventos que podem abranger orogenias, intensa diagênese, ou até mesmo metamorfismo. O Grupo Port au Port está inserido em uma porção menos afetada pela Orogênese Apalachiana. Apesar disso, suas rochas sofreram intensa alteração diagenética.

A diagênese do Grupo Port au Port afetou fortemente a sequência, sendo mais expressiva nos bancos oolíticos. Entretanto, apesar da intensa dolomitização, a assinatura isotópica de carbono não foi afetada, e a magnitude reduzida do SPICE na localidade se deve ao fato desta estar em uma posição mais rasa da plataforma. O mesmo se observa nos isótopos de estrôncio. Ao longo do grupo são observados valores médios característicos do Cambriano Médio/Superior, mas a redução das razões equivale às camadas onde ocorre o SPICE. Desta forma, os valores reduzidos se devem ao fato da regressão que dá origem à excursão positiva de carbono expor rochas carbonáticas mais antigas (Cambriano Inferior).

A análise dos processos diagenéticos da sequência evidencia que processos eodiagenéticos marinhos promoveram a formação de hardgrounds que deram origem aos intraclastos observados nas diferentes litologias. A dolomitização fina, que ocorreu ainda na eodiagênese, auxiliou na preservação da estrutura das partículas, assim como sua micritização. A calcita ocorre ainda como cimentos eodiagenéticos e neomorfismo, associada aos processos da zona freática meteórica, que resultaram na primeira fase de dissolução e criação de porosidade móldica. Com o avanço do soterramento e implementação da mesodiagênese, a dolomitização se intensifica, sendo posteriormente dissolvida e calcitizada durante processos telodiagenéticos relacionados ao soerguimento e exposição da sequência durante o evento orogênico que deu origem aos Apalaches.

A análise petrográfica de amostras com menores graus de dolomitização evidenciam hábitos que remetem a uma mineralogia de composição aragonítica ou de calcita magnesiana (*HMC*), dentre as quais encontram-se as franjas fibrosas. Partículas biminerálicas mostram dissolução e recristalização seletivas, com micritização das fases minerais mais instáveis ainda na eodiagênese. Adicionalmente, teores mais elevados de Sr em franjas e envelopes oolíticos, mesmo após neomorfismo, indicam possível mineralogia originalmente aragonítica

Referências Bibliográficas

Allen, J.S. 2009. Stratigraphy and Structure of the Laurentian Rifted Margin in the Northern Appalachians: A Low-Angle Detachment Rift System. *Geology* 37(4):335–338.

Barili, R., Neilson, J.E., Brasier, A. T., Goldbenrg, K., Bardola, T. P., De Ros, L. F. & Leng, M. 2018. Carbon Isotopes, Stratigraphy, and Environmental Change: The Middle–Upper Cambrian Positive Excursion (SPICE) in Port Au Port Group, Western Newfoundland, Canada. *Canadian Journal of Earth Sciences* 55(11):1209–1222.

Chow, N. & James, N. P. 1992. Synsedimentary Diagenesis of Cambrian Peritidal Carbonates: Evidence from Hardgrounds and Surface Paleokarst in the Port Au Port Group, Western Newfoundland. *Bulletin of Canadian Petroleum Geology* 40(2):115–127.

Chow, N. 1985. Sedimentology and Diagenesis of Middle and Upper Cambrian Platform Carbonates and Siliciclastics, Port Au Port Peninsula, Western Newfoundland. 458p.*Tese de doutorado.* Departamento de ciências da Terra, Memorial University.

Chow, N. & James, N. P. 1987a. Cambrian Grand Cycles : A Northern Appalachian Perspective. *Geological Society of America Bulletin* 98(4):418–429.

C Chow, N. & James, N. P. 1987b. Facies Specific, Calcitic and Bimineralic Ooids from Middle and Upper Cambrian Platform Carbonates, Western Newfoundland, Canada. *Journal of Sedimentary Petrology* 57(5):907–921.

Cowan, C. A. & James, N. P. 1993. The Interactions of Sea-Level Change, Terrigenous-Sediment Influx, and Carbonate Productivity as Controls on Upper Cambrian Grand Cycles of Western Newfoundland, Canada. *Geological Society of America Bulletin* 105(12):1576–1590.

Dickson, J. A. D. 2014. *Marine Beachrocks*. Newmarket, Carbonate Diagenesis Ltd. 41p.

Dunham, R.J. 1962. Classification of Carbonate Rocks According to Depositional Textures. *in* Ham, W. E. (Ed.). *Classification of Carbonate Rocks--A Symposium*. AAPG. p. 108–122

Embry III, A. F.& Klovan, J. E. 1971. A Late Devonian Reef Tract on Northeastern Banks Island, NWT. *Bulletin of Canadian Petroleum Geology* 19(4):730–781.

Flügel, E. 1982. *Microfacies Analysis of Limestones.* Berlin, Springer-Verlag, 984p.

Fritz, R.D.,. Morgan, W. A., Longacre, S., Derby, J.R., & Sternbach, C. A. 2012. *AAPG*

Memoir 98 Great American Carbonate Bank. Tulsa. AAPG. 528p.

James, N. P. & Choquette, P. W. 1983. Diagenesis 6. Limestones — The Sea Floor Diagenetic Environment. *Geoscience Canada* 10(4):162–179.

James, N.P., Stevens, R. K., Barnes, C.R., & Knight, I. 1989. Evolution of a Lower Paleozoic Continental-Margin Carbonate Platform, Northern Canadian Appalachians. *In* Paul Crevello, P., Wilson, P., Sarg, F. & Read, F. *Controls on Carbonate Platforms and Basin Development*. SEPM Society for Sedimentary Geology. Tulsa, Oklahoma. 379p.

Kindle, C. H.& Whittington, H. B. 1965. New Cambrian and Ordovician Fossil Localities in Western Newfoundland. *Geological Society of America Bulletin* 76(6):683–688.

Knoll, A. H. 2000. Learning to Tell Neoproterozoic Time. *Precambrian Research* 100(1–3):3–20.

Kouchinsky, S.B., Gallet, Y., Korovnikov, I., Pavlov, V., Runnegar, B., Shields, G., Veizer, J., Young, E., & Ziegler, K. 2008. The SPICE Carbon Isotope Excursion in Siberia: A Combined Study of the Upper Middle Cambrian–lowermost Ordovician Kulyumbe River Section, Northwestern Siberian Platform. *Geological Magazine* 145(05):609–622.

Lavoie, D., Desrochers, A., Dix, G., Knight, I., & Hersi, O.S. 2012. The Great American Carbonate Bank in Eastern Canada: An Overview. *In* Derby, J., Fritz, R., Longacre, S., Morgan, W., & Sternbach, C. (Eds). *Memoir 98 Great American Carbonate Bank*. Tulsa. AAPG. p. 499–523.

Levesque, R. J.. 1977. Stratigraphy and Sedimentology of Middle Cambrian to Lower Ordovician Shallow Water Carbonate Rocks, Western Newfoundland. 325p.Dissertação de mestrado. Departamento de ciências da Terra, Memorial University

Lohman, K. C. & Meyers, W. J. 1977. Microdolomite Inclusions in Cloudy Prismatic Calcites: A Proposed Criterion for Former High-Magnesium Calcite. *Journal of Sedimentary Petrology* 47(3):1078–1088.

Longman, M. W. 1980. Carbonate Diagenetic Textures from Nearsurface Diagenetic Environments^. *American Association of Petroleum Geologists Bulletin* 64(4):461–487.

McMahon, S., Hood, A. van S., & McIlroy, D. 2017. The Origin and Occurrence of Subaqueous Sedimentary Cracks. *Geological Society, London, Special Publications* 448(1):285–309.

Miall, A. D. 1978. Lithofacies Types and Vertical Profile Models in Braided River Deposits: A Summary. *In* Miall, A.D (Ed.). *Fluvial Sedimentology*. Cambridge. Cambridge Unibersity

Press. p. 597–604

Montañez, Isabel P., Jay L. Banner, David A. Osleger, Lars E. Borg, and Paula J. Bosserman. 1996. Integrated Sr Isotope Variations and Sea-Level History of Middle to Upper Cambrian Platform Carbonates: Implications for the Evolution of Cambrian Seawater 87Sr/86Sr. *Geology* 24(10):917–920.

Montañez, I.P., Osleger, D. A., Banner, J. L., Mack, L. E., & Musgrove, M. 2000. Evolution of the Sr and C Isotope Composition of Cambrian Oceans. *GSA Today* 10(5):1–7.

Morad, S., Ketzer, J. M., &De Ros, L. F. 2012. Linking Diagenesis to Sequence Stratigraphy: An Integrated Tool for Understanding and Predicting Reservoir Quality Distribution. *Linking Diagenesis to Sequence Stratigraphy* 45:1–36.

Neilson, J. E., Brasier, A.T., & North, C. P. 2016. Primary Aragonite and High-Mg Calcite in the Late Cambrian (Furongian). Potential Evidence from Marine Carbonates in Oman. *Terra Nova* 28(5):306–315.

Peters, S. E. & Gaines, R. R. 2012. Formation of the ’ Great Unconformity’ as a Trigger for the Cambrian Explosion. *Nature* 484(7394):363–366.

Saltzman, M. R., Cowan, C. A., Runkel, A. C., Runnegar, B., Stewart, M. C., & Palmer, A. R. 2004. The Late Cambrian Spice (13C) Event and the Sauk II-SAUK III Regression: New Evidence from Laurentian Basins in Utah, Iowa, and Newfoundland. *Journal of Sedimentary Research* 74(3):366–377.

Saltzman, M.R., Ripperdan, R.L., Brasier, M. D., Lohmann, K. C., Robison, R. A., Chang, W. T.,Peng, S., Ergaliev, E. K., & Runnegar, B. 2000. A Global Carbon Isotope Excursion (SPICE) during the Late Cambrian: Relation to Trilobite Extinctions, Organic-Matter Burial and Sea Level. *Palaeogeography, Palaeoclimatology, Palaeoecology* 162(3–4):211–223.

Saltzman, M. R., Runnegar, B, & Lohmann, K. C. 1998. Carbon Isotope Stratigraphy of Upper Cambrian (Steptoean Stage) Sequences of the Eastern Great Basin: Record of a Global Oceanographic Event. *Bulletin of the Geological Society of America* 110(3):285–297.

Saltzman, M.R., Young, S., Kump, L. R., Gill, B. C., Lyons, T.W., & Runnegar, B. 2011. Pulse of Atmospheric Oxygen during the Late Cambrian. *Proceedings of the National Academy of Sciences of the United States of America* 108(10):3876–3881.

Schmid, S., Smith, P.M., & Woltering, M. 2018. A Basin-Wide Record of the Late Cambrian Steptoean Positive Carbon Isotope Excursion (SPICE) in the Amadeus Basin, Australia.

Palaeogeography, Palaeoclimatology, Palaeoecology 508(July):116–128.

Schuchert, Charles & Carl Owen Dunbar. 1934. *GSA Memoirs n°1: Stratigraphy of Western Newfoundland*. Washington, Juddn & Detwaeiler Inc. 154p.

Jacobsen, S. B. & Kaufman, A. J. 1999. The Sr, C and O Isotopic Evolution of Neoproterozoic Seawater. *Chemical Geology* 161(1–4):37–57.

Thomas, W. A. 1977. Evolution of Appalachian-Ouachita Salients and Recesses from Reentrants and Promontories in the Continental Margin. *American Journal of Science* 277(10):1233–1278.

Thomas, W. A. 1991. The Appalachian-Ouachita Rifted Margin of Southeastern North America. *Geological Society of America Bulletin* 103(3):415–31.

Tucker, M. E. 1992. The Precambrian-Cambrian Boundary: Seawater Chemistry, Ocean Circulation and Nutrient Supply in Metazoan Evolution, Extinction and Biomineralization. *Journal of the Geological Society* 149(4):655–668.

Tucker, M. E. 1985. Calcitized Aragonite Ooids and Cements from the Late Precambrian Biri Formation of Southern Norway. *Sedimentary Geology* 43(1–4):67–84.

Tucker, M. E. 1993. Carbonate Diagenesis in a Sequence Stratigraphic Framework. *In*: Wright, V. P. (Ed.). *Sedimentology Review*. Oxford, Blackwell Scientific Publications p.51–72.

Tucker, M. E. 2001. *Sedimentary Geology: An Introduction to the Origin of Sedimentary Rocks*. Oxford, Blackwell Scientific Publications. 272 p.

Tucker, M. E. & Paul Wright. 1990. *Carbonate Sedimentology*. Oxford, Wiley-Blackwell. 496p.

Whittington, H. B. & Kindle, C. H. 1963. Middle Ordovician Table Head Formation, Western Newfoundland. *Geological Society of America Bulletin* 74(6):745–758.

Whittington, H. B. & Kindle, C. H. 1969. Cambrian and Ordovician Stratigraphy of Western Newfoundland: Chapter 47: Northwestern Border of the Orogenic Belt. *In M 12: North Atlantic: Geology and Continental Drift*. p. 655–664.

Williams, H. 1976. Tectonic Stratigraphic Subdivision of the Appalachian Orogen. *Geological Society of America Abstracts* 8(2):300.

Williams, H. 1979. Appalachian Orogen in Canada. *Canadian Journal of Earth Sciences* 16(3):792–807.

Williams, H. 1995. Geology of the Appalachian—Caledonian Orogen in Canada and Greenland*.* *In:* Williams, H. (Ed). *Geology of Canada – nº 6.* Otawa, Canada Communications Group. 925p.

Woods, M., Wilby, P., Leng, M., Rushton, A., & Williamsm, M. 2011. The Furongian (Late Cambrian) Steptoean Positive Carbon Isotope Excursion (SPICE) in Avalonia. *Journal of the Geological Society* 168(4):851–862.

PARTE II

ARTIGO 1

CARBON ISOTOPES, STRATIGRAPHY, AND ENVIRONMENTAL CHANGE: THE MIDDLE-UPPER CAMBRIAN POSITIVE EXCURSION (SPICE) IN PORT AU PORT GROUP, WESTERN NEWFOUNDLAND, CANADA.

Artigo completo publicado no número especial do periódico ***Canadian Journal of Earth Sciences***, referente aos trabalhos apresentados durante o *International Symposium of Ediacaran-Cambrian Transition* (ISECT, 2017). O artigo está reproduzido na íntegra nas páginas a seguir.

NRC Research Press

ARTICLE

Carbon isotopes, stratigraphy, and environmental change: the Middle–Upper Cambrian Positive Excursion (SPICE) in Port au Port Group, western Newfoundland, Canada[1]

Rosalia Barili, Joyce Elaine Neilson, Alexander Thomas Brasier, Karin Goldberg, Tatiana Pastro Bardola, Luiz Fernando De Ros, and Melanie Leng

Abstract: In many basins, Upper Cambrian carbonate successions display intervals with a positive carbon isotope excursion (CIE) of up to +5‰. In North America, this marks the boundary between the Sauk II–III super-sequences. A Steptoean positive carbon isotope excursion (SPICE) locality previously identified in the Port au Port peninsula, western Newfoundland, has been revisited and an additional potential SPICE locality found. In both locations, a CIE is found to be associated with a prominent bioherm and sandstone layer within a sequence of carbonate rocks. At March Point columnar stromatolites occur, whereas at Felix Cove thrombolites can be seen. In the latter, the sandstone immediately overlies the thrombolites coincident with the CIE, whereas at March Point a dolomitized grainstone occurs above the stromatolites. The sandstone at this locality post-dates the CIE. Although lower than the SPICE in some localities, a positive CIE is present in both sections: March Point (+1.1‰) and Felix Cove (+1.8‰). Additionally, $\delta^{13}C_{org}$ rises from –30.0‰ to –22.0‰ at March Point and from –27‰ to –24.0‰ at Felix Cove and, in accordance with previously published work, we suggest that this could be the SPICE. Comparison of the stratigraphy and petrography between the two localities suggest that both depositional and diagenetic factors could have influenced the nature of the interpreted SPICE in Newfoundland. It is also possible that the local carbon isotopic signature may have been influenced by a semi-restricted depositional and early diagenetic environment related to the paleogeographic configuration rather than the global marine excursion.

Résumé : Dans de nombreux bassins, les séquences de carbonates du Cambrien supérieur présentent des intervalles caractérisés par une excursion des isotopes du carbone (EIC) positive de jusqu'à +5‰. En Amérique du Nord, cette excursion marque la limite entre les superséquences de Sauk II et III. Une localité d'excursion des isotopes du carbone positive steptoienne (SPICE) déjà reconnue dans la péninsule de Port au Port de l'ouest de Terre-Neuve a été revisitée, et une autre localité SPICE potentielle a été trouvée. Dans les deux endroits, une EIC est associée à une couche bien en évidence de bioherme et de grès dans une séquence de roches carbonatées. À March Point, des stromatolithes en colonnes sont présents, alors qu'à Felix Cove, des thrombolithes sont observés. Dans ce dernier site, le grès se trouve immédiatement au-dessus des thrombolithes coïncidant avec l'EIC, alors qu'à March Point, un grainstone dolomitisé repose sur les stromatolithes. Le grès dans cette localité est plus jeune que l'EIC. Bien qu'elle soit plus faible que la SPICE dans certaines localités, une EIC positive est présente dans les deux coupes, de March Point (+1,1 ‰) et de Felix Cove (+1,8 ‰). En outre, le $\delta^{13}C_{org}$ augmente de –30,0 ‰ à –22,0 ‰ à March Point, et de –27 ‰ à –24,0 ‰ à Felix Cove et, à l'instar de travaux déjà publiés, nous suggérons qu'il pourrait s'agir de la SPICE. La comparaison de la stratigraphie et de la pétrographie des deux localités donne à penser que des facteurs associés tant au dépôt qu'à la diagenèse pourraient avoir influencé la nature de l'excursion interprétée comme étant la SPICE à Terre-Neuve. Il est aussi possible que la signature locale des isotopes du carbone ait été influencée par un milieu semi-restreint de dépôt et de diagenèse précoce associé à la configuration paléogéographique plutôt qu'à l'excursion marine planétaire. [Traduit par la Rédaction]

Introduction

Upper Cambrian (Steptoean Stage) carbonate successions are found worldwide, including examples in North America, Siberia, Kazakhstan, China, Australia, and Oman (Fig. 1), with a positive carbonate carbon isotope ($\delta^{13}C_{carb}$) excursion (CIE) of up to +5‰, lasting nearly 4 Ma (Saltzman et al. 2000, 2004; Kouchinsky et al. 2008; Woods et al. 2011; Neilson et al. 2016). This excursion has also been observed in the $\delta^{13}C$ of organic-rich ($\delta^{13}C_{org}$) mudstones and shales (Ahlberg et al. 2009; Saltzman et al. 2011). This CIE was first reported from the John's Wash Limestone of Utah by Brasier (1993), followed by sections described in the House Range in Utah, McGill in Nevada, and Wind Rover Range and Gros Ventre Range in Wyoming (Saltzman et al. 1995). The term Steptoean positive carbon isotope excursion (SPICE) was proposed by Saltzman et al.

Received 23 January 2018. Accepted 6 July 2018.

Paper handled by Special Editor Marc Laflamme.

R. Barili. Universidade Federal do Rio Grande do Sul, Instituto de Geociências, Av. Bento Gonçalves, 9500, Porto Alegre, RS, Brazil; Instituto do Petróleo e dos Recursos Naturais, Pontifícia Universidade Católica do Rio Grande do Sul, Av. Ipiranga, 6681, prédio 96J, Porto Alegre, RS, Brazil.
J.E. Neilson and A.T. Brasier. University of Aberdeen, School of Geosciences, King's College, Aberdeen, UK.
K. Goldberg. Department of Geology, Kansas State University, 207 Thompson Hall, Manhattan, KS, 66506, USA.
T. Pastro Bardola and L.F. De Ros. Universidade Federal do Rio Grande do Sul, Instituto de Geociências, Av. Bento Gonçalves, 9500, Porto Alegre, RS, Brazil.
M. Leng. NERC Isotope Geosciences Laboratory, British Geological Survey, Keyworth, Nottingham NG12 5GG, UK.
Corresponding author: Rosalia Barili (email: rosalia.barili@gmail.com).

[1]This paper is part of a Special Issue entitled "Geobiology of the Ediacaran–Cambrian Transition: ISECT 2017".

Fig. 1. Record of the Steptoean positive carbon isotope excursion (SPICE) excursion and global chronostratigraphic framework (after Saltzman et al. 2004).

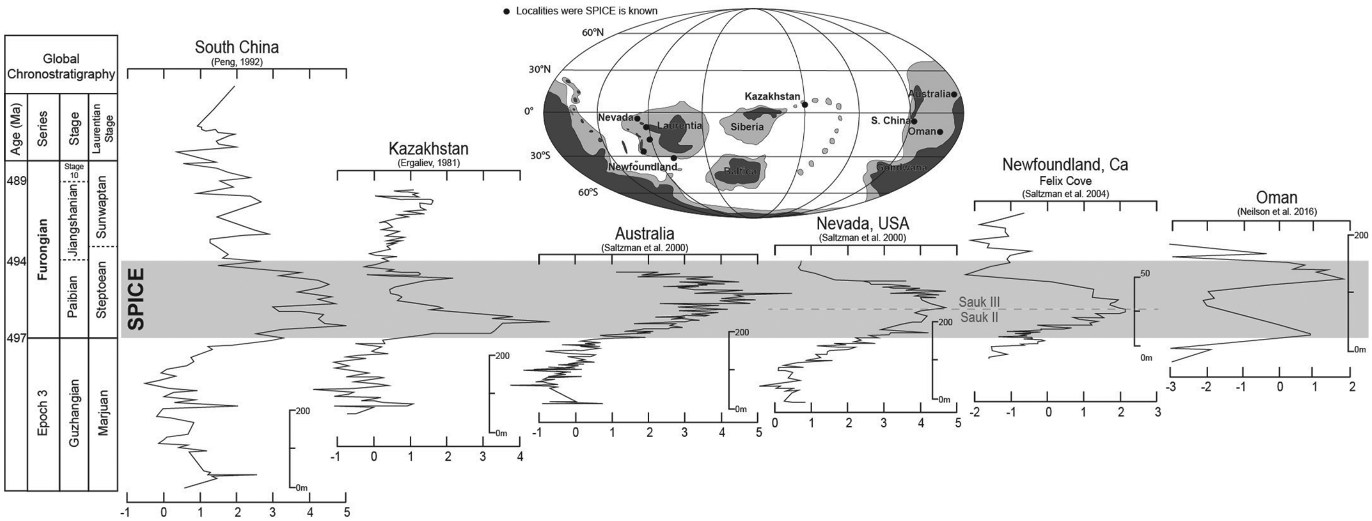

Fig. 2. Study area in the Port au Port Peninsula. Location of the logged sections are shown by black rectangles: (1) March Point and (2) Felix Cove.

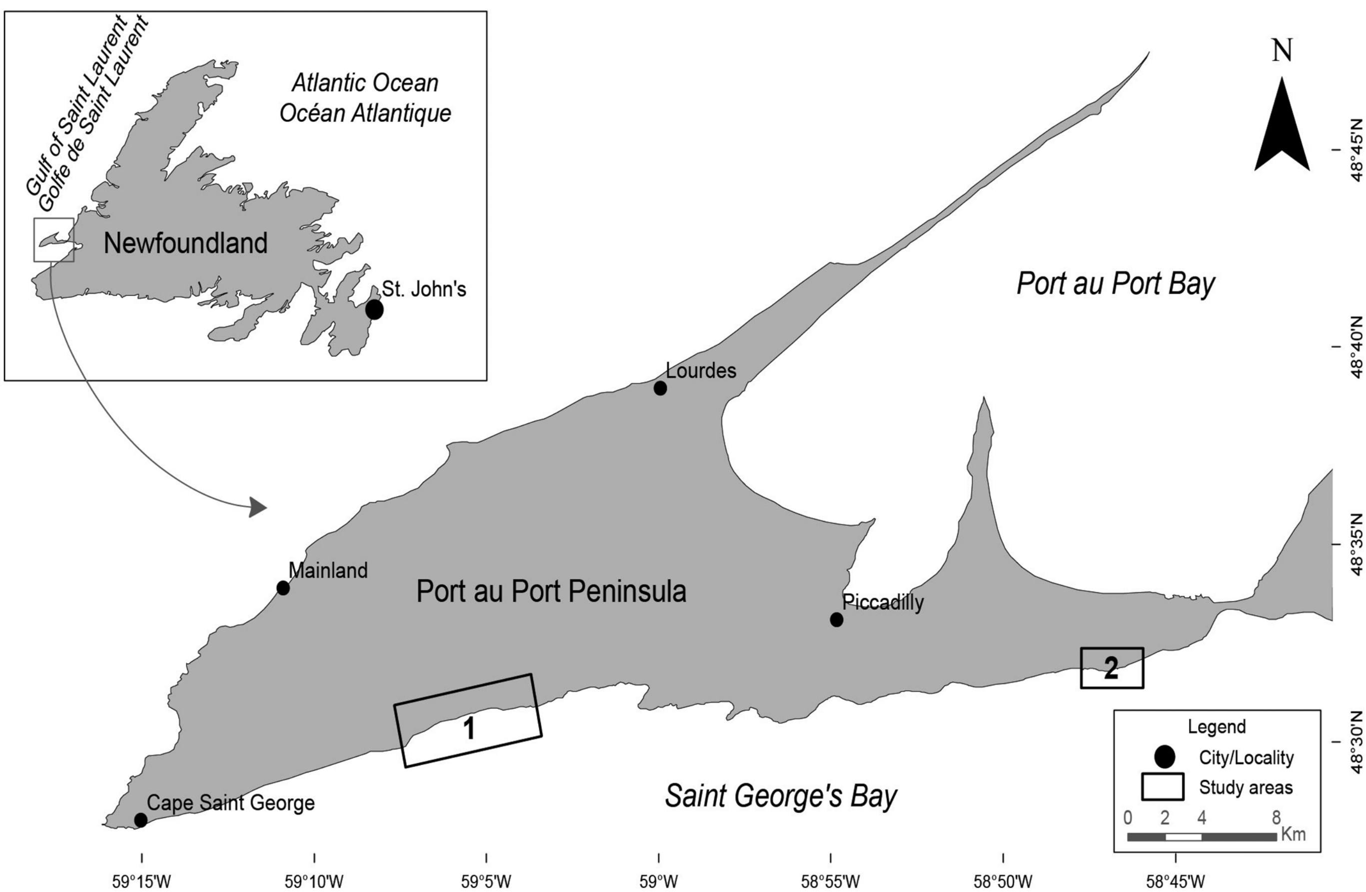

(1998), who suggested a global occurrence comparing data from South China, Kazakhstan, Australia, and Laurentia (Shingle Pass, Nevada) (Saltzman et al. 2000). This positive carbon isotope excursion is coeval with a trilobite mass extinction horizon (Palmer 1965; Sepkoski 1982; Yochelson 1984; Saltzman et al. 1995, 1998, 2000; Bond and Grasby 2017). Saltzman et al. (2004, 2011) and Bond and Grasby (2017) suggested that the positive excursion represents a perturbation in the global carbon cycle that occurs on the boundary between the Sauk II and Sauk III second-order supersequences from the Sauk megasequence (Sloss 1963).

Other CIEs of similar magnitude and duration have been described from the Late Ordovician, late Silurian, Upper Devonian, early Mississippian, and early late Permian (Gruszczyński et al. 1989; Brenchley 1994; Joachimski et al. 2002; Saltzman 2002; Saltzman et al. 2011). Each positive CIE may correspond to different causes, but in general they are thought to reflect an increased burial of isotopically lighter organic carbon (resulting in higher δ13C in the residual pool) related to increased organic productivity, with organic preservation due to high sedimentation rates and (or) anoxic conditions (Arthur et al. 1987; Derry et al. 1992; Schidlowski et al. 1992; Schrag et al. 2002).

The SPICE was first described in western Newfoundland in the Petit Jardin Formation (Felix and overlying Man O' War members) at Felix Cove by Saltzman et al. (2004). In this unit, δ13C values of carbonates rise from −1‰ to 0‰ Vienna Pee Dee Belemnite (V-PDB), reaching a peak δ13C of +2.2‰ just above a quartz sandstone layer that marks the Sauk II – Sauk III boundary. Although the presence of an excursion has been reported in the Port au Port rocks (Saltzman et al. 2004), the magnitude of the SPICE excursion in the Petit Jardin Formation is smaller than observed around the world (Glumac and Walker 1998).

This raises questions about whether the presence of the global SPICE excursion in the Port au Port Peninsula rocks is real, or whether it is just a local environmental or diagenetic shift. In an attempt to address this issue, two western Newfoundland stratigraphic sections were logged in detail, followed by petrographic analysis of the carbonates, and δ13C analysis of both carbonate and organic carbon samples.

Geologic setting

The study area is located on the southern coast of the Port au Port Peninsula, western Newfoundland (Fig. 2). The SPICE was identified in Felix Cove (48°31′49.2″N/58°47′12″E), a section previously studied by Saltzman et al. (2004), and another potential SPICE locality was identified at March Point (48°30′42.1″N/59°05′31.1″E).

The Port au Port Group forms part of the autochthonous Cambrian–Ordovician sequence of the tectono-stratigraphic Humber zone of the northern Appalachian orogeny (Williams 1976, 1979). It is interpreted as shallow-marine deposits from the outer part of a stable carbonate platform that surrounded the Iapetus Ocean (Williams 1976, 1979; Palmer and James 1979). These mixed carbonate–siliciclastic deposits record the gradual transition from early Cambrian siliciclastic deposition to predominantly carbonate sedimentation in the Early Ordovician (Chow 1985; Chow and James 1987*b*; Cowan and James 1993). The group is composed of three formations, namely the March Point, Petit Jardin (Cape Ann, Campbells, Big Cove, Felix and Man O' War Members), and Berry Head Formations.

Transgressive–regressive Grand Cycles are identified through the Port au Port Group (Chow 1985; Chow and James 1987*a*, 1987*b*) (Fig. 3). The marine transgression at the beginning of the Grand Cycles resulted in a shallow subtidal–intertidal environment, where relatively muddy carbonates were deposited (shaley packages and parted limestone; Chow and James 1987*b*). These deposits pass upwards into more open marine oolitic shoals, probably deposited near the platform edge (carbonate packages; Chow and James 1987*b*). As sea level dropped at the top of the cycles, the environment returned to a more restricted water circulation situation, although according to Chow and James (1987*b*) extensive evidence of subaerial exposure at the top of cycle B is absent. Carbon isotope data, previously collected in the Port au Port Group at Felix Cove, show a strong positive $\delta^{13}C_{carb}$ excursion between the Felix and Man O' War Members (Fig. 1), which has been interpreted as the SPICE (Saltzman et al. 2004).

Methodology

The field work was performed along two main outcrops on the Port au Port Peninsula—March Point and Felix Cove. Detailed sedimentological logging on a centimeter scale (1:50) and systematic sampling was carried out at 1 m resolution, from the base of accessible units in the Petit Jardin Formation to the top of each

Fig. 3. Schematic stratigraphic log of the Port au Port Group (after Chow 1985). Each of the grand cycles (A, B, and C) consists of a lower shaley half-cycle mainly composed of parted limestone (interbedded shale and mudstone) and an upper carbonate half-cycle of oolitic grainstone/bioherms. Estimated Sauk II–III sequence limit is indicated (Chow and James 1987*b*; Saltzman et al. 2004).

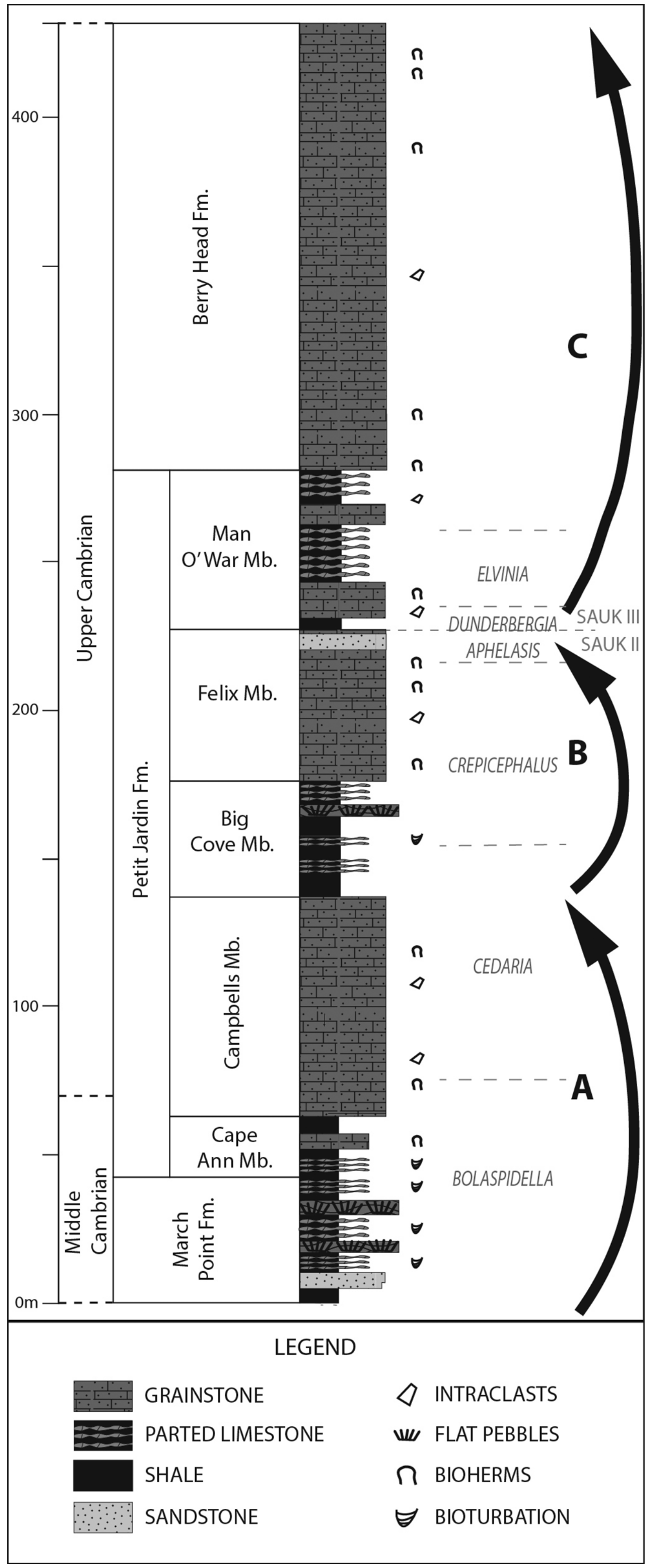

Fig. 4. Outcrop photos of Steptoean positive carbon isotope excursion bearing layers. (*a*) Felix Cove outcrop at 22.5 m showing the massive sandstone (S) that overlies the thrombolite layer at 22.25 m. Some intervals in the thrombolite contains vugs parallel to bedding that may also occur in the sandstone (arrow). (*b*) Detail from Felix Cove of thrombolite at 22.25 m. (*c*) West Felix Cove outcrop with pillow thrombolites (T) and the overlying sandstone (S). (*d*) Detail from March Point of columnar stromatolite at 222.5 m. (*e*) Detail of the dolomitized glauconitic grainstone (DG) above the stromatolite (STR). (*f*) View of the outcrop with the dolomitized glauconitic grainstone (DG) overlying the stromatolite. [Colour online.]

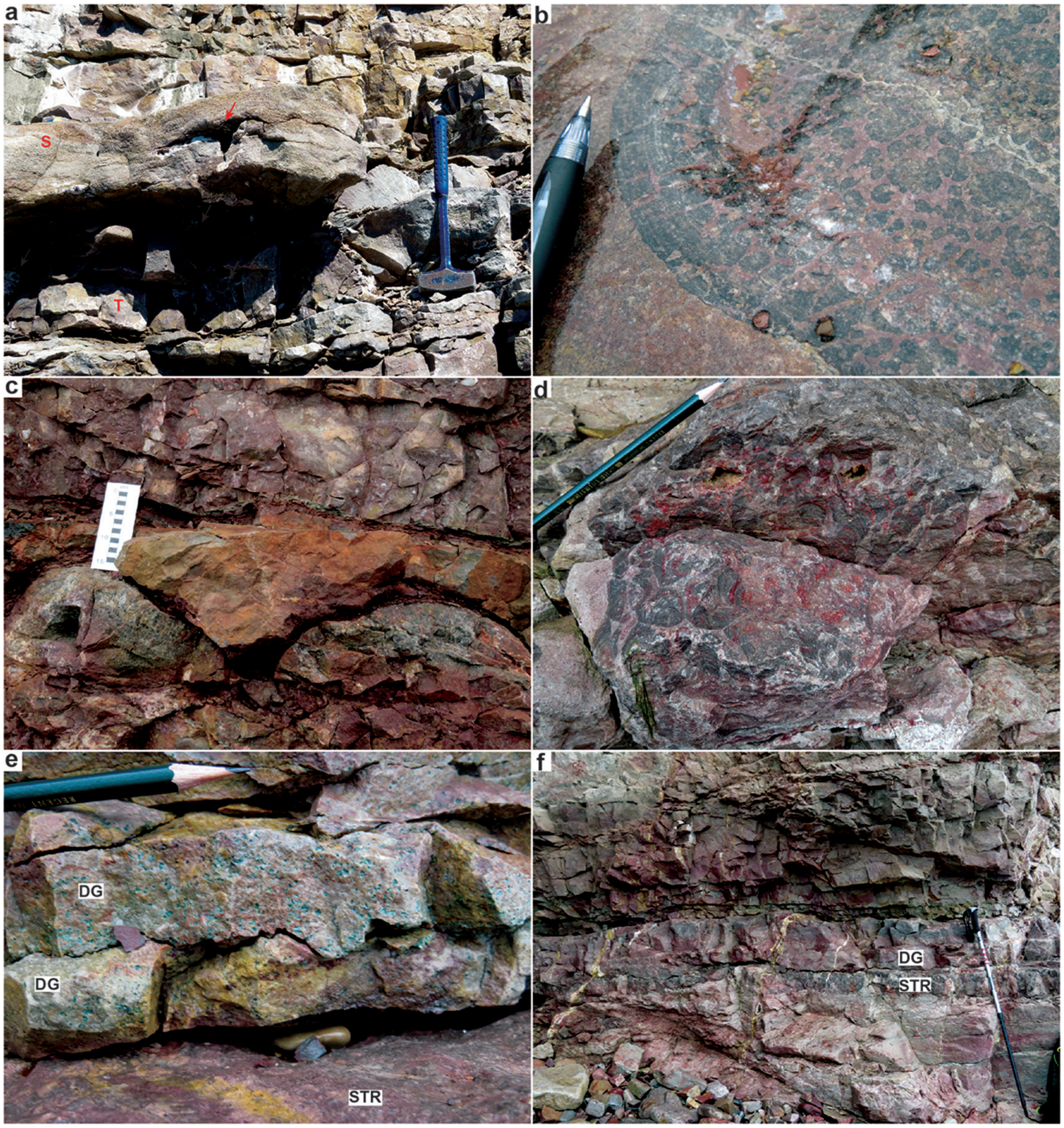

exposed Petit Jardin or Berry Head Formation section. The stratigraphic section logged in the March Point locality was 270 m thick and in the Felix Cove locality it was 40 m thick. A third outcrop was found in which the diagnostic sedimentological characteristics of the SPICE layer in the Port au Port peninsula are exhibited (West Felix Cove 48°31′51.6″N/58°47′49.1″E), but logging was not carried out at this location.

Representative layers were selected for thin sections (March Point: 45; Felix Cove: 8), carbonate $\delta^{13}C$ and $\delta^{18}O$ analyses (March Point: 41; Felix Cove: 16), and organic carbon ($\delta^{13}C_{org}$) (March Point: 14; Felix Cove: 4). Polished thin sections were prepared at the Mineral and Rock Analyses Laboratory (LAMIR) at the Universidade Federal do Paraná (UFPR) and at Petrografia BR after impregnation with blue resin for porosity identification. Petrographic analysis was performed at the Universidade Federal do Rio Grande do Sul. For carbonate identification, the thin sections were stained with a solution of alizarin red.

Carbonate stable isotope ($\delta^{13}C_{carb}$ and $\delta^{18}O_{carb}$) analysis was carried out at LAMIR/UFPR in Brazil and at the British Geological Society (BGS) in the UK. For isotope analyses, carbonate samples were collected using a micro-drill (0.5 mm diamond drill), to avoid mixing of primary and diagenetic constituents whenever possible. At LAMIR, the amount of material drilled was around 0.3 mg, whereas a larger amount of powder was required by the BGS for the analysis (10 mg). At LAMIR, the isotope ratios were determined using a GasBench II attached to a Thermo Scientific Delta Advantage continuous flow isotope ratio mass spectrometer, following the Spötl and Vennemann (2003) and Paul and Skrzypek (2007) routine with a reproducibility <0.1‰ (1σ). At BGS, isotopic analysis was carried out using a vacuum extraction technique and a VG Optima

Fig. 5. Felix cove section: (*a*) Photomicrograph of the sandstone at 22.5 m (peak Steptoean positive carbon isotope excursion (SPICE)), with quartz (Qz), crinoid bioclasts (Cr), and a few glauconite grains (G) and peloids (P), cemented by calcite (pinkish stain), with minor dolomite replacement (uncrossed polarizers). (*b*) Photomicrograph of the equivalent sandstone layer in West Felix Cove cemented by dolomite replacing calcite (pinkish stain), with minor dolomite replacement (uncrossed polarizers). March Point section: (*c* and *d*) Photomicrographs of dolomitized (D), glauconitic (G), bioclastic (Cr), peloidal grainstone at 222.6 m (peak SPICE). (*d*) Detail of the glauconite (G) glauconite peloid partially replaced by dolomite (D) in (*c*). (*e* and *f*) Photomicrographs of glauconitic (G) sandstone partially cemented by euhedral dolomite rhombs (D) at 226.5 m. [Colour online.]

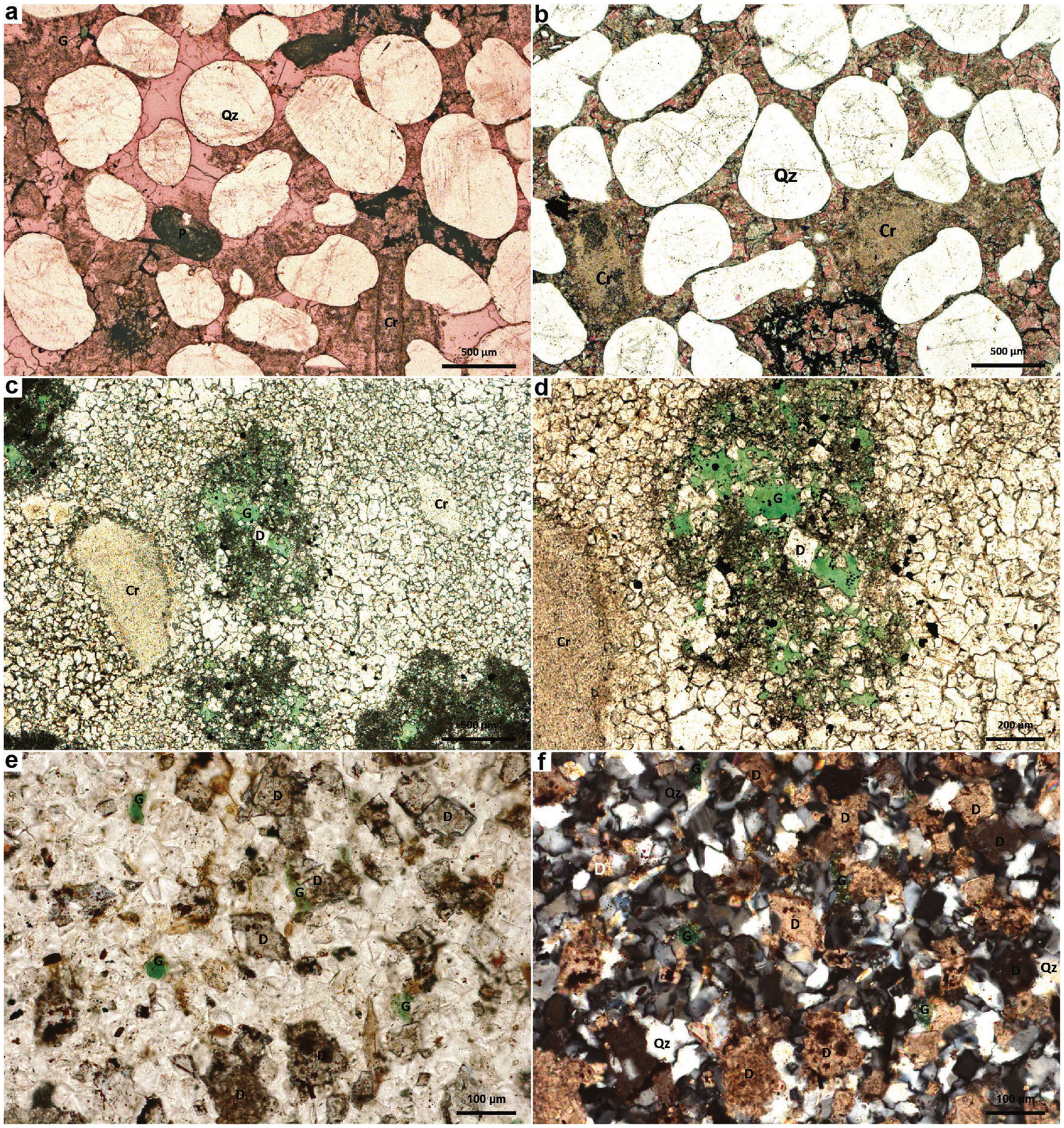

mass spectrometer with overall analytical reproducibility better than <0.1‰ (1σ) for $\delta^{13}C_{carb}$ and $\delta^{18}O_{carb}$. The main difference in the carbonate isotope methodology of the two laboratories is the time of carbonate–acid reaction. At the BGS a quick reaction at low temperature (16 °C) was performed over two hours to release CO_2 from calcite with minimal contribution from any CO_2 derived from secondary dolomite. However at LAMIR, the time taken for reaction was between one and two hours at a temperature of 72 °C. The isotope composition of samples is reported in the standard δ notation, defined as the relative difference, in parts per thousand (‰) without any further conversion. Each laboratory used its own in-house standards previously calibrated to V-PDB.

For organic carbon isotope ($\delta^{13}C_{org}$) analysis at the BGS, the samples were reacted with 5% HCl overnight to remove carbonate, and dried down at 40 °C. After being cleaned, homogenized, and dried, c. 15–25 mg of decarbonized sediment were used for determination of carbon isotope ratios using a carbon isotopic ratio Carlo Erba 1500 on-line to a VG TripleTrap (with a secondary cryo-

Table 1. Quartz grain size for March Point and Felix Cove sections.

Quartz grain size	March Point		Felix Cove		
Height, m	222.3	222.5	23	23.4	24
Average, µm	88	89	473	466	456
Maximum, µm	338	224	734	815	858
Minimum, µm	37	36	116	227	138
Median, µm	75	78	504	439	409
n	31	31	31	31	31

Fig. 6. Photomicrographs of March Point dolomitized layers. (*a*) Dolomitized grainstone at 189.5 m. (*b*) Dolomitized grainstone at 208 m with ghost of ooids (black arrows). (*c*) Dolomitized grainstone at 215.5 m. (*d*) Hybrid arenite with quartz grains (Q) replaced and cemented by dolomite (D) at 239.5 m. [Colour online.]

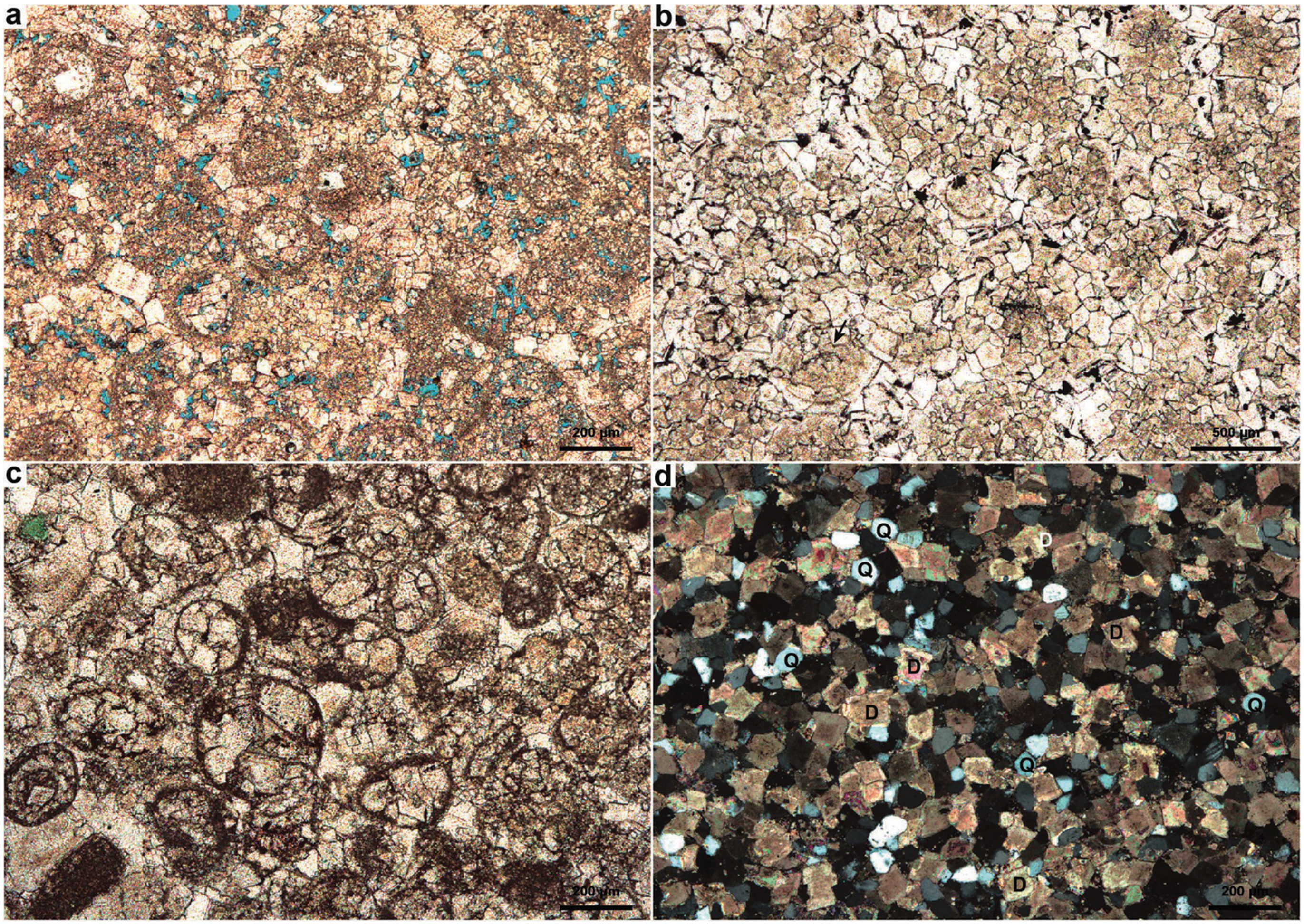

genic trap for very low carbon content samples) and Optima dual-inlet mass spectrometer. $\delta^{13}C_{org}$ values were calculated to the V-PDB scale using a within-run laboratory standard (BROC1) calibrated against NBS-19 and NBS-22. Replicate analysis of well-mixed samples embraces a precision of ±<0.1‰ (1σ).

Results

The stratigraphic interval that comprises the purported SPICE in Felix Cove (as identified by Saltzman et al. 2004; at 22.5 m, Fig. 4*a*) comprises several sets of fining-upward oolitic grainstones (20–40 cm thickness), followed by a layer of pillow-shaped thrombolite, around 25 cm thick, with a clotted center tending to a more regular shape at the edges (Fig. 4*b*). The sedimentary layers that underly the thrombolite layer contain trilobites of the *Crepicephalus* Zone (*Terranovella dorsalis* and *Crepicephalus iowensis* in the FC1 and FC2 collections of Westrop 1992). Westrop (1992) also records the occurrence of the trilobite *Dytremacephalus strictus* in the thrombolite layer itself (R. Levesque, Geological Survey of Canada, location 96635), indicating that it belongs to the *Aphelaspis* Zone (Fig. 3). These bioherms are overlain by a thin glauconitic sandstone layer (~25 cm thickness) before returning upwards to grainstones and parted limestone sets. These sets show different degrees of dolomitization, but it is still possible to identify primary constituents. Saltzman et al. (2004) note that Elvinia Zone fauna (A.R. Palmer, Institute for Cambrian Studies collection ICS-1406) were found approximately 8 m above the quartz sandstone. The trilobite data confirms the CIE as being the SPICE. A similar lithological succession is observed in West Felix Cove (Fig. 4*c*).

In the March Point section, the interval that comprises the positive carbon excursion, between 222 m and 226 m, consists of a layer of columnar stromatolites (Fig. 4*d*), around 20 cm thick, either forming as separated columns or laterally continuous mats. These are overlain by a thin dolomitized glauconitic grainstone, 20 cm thick (Fig. 4*e*). A meter-thick glauconitic, fine-grained sandstone (Fig. 4*f*) occurs 3–4 m above. Below the stromatolite layer, the oolitic grainstone sets are extensively dolomitized. No well-constrained faunal information is available for this layer.

The uncompacted bioclastic sandstone that overlies the bioherms in Felix Cove is cemented by calcite with very minor replacive dolomite (Fig. 5*a*) although in West Felix Cove the dolomite content is considerably higher, showing small relict calcite areas (pinkish stain) (Fig. 5*b*). Quartz grains are well rounded and well sorted, medium coarse – coarse sand, with 465 μm diameter average (Table 1). The glauconitic grainstone that overlies the stromatolites at March Point is extensively dolomitized (Fig. 5*c*) including the glauconite peloids (Fig. 5*d*). The glauconitic sandstone layer, 3–4 m above it, contains very poorly sorted, sub-rounded to angular silt to medium sand grains (89 μm diameter average) is also partially cemented by dolomite (Figs. 5*e* and 5*f*) and is very compacted. The sets of oolitic grainstones that underlie the potential SPICE layer in March Point are extensively dolomitized although the ooids outlines may be partially preserved (Figs. 6*a*–6*c*). For

Table 2. March point section isotopic results.

Sample description	Sample height (m)	$\delta^{13}C_{org}$ (‰)*	%C	$\delta^{13}C_{carb}$ (‰)†	$\delta^{18}O_{carb}$ (‰)†	Laboratory
Glauconitic grainstone	9.25	—	—	−0.96	−8.09	LAMIR
Grainstone	56.75	—	—	−1.79	−5.51	LAMIR
Grainstone	59.00	—	—	−1.32	−5.70	LAMIR
Grainstone	67.00	—	—	−0.41	−7.63	LAMIR
Grainstone	83.50	—	—	−1.80	−7.37	LAMIR
Grainstone	86.50	—	—	−1.26	−7.28	LAMIR
Grainstone	106.00	—	—	−2.46	−6.74	LAMIR
Grainstone	109.50	—	—	−3.84	−7.62	BGS
Grainstone interbedded with mudstone	115.25	—	—	−1.77	−6.55	LAMIR
Glauconitic grainstone	122.5	−29.2	0.2	—	—	BGS
Reddish grainstone interbedded with shale	126.00	—	—	−2.16	−8.01	LAMIR
Shale	132.50	−28.41	0.4	—	—	BGS
Shale	133	−27.9	0.3	—	—	BGS
Shale	133.50	−29.47	—	—	—	BGS
Grainstone interbedded with mudstone	136.25	—	—	−3.18	−7.38	BGS
Shale	136.5	−30.8	—	—	—	BGS
Grainstone interbedded with mudstone	137.00	—	—	−4.16	−7.57	LAMIR
Grainstone	140.25	—	—	−2.54	−8.19	LAMIR
Shale	145.00	−27.48	0.1	—	—	BGS
Glauconitic bioclastic grainstone	152.25	—	—	−1.29	−8.00	LAMIR
Glauconitic bioclastic grainstone	152.50	—	—	−0.82	−7.84	BGS
Shale	153.25	−28.71	0.1	—	—	BGS
Shale	154.25	−26.61	0.1	—	—	BGS
Shale	155.25	−27.50	0.1	—	—	BGS
Shale	157.25	−28.40	0.1	—	—	BGS
Shale	157.25	−28.70	0.1	—	—	BGS
Mudstone interbedded with shale	160.25	−26.68	0.3	—	—	BGS
Mudstone interbedded with shale	162.25	−27.07	0.1	—	—	BGS
Mudstone interbedded with shale	166.75	−26.79	0.04	—	—	BGS
Glauconitic grainstone	167.00	—	—	−0.90	−7.94	LAMIR
Glauconitic grainstone	167.50	−27.88	0.3	—	—	BGS
Glauconitic grainstone	167.75	−27.35	0.1	—	—	BGS
Mudstone	168.75	−27.82	0.3	—	—	BGS
Glauconitic grainstone	170.75	−28.01	1.9	—	—	BGS
Glauconitic grainstone interbedded with mudstone	174.00	−27.70	0.5	—	—	BGS
Glauconitic grainstone interbedded with mudstone	175.50	—	—	−1.16	−5.90	BGS
Mudstone	175.50	−27.97	0.2	—	—	BGS
Glauconitic grainstone interbedded with mudstone	176.50	—	—	−1.49	−6.72	LAMIR
Glauconitic grainstone interbedded with mudstone	176.50	−24.77	0.3	—	—	BGS
Parted limestone dolomitized	179.00	—	—	−0.84	−7.19	LAMIR
Dolomitized parted limestone	179.00	—	—	−0.82	−6.50	LAMIR
Dolomitized parted limestone	179.75	−25.67	0.4	—	—	BGS
Glauconitic grainstone	180.50	−27.36	2.1	—	—	BGS
Dolomitized oolitic grainstone	183.75	−30.02	0.2	—	—	BGS
Dolomitized oolitic grainstone	184.50	—	—	−1.72	−6.87	LAMIR
Dolomitized oolitic grainstone	189.50	—	—	−1.53	−6.56	LAMIR
Mudstone	194.00	−22.47	0.3	—	—	BGS
Dolomitized oolitic grainstone	194.25	−27.21	0.5	—	—	BGS
Dolomitized oolitic grainstone	194.75	−26.68	0.5	—	—	BGS
Dolomitized oolitic grainstone interbedded with mudstone	198.50	−28.24	0.1	—	—	BGS
Parted limestone	199.50	−28.55	0.04	—	—	BGS
Dolomitized oolitic grainstone	200.25	—	—	−1.61	−6.76	LAMIR
Dolomitized oolitic grainstone	201.50	−28.17	0.1	—	—	BGS
Dolomitized oolitic grainstone	206.00	−21.31	0.8	—	—	BGS
Dolomitized oolitic grainstone	208.00	—	—	−1.29	−6.66	LAMIR
Dolomitized oolitic grainstone	215.50	—	—	−0.68	−6.93	LAMIR
Dolomitized oolitic grainstone	218.50	—	—	−0.46	−5.27	BGS
Parted limestone	218.50	−22.55	0.5	—	—	BGS
Dolomitized oolitic grainstone	222.75	—	—	+1.13	−5.08	BGS
Dolomitized oolitic grainstone	223.60	—	—	+0.52	−4.58	BGS
Dolomitized oolitic grainstone	223.75	—	—	+0.79	−5.76	BGS
Parted limestone	224.75	−25.79	0.1	—	—	BGS
Parted limestone	225.50	—	—	−0.31	−4.75	BGS
Parted limestone	226.25	—	—	−0.18	−4.04	BGS
Parted limestone	226.25	−25.55	0.1	—	—	BGS
Parted limestone	226.75	−26.3	1.1	—	—	BGS

Table 2 (*concluded*).

Sample description	Sample height (m)	$\delta^{13}C_{org}$ (‰)*	%C	$\delta^{13}C_{carb}$ (‰)†	$\delta^{18}O_{carb}$ (‰)†	Laboratory
Glauconitic grainstone	230.00	—	—	–1.74	–7.73	BGS
Glauconitic grainstone	230.00	–26.24	—	—	—	BGS
Mudstone	230.75	—	—	–1.35	–8.18	BGS
Mudstone	231.50	—	—	–1.83	–8.47	BGS
Mudstone	233.50	—	—	–1.05	–7.95	BGS
Mudstone	235.00	—	—	–1.19	–8.08	BGS
Glauconitic grainstone	236.00	—	—	–1.73	–8.32	BGS
Glauconitic grainstone	236.00	—	—	–1.67	–8.62	BGS
Glauconitic grainstone	236.75	—	—	–2.01	–7.86	BGS
Grainstone	239.25	—	—	–1.07	–6.57	LAMIR
Grainstone	239.25	–23.05	—	—	—	BGS
Dolomitized oolitic grainstone	244.50	—	—	–1.38	–3.32	LAMIR

*Overall analytical reproducibility for $^{13}C_{org}$ (1SD): BGS – ±<0.1‰.
†Overall analytical reproducibility for ^{13}C and ^{18}O (1σ): BGS – 0.1‰; LAMIR: not determined.

Fig. 7. March Point isotope results, showing $\delta^{13}C_{org}$, $\delta^{13}C_{carb}$, and $\delta^{18}O_{carb}$ isotopic data. Dolomitized samples indicated in grey.

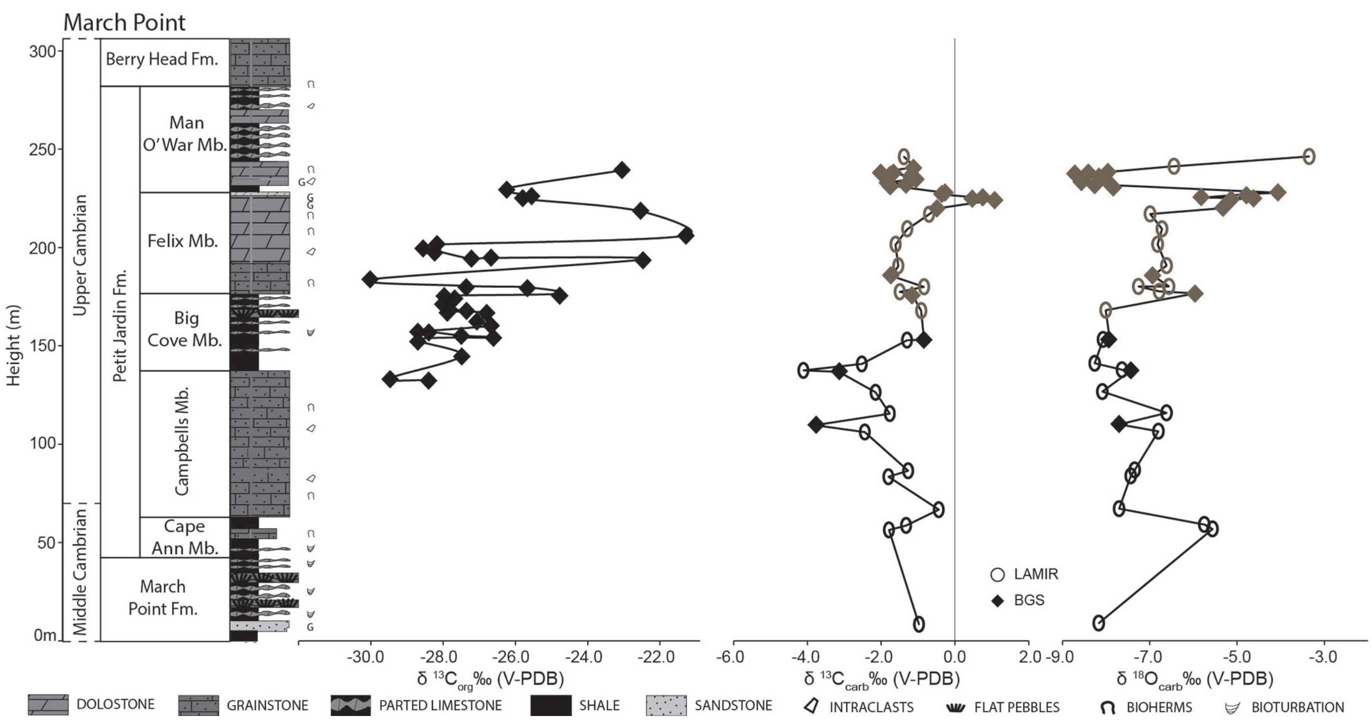

several meters above the potential SPICE layer, carbonate-clastic sandstones (composed of quartz grains and carbonate particles) occur (Fig. 6*d*), replaced by dolomite.

The isotope data ($\delta^{13}C_{carb}$, $\delta^{18}O_{carb}$, $\delta^{13}C_{org}$, and %C) analysis for the March Point section are presented in Table 2 and Fig. 7. The $\delta^{13}C_{org}$ data are relatively stable below the base of the Felix Member, with values between –29.5‰ and –24.8‰. Above this point, however, the values become more variable, between –30‰ and –21.3‰, showing a general enrichment in ^{13}C organic carbon up section, with a maximum within the Felix Member. The total organic carbon level (%C), however, is generally very low, ranging between 0.04% and 0.3%, except for layers at 170 and 180 m, with 1.9% and 2.1%, respectively. The $\delta^{13}C_{carb}$ data show significant depletion at the top of the Campbells Member (–4.1‰) and a maximum (+1.1‰) at the boundary between the Felix and Man O' War Members. Above this, the $\delta^{13}C_{carb}$ general trend is towards lower values between –2 and –1‰. In the March Point section the best defined carbonate carbon excursion occurs over a thickness of approximately 5 m (Fig. 7). The $\delta^{18}O_{carb}$ values are not directly related to the $\delta^{13}C_{carb}$ values ($r^2 = 0.21$, $n = 41$), although they show similar trends. However, $\delta^{18}O_{carb}$ becomes less variable in the Felix Member, showing a more positive peak, around –4.5‰, which coincides with the positive shift in $\delta^{13}C_{carb}$ at the boundary between the Felix Cove and Man O' War Members.

In the Felix Cove section, only part of the Petit Jardin Formation is exposed, starting within the Felix Member. The $\delta^{13}C_{carb}$, $\delta^{18}O_{carb}$, $\delta^{13}C_{org}$ and %C data are given in Table 3 and Fig. 8. Near the lowermost part of the outcrop exposed in the Felix Member, the $\delta^{13}C_{carb}$ value is around –2.0‰, reaching a high of +1.8‰ near to the transition between the Felix and Man O' War Members (Fig. 8). This section corresponds to the same interval studied by Saltzman et al. (2004). The data present a general upward increase in $\delta^{13}C_{carb}$ values (Fig. 8). Compared with $\delta^{13}C_{carb}$, the $\delta^{18}O_{carb}$ data show a relatively stable trend, as observed for the Felix Member in the March Point section, with a negative trough (though only of one data point) of –9.0‰ just before an interval of higher values that reach –5.4‰. A weak correlation between $\delta^{13}C_{carb}$ and $\delta^{18}O_{carb}$ occurs for the Felix Cove section ($r^2 = 0.57$, $n = 16$). As in the March Point section, %C is low, ranging between 0.04% and 0.17%.

Table 3. Felix Cove section isotopic results.

Sample description	Sample height (m)	$\delta^{13}C_{org}$ (‰)*	%C	$\delta^{13}C_{carb}$ (‰)†	$\delta^{18}O_{carb}$ (‰)†	Laboratory
Grainstone	1.00	—	—	−2.0	−7.3	BGS
Grainstone	6.50	—	—	−1.3	−5.9	BGS
Shale	9.00	−26.6	1.0	—	—	BGS
Grainstone	13.00	—	—	−1.2	−7.0	BGS
Grainstone	16.80	—	—	−1.2	−7.5	BGS
Shale	17.25	−26.4	0.1	—	—	BGS
Shale	17.50	−27.5	0.17	—	—	BGS
Dolomitized oolitic grainstone	19.00	—	—	−0.5	−6.5	BGS
Dolomitized oolitic grainstone	22.25	—	—	−1.1	−9.0	BGS
Dolomitized oolitic grainstone	23.40	—	—	+0.4	−5.4	BGS
Dolomitized oolitic grainstone	24.00	—	—	+0.9	−5.4	BGS
Dolomitized oolitic grainstone	24.00	—	—	+0.87	−5.55	BGS
Dolomitized oolitic grainstone	25.50	—	—	+0.8	−5.4	BGS
Dolomitized oolitic grainstone	26.00	—	—	+1.02	−5.57	BGS
Shale	26.60	−23.5	0.01	—	—	BGS
Dolomitized oolitic grainstone	27.25	—	—	+0.9	−5.7	BGS
Dolomitized oolitic grainstone	27.50	—	—	+1.59	−5.76	BGS
Dolomitized oolitic grainstone	29.75	—	—	+1.83	−5.34	BGS
Shale	30.75	−25.7	0.04	—	—	BGS
Shale	33	−25.0	0.04	—	—	BGS
Dolomitized oolitic grainstone	35.25	—	—	+1.70	−5.46	BGS
Shale	36.00	−26.1	0.19	—	—	BGS
Mudstone	36.50	—	—	+1.10	−5.30	BGS

*Overall analytical reproducibility for $^{13}C_{org}$ (1σ): BGS – ±<0.1‰.
†Overall analytical reproducibility for $^{13}C_{carb}$ and ^{18}O (1σ): BGS – 0.1‰.

Fig. 8. Felix Cove isotope results, showing $\delta^{13}C_{org}$, $\delta^{13}C_{carb}$, and $\delta^{18}O_{carb}$ isotopic data. Dolomitized samples are indicated in grey.

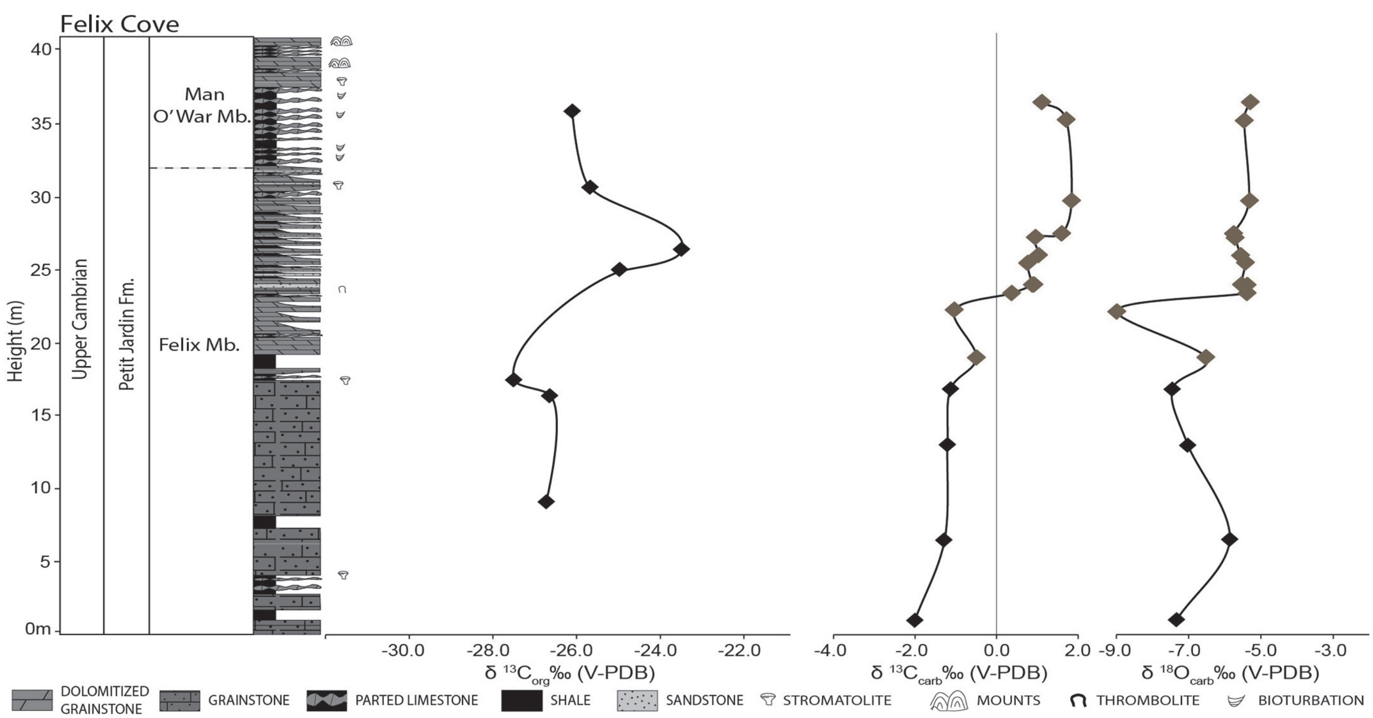

The stratigraphic thickness of the excursion upwards from 22.25 m, is about 15 m (Fig. 8).

Discussion

In the Port au Port Peninsula, particular lithologies were found to be related to the peak $\delta^{13}C$ values in outcrop. This positive $\delta^{13}C$ excursion was observed and identified by Saltzman et al. (2004) at Felix Cove and, based on trilobite data presented by Westrop (1992), identified as the SPICE. The positive $\delta^{13}C$ excursion occurs at a time when there was an influx of glauconitic quartzose sand believed to be a result of a decrease in water depth (regression). This was followed by a rise in sea level and deepening (Saltzman et al. 2004), reflected in the resumption of carbonate deposition. Detailed logging of the SPICE section at Felix Cove has shown that the positive peak is characterized by a lithological sequence of bioherms, overlain by glauconitic sand rich layers, also observed by Saltzman et al. (2004). A very similar lithological sequence has also been identified during this study approximately 0.8 km

Fig. 9. Comparison between the expression of the Steptoean positive carbon isotope excursion in the March Point (1) and Felix Cove (2) sections. The grey shaded area indicates the correlation based on the carbonate carbon signature.

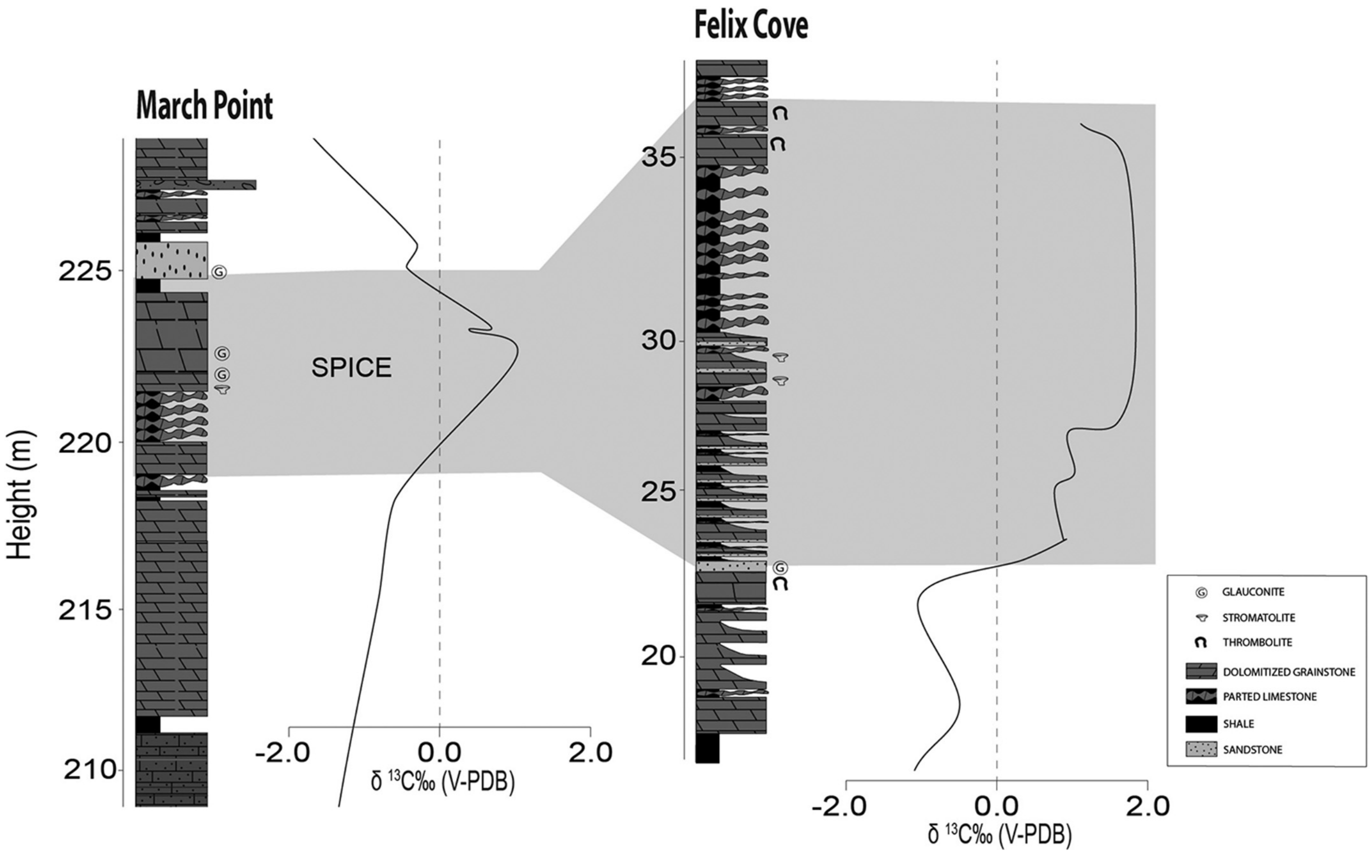

west of Felix Cove (West Felix Cove) although limited data are available.

In the March Point section (approximately 25 km further west, Fig. 2), a similar lithological sequence of bioherms and glauconitic sandstone occur in the interval and is accompanied by a positive carbon isotope excursion (Fig. 7). No biostratigraphic data are available for the upper part of the Felix Member. Westrop (1992) provided data for the underlying Big Cove Member, but this lies well below where the SPICE would be expected in that section.

Although there are similarities in the lithological sequence between these localities, there are also differences. Folk (1951) suggested that textural and compositional maturity of the sediment are products of the degree of reworking, energy, and distance of transport. The fine-grained, poorly-sorted, slightly immature sandstones at March Point (Figs. 5*e* and 5*f*, Table 1) contrast with the clean, coarse and mature sandstone observed at Felix Cove (Figs. 6*a* and 6*b*). Also, the position of the distinctive glauconitic sandstone is different. At Felix Cove it directly overlies the thombolites, whereas at March Point it occurs 3–4 mm above it. At March Point, the stromatolite is overlain by a dolomitized glauconitic grainstone prior to deposition of the glauconitic sandstone. Moreover, even though it is unlikely that the morphology of specific microbial buildups was related to particular environments, lateral differences do exist. The bioherm morphology at March Point comprises columnar stromatolites (Fig. 4*e*), whereas thrombolites are observed in this layer at Felix Cove (Figs. 4*a*–4*c*). The interval at March Point can therefore be identified as a potential SPICE locality.

The Felix Cove section indicates that the lead up to the SPICE occurred in a shallow marine environment with bioclastic grainstone shoals (e.g., echinoderms) and bioherms. The influx of coarse, well-rounded, quartz sandstone marks the base of the positive carbon excursion and start of a regression. The sandstone layer is followed by several sets of fining upward oolitic bioclastic grainstones, up to the Felix and Man O' War member transition, where parted limestone and shale become abundant. These deposits have been interpreted by Chow and James (1987*b*) as subtidal to intertidal. Comparatively, in the March Point section the positive carbon excursion (potential SPICE) occurs within a set of a glauconitic grainstones. The fine, angular, carbonate-clastic sandstone occurs a few meters above the peak of the positive $\delta^{13}C_{carb}$ excursion rather than at its beginning, near to the transition between Felix and Man O' War members. This suggests that the sandstones at the two locations are diachronous and may have been deposited in different environments with the start of the regression being slightly later at March Point than at Felix Cove.

While the SPICE interval is 200 m thick in Nevada (Saltzman et al. 1998) and 80 m in the Southern Appalachians (Glumac and Walker 1998), it is only 15 m thick in the Felix Cove section and the potential SPICE only 5 m thick in the March Point section (Fig. 9). This has already been noted by James and Stevens (1986), who found a thickness of less than 20 m, similar to our observations at Felix Cove. However we observed a much thinner interval in the March Point section. Additionally, the $\delta^{13}C_{carb}$ of the SPICE has a relatively lower magnitude than observed in other suggested localities around the world. Globally, the SPICE is described as a $\delta^{13}C_{carb}$ positive shift of around +5‰ (Saltzman et al. 2000, 2004; Kouchinsky et al. 2008; Woods et al. 2011) in carbonates. The results presented here reach a $\delta^{13}C_{carb}$ peak of about +1.13‰ for the March Point section and +2.2‰ (Saltzman et al. 2004) and +1.8‰ (this work) for the Felix Cove section, with an average shift of about +2‰, half of the typical global value. There are other locations that have lower values, for example ~+3‰ in the Southern Appalachians and South China (Fan et al. 2011).

Fig. 10. $\delta^{13}C_{org}$ and $\delta^{13}C_{carb}$ data for (A) March Point Sections and (B) Felix Cove Section. The comparison between the curves shows a peak of organic excursion a few meters below (but nearly coincident with) the peak of the carbonate carbon excursion in the March Point section, while in Felix Cove both peaks occurs at same level.

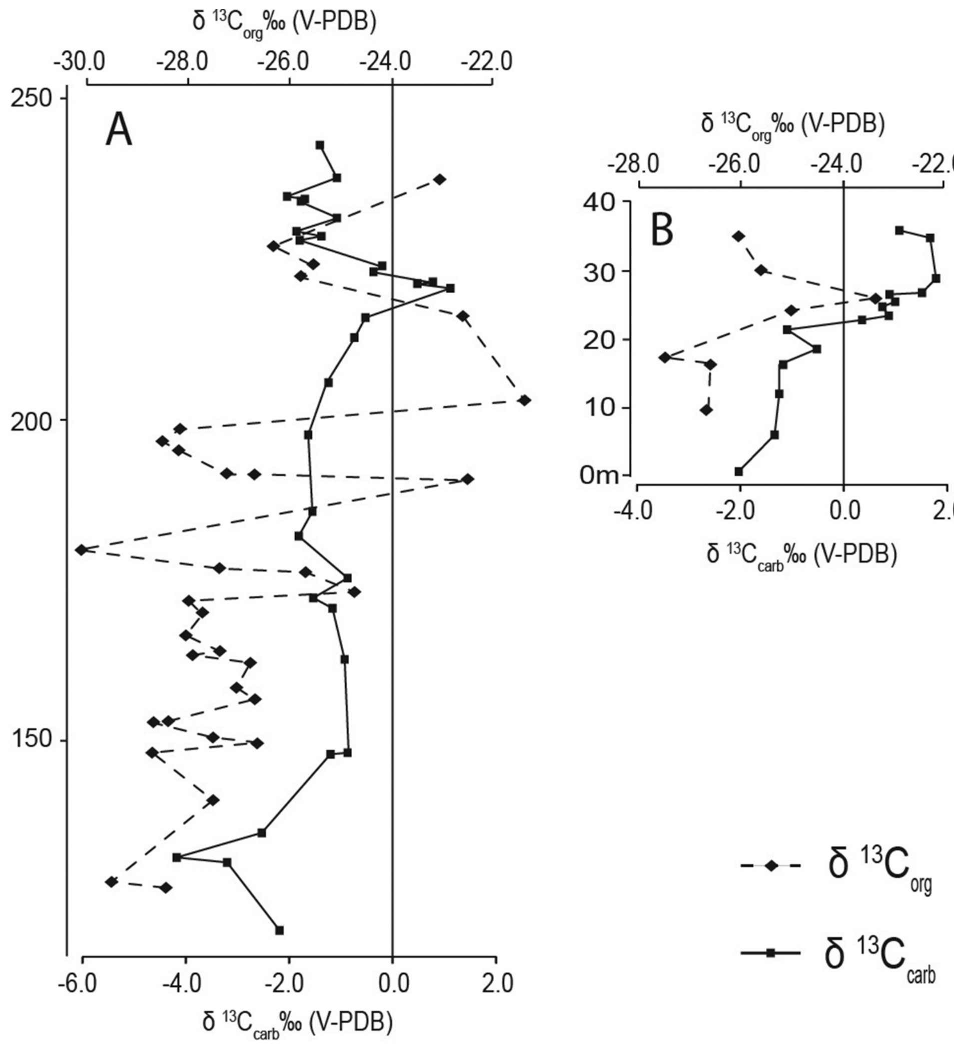

At March Point, dolomitisation is significant in the immediate lead-up to and around the potential SPICE interval, and this may have affected the isotopic results. To minimize the effect of this, the data around the potential SPICE interval itself were collected at the BGS (Fig. 7) using a quick acid reaction time. This was performed over two hours at low temperature (16 °C) to release CO_2 mainly from calcite and to minimize the contribution from dolomite. At March Point, the higher $\delta^{13}C_{carb}$ values are accompanied by an increase in $\delta^{18}O_{carb}$ (up to c. –4‰, Fig. 7). A similar pattern in $\delta^{18}O_{carb}$ values was recorded from early dolomites in the Lower–Middle Triassic Moenkopi Formation (Marenco et al. 2008). The early, relatively heavy Moenkopi Formation dolomites were contemporaneous with inner–middle shelf limestones that showed much lighter $\delta^{18}O_{carb}$ values of –9 to –6‰. The $\delta^{18}O_{carb}$ data observed here may therefore reflect a contribution from early dolomitisation that may be more likely to have retained the original carbon isotopic signature due to a lack of subsequent recrystallisation.

Considering the wider effects of diagenesis, the more negative $\delta^{18}O_{carb}$ data observed in both sections could be the result of burial and interaction with hot or meteoric diagenetic fluids (Scholle 1977; Moore 2001). Thus, the large depletion in $\delta^{18}O_{carb}$ values (down to –9‰, Figs. 7 and 8) could be interpreted as a diagenetic effect, marked by resetting of the original isotope ratios (Brand and Veizer 1980). Despite different diagenetic patterns around the SPICE and potential SPICE intervals, both sections show similar $\delta^{18}O$ values at that level (between –4.5 and –5.75‰, Figs. 7 and 8). These values are heavier than most of the samples that lie stratigraphically below or above the potential SPICE at March Point. This may suggest that the original signature has been preserved better around the SPICE and potential SPICE interval.

A positive excursion was observed in $\delta^{13}C_{org}$ data from Avalonia (Woods et al. 2011), Australia, China, and North America (Iowa) (Saltzman et al. 2011). In Newfoundland this is also observed although an offset between $\delta^{13}C_{org}$ and $\delta^{13}C_{carb}$ occurs in the March Point section and, to a lesser degree, in the Felix Cove section (Fig. 10). The isotope offset between $\delta^{13}C_{org}$ and $\delta^{13}C_{carb}$ curves has been noted previously in Queensland, Australia, and Iowa, USA, by Saltzman et al. (2011). There, $\delta^{13}C_{org}$ was found to track the $\delta^{13}C_{carb}$ curve on the rising limb, with $\delta^{13}C_{org}$ shifting back to lighter values before peak SPICE in the inorganic data. Although the pattern is clear at March Point, the reduced thickness of the Felix Member exposed at Felix Cove makes it more difficult to identify there. The highly variable trend in $\delta^{13}C_{org}$ below the potential SPICE at March Point is most likely due to the low %C values in most of the samples.

Fig. 11. Laurentia paleogeographic map (Blakey 2016), showing its evolution between 510 Ma and 485 Ma. The red square indicates the position of western Newfoundland, yellow square indicates the position of southern Appalachians (Glumac and Walker 1998), and black squares indicates the positions of other SPICE localities in the United States (Nevada, Utah, Iowa, and Minnesota) (Saltzman et al. 2004). Detail of Newfoundland (NF) paleogeography and paleolatitudes are indicated on the map. [Colour online.]

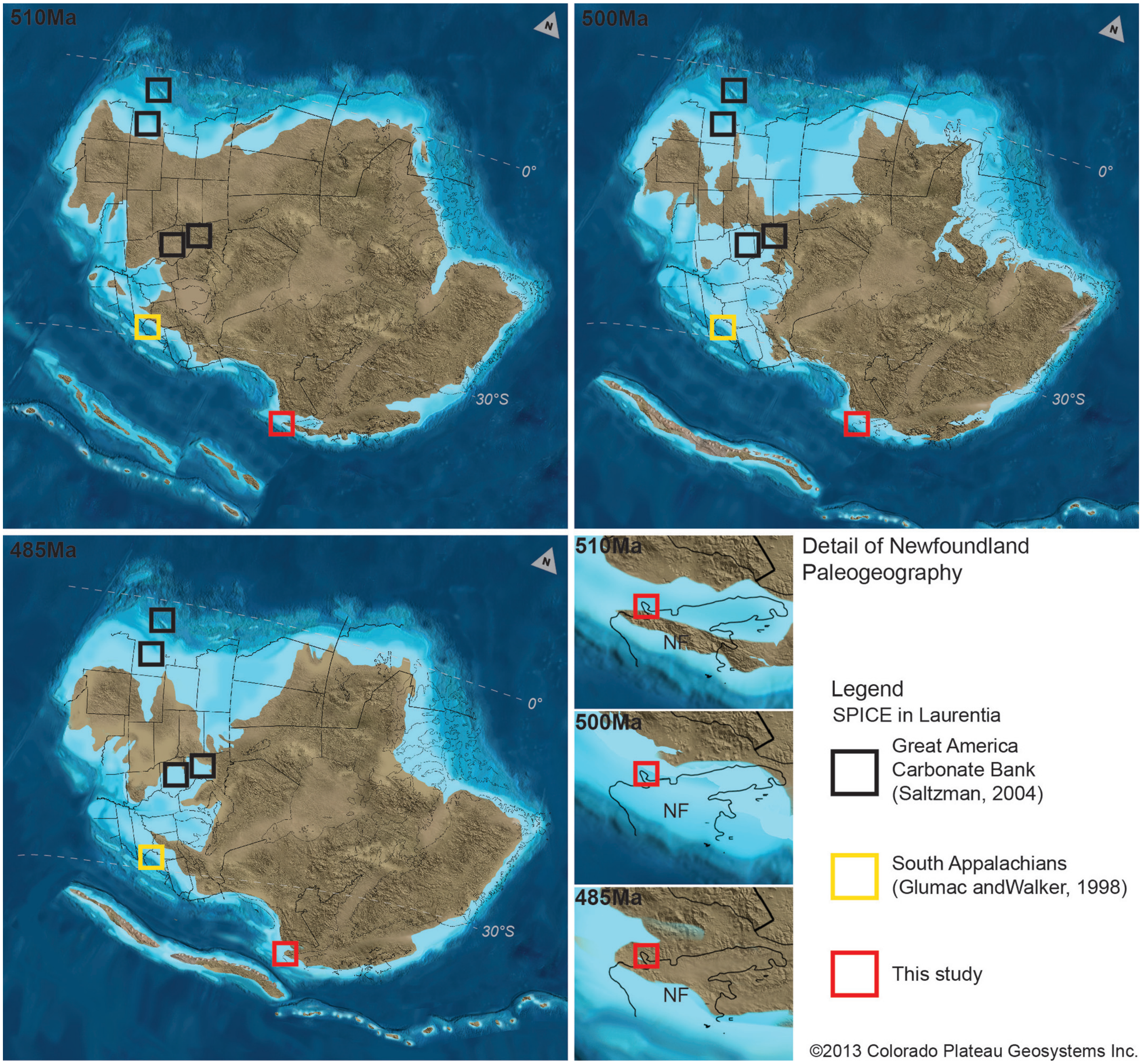

The SPICE is a global phenomenon and represents the characteristics of open ocean seawater at that time. However, as shown earlier, the Petit Jardin Formation was deposited in a more marginal marine environment (Chow and James 1987*b*) rather than open marine. Gilleaudeau and Kah (2013) showed that carbonates deposited in epicratonic seas are typically 2–4‰ lighter in $\delta^{13}C$ than those deposited in open-marine pericratonic environments. Gilleaudeau and Kah (2013) suggested that general mechanisms for this include ^{13}C-depletion due to marine upwelling, ^{13}C-depletion from terrigenous plant material (even in pre-Silurian environments from early bryophytes), or ^{13}C-depletion from in situ organic remineralisation.

Local tectonics may also have played a part in reducing the extent of the CIE. It has been suggested that local tectonics influenced the sedimentation patterns observed in the Port au Port peninsula in the inner flexural wedge of the Laurentian cratonic margin (Cowan and James 1993; Lavoie et al. 2012). Even for relatively adjacent locations such as Felix Cove and March Point (c. 25 km apart), local tectonics could have accounted for the variations in input and timing of the clastics observed related to the SPICE, and potential SPICE (Fig. 9) and could have generated local, more restricted environments. These environments would have had differences in energy (Knight and Boyce 2009) that again could have affected the geochemical signature (Gilleaudeau and Kah 2013).

As the platforms evolved due to closure of Iapetus, western Newfoundland and its surroundings, located in southern Laurentia, became progressively more restricted whereas SPICE outcrops situated on the west/northwest of Laurentia maintained open circulation (Fig. 11). Likewise, deposition in the southern Appalachians also occurred in a similar progressively restricted environment. The CIE in the southern Appalachians, like the SPICE and potential SPICE in Newfoundland, is thinner with a reduced magnitude.

The isotopic signal observed in the Petit Jardin Formation therefore, could reflect superposition of a regional and local signature onto ocean chemistry as a result of semi-restricted or restricted water circulation in the Newfoundland area due to sea level changes and closure of the Iapetus Ocean (Cowan and James 1993; Patterson and Walter 1994; Saltzman et al. 2004). Hence, despite recording a positive excursion plausibly related to the SPICE, the Petit Jardin Formation may have imparted its own isotopic signature onto the SPICE, driven by local tectonic, sedimentary and diagenetic processes.

Conclusions

Two upper Cambrian sections in the Port au Port peninsula, western Newfoundland, have been studied and compared in detail (March Point and Felix Cove). These are predominantly carbonate in lithology but contain specific sandstone horizons that occur in close proximity to bioherms. At March Point, this bioherm is of stromatolitic character and a poorly sorted glauconitic sandstone layer occurs 3–4 m above it. At Felix Cove, the bioherm is thrombolitic and directly overlain by a coarse glauconitic sandstone. The sandstones are therefore diachronous.

Carbon isotope data (from both carbonate carbon and organic carbon) show a positive excursion (at the level which marks the boundary between Sauk II and III). Saltzman et al. (2004) presented data for the section at Felix Cove that has been dated by trilobite fauna and identified as the SPICE. New data from a potential SPICE horizon at March Point is presented in this work but no biostratigraphic data are available.

The $\delta^{13}C_{carb}$ excursion presented here and by Saltzman et al. (2004) is reduced in magnitude compared with other global occurrences of the SPICE. This may be driven by local tectonic, sedimentary, and (or) diagenetic processes. A restricted environment would result in a less well-developed excursion rather than the expected global CIE due to ocean chemistry. The stratigraphic and isotope variations observed in the Port au Port peninsula associated with the SPICE suggest that local as well as global conditions were important in determining its character.

Acknowledgements

This work is a part of the Ph.D. of the first author, developed at Universidade Federal do Rio Grande do Sul (UFRGS) and University of Aberdeen (UoA). The authors gratefully acknowledge support from Shell Brasil through the “BG05: UoA-UFRGS-SWB Sedimentary Systems” project at UFRGS and the strategic importance of the support given by ANP through the R&D levy regulation. BGS and LAMIR staff are also acknowledged for assisting with stable isotope analysis. We also would like to thank Dr. Duncan McIlroy for all his help during the field work, and Dr. Marc Laflamme, Dr. Pedro Jose Marenco, and an anonymous reviewer for their help in improving the manuscript.

References

Ahlberg, P., Axheimer, N., Babcock, L.E., Eriksson, M.E., Schmitz, B., and Terfelt, F. 2009. Cambrian high-resolution biostratigraphy and carbon isotope chemostratigraphy in Scania, Sweden: first record of the SPICE and DICE excursions in Scandinavia. Lethaia, **42**: 2–16. doi:10.1111/j.1502-3931.2008.00127.x.

Arthur, M.A., Schlanger, S.O., and Jenkyns, H.C. 1987. The Cenomanian-Turonian Oceanic anoxic event, II. Palaeoceanographic controls on organic-matter production and preservation. Geological Society, London, Special Publications, **26**: 401–420. doi:10.1144/GSL.SP.1987.026.01.25.

Blakey, R. 2016. Deep time maps [online]. Available from https://deeptimemaps.com/.

Bond, D.P.G., and Grasby, S.E. 2017. On the causes of mass extinctions. Palaeogeography, Palaeoclimatology, Palaeoecology, **478**: 3–29. doi:10.1016/j.palaeo.2016.11.005.

Brand, U., and Veizer, J. 1980. Chemical diagenesis of a multicomponent carbonate system; 1, trace elements. Journal of Sedimentary Research, **50**(4): 1219–1236. doi:10.1306/212F7BB7-2B24-11D7-8648000102C1865D.

Brasier, M.D. 1993. Towards a carbon isotope stratigraphy of the Cambrian System: potential of the Great Basin succession. Geological Society, London, Special Publications, **70**: 341–350. doi:10.1144/GSL.SP.1993.070.01.22.

Brenchley, P.J., Marshall, J.D., Carden, G.A.F., Robertson, D.B.R., Long, D.G.F., Meidla, T., et al. 1994. Bathymetric and isotopic evidence for a short-lived late Ordovician glaciation in a greenhouse period. Geology, **22**: 295–298. doi:10.1130/0091-7613(1994)022<0295:BAIEFA>2.3.CO;2.

Chow, N. 1985. Sedimentology and diagenesis of Middle and Upper Cambrian platform carbonates and siliciclastics, Port au Port Peninsula, western Newfoundland. Ph.D. thesis, Memorial University of Newfoundland, St. John's, N.L. Unpublished.

Chow, N., and James, N. 1987*a*. Facies-specific, calcitic and bimineralic ooids from Middle and Upper Cambrian platform carbonates, western Newfoundland, Canada. Journal of Sedimentary Research, **57**: 907–921. doi:10.1306/212F8CA1-2B24-11D7-8648000102C1865D.

Chow, N., and James, N.P. 1987*b*. Cambrian Grand Cycles: a northern Appalachian perspective. Geological Society of America Bulletin, **98**: 418–429. doi:10.1130/0016-7606(1987)98<418:CGCANA>2.0.CO;2.

Cowan, C.A., and James, N.P. 1993. The interactions of sea-level change, terrigenous-sediment influx, and carbonate productivity as controls on Upper Cambrian Grand Cycles of western Newfoundland, Canada. Geological Society of America Bulletin, **105**: 1576–1590. doi:10.1130/0016-7606(1993)105<1576:TIOSLC>2.3.CO;2.

Derry, L.A., Kaufman, A.J., and Jacobsen, S.B. 1992. Sedimentary cycling and environmental change in the late Proterozoic: evidence from stable and radiogenic isotopes. Geochimica et Cosmochimica Acta, **56**: 1317–1329. doi:10.1016/0016-7037(92)90064-P.

Fan, R., Deng, S.H., and Zhang, X.L. 2011. Significant carbon isotope excursions in the Cambrian and their implications for global correlations. Science China Earth Sciences, **54**: 1686–1695. doi:10.1007/s11430-011-4313-z.

Folk, R.L. 1951. Stages of textural maturity in sedimentary rocks. Journal of Sedimentary Research, **21**: 127–130. doi:10.2110/jsr.21.127.

Gilleaudeau, G.J., and Kah, L.C. 2013. Carbon isotope records in a Mesoproterozoic epicratonic sea: carbon cycling in a low-oxygen world. Precambrian Research, **228**: 85–101. doi:10.1016/j.precamres.2013.01.006.

Glumac, B., and Walker, K.R. 1998. A late Cambrian positive carbon-isotope excursion in the southern Appalachians; relation to biostratigraphy, sequence stratigraphy, environments of deposition, and diagenesis. Journal of Sedimentary Research, **68**: 1212–1222. doi:10.2110/jsr.68.1212.

Gruszczyński, M., Hałas, S., Hoffman, A., and Małkowski, K. 1989. A brachiopod calcite record of the oceanic carbon and oxygen isotope shifts at the Permian/Triassic transition. Nature, **337**: 64–68. doi:10.1038/337064a0.

James, N.P., and Stevens, R.K. 1986. Stratigraphy and correlation of the cambro-ordovician Cow Head Group, western Newfoundland. Bulletin 366. Geological Survey of Canada, Ottawa. pp. 143.

Joachimski, M.M., Pancost, R.D., Freeman, K.H., Ostertag-Henning, C., and Buggisch, W. 2002. Carbon isotope geochemistry of the Frasnian-Famennian transition. Palaeogeography, Palaeoclimatology, Palaeoecology, **181**: 91–109. doi:10.1016/S0031-0182(01)00474-6.

Knight, I., and Boyce, W.D. 2009. The Reluctant Head Formation, Goose Arm Thrust Stack, Newfoundland Humber Zone: new observations on the stratigraphy, biostratigraphy and implications for the evolution of the Cambrian—Ordovician shelf. Report 09-1. Current Research, Geological Survey, Newfoundland and Labrador Department of Natural Resources, St. John's, N.L.

Kouchinsky, A., Bengtson, S., Gallet, Y., Korovnikov, I., Pavlov, V., Runnegar, B., et al. 2008. The SPICE carbon isotope excursion in Siberia: a combined study of the upper Middle Cambrian–lowermost Ordovician Kulyumbe River section, northwestern Siberian Platform. Geological Magazine, **145**: 609–622. doi:10.1017/S0016756808004913.

Lavoie, D., Desrochers, A., Dix, G., Knight, I., and Hersi, O. 2012. The great American carbonate bank in eastern Canada: an overview. *In* Great American carbonate bank: the geology and economic resources of the Cambrian-Ordovician sauk megasequence of Laurentia. American Association of Petroleum Geologists. Vol. 98, 499–523. doi:10.1306/13331504M983503.

Marenco, P.J., Corsetti, F.A., Kaufman, A.J., and Bottjer, D.J. 2008. Environmental and diagenetic variations in carbonate associated sulfate: an investigation of CAS in the Lower Triassic of the western USA. Geochimica et Cosmochimica Acta, **72**, 1570–1582. doi:10.1016/j.gca.2007.10.033.

Moore, C.H. 2001. Carbonate reservoirs: porosity, evolution and diagenesis in a sequence stratigraphic framework. Elsevier Science, New York. Vol. 55.

Neilson, J.E., Brasier, A.T., and North, C.P. 2016. Primary aragonite and high-Mg calcite in the late Cambrian (Furongian). Potential evidence from marine carbonates in Oman. Terra Nova, **28**: 306–315. doi:10.1111/ter.12222.

Palmer, A.R. 1965. Trilobites of the Late Cambrian Pterocephaliid Biomere in the Great Basin, United States. Professional Paper 243. United States Geological Survey, Reston, Va. pp. 1–105.

Palmer, A.R. 1984. The biomere problem: evolution of an idea. Journal of Paleontology, **58**: 599–611.

Palmer, A.R., and James, N.P. 1979. The Hawke Bay event: a circum-Iapetus regression near the lower middle Cambrian boundary. Memoir 2. Department of Geological Sciences, Virginia Polytechnic Institute & State University, Blacksburg, Va. pp. 15–18.

Patterson, W.P., and Walter, L.M. 1994. Depletion of 13C in seawater ΣCO2 on modern carbonate platforms: significance for the carbon isotopic record of carbonates. Geology, **22**, 885–888. doi:10.1130/0091-7613(1994)022<0885:DOCISC>2.3.CO;2.

Paul, D., and Skrzypek, G. 2007. Assessment of carbonate-phosphoric acid analytical technique performed using GasBench II in continuous flow isotope ratio mass spectrometry. International Journal of Mass Spectrometry, **262**: 180–186. doi:10.1016/j.ijms.2006.11.006.

Saltzman, M.R. 2002. Carbon and oxygen isotope stratigraphy of the Lower Mississippian (Kinderhookian–lower Osagean), western United States: implications for seawater chemistry and glaciation. Geological Society of America Bulletin, **114**, 96–108. doi:10.1130/0016-7606(2002)114<0096:CAOISO>2.0.CO;2.

Saltzman, M.R., Davidson, J.P., Holden, P., Runnegar, B., and Lohmann, K.C. 1995. Sea-level-driven changes in ocean chemistry at an Upper Cambrian\rextinction horizon. Geology, **23**: 893–896. doi:10.1130/0091-7613(1995)023<0893:SLDCIO>2.3.CO;2.

Saltzman, M.R., Runnegar, B., and Lohmann, K.C. 1998. Carbon isotope stratigraphy of upper Cambrian (Steptoean stage) sequences of the eastern Great Basin: record of a global oceanographic event. Geological Society of America Bulletin, **110**: 285–297. doi:10.1130/0016-7606(1998)110<0285:CISOUC>2.3.CO;2.

Saltzman, M.R., Ripperdan, R.L., Brasier, M.D., Lohmann, K.C., Robison, R.A., Chang, W.T., et al. 2000. A global carbon isotope excursion (SPICE) during the Late Cambrian: relation to trilobite extinctions, organic-matter burial and sea level. Palaeogeography, Palaeoclimatology, Palaeoecology, **162**: 211–223. doi:10.1016/S0031-0182(00)00128-0.

Saltzman, M.R., Cowan, C.A., Runkel, A.C., Runnegar, B., Stewart, M.C., and Palmer, A.R. 2004. The Late Cambrian SPICE (δ13C) event and the Sauk II-Sauk III regression: new evidence from Laurentian Basins in Utah, Iowa, and Newfoundland. Journal of Sedimentary Research, **74**: 366–377. doi:10.1306/120203740366.

Saltzman, M.R., Young, S.A., Kump, L.R., Gill, B.C., Lyons, T.W., and Runnegar, B. 2011. Pulse of atmospheric oxygen during the late Cambrian. Proceedings of the National Academy of Sciences, **108**: 3876–3881. doi:10.1073/pnas.1011836108.

Schidlowski, M., Golubic, S., Kimberley, M., McKirdy, D., and Trudinger, P.A. (*Editors*). 1992. Early organic evolution: implications for mineral and energy resources. Springer-Verlag, Berlin, Heidelberg. doi:10.1007/978-3-642-76884-2.

Scholle, P.A. 1977. Deposition, diagenesis, and hydrocarbon potential of deeper-water limestones. *In* Short course notes. American Association of Petroleum Geologists, Midland, Tex.

Schrag, D.P., Berner, R.A., Hoffman, P.F., and Halverson, G.P. 2002. On the initiation of a snowball Earth. Geochemistry, Geophysics, Geosystems, **3**(6): 1–21. doi:10.1029/2001GC000219.

Sepkoski, J.J., Jr. 1982. Mass extinctions in the Phanerozoic oceans: a review. *In* Geological implications of impacts of large asteroids and comets on the Earth. Geological Society of America, Boulder, Colo. Vol. 190, 283–289. doi:10.1130/SPE190-p283.

Sloss, L.L. 1963. Sequences in the cratonic interior of North America. Geological Society of America Bulletin, **74**: 93–114. doi:10.1130/0016-7606(1963)74[93:SITCIO]2.0.CO;2.

Spötl, C., and Vennemann, T.W. 2003. Continuous-flow isotope ratio mass spectrometric analysis of carbonate minerals. Rapid Communications in Mass Spectrometry, **17**: 1004–1006. doi:10.1002/rcm.1010.

Westrop, S. 1992. Upper Cambrian (Marjuman-Steptoean) trilobites from the Port au Port Group, western Newfoundland. Journal of Paleontology, **66**: 228–255. doi:10.1017/S0022336000033758.

Williams, H. 1976. Tectonic stratigraphic subdivision of the Appalachian orogen. Geological Society of America, Abstracts with Programs, **8**: 300.

Williams, H. 1979. Appalachian orogen in Canada. Canadian Journal of Earth Sciences, **16**: 792–807. doi:10.1139/e79-070.

Woods, M., Wilby, P., Leng, M., Rushton, A., and Williams, M. 2011. The Furongian (late Cambrian) Steptoean positive carbon isotope Excursion (SPICE) in Avalonia. Journal of the Geological Society, **168**: 851–862. doi:10.1144/0016-76492010-111.

ARTIGO 2

CAMBRIAN OCEAN CHEMISTRY IMPLICATIONS FROM SEDIMENTARY FACIES AND CHEMICAL STRATIGRAPHY OF THE PORT AU PORT GROUP, NEWFOUNDLAND, CANADA.

Artigo completo submetido ao periódico Sedimentary Geology.

Acknowledgement of receipt of your submitted article
1 mensagem

Sedimentary Geology <eesserver@eesmail.elsevier.com> 13 de setembro de 2019 16:53
Responder a: Sedimentary Geology <sedgeo-eo@elsevier.com>
Para: rosalia.barili@gmail.com

*** Automated email sent by the system ***

Dear %TITLE% Barili,

Your submission entitled "Cambrian ocean chemistry implications from sedimentary facies and chemical stratigraphy of the Port au Port Group, Newfoundland, Canada" has been received by Sedimentary Geology.

Your paper will be considered as belonging to the category Research Paper. Please contact us if this is not correct.

Please note that submission of an article is understood to imply that the article is original and is not being considered for publication elsewhere. Submission also implies that all authors have approved the paper for release and are in agreement with its content.

You will be able to check on the progress of your paper by logging on to https://ees.elsevier.com/sedgeo/ as Author.

Your manuscript will be given a reference number in due course.

Thank you for submitting your work to this journal.

Kind regards,

Elsevier Editorial System
Sedimentary Geology

Title: Cambrian ocean chemistry implications from sedimentary facies and chemical stratigraphy of the Port au Port Group, Newfoundland, Canada

Barili, R.*, UFRGS/PUCRS, Porto Alegre, Brasil. Rosalia.barili@gmail.com; Rosalia.cunha@pucrs.br

Neilson, J. E., University of Aberdeen, Aberdeen. J.neilson@abdn.ac.uk

Goldberg, K., Kansas State University, Manhattan, Kansas, USA. kgoldberg@ksu.edu

Carol-Ann Craig, James Hutton Institute, Aberdeen. Carol-Ann.Craig@hutton.ac.uk

De Ros, L.F, UFRGS, Porto Alegre, Brazil. lfderos@inf.ufrgs.br

*Corresponding author

Abstract

The Port au Port Group, western Newfoundland, is a shallow marine record from the outer part of a stable carbonate platform that surrounded the Iapetus Ocean, and marks the gradual transition from siliciclastic deposition in underlying Hawke Bay Formation to carbonate sedimentation up to the lower Ordovician. Shallowing-upward 'Grand Cycles' consist of subtidal deposits in the lower hybrid half-cycle (heterolite, shale, mudstone and subordinate wackestone) and a upper carbonate half-cycle (oolitic grainstones, packstones and laminated carbonates) resulting from vertical and lateral accretion of subtidal, intertidal and supratidal deposits.The Port au Port Group has a well-known stratigraphy framework, however there is a lack of chemostratigraphy data. In this study, we integrate stratigraphy and stable isotopic data to unpublished $^{87}Sr/^{86}Sr$ and XRF results. The previous dissecation cracks are now interpreted as syneresis cracks, and the lack of exposure features associated to marine fauna evidences prevailing subtidal conditions when before interpreted as intertidal environment. The occurrence of SPICE in Port au Port Group has lower magnitude and thickness than expected for the global measured excursion and, although a subtidal environment, this local superimposed signature may reflects a shallower shelf position, which is similar to the SPICE observed for shallower portion of Amadeus Basin/Australia. The chemostratigraphic data reveals Mn/Sr ratios > 2 for Felix Cove section (0.53-17) and March Point section (0.38-33.31), corroborating the extensive diagenetic influence. However, the $^{87}Sr/^{86}Sr$ results are the expected range to Middle/Upper Cambrian (~0.7093-0.7095), with exception of those related to the SPICE (~0.7089), and therefore related to the regression event, which exposed older carbonate Cambrian rocks.

Keywords: SPICE, CHEMOSTRATIGRAPHY, CAMBRIAN, PORT AU PORT GROUP

1. Introduction

The first studies of the Port au Port Group (PAP), Western Newfoundland, date back to 1861-1863, published by Logan (1863). According to Chow (1985), these studies integrated the stratigraphic data from Schuchert and Dunbar (1934), who first proposed the March Point Formation as an Upper Cambrian sequence. Several studies succeeded, improving little by little the knowledge regarding sedimentology and biostratigraphy. Chow (1985), integrating the sedimentology, stratigraphy and diagenesis of the Port au Port Group, is one of the most complete studies to date and also the first to integrate stratigraphic and stable isotope data in the area. This paper presents a new detailed sedimentary study of the March Point section (the most complete section through the Petit Jardin Formation of the Port au Port Group) and a detailed sedimentary analysis of the Felix Cove section. The addition of stable isotope, Sr-isotope and X-ray fluorescence data allowed the construction of a detailed chemical stratigraphy for the Upper Cambrian in Newfoundland.

Previous studies by Saltzman et al (2004) showed that the Steptoean Positive Carbon Isotope Excursion (SPICE) that is coeval with a trilobite mass extinction horizon (Bond and Grasby, 2017; Palmer, 1965; Saltzman et al., 2000, 1998, 1995; Sepkoski, 1982; Yochelson, 2010), is present in the Petit Jardin Formation at the Felix Cove location. This has been confirmed during this study and a further new locality of the SPICE identified (Barili et al., 2018).

The Cambrian is a key time in the evolution of life on the planet with two major extinctions of marine faunas occurring during that time, the second of which coincides with the SPICE relating to rapid ocean changes (Zhuravlev and Wood, 2018). It is therefore essential to understand the stratigraphy and oceanic conditions at that time. Although there is a well-developed stratigraphic framework and biostratigraphic control proposed by several authors (e.g. Chow, 1985; Chow & James, 1987a; Cowan & James, 1993), the unpublished data presented here help to elucidate the environmental conditions at the time in the carbonate shelf surrounding Laurentia.

2. Geological setting

The study area is located on the southern coast of the Port au Port Peninsula, western Newfoundland (Figure 1). The SPICE was identified at Felix Cove (48°31’49.2”N / 58°47’12”E), a section previously studied by Saltzman et al. (2004)

and another potential SPICE locality was identified at March Point (48°30'42.1"N / 59°05'31.1"E).

The Port au Port Group forms part of the autochthonous Cambrian-Ordovician sequence of the tectono-stratigraphic Humber zone of the northern Appalachian orogeny (Williams, 1976, 1979). It is interpreted as shallow-marine deposits from the outer part of a stable carbonate platform that surrounded the Iapetus Ocean (Palmer and James, 1979; Williams, 1979, 1976). These mixed carbonate-siliciclastic deposits record the gradual transition from Early Cambrian siliciclastic deposition to predominantly carbonate sedimentation in the Early Ordovician (Chow, 1985; Chow & James, 1987b; Cowan & James, 1993). The Group is composed of three formations, namely the March Point, Petit Jardin (Cape Ann, Campbells, Big Cove, Felix and Man O' War Members) and Berry Head Formations.

Transgressive-regressive Grand Cycles are identified through the Port au Port Group (Chow, 1985; Chow & James, 1987a, 1987b). The marine transgression at the beginning of the Grand Cycles resulted in a shallow subtidal-intertidal environment, where relatively muddy carbonates were deposited (shaley packages and parted limestone; Chow and James 1987b). These deposits pass upwards into more open marine oolitic shoals, probably deposited near the platform edge (carbonate packages; Chow and James 1987a). As sea level dropped at the top of the cycles, the environment returned to more restricted water circulation, although extensive evidence of subaerial exposure is absent (Chow, 1985; Chow and James, 1987a). Carbon isotope data, previously collected in the Port au Port Group at Felix Cove, show a strong positive $\delta^{13}C_{carb}$ excursion between the Felix and Man O' War Members (top of cycle B, Figure 2), which has been interpreted as the SPICE (Barili et al., 2018; Saltzman et al., 2004).

3. Methods

3.1. Sedimentogical logs and petrography

The fieldwork was performed along two main outcrops on the Port au Port Peninsula – March Point and Felix Cove. Detailed sedimentological logging on a cm scale (1:50) and systematic sampling was carried out at 1m resolution, from the base of accessible units in the Petit Jardin Formation to the top of each exposed Petit Jardin or Berry Head Formation section. The stratigraphic section logged in the March Point locality (MP) was 270m thick, and in the Felix Cove locality (FC), 40m thick.

Representative layers were selected for thin section preparation (March Point: 45; Felix Cove: 8). Polished thin sections were prepared at the Mineral and Rock Analyses Laboratory (LAMIR) of the Universidade Federal do Paraná (UFPR) and at Petrografia BR, after impregnation with blue resin for porosity identification. Petrographic analysis was performed at the Universidade Federal do Rio Grande do Sul (UFRGS) and University of Aberdeen (UoA). For identification of the carbonate minerals, the thin sections were stained with a solution of alizarin red and potassium ferrocyanide (Dickson, 1966) at UFRGS.

3.2. pXRF analysis

Bulk crushed samples were analyzed for their bulk elemental composition using an Olympus InnovX portable XRF instrument and innovX software at the University of Aberdeen. A total of 40 samples from the March Point section and 20 from Felix Cove section were analyzed. An average was calculated after each sample was run twice through the geochemistry mode. The instrument was calibrated at the beginning of each run using a steel calibration check disc, with standards and a SiO_2 blank supplied by Olympus. The XRF data was further calibrated using an in-house sample database (40 Precambrian shales) analyzed by both pXRF and ICP-MS (D. Kemp *pers.comm.*). The standard deviation for the elemental analysis was: Mg (18.44%), Al (4.46%), Si (3.89%), Ca (2.05%) and Sr (0.77%).

3.3. Strontium Ratios

The sample preparation, digestion and analytical procedures followed the James Hutton Institute (Aberdeen, UK) approach. Bulk samples crushed to a fine powder, were washed multiple times in deionized water to remove residual salts. The powder was then digested in 5 ml of 0.5M trace grade HCl and centrifuged to remove any remaining undigested material. The supernatant was dried out under hot lamps. The strontium was isolated by cation exchange chromatography and the isotopic composition determined by thermal ionization mass spectrometry using a VG Sector 54 TIMS.

4. Results

4.1. Sedimentology

Detailed sedimentary description of the studied outcrop sections allowed the identification of 8 facies for the Port au Port Group (**Error! Reference source not found.**). These facies were grouped in four facies associations (F.A) formed in a tide-dominated shelf, comprising subtidal, shallow subtidal, shallow subtidal to intertidal transition, and shoreface facies associations.

4.1.1. Subtidal F.A.

The Subtidal F.A. is composed of facies Sh, M, G, M/W, HS, FPC and Ht. Ht is interbedded with HS and Sh, predominantly in the lower March Point Formation, and with Sh and G in the other units. Due to the variable thickness of the interbedded layers, some beds were named according to specific facies (M/W or Sh), rather than heterolites, where parting layers were thicker than 0.10 m.

Sh may occur as thick beds (up to 3 m), or as partings within M/W and G. Sh has more expressive intervals in the March Point Formation and Big Cove Member, the latter with occasional G and FPC layers. HS may also alternate with Sh and M, mostly in the lower March Point, but also with occasional layers interbedded with G in the Campbells Member of the Petit Jardin Formation.

The dominance of fine-grained facies indicates predominantly low-energy conditions, with settling from suspension below fair-weather wave base. Periodic increase in the energy levels, probably related to tidal processes and/or storm waves, are marked by the occurrence of HS, G and FPC. Marine biota and glauconite peloids points to a seaward shoal position and rip-up clasts formed by storm action suggests the early formation of hardgrounds, associated with low depositional rates in deeper water.

4.1.2. Shallow subtidal oolitic shoal F.A.

The Shallow subtidal oolitic shoal F.A. comprises facies G, B, Sh, Ht, FPC. Oolitic and bioclastic G are interbedded with minor Ht and Sh, and laterally associated with B. The boundstones locally use FPC as a substrate. Thicker and predominantly oolitic G and B intervals occur in the Campbells Member, where these facies are interbedded with minor bioturbated Ht and Sh, the latter progressively thicker when transitioning into the Big Cove members.

The dominance of high-energy facies in this facies association represents the transition from a seaward, subtidal into a shallow subtidal oolitic shoal. The interbedding with Ht and Sh suggest a mobile shoal fringe. Thick oolitic G layers with herringbone cross stratification evidence a well-developed oolitic shoal under tidal influence. A shallower position in the depositional environment is also attested by the development of B.

4.1.3. Shallow subtidal to intertidal F.A.

The Shallow subtidal to intertidal F.A. includes facies B, G, Ht, FPC, mostly B laterally associated with oolitic G, minor Ht and occasional FPC. The lack of marine biota and the dominance of boundstones reflect the existence of a protected, shallow area without grazing biota that allowed the development of stromatolites and thrombolites. The depositional position was likely in the shoal leeward, within the tidal range, with no clear transition between shallow subtidal oolitic shoals and intertidal areas.

4.1.4. Shoreface F.A.

This facies association includes only facies S, which occurs exclusively in this F.A. It overlies the SPICE-related thrombolite deposits in Felix Cove, but it is not present in the coeval layer in March Point. This sandstone layer has been interpreted by Saltzman (2004) as shoreface deposits resting on a subtidal/intertidal microbial layer due to a regressive event.

In order to help the visualization of facies distribution, the sedimentary were divided accord the PAP units (Chow, 1985) observed in the field sections.

4.2. March Point Section

March Point Formation

The March Point Formation shows into two different trends within the subtidal facies association (Figure 3). Between 0 and 11m, the main facies comprises glauconitic, bioclastic (trilobites, brachiopods and echinoderms, mostly crinoids) HS (Figure 4), interbedded with Ht with variable degree of bioturbation, frequent syneresis cracks and occasional microbial mats. The facies of the upper half comprises Ht and FPC within 0.5 to 1.0 meter cycles, between 11 and 43m, with abrupt facies transition related to an oolitic G mobile fringe. At the very top (39.5 m to 40.25 m), this formation is composed of partially dolomitized oolitic grainstones and thrombolites with thicker shale layers (>0.5m).

Cape Ann Member

The Cape Ann Member (43 m to 53.25 m; Figure 5) comprises the subtidal facies associations, being also associated with a mobile fringe. The Sh facies is predominant in this unit, with several sets, up to 1m thick, interbedded with oolitic G. The grainstones show partial dolomitization and display relic porosity filled by dolomite. Despite the variable degrees of bioturbation in the shaley layers, in thin sections bioclasts are absent in the oolitic grainstone.

Campbells Member

Sedimentary logs of lower and upper Campbells Member are presented in Figure 6 and Figure 7 representing the transition between shallow subtidal oolitic shoal and subtidal to intertidal, with at least two repetitions of each facies association. The lower Campbells Mbr (53.25 m to 100.75 m) comprises several sets of oolitic G interbedded with minor Ht and Sh with abrupt facies transition between, forming the shallow subtidal oolitic shoal facies association (Figure 6). Occasional glauconite and bioclasts are observed and the finer-grained levels are bioturbated.

The upper Campbells Mbr (100.75 m to 138.5 m) is dominated by oolitic G, interbedded with Sh and bioturbated Ht with recurrent syneresis cracks and frequent B using FPC as a substrate (Figure 7). In this part of the Cambells Mbr, passes into a shallow subtidal oolitic shoal F.A., overlain by another subtidal to intertidal F.A. before transitioning to the Big Cove Member. In thin sections, fibrous fringes and oomoldic porosity, in part filled by dolomite, are frequent (Figure 8A). Decametric HS incursions are observed between 119 m and 138.5m, comprising fine to very fine angular quartz grains layers, mud intraclasts as pseudomatrix and ooids (Figure 8D).

Big Cove Member

The transition between the Campbells and Big Cove members is marked the occurrence of large thrombolite in B/G facies (Figure 9) that transitions into a glauconitic-bioclastic HS (Figure 10), followed abruptly by a thick Sh/Ht layer. The Big Cove Member comprises Ht interbedded with Sh, forming in the subtidal facies association (Figure 9). Occasional layers of FPC, oolitic G and bioclastic-glauconitic HS, without any apparent stacking pattern, are observed throughout the unit.

Felix Member

The Felix member (179.25m to 222.5m, Figure 11) comprises thick layers of dolostones and dolomitized G (Figure 11 and Figure 12), interbedded with Ht and Sh. Herringbone and low-angle cross stratification are frequent, with layers of B/G being more common above the unit top half. Occasional bioclasts (trilobite and echinoderm fragments), with glauconite marks the transition to Man of War Member, at the base of which is marked by the SPICE excursion.

Man O' War Member

The Man O' War Mbr. (222.25m to 249.25m, Figure 13) comprises a subtidal facies association, formed by the interbedding of dolomitized G (Figure 14A and B), Ht and Sh. A layer of glauconitic HS is observed near to the lower boundary, between 225.25 and 225.50m. B facies is frequent and generally associated with Ht layers that, in this unit and above, also includes decametric layers of grainstone interbedded with Sh and W/M.

Berry Head Formation

The Berry Head Fm. (249 m to >270m, Figure 15) comprises thin bedded dolostones (Figure 14C and D) /oolitic G and Ht and very minor Sh forming to the Shallow subtidal oolitic shoal F.A. Well-developed but extensively dolomitized stromatolites occur throughout the formation within B/G facies. The upper boundary of this unit was not reached during the field work.

4.3. Felix Cove Section

The Felix Cove section comprises a smaller portion of PAP, including Felix and Man O'War members (Figure 16). In this section, despite dolomitization is also present, the sedimentary structures are better preserved that at the March Point Section. The Felix Member comprises oolitic G interbedded with minor Ht and Sh. At the transition with the Man O'War member (19 m to 27 m), several finning upward cycles, ranging between 0.5 and 1 m thick are present. Occasionally, the basal contact of these cycles is marked by FPC. The actual base of the Felix Mb is not exposed but a an erosive contact between the bottom shaley/muddy layer and the oolitic G above is observed. The limit between Felix and Man O'War Members is the SPICE layer, with the peak excursion marked between 22 and 23m in the studied section, coinciding with the only occurrence of S facies covers a thrombolite (B) layer.

4.4. Chemical composition from X-Ray Fluorescence

The standard deviation for Mg measured is very high (18.44%), whereas the standard deviation for Ca is 2.05%. Therefore, at least for the carbonate layers of the PAP, the Ca value is a better indicator of the degree of dolomitization. Calcite has a molecular weight of 100, the elemental percentage of Ca in calcite being 40%. Dolomite has a molecular weight of 184, the elemental percentage of Ca in dolomite being 22%. The pXRF Ca elemental % therefore gives a reliable indication of the degree of dolomitization that the samples have undergone.

Based on this, in the March Point section, the dolomitization was significant in the upper part of the Petit Jardin Fm (e.g. Felix and Man o' War Members - Ca c. 20%), while it was only partial at Felix Cove, with Ca ranging between 20-40% (*Figure 17 and Figure 18*). These data are corroborated by the petrographic characterization, which indicates more intense dolomitization in the Felix Mbr. in the March Point section. Regarding major and trace elements ratios, Mn/Sr present elevated values, ranging between 0.67 and 29.12 for March point and 0.53 and 17 for Felix Cove. Mg/Ca ratios shown lower ratios (<0.5) in the lower half of March Point section and higher values from Felix member and above, being little variable within these trends. The Sr/Ca is below 0.0001 for all samples in both sections, and hence not displayed in Figures 17 and 18.

High levels of Al and Si in the pXRF data also can be correlated with glauconitic hybrid arenites, sandstones or shales. In general, hybrid sandstones occur at the tops of the grand cycles (Figure 2), where the grains include very fine to fine-sized, angular, quartz and feldspar. A well sorted, rounded, medium to coarse, massive quartz sandstone is only found at the top of Grand Cycle B at Felix Cove section, which is coeval with the SPICE (Figure 16). The main Si peak in March Point is found at 223.6 m (Figure 17), a meter above the SPICE in a thick dolomitized, glauconitic, very fine peloidal dolomitized grainstone with angular quartz grains. Glauconite is most abundant in the lower half of the March Point Formation, where it occurs associated with bioclastic grainstones and hybrid limestones, with occasional biotite feldspar. In these layers, the Si and Al contents are higher, but the Mg is less than 5%, while the Ca is generally greater than 20%.

In the Felix Cove section, a similar pattern is observed. Higher Si and Al occur near to the SPICE layer, which is coeval with the sandstone layer. The amount of Ca ranges between 20 and 40%, but the Mg content is more variable, ranging between 0 and 25%. The Sr is generally lower than 200ppm, but can reach up to 500ppm. As in the March Point section, the higher Si is found close to the SPICE at 23.4m (Figure 18). However, here this layer is composed of a medium to coarse sandstone that directly overlies the SPICE level.

4.3 Stable isotopes

The March Point section shows significant depletion in $\delta^{13}C$ at the top of the Campbells Member (–4.1‰), with a maximum (+1.1‰) at the boundary between the Felix and Man O' War Members (Figure 19). Above this interval, values return to –2 and –1‰. The isotope carbon excursion is detected across a thickness of ~5 m. $\delta^{18}O$ and $\delta^{13}C$values show similar trends but are not directly related. However, $\delta^{18}O$ is less variable in the Felix Member, showing a more positive peak, around –4.5‰, which coincides with the positive shift in $\delta^{13}C$ at the boundary between the Felix Cove and Man O' War Members

At Felix Cove section, Barili *et al.* (2018) data indicated that the $\delta^{13}C$ values range from –2.0‰, reaching +1.8‰ near the transition between the Felix and Man O' War Members (*Figure 20*), which corresponds to the same interval studied by Saltzman et al. (2004). The $\delta^{18}O$ values show a relatively stable trend, as observed at the March Point section, with a negative trough of –9.0‰ just before an interval of higher values reaching –5.4‰, with a weak correlation between $\delta^{13}C$ and $\delta^{18}O$. The stratigraphic thickness of the positive carbon excursion is about 15 m.

4.4 Sr isotopes

Bulk Sr-isotopes were collected throughout the Petit Jardin Formation at the March Point section. $^{87}Sr/^{86}Sr$ values are mostly in the range 0.7092 to 0.7096 (Figure 19). However, through the Felix Member, the values decrease towards a minimum of 0.7089 at the SPICE and then increase towards typical values of 0.7093 at the top of the Petit Jardin Formation. For the Felix Cove section, $^{87}Sr/^{86}Sr$ values display a similar behavior, ranging from 0.7089 to 0.7095, with lower values in the SPICE layer (Figure 20).

5. Discussion

5.1 Sedimentology

The PAP was divided the into a series of relative transgressive-regressive sequences generated by the rate of relative sea-level rise during the Upper Cambrian. These variations were used by Chow (1985) and Chow and James (1987a; 1987b) to separate the group units. Each Grand Cycle in the PAP. The depositional environment proposed encompasses a shallow subtidal-intertidal environment, where relatively muddy carbonates were deposited (‘shaley packages and parted limestone’; Chow & James, 1987a). These deposits were interpreted as passing upwards into more open marine oolitic shoals, probably deposited near the platform edge (‘carbonate packages’; Chow and James, 1987b). As the accommodation space that was generated by the relatively rapid sea-level rise was filled at the top of the cycles, the environment returned to a situation with more restricted water circulation situation, although extensive evidence of subaerial exposure at the top of cycle B is absent (Chow and James, 1987a). The Grand Cycles in observed in Newfoundland are coeval with the Laurentian Great American Banks Grand Cycles (Lavoie et al., 2012). Cowan and James (1993) however reinterpreted the PAP as being subtidal and composed of stacked shelf cycles. They renamed the half-cycles of Chow and James (1987a) as being ribbon (previously ‘shaley’) and oolitic (previously “carbonate”) packages.

Lower Half cycles

The March Point Formation, and the Big Cove and Man O’ War Members of the Petit Jardin Formation are characterized by frequent intercalations of heterolite (ribbon to parted limestones), shales and flat pebble conglomerates. They also contain marine bioclasts, glauconite and quartz-rich layers. The main facies association in these units is the the subtidal F.A. (Figure 3, Figure 9 and Figure 13).

Chow and James (1987a) suggested that these cycles were deposited in inter to subtidal environments. However, the presence of marine bioclasts (trilobites, echinoderms and brachiopods) in these units suggests relatively open marine conditions that support the subtidal interpretation by Cowan and James (1993).

Glauconite is also often found in these horizons, mainly in the lower part of the March Point Formation and in coarser layers within the Big Cove Member. However, glauconite is also found in the upper Cambells Member (Figure 7) and in the Felix Member above the SPICE (Figure 11).

Glauconite is also often found in these horizons, mainly in the lower part of the March Point Formation (Figure 4) and in coarse layers within the Big Cove Member (Figure 9). Glauconite is also found in the upper Campbells Member (Figure 7) and in the Felix Member above the SPICE (Figure 11). In modern marine environments, glauconite is forming in relatively deep water at platform edge, where sedimentation rates are low. However, in the Cambrian it was also abundant in shallow marine waters (Peters and Gaines, 2012). Peter and Gaines (2012) suggest that the more extensive formation of glauconite in the Cambrian was due to unusually high levels of K^{+}, Fe^{3+} and $H_3SiO_4^{-}$ flushed into shelf waters as a result of erosion the hinterland along the Precambrian-Cambrian ‘Great Unconformity’. The recurrence of glauconite during the Cambrian may be therefore indicated a subtidal environment.

As evidence of intertidal conditions in the shaley half-cycles, Chow (1985) and Chow & James (1992) pointed to the occurrence of desiccation cracks, mainly in the lower half cycles. However, our observations, at least for the March Point Formation, suggest that these are actually syneresis cracks. These features occur near to the glauconite and bioclast rich layers with entire (unbroken) brachiopod shells, reflecting a low-energy, subaqueous environment. In the PAP, mud cracks that display a linear shape in a plane view or V or septarian shape in vertical cross section (Figure 21) are frequent. They are occasionally filled by ooids and bioclasts, suggesting accumulation in a subtidal environment, seaward towards a shoal position.

Often misinterpreted as desiccation cracks, syneresis cracks are related to subaqueous shrinkage due to salinity changes (Pratt, 1998). Subaqueous sedimentary cracks can also be formed due to other processes. McMahon *et al.* (2017) indicated a series of processes, commonly related to heterolithic carbonates, including, among others, loading and wave stress. The shape of these cracks include polygonal networks, isolated linear cracks or curlicue cracks in the upper bed, and V or U-shaped linear morphology or anastomosing (spindle or cuspate) shape in vertical cross sections. These features may be filled by the associated sediments or even spar cement (McMahon et al., 2017). Cowan and James (1993) concluded that the cracks were subtidal 'diastasis' cracks.

Hardgrounds were described by Chow (1985) and Chow & James (1992). These may indicate an early lithification process associated to interruption of sedimentation. In the PAP, Chow (1985) noted hardgrounds associated with mudstones in the parted limestones. They were pervasively mineralized and overlain by glauconitic and phosphatic layers, fand interpreted as the product of sea-floor cementation under low-energy, intermittent sedimentation. The frequent intraclasts reworked from PAP hardgrounds are interpreted as storm deposits, and described as flat pebble conglomerate. The latter indicates early lithification of shallow subtidal sediments. Unidirectional orientation and wave ripples are common in these conditions and also related to flat pebble generation (Pratt, 2010). These layers are frequent in the upper half of the March Point Formation, and in the Big Cove and Man o' War Members and suggest deposition in a subtidal environment. In the lower half, shaley cycles therefore, there is significant evidence of deposition in a subtidal environment as suggested by Cowan and James (1993).

Upper half cycles

The carbonate-rich layers of the Cape Ann, Campbells and Felix Members and Berry Head Formation are rich in oolitic grainstones and microbial deposits, with subordinated heterolites and bioclasts. These layers correspond to the upper part of the relative transgressive-regressive cycles (Figure 2) of Chow and James (1987a) and oolitic upper half cycles of Cowan and James (1993). The facies associations in these units include shallow subtidal oolitic shoal and subtidal to intertidal F.A. The shoreface facies association, present only in the SPICE related massive sandstone at Felix Cove section, is discussed later.

Frequent microbial buildups occur in the PAP both as thrombolites and stromatolites (Figure *22*A and B), developed mostly in a more restricted/protected shelf position (upper subtidal to intertidal), with occasional glauconite and bioclasts carried to the shoal area due to storms. Stromatolites growing over flat pebble conglomerate are common in the lower Campbells Member (Figure 22C). Often, oolitic sands may locally fill the inter buildup space. Ooids and quartz grains observed with incursions of glauconite and bioclasts, may also be trapped in the stromatolites, suggesting that the mats and buildups may have occurred between oolitic shoals, as discussed by Cowan and James (1993). Microbial mats with wrinkle structure also occur (Figure *22*D). The thrombolites in the upper Campbells Member, near to the transition with the Big Cove Member, are wider and higher than ones observed in the same unit within the oolitic shoal facies association, possibly reflecting greater water depths that allowed the development of larger structures.

Boundstones show different morphologies depending on the shelf position, and they did not formed onl in protected intertidal areas but also in deep subtidal environments, mainly as microbial mats associated with trilobite and brachiopod faunas. While in the March Point section, microbial deposits below the SPICE layer are columnar stromatolites, in the Felix Cove section it is a thrombolite, equivalent to the oblate thrombolite of the type described by Cowan and James (1993). These differences may reflect possible environmental differences between the two localities, where the Felix Cove locality would being shallower than the March Point locality.

The oolitic shoal complexes are typically massive but occasionally exhibit herringbone and low angle and incipient stratifications, evidencing a tidal influence, possibly related to the upper subtidal. At the top of the oolitic half cycles as defined by Cowan and James (1993), relic oomouldic porosity occurs which has often been infilled by dolomite rhombs. Regarding the oolitic grains in the upper half cycles, there are differences among the units. Chow (1985) and Chow and James (1987b) describe two different ooids types forming oolitic grainstones of PAP.

The grey oolites are associated with parted limestones and flat pebble conglomerates, displaying radial cortexes and showing variable degree of preservation, with limited micritization. They also often display well developed, isopachous fibrous to prismatic cement fringes. Hardgrounds formed these oolites suggested that although they were related to a subtidal mobile fringe in a high-energy environment, at times, cementation was a major lithification process. Comparatively, the brown oolites consist of micritized, commonly superficial ooids, associated with peloids, bioclasts, quartz and feldspar sand and silt grains, and with poorly-developed fibrous cement fringes.

Although Chow (1985) and Chow and James (1987b), suggested that the brown and grey ooids formed in different environments, many samples contain a variety of ooid types (e.g. Figure 8). There is also limited evidence of subaerial exposure; rather many of the sedimentary structures observed suggests subtidal and shallow subtidal conditions (e.g. syneresis cracks, hardgrounds and herringbone stratification). Additionally, since ooid morphology is not diagnostic of environmental conditions itself (Tucker and Wright, 1990), it cannot reflect the position in the shelf.

Influx of siliciclastic sand (Desrochers et al., 2012) occurred at the top of some of the oolitic upper half cycles, as sandy limestones (angular, fine sand to silt quartz) . The occurrence of at the SPICE excursion in laterally different lithologies also may be a result of different shelf positions. At March Point section, the SPICE is characterized by digitate stromatolites and glauconitic dolostones while at Felix Cove section, the SPICE is characterized by a lobate thrombolite and well-developed medium-coarse grained sandstone. Wind-blown, angular, fine quartz grains that are present within the carbonate layers are likely to have been subtidally reworked (Cowan and James, 1993) while the coarser grained, well sorted sandstone in the Felix Member is related to the siliciclastic shoreface reworking due to the transgression that resulted in the SPICE event (Lavoie et al., 2012). Such lateral but coeval differences as suggested by the SPICE, suggest an irregular Cambrian coastline.

5.2 Sequence Stratigraphy

Although the Cambrian period was a time of overall transgression (e.g. James *et al.*, 1989; Knight *et al.*, 2007; Peters & Gaines, 2012), the cyclic nature of the PAP is believed to reflect third-order eustatic fluctuations (Cowan and James, 1993) with periods of regression, particularly at the SPICE (e.g. Saltzman, 2004, Barili et al. 2018). This order of eustatic variation is a result of regional plate kinematics and/or glacioeustatic variations. According to Cowan & James (1993), each Grand Cycle has highstand, lowstand and sequence boundaries deposits, marked respectively by ribbon rocks, oolitic grainstones and heterolithic peritidal carbonates. The latter however is not seen to any significant extent in the PAP (Cowan and James, 1993) although the oblate bioherms observed at the SPICE locality in Felix Cove and nearby (Barili et al., 2018) may suggest minor peritidal cycles in places at the top of the Felix Mbr.

5.3 Chemical Stratigraphy

5.3.1 Stable isotopes

Stable isotope data published by Chow (1985) did not reveal the positive carbon excursion (SPICE) but it was identified by Saltzman et al. (2004) in the Felix Cove section and also at March Point by Barili et al. (2018). Saltzman et al. (2004) observed an excursion of ca. +3.5 ‰ and Barili et al. (2018) it was found to be slightly smaller variations (ca.+2.5 ‰ to +3 ‰). In a study of the Amadeus Basin, Australia, Schmid *et al.* (2018) showed that the extent of the excursion depended on the position within the basin. Open marine sequences showed the full +5 ‰ carbon isotope excursion whereas sequences deposited nearshore shelf displayed a reduced excursion with marine subtidal deposits showing $\delta^{13}C$ excursions of +2 to +3.5 ‰. The data presented here and by Saltzman et al.(2004) suggests that the SPICE in the PAP occurs in a shallow positions within the sequence.

The thickness of the SPICE interval is also variable in the Amadeus Basin, ranging from 14 to 119 m. The excursion observed in the Petit Jardin Formation is detected across a thickness of 5 - 15 m also comparable to a shallow, subtidal position in the Amadeus Basin. According to Schmid *et al.* (2018), a lower $\delta^{13}C$ values occur nearshore and higher values in the deep shelf, suggesting a possible isotopic gradient between dissolved inorganic carbon (DIC) in seawater and atmospheric CO_2

The effect of diagenesis on the isotopic signature is a matter of concern in ancient rocks. Meteoric diagenesis can reduce both $\delta^{13}C$ and $\delta^{18}O$ signatures, due to its depleted isotopic content, however, burial diagenesis also may lead to a $\delta^{18}O$ negative shift due to the increasing temperature and consequent fractionation (Hoefs, 2018). The $\delta^{18}O$ signature of dolomites is controlled by pore fluid temperature, while the $\delta^{13}C$ is defined by the composition of the carbonate precursor (Hoefs, 2018). The XRF data confirms that the Felix Member in the March Point section was more affected by dolomitization, (Ca <20% and higher Mn/Sr) than in Felix Cove, as observed in the petrography and discussed by Barili et al. (2018). Nonetheless, despite this variation in dolomitization intensity, carbon isotope signatures do not differ much between these two sections. While March Point has a maximum positive excursion peak of +2.5‰, Felix Cove data reaches c. + 3‰ (Barili et al., 2018). Since the dolomite $\delta^{13}C$ is normally close to the original signature, and considering that SPICE amplitudes may vary according to the shelf position (Schmid et al., 2018), even if meteoric diagenesis may have reduced the original signature before dolomitization, these isotopic results ,indicate that its effect was minimal on the original signature.

Comparing with other Laurentian SPICE occurrences, depending on the craton position, there are visible differences between excursion thickness and amplitude. While in the southern to the northern Appalachians, the excursion is progressively thinner (~80m to < 20m) with a reduced magnitude (c. +4 to +2‰), while in the northwest of paleo Laurentia, the excursion occurrences are thicker (>200m) reaching the maximum amplitude observed (~5‰) (Barili et al., 2018; Glumac and Walker, 1998; Saltzman, 1999; Saltzman et al., 2004). These differences,can be related to the shelf position and then a local signature (Barili et al., 2018; Schmid et al., 2018), with deeper and open shelf circulation in the Laurentian Northeast, and a shallow, possible more restrict position, in the south Laurentia.

5.3.2 $^{87}Sr/^{86}Sr$ ratios and Mn/Sr ratios

The $^{87}Sr/^{86}Sr$ ratios for most of the Upper Cambrian at March Point are within typical values of , between 0.7091 and 0.7096 (Montañez et al., 2000; Peters and Gaines, 2012). This very high ratio is due to the exposure and long-term erosion of granitic rocks at the Precambrian-Cambrian Great Unconformity, with a maximum (~0.7096) reached at the end of the Sauk transgression (510-500 Ma), followed by a declined (Montañez et al., 2000; Peters and Gaines, 2012). The maximum continental flood of the Sauk II transgression occurred between 505 and 500 Ma, followed by a regression associated with the SaukII-III sequence boundary that originated the SPICE (Karlstrom et al., 2018; Saltzman et al., 2004) during which time the $^{87}Sr/^{86}Sr$ ratios reach a minimum of 0.7088. At Felix Cove, the $^{87}Sr/^{86}Sr$ ratios are similar, typically 0.7092 – 0.7093 but dropping to c. 0.7090 at the SPICE, slightly higher than at March Point.

Lower $^{87}Sr/^{86}Sr$ ratios are typically attributed to increased ^{86}Sr from the hydrothermal alteration of mid-ocean ridges (~0.703), while values of ~0.711 and ~0.708 result from continental weathering and the diagenetic processes of dissolution and recrystallization that affecting carbonate rocks (Faure, 1986; Montañez *et al.*, 2000; Wierzbowski, 2014).

Given that the analyses are from bulk samples, although Cambrian mean $^{87}Sr/^{86}Sr$ ratios are exhibited for most of the samples, diagenetic alteration cannot be ruled out; especially for the SPICE interval in the March Point section, which is more affected by dolomitization and has a slightly lower $^{87}Sr/^{86}Sr$ ratio than at Felix Cove. Although carbon stable isotopes normally hold a signature similar to the original rock or sediments, other trace metals such as Sr are affected by diagenesis (Veizer, 1989). The $^{87}Sr/^{86}Sr$ ratio of the rock represents the marine environment and/or the fluid associated with diagenetic processes, since there is no fractionation of Sr isotopes in nature due to temperature changes (Faure, 1986). Although a relatively closed early diagenetic system could maintain the original isotopic signature buffered by the surrounding rocks, burial diagenesis imposes limits of preservation in marine sediments (Veizer, 1989). However. as diagenesis tends to increase $^{87}Sr/^{86}Sr$ values (Knoll, 2000), the values range around the SPICE layers are lower than the expected and perhaps warrant further research.

The extent of diagenesis can be identified using geochemical screening proxies such as the Mn/Sr ratio. Different levels of cutoff can be used for the Mn/Sr ratio, that is widely used for detecting the intensity of Sr alteration due to diagenesis (Derry *et al.*, 1992; Stein & Kaufman, 1999; Derry, 2010). For most of the samples, Mn/Sr ratios are higher than 2, indicating a possible diagenetic imprint (Stein & Kaufman, 1999). However, Hood *et al.* (2018) emphasizes that the cutoffs generally applied to younger rocks may not necessarily apply to ancient rocks. Additionally, although for Fe and Mn enrichment and reduction of Sr concentrations may be due to meteoric diagenesis, samples with higher Mn/Sr may have been affected by reducing diagenetic fluids (Hood et al., 2018).

6. Conclusions

Following work by Chow (1985), Chow and James (1987b) and Cowan and James (1993), the Port au Port Gp has been separated transgressive-regressive cycles which coincides with the North American Grand Cycles. New, detailed sedimentary logs are presented for March Point (the most complete section through the Port au Part Gp) in Western Newfoundland and Felix Cove, coupled with chemical stratigraphy (XRF and stable/Sr isotopes) for both localities.

Four facies associations have been constructed ranging from subtidal to intertidal. However, the Port au Port Gp has been found to have been largely deposited in a subtidal marine environment as suggested by Cowan and James (1993). Evidence includes the lack of subaerial exposure, syneresis and subaqueous cracks, the frequent occurrence of hardgrounds marine bioclasts and glauconite.

The SPICE is observed in both the March Point and Felix Cove sections. By comparison with the SPICE in the Amadeus Basin (Schmidt, 2018) the magnitude of the SPICE excursion (.+2.5 ‰ to +3 ‰) suggests deposition of sediment in the shallow subtidal with Felix Cove being nearest of the shoreface while the March Point section was in a slightly more basinward position. Although Mn/Sr for most of samples are higher than two, strontium ratios are very similar to those expected for the Middle/Upper Cambrian, with exception of those related to the SPICE which are lower than and therefore related to the regression event and consequent weathering of older carbonate rocks. Although the evident relation between the Sr ratios and the SPICE event, these lower, values warrant further investigation regarding other SPICE occurrences and diagenetic influences.

Acknowledgements

This work is a part of the PhD of the first author, developed at Universidade Federal do Rio Grande do Sul (UFRGS), fully funded by Shell during the first three years. The authors gratefully acknowledge support from Shell Brasil through the “BG05: UoA-UFRGS-SWB Sedimentary Systems” project at UFRGS and the strategic importance of the support given by ANP through the R&D levy regulation. We also would like to thank the University of Aberdeen (UoA) for funding XRF and $^{87}Sr/^{86}Sr$ analysis, and the Petroleum and Natural Resources Institute (IPR/PUCRS) colleagues for the support during the last months.

References

Barili, R., Neilson, J.E., Brasier, A.T., Goldberg, K., Pastro Bardola, T., De Ros, L.F., Leng, M., 2018. Carbon isotopes, stratigraphy, and environmental change: the Middle–Upper Cambrian Positive Excursion (SPICE) in Port au Port Group, western Newfoundland, Canada. Can. J. Earth Sci. 55, 1209–1222. https://doi.org/10.1139/cjes-2018-0025

Bond, D.P.G., Grasby, S.E., 2017. On the causes of mass extinctions. Palaeogeogr. Palaeoclimatol. Palaeoecol. 478, 3–29. https://doi.org/10.1016/j.palaeo.2016.11.005

Chow, N., 1985. Sedimentology and diagenesis of Middle and Upper Cambrian platform carbonates and siliciclastics, Port au Port Peninsula, western Newfoundland. Thesis (Unpublished) 458.

Chow, N., James, N.P., 1992. Synsedimentary diagenesis of Cambrian peritidal carbonates: evidence from hardgrounds and surface paleokarst in the Port au Port Group, western Newfoundland. Bull. Can. Pet. Geol. 40, 115–127.

Chow, N., James, N.P., 1987a. Cambrian Grand Cycles : A northern Appalachian perspective. Geol. Soc. Am. Bull. 98, 418–429. https://doi.org/10.1130/0016-7606(1987)98<418

Chow, N., James, N.P., 1987b. Facies specific, calcitic and bimineralic ooids from Middle and Upper Cambrian platform carbonates, Western Newfoundland, Canada. J. Sediment. Petrol. 57, 907–921.

Cowan, C.A., James, N.P., 1993. The interactions of sea-level change, terrigenous-sediment influx, and carbonate productivity as controls on Upper Cambrian

Grand Cycles of western Newfoundland, Canada. Geol. Soc. Am. Bull. 105, 1576–1590. https://doi.org/10.1130/0016-7606(1993)105<1576:TIOSLC>2.3.CO;2

Derry, L.A., 2010. A burial diagenesis origin for the Ediacaran Shuram-Wonoka carbon isotope anomaly. Earth Planet. Sci. Lett. 294, 152–162. https://doi.org/10.1016/j.epsl.2010.03.022

Derry, L.A., Kaufman, A.J., Jacobsen, S.B., 1992. Sedimentary cycling and environmental change in the late Proterozoic: evidence from stable isotopes. Geochim. Cosmochim. Acta 56, 1317–1329.

Desrochers, A., Brennan-Alpert, P., Lavoie, D., Chi, G., 2012. Regional Stratigraphic, Depositional, and Diagenetic Patterns of the Interior of St. Lawrence Platform: The Lower Ordovician Romaine Formation, Western Anticosti Basin, Quebec. AAPG Mem. 98, 525–544. https://doi.org/10.1306/13331505M983504

Glumac, B., Walker, K.R., 1998. A Late Cambrian positive carbon-isotope excursion in the Southern Appalachians; relation to biostratigraphy, sequence stratigraphy, environments of deposition, and diagenesis. J. Sediment. Res. 68, 1212–1222. https://doi.org/10.2110/jsr.68.1212

Hoefs, J., 2018. Stable Isotope Geochemistry. https://doi.org/10.1007/978-3-662-02290-0

Hood, A. v. S., Planavsky, N.J., Wallace, M.W., Wang, X., 2018. The effects of diagenesis on geochemical paleoredox proxies in sedimentary carbonates. Geochim. Cosmochim. Acta 232, 265–287. https://doi.org/10.1016/j.gca.2018.04.022

Karlstrom, K., Hagadorn, J., Gehrels, G., Matthews, W., Schmitz, M., Madronich, L., Mulder, J., Pecha, M., Giesler, D., Crossey, L., 2018. Cambrian Sauk transgression in the Grand Canyon region redefined by detrital zircons. Nat. Geosci. 11, 438–443. https://doi.org/10.1038/s41561-018-0131-7

Knoll, A.H., 2000. Learning to tell Neoproterozoic time. Precambrian Res. 100, 3–20. https://doi.org/10.1016/S0301-9268(99)00067-4

Lavoie, D., Desrochers, A., Dix, G., Knight, I., Hersi, O., 2012. The great American carbonate bank in eastern Canada: An overview, in: Derby, J., Fritz, R., Longacre, S., Morgan, W., Sternbach, C. (Eds.), AAPG Memoir 98 Great American Carbonate Bank. AAPG, pp. 499–523. https://doi.org/10.1306/13331504M983503

McMahon, S., van Smeerdijk Hood, A., McIlroy, D., 2017. The origin and occurrence of subaqueous sedimentary cracks. Geol. Soc. London, Spec. Publ. 448, 285–309. https://doi.org/10.1144/sp448.15

Montañez, I.P., Osleger, D.A., Banner, J.L., Mack, L.E., Musgrove, M., 2000. Evolution of the Sr and C Isotope Composition of Cambrian Oceans. GSA Today 10, 1–7.

Palmer, A.R., 1965. Trilobites of the Late Cambrian Pterocephaliid Biomere in the Great Basin, United States. United States Geol. Surv. Prof. Pap. 493, 1–105.

Palmer, A.R., James, N.P., 1979. The Hawke Bay event: A circum- Iapetus regression near the lower middle Cambrian boundary. Virginia Polytech. Inst. State Univ. Dep. Geol. Sci. Mem. 2, 15–18.

Peters, S.E., Gaines, R.R., 2012. Formation of the ’ Great Unconformity’ as a trigger for the Cambrian explosion. Nature 484, 363–366. https://doi.org/10.1038/nature10969

Pratt, B., 2010. Peritidal carbonates. Facies Model. 4 401–420.

Pratt, B.R., 1998. Syneresis cracks: Subaqueous shrinkage in argillaceous sediments caused by earthquake-induced dewatering. Sediment. Geol. 117, 1–10. https://doi.org/10.1016/S0037-0738(98)00023-2

Saltzman, M.R., 1999. Upper Cambrian carbonate platform evolution, Elvinia and Taenicephalus zones (pterocephaliid-ptychaspid biomere boundary), northwestern Wyoming. J. Sediment. Res. 69, 926–938. https://doi.org/10.2110/jsr.69.926

Saltzman, M.R., Cowan, C. a., Runkel, A.C., Runnegar, B., Stewart, M.C., Palmer, a. R., 2004. The Late Cambrian Spice (13C) Event and the Sauk II-SAUK III Regression: New Evidence from Laurentian Basins in Utah, Iowa, and Newfoundland. J. Sediment. Res. 74, 366–377. https://doi.org/10.1306/120203740366

Saltzman, M.R., Davidson, J.P., Holden, P., Runnegar, B., Lohmann, K.C., 1995. No statistical support for sudden (or Sea-level-driven changes in ocean chemistry at an Upper Cambrian\rextinction horizon. Geology 23, 893–896. https://doi.org/10.1130/0091-7613(1995)023<0893:SLDCIO>2.3.CO;2

Saltzman, M.R., Ripperdan, R.L., Brasier, M.D., Lohmann, K.C., Robison, R.A., Chang, W.T., Peng, S., Ergaliev, E.K., Runnegar, B., 2000. A global carbon isotope excursion (SPICE) during the Late Cambrian: Relation to trilobite extinctions, organic-matter burial and sea level. Palaeogeogr. Palaeoclimatol.

Palaeoecol. 162, 211–223. https://doi.org/10.1016/S0031-0182(00)00128-0

Saltzman, M.R., Runnegar, B., Lohmann, K.C., 1998. Carbon isotope stratigraphy of upper Cambrian (Steptoean stage) sequences of the eastern Great Basin: Record of a global oceanographic event. Bull. Geol. Soc. Am. 110, 285–297. https://doi.org/10.1130/0016-7606(1998)110<0285:CISOUC>2.3.CO;2

Schmid, S., Smith, P.M., Woltering, M., 2018. A basin-wide record of the Late Cambrian Steptoean positive carbon isotope excursion (SPICE) in the Amadeus Basin, Australia. Palaeogeogr. Palaeoclimatol. Palaeoecol. 508, 116–128. https://doi.org/10.1016/j.palaeo.2018.07.027

Sepkoski, J.J., 1982. Mass extinctions in the Phanerozoic oceans: a review. Geol. Soc. Am. Spec. Pap. 190, 283–289. https://doi.org/10.1130/SPE190-p283

Stein B., J., Alan J.， Kaufman, 1999. The Sr, C and O isotopic evolution of neoproterozoic seawater. Chem. Geol. 161, 37–57. https://doi.org/10.1016/S0009-2541(01)00268-6

Tucker, M.E., Wright, P., 1990. Carbonate Sedimentology. John Wiley & Sons.

Veizer, J., 1989. Strontium Isotopes in. Ann. Rev. Earth Planet Sci. 717, 141–167.

Wierzbowski, H., 2014. Strontium isotope composition of sedimentary rocks and its application to chemostratigraphy and palaeoenvironmental reconstructions. Ann. UMCS, Sect. AAA Phys. 68. https://doi.org/10.2478/v10246-012-0017-2

Williams, H., 1979. Appalachian Orogen in Canada. Can. J. Earth Sci. 16, 792–807. https://doi.org/10.1139/e79-070

Williams, H., 1976. Tectonic stratigraphic subdivision of the Appalachian Orogen.

Williams, H. (1976). Tecton. Stratigr. Subdiv. Appalach. Orogen. Geol. Soc. Am. Abstr. with Programs 8, 300.

Yochelson, E.L., 2010. Paleontological Society. Society 59, 85–95.

Zhuravlev, A.Y., Wood, R.A., 2018. The two phases of the Cambrian Explosion. Sci. Rep. 8, 1–10. https://doi.org/10.1038/s41598-018-34962-y

Figures and tables captions

Figure 1. Study area in the Port au Port Peninsula. Location of the logged sections are shown by RED rectangles: March Point and Felix Cove. (Source: ESRI Digital Globe, datum WGS84).

Figure 2. Schematic stratigraphic log of the Port au Port Group (after Chow, 1985). Each of the Grand Cycles (A, B and C) consists of a lower shaley half-cycle mainly composed of parted limestone (interbedded shale and mudstone) and an upper carbonate half-cycle of oolitic grainstone / bioherms. Estimated Sauk II-III sequence limit and SPICE peak is indicated (Barili et al., 2018; Chow and James, 1987a; Saltzman et al., 2004)

Figure 3. Detailed sedimentary log of March Point Formation in the March Point section. Field photographs are indicated in the log. A) Glauconitic bioclastic HS (bottom) interbedded with Sh and Ht. B) Ht (limestone and shale interbedded). C) Detail of a thick FPC layer.

Figure 4. Photomicrographs of March Point Formation. PPL except where stated A) Glauconitic bioclastic hybrid sandstone cemented by calcite (9.25m); uncrossed polarizers (//P). B) Glauconitic bioclastic hybrid sandstone cemented by calcite (7.5m); crossed polarizers (XP). C) Bioclastic peloidal grainstone cemented by calcite and partially dolomitized (22.75m); //P. D) Hybrid siliciclastic-carbonate sandstone (2.25m) (XP).

Figure 5. Detailed sedimentary log of Cape Ann Member of Petit Jardin Formation in the March Point section. Field photographs are indicated in the log. A) Ht (upper part) and oolitic G (bottom).

Figure 6. Detailed sedimentary log of Lower Campbells Member of Petit Jardin Formation in the March Point section. Field photographs are indicated in the log. A) Massive Oolitic grainstone. B) Grey grainstones with several stylolites. C) Reddish oolitic grainstone with herringbone stratification.

Figure 7. Detailed sedimentary log of Upper Campbells Member of Petit Jardin Formation. A) Ht between two sets of reddish oolitic G. B) Thrombolite (B facies).

Figure 8. Photomicrographs of Campbells Member. PPL A) Dolostone with remnants of micritized and dolomitized ooids (67m); //P. B) Oolitic grainstone composed by partially micritized and recrystallized ooids, cemented by coarse calcite mosaic; //P. C) oolitic grainstone cemented by well-developed fibrous to prismatic fringes (126m); //P. and D) Sandy intraclastic limestone with minor ooids at top of the member (136m); //P.

Figure 9. Detailed sedimentary log of Big Cove Member of Petit Jardin Formation in the March Point Section. Field photographs are indicated in the log. A) Interbedding of parted limestone and oolitic grainstone interbedded. B) Flat pebble conglomerate covered by parted limestone. C) Flat pebble conglomerate.

Figure 10. Photomicrographs of Big Cove Member. A) Partially recrystallized, bioclastic-glauconitic HS (140.25m); //P. B) Bioclastic G (152.25m); //P. C) Stylolitic contact between bioclastic, partially dolomitized G and silty bioclastic G in the bottom (167m); //P. D) Oolitic-bioclastic-glauconitic G (167.5m).

Figure 11. Detailed sedimentary log of Felix Member of Petit Jardin Formation in the March Point Section. Field photographs are indicated in the log. A) Ht. B) Sets of oolitic G. C) Layers that contain the positive carbon excursion SPICE.

Figure 12. Photomicrographs of Felix Member. PPL A) Dolostone with calcite (stained pink) filling moldic and vugular pores (177.75m); //P. B) Dolomitized G with relic of micritized ooid and porosity impregnated by blue resin (189.5m); //P. C) Dolostone with occasional ooid grains and relic ooid (199.5m); //P. D) Dolomitized G with occasional ooid grains and relic ooid (215.5m); //P.

Figure 13. Detailed sedimentary log of Man O' War Member of Petit Jardin Formation. Field photographs are indicated in the log. A) Ht. B) Sets of oolitic G in the lower part and Ht in the upper part. C) Shale covered by oolitic G.

Figure 14. Photomicrographs of Man O' War Member (A and B) and Berry Head Formation C and D). A) Dolomitized G with partially preserved ooids (230m); //P. B) Dolostone with pink-stained calcite cement (239.25m); //P. C and D) Massive dolostones (251 and 265m).

Figure 15. Detailed sedimentary log of Berry Head Formation in the March Point section. Field photographs are indicated in the log. A and B) Ht. C) B/G covered by Ht.

Figure 16. Detailed sedimentary log of Felix and Man of War Members of Petit Jardin Formation in Felix Cove section. Field photographs are indicated in the log. A) View of the SPICE layers. B) Detail of thrombolite (B facies). C) G/B covered by a thick layer of Ht/Sh.

Figure 17. XRF results in the March Point Section

Figure 18. XRF results in the Felix Cove Section.

Figure 19. Isotopic results for March Point section. $\delta^{13}C$ and $\delta^{18}O$ isotopic data from Barili et al. (2018) and $^{87}Sr/^{86}Sr$ presented in this work.

Figure 20. Isotopic results for Felix Cove section. $\delta^{13}C$ and $\delta^{18}O$ isotopic data from Barili *et al.* (2018) and $^{87}Sr/^{86}Sr$ presented in this work.

Figure 21. Subaqueous sedimentary cracks in the March Point Formation. A and B) Plane view of syneresis cracks (at 12 m and 17 m along vertical log). C) Side view with V and anastomosing morphology (at ~14m). D) Linear cracks that are occasionally conformed in a polygonal shape (at ~15m).

Figure 22. Microbial deposits in the Port au Port Group. A) A stromatolite from lower Campbells Member (at 84 m along vertical log). B) Thrombolites from upper Campbells Member (at 138m). C) Microbial mat growing over flat pebble conglomerate (at 111m). D) Wrinkle structure in microbial mat near to the boundary between Campbells and Big Cove members (at 139m).

Table 1. XRF and isotopic results for Felix Cove section.

Table 2. XRF and isotopic results for March Point section.

Figure 1
Click here to download high resolution image

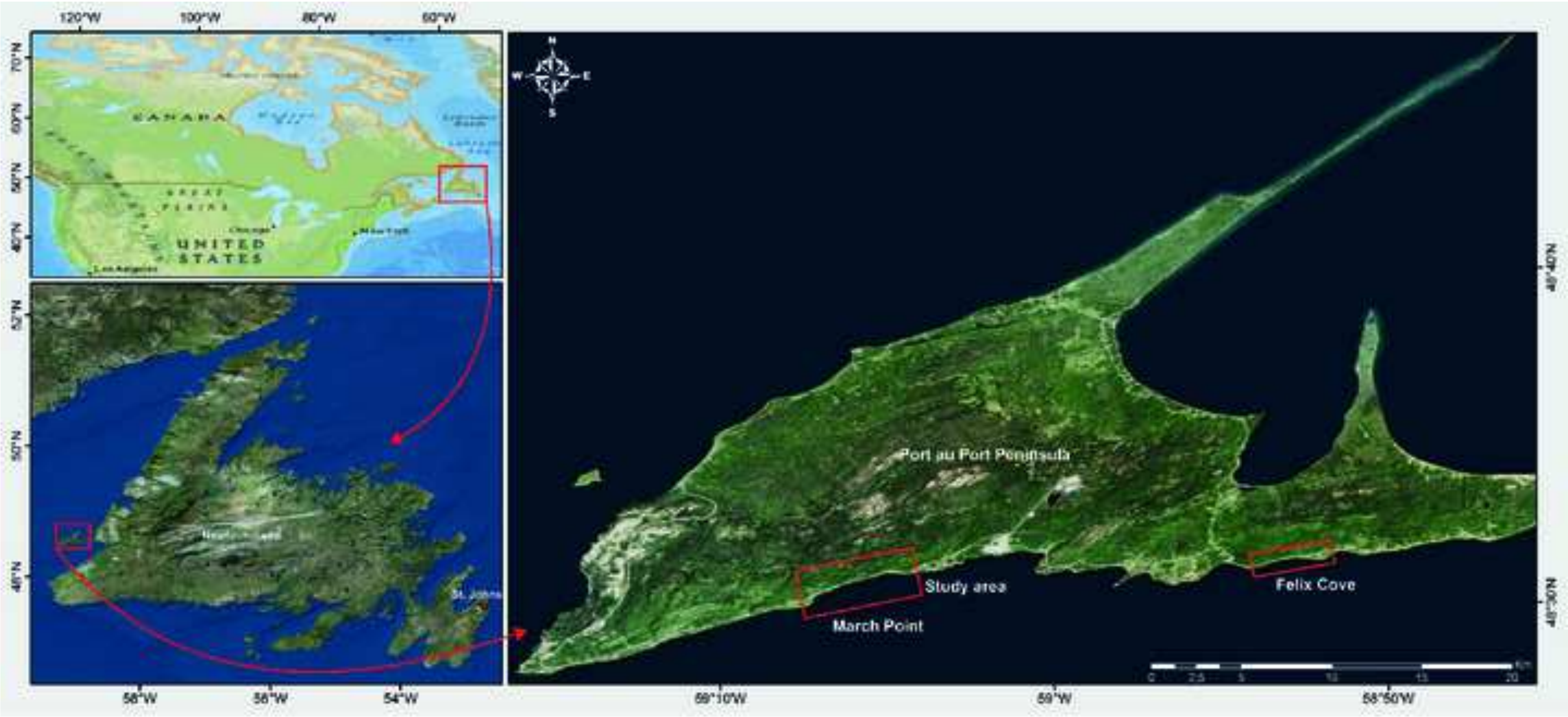

Figure 2

Click here to download high resolution image

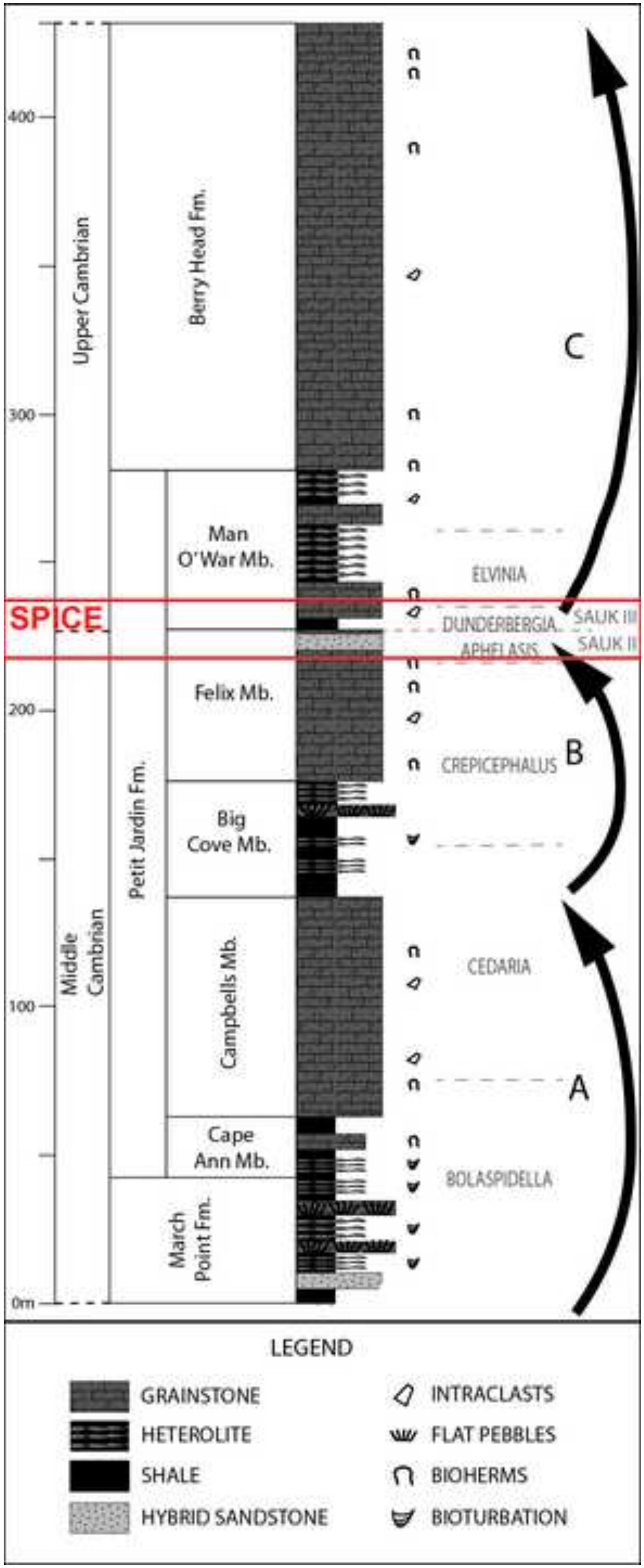

Figure 3
Click here to download high resolution image

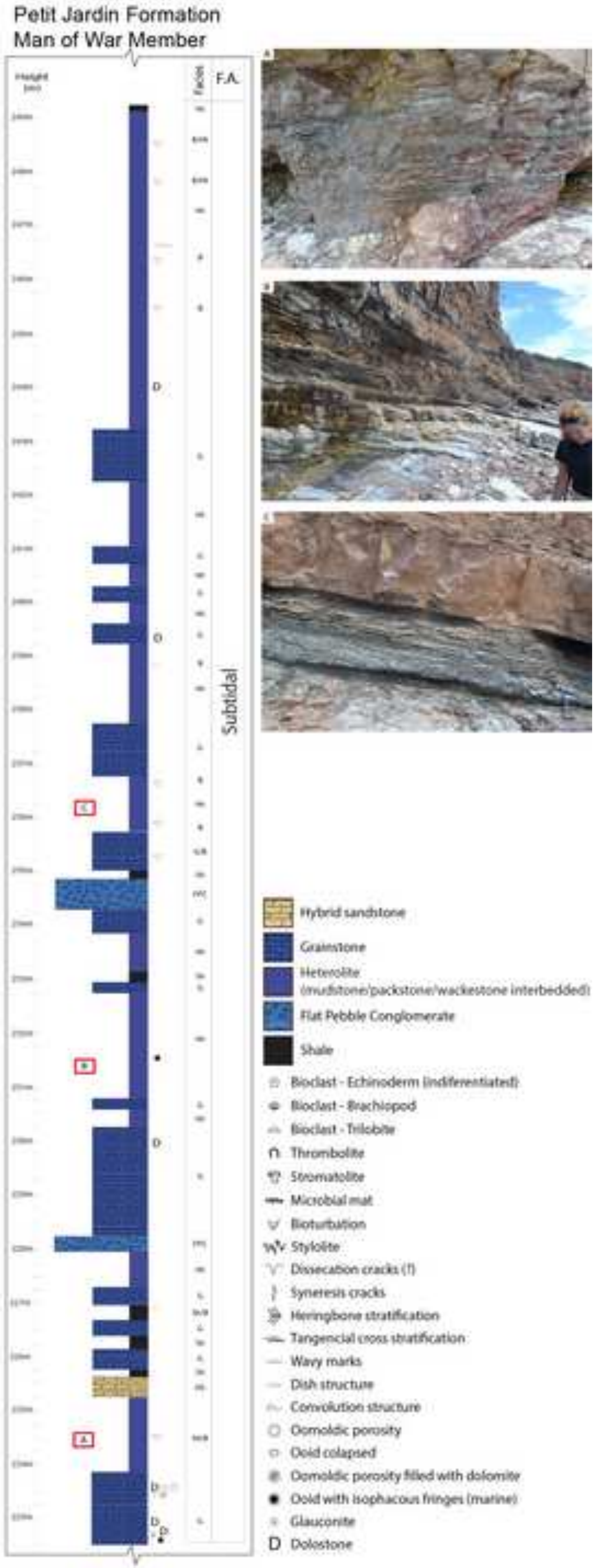

Figure 4
Click here to download high resolution image

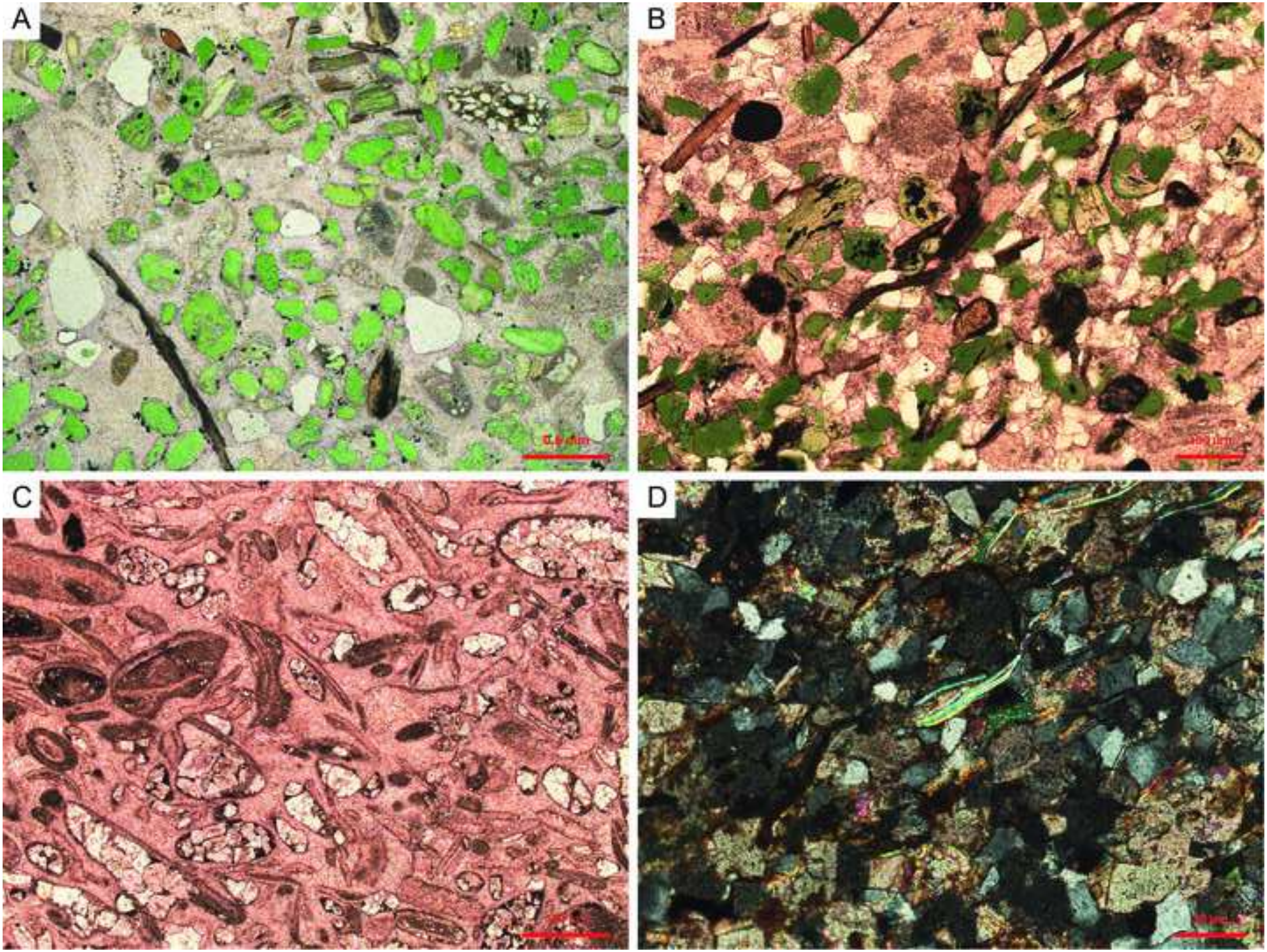

Figure 5

Click here to download high resolution image

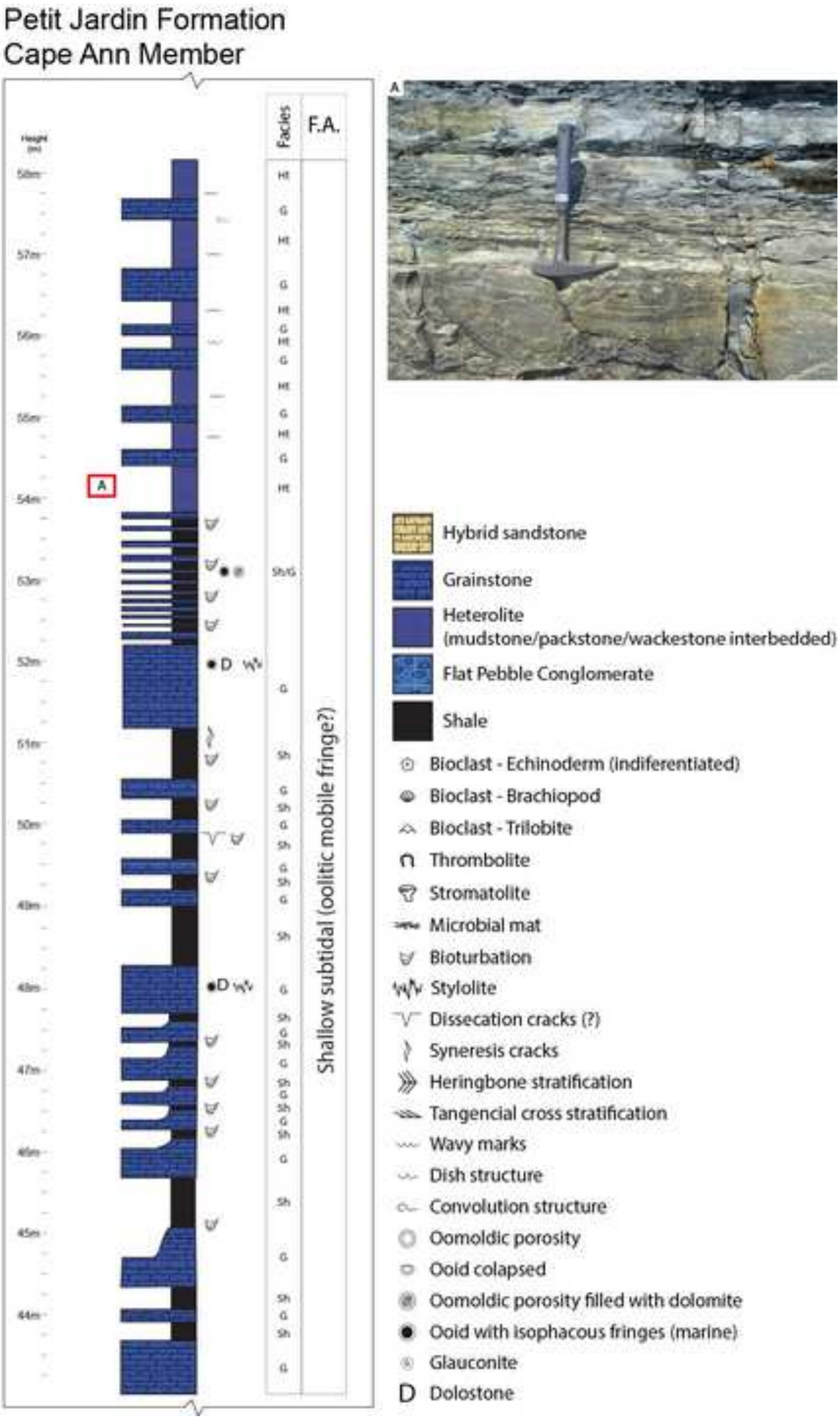

Figure 6

Click here to download high resolution image

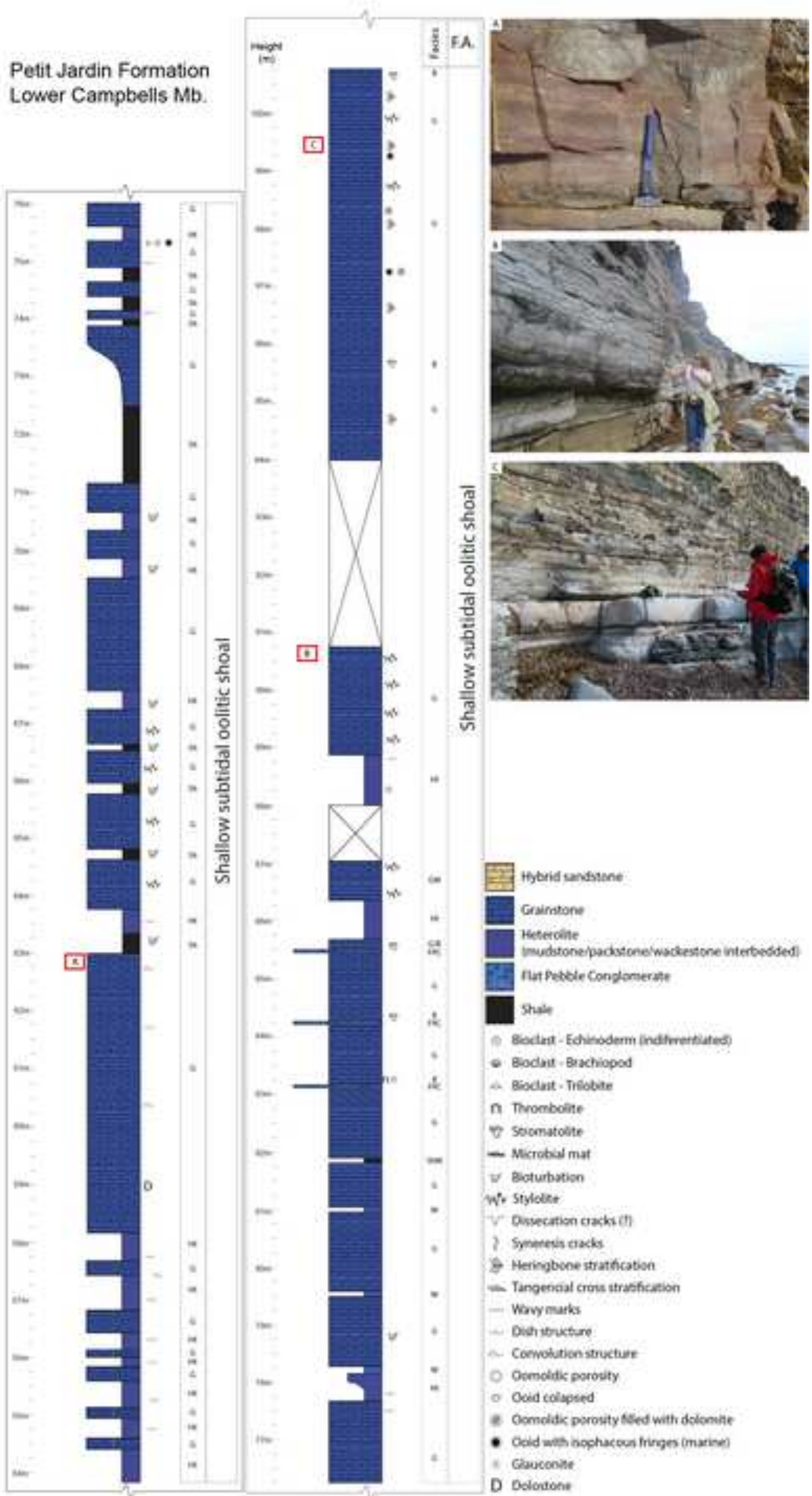

Figure 7

Click here to download high resolution image

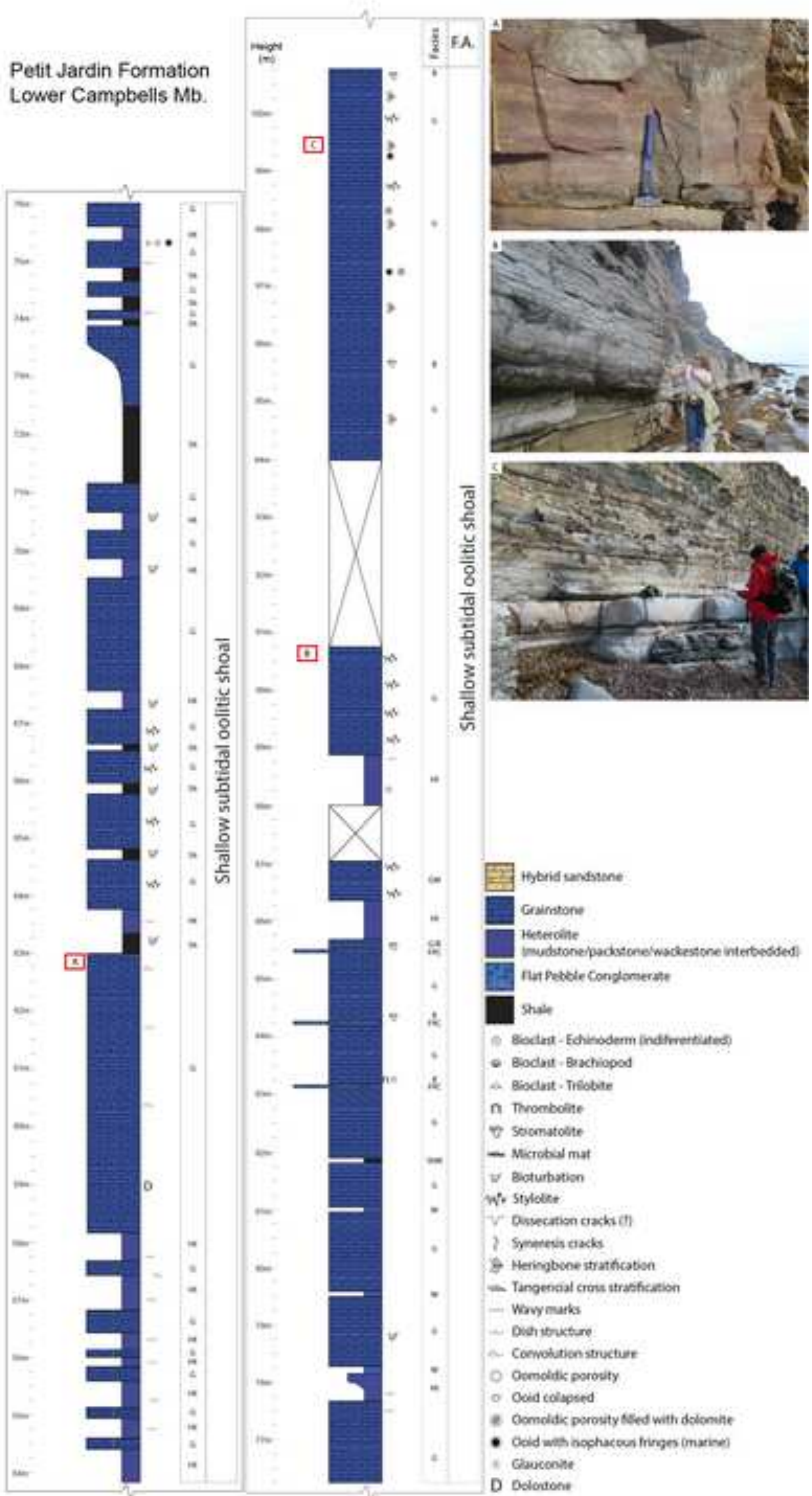

Figure 8
Click here to download high resolution image

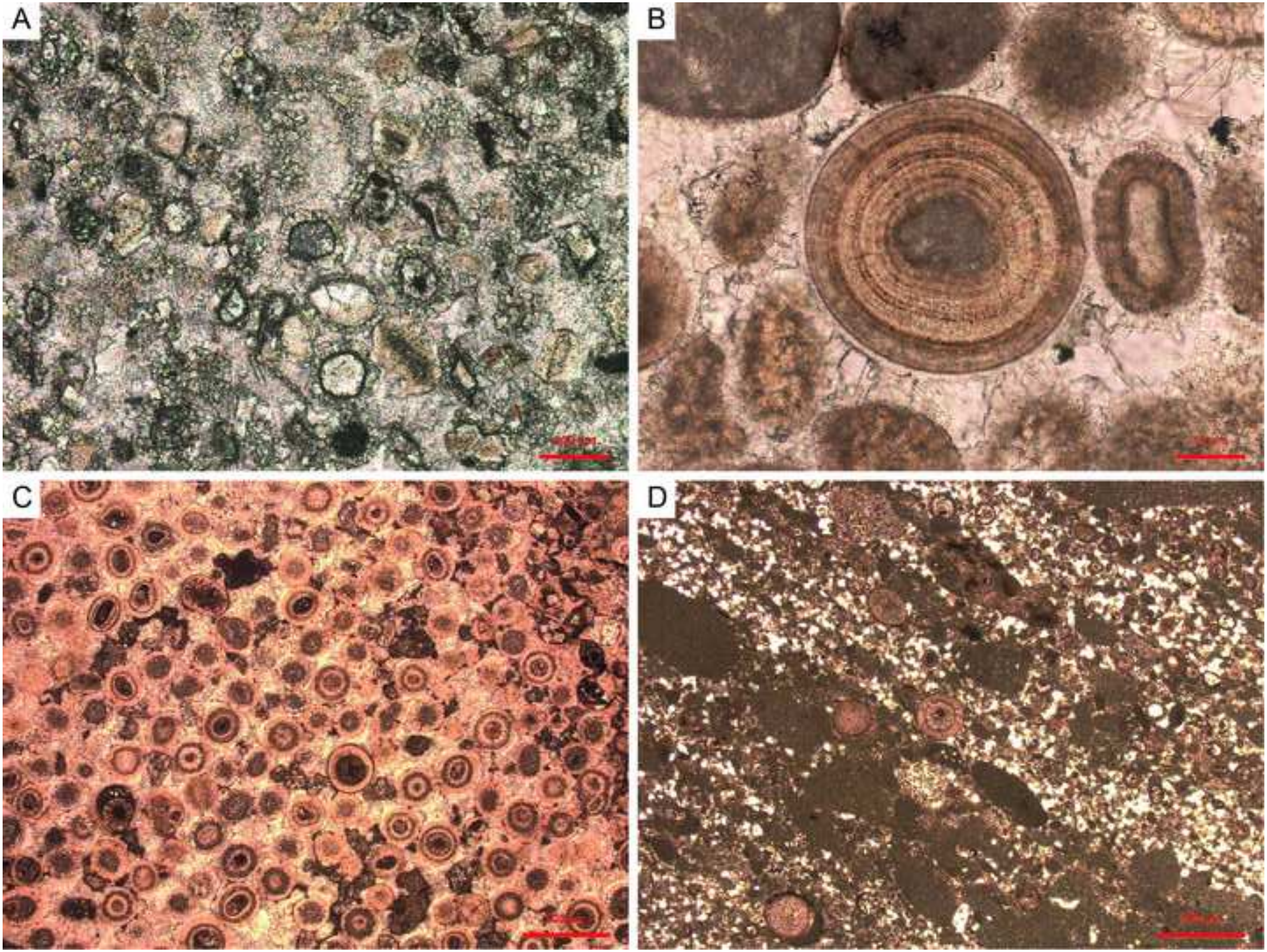

Figure 9

Click here to download high resolution image

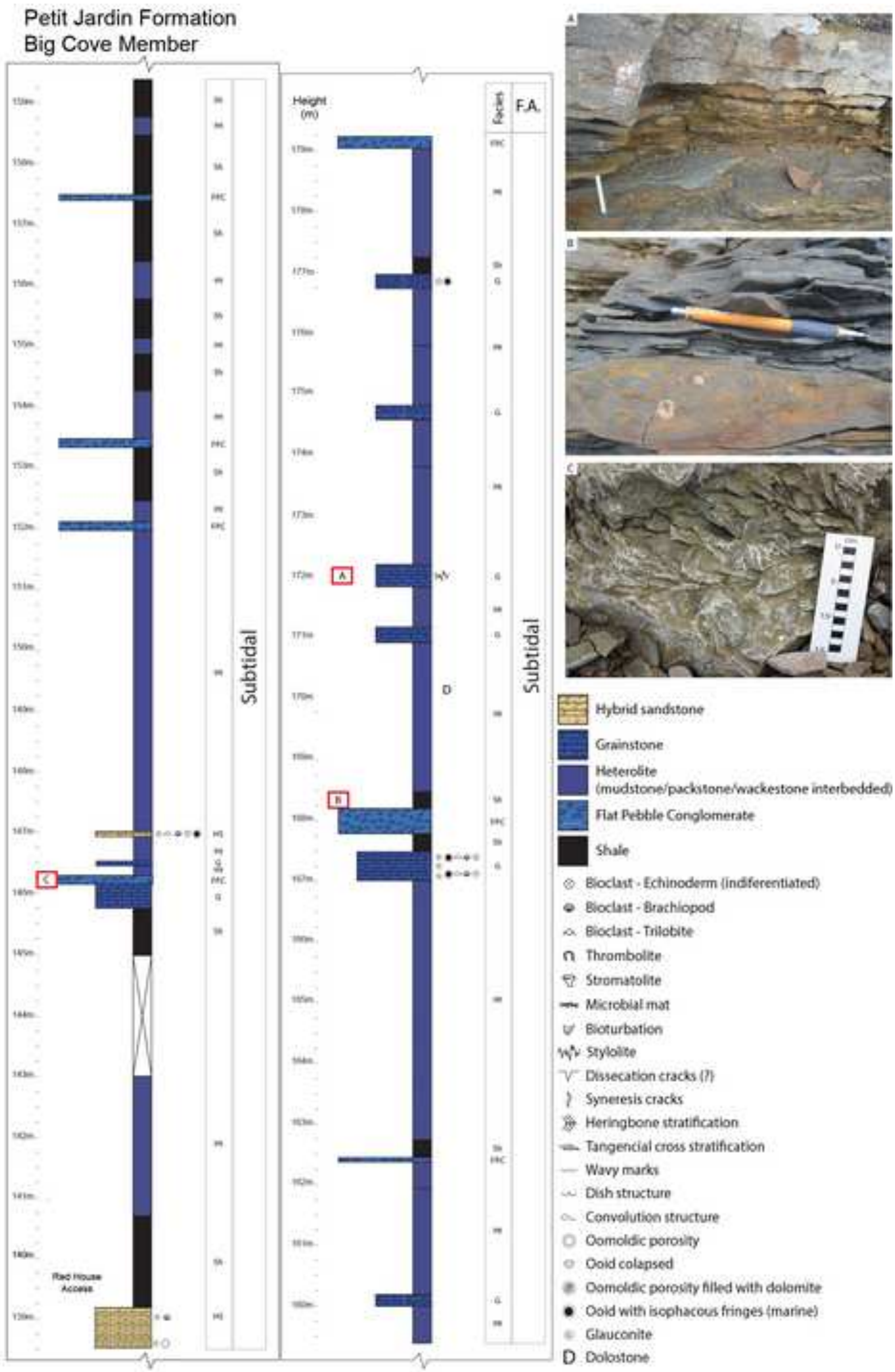

Figure 10
Click here to download high resolution image

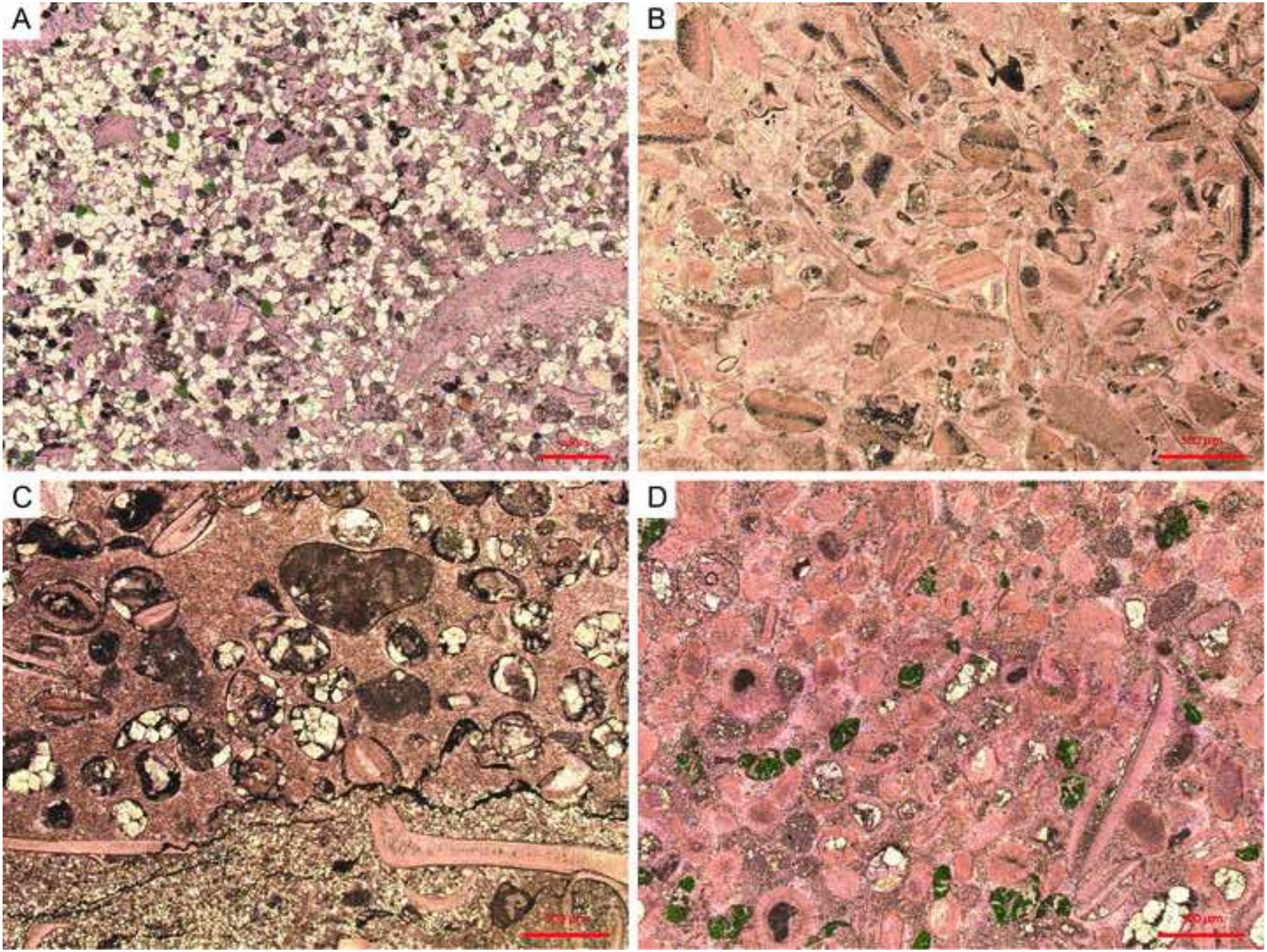

Figure 11

Click here to download high resolution image

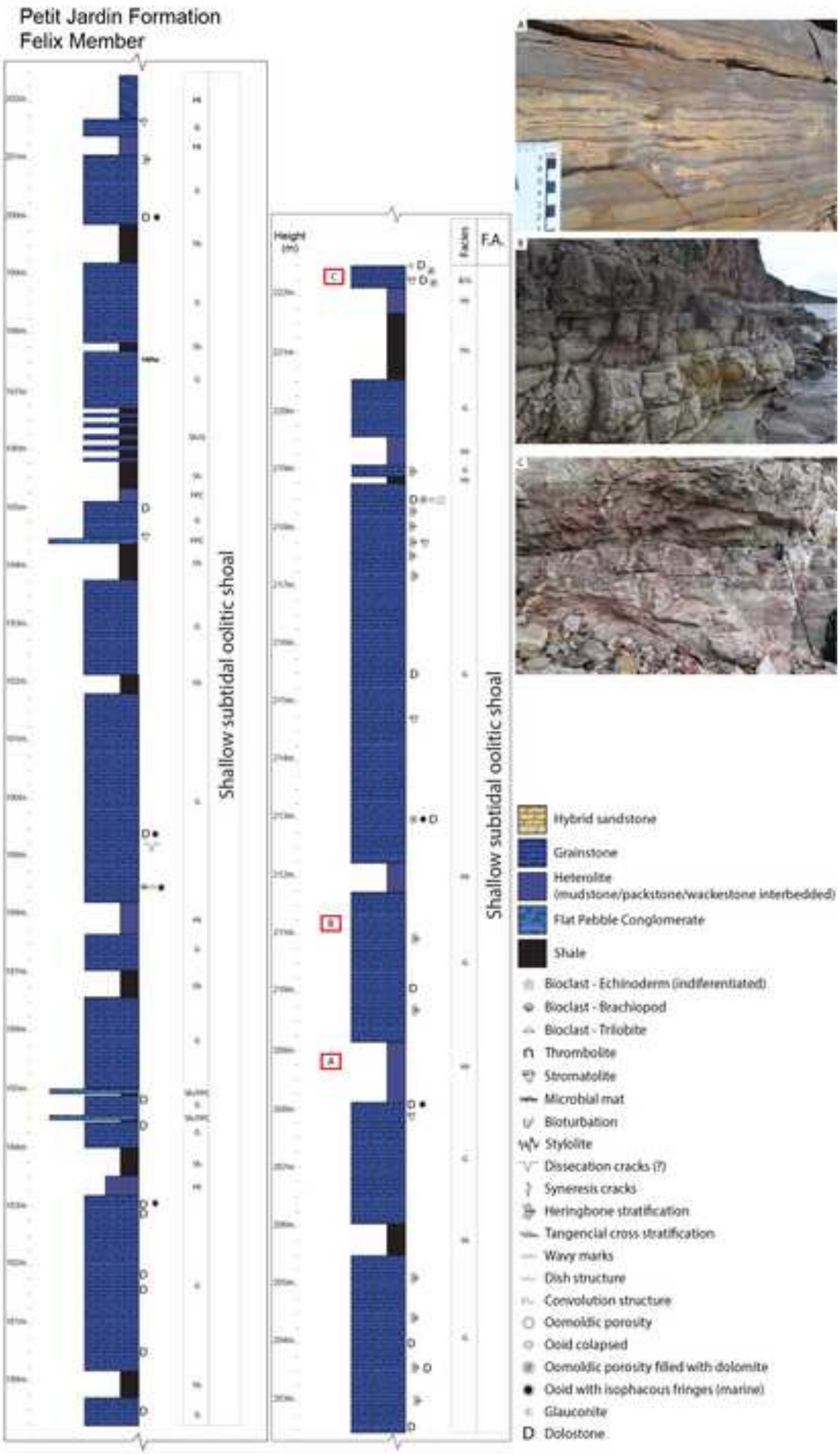

Figure 12

Click here to download high resolution image

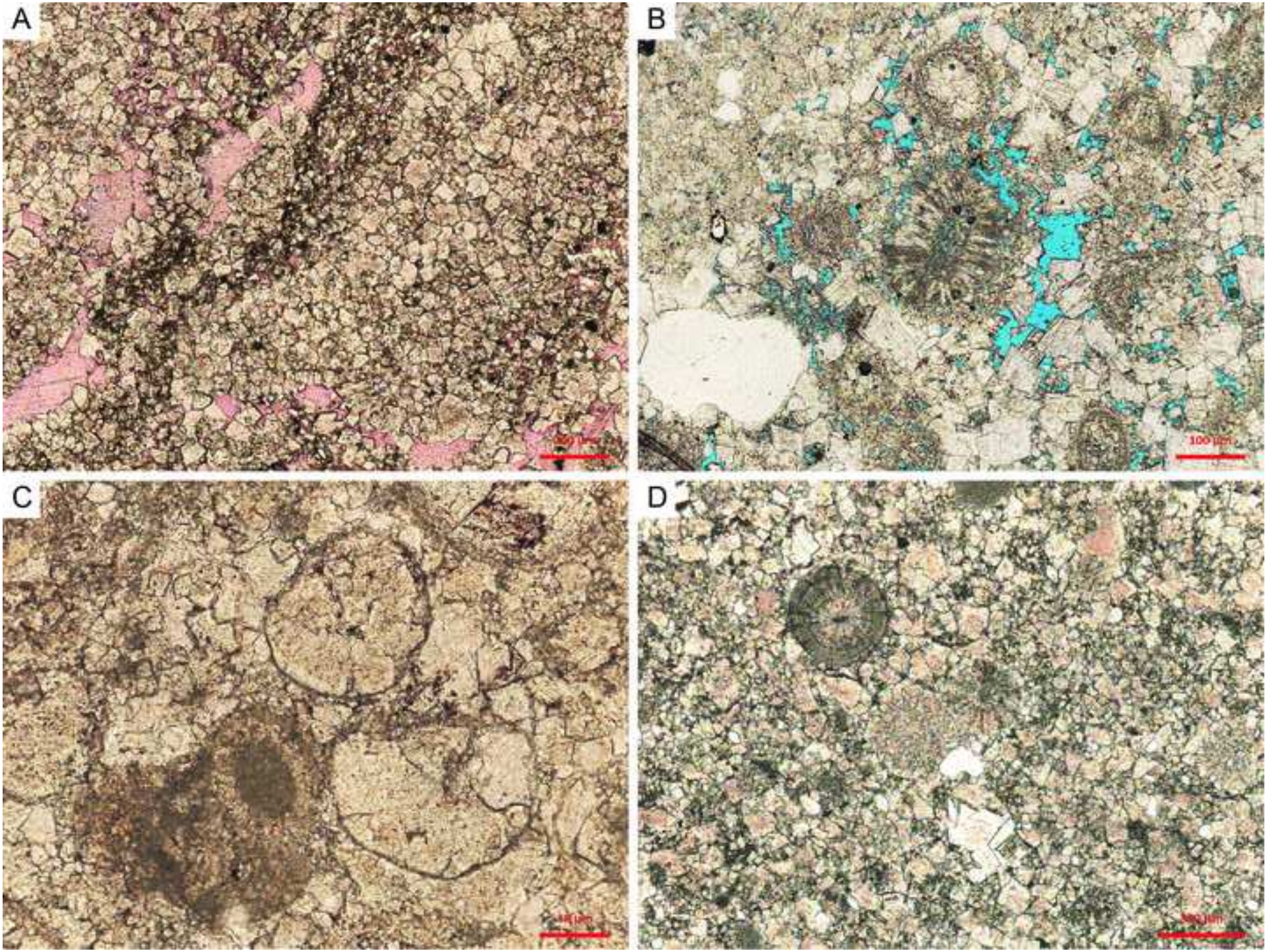

Figure 13
Click here to download high resolution image

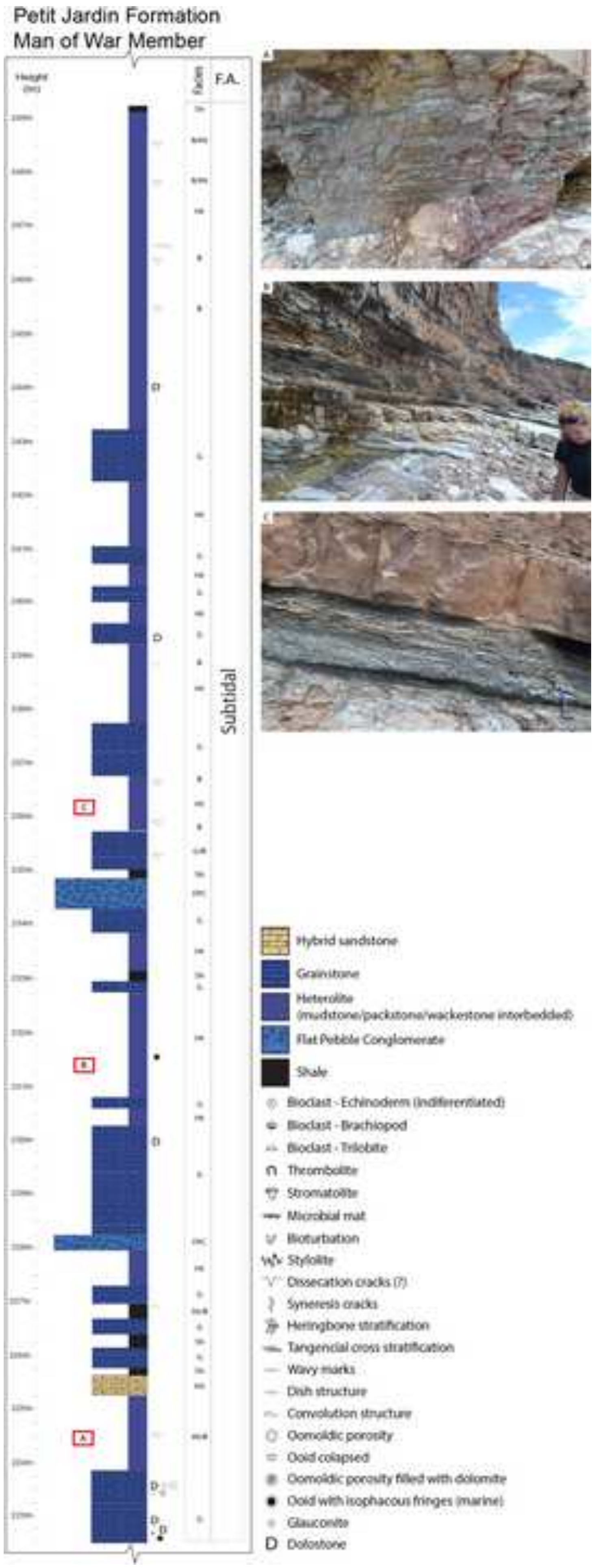

Figure 14

Click here to download high resolution image

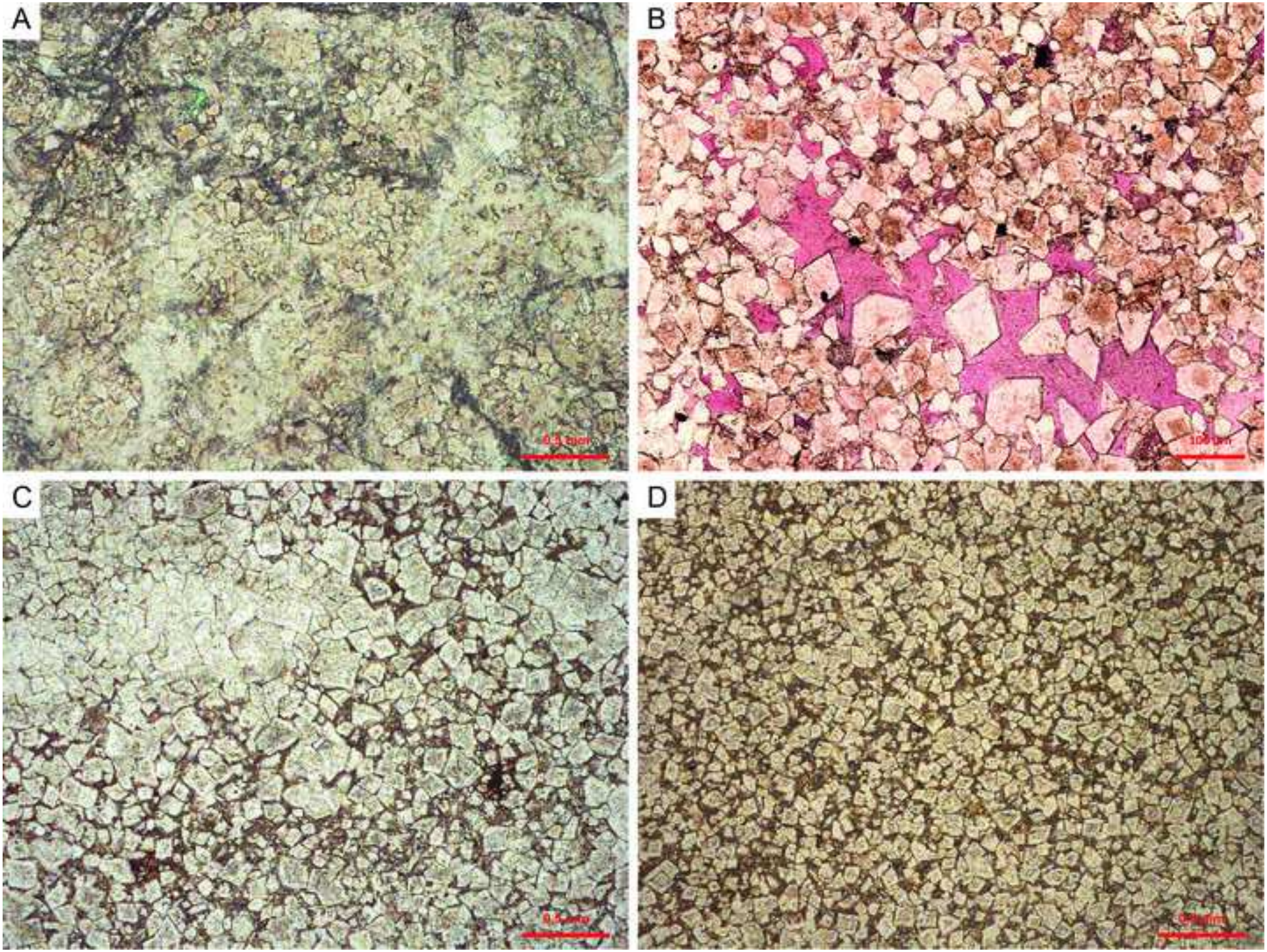

Figure 15

Click here to download high resolution image

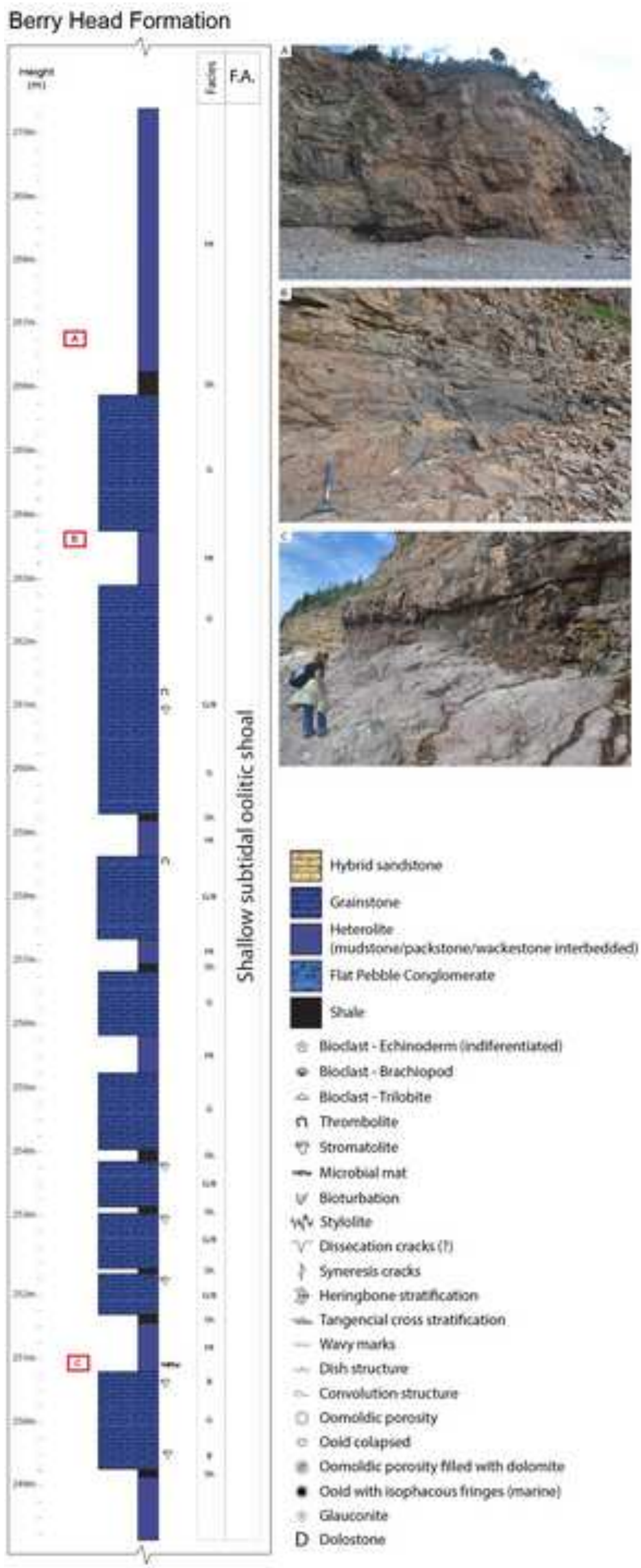

Figure 16

Click here to download high resolution image

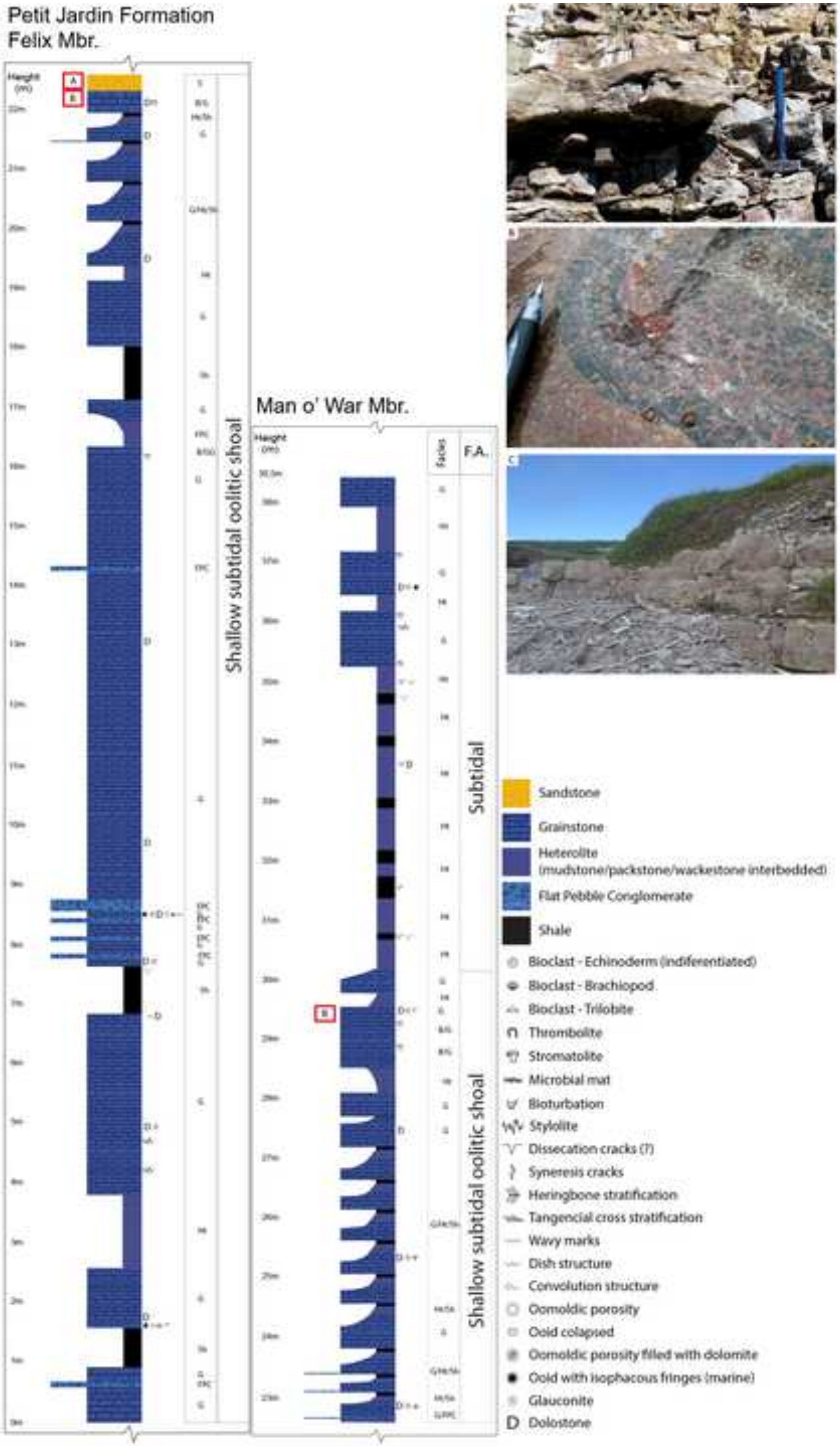

Figure 17

Click here to download high resolution image

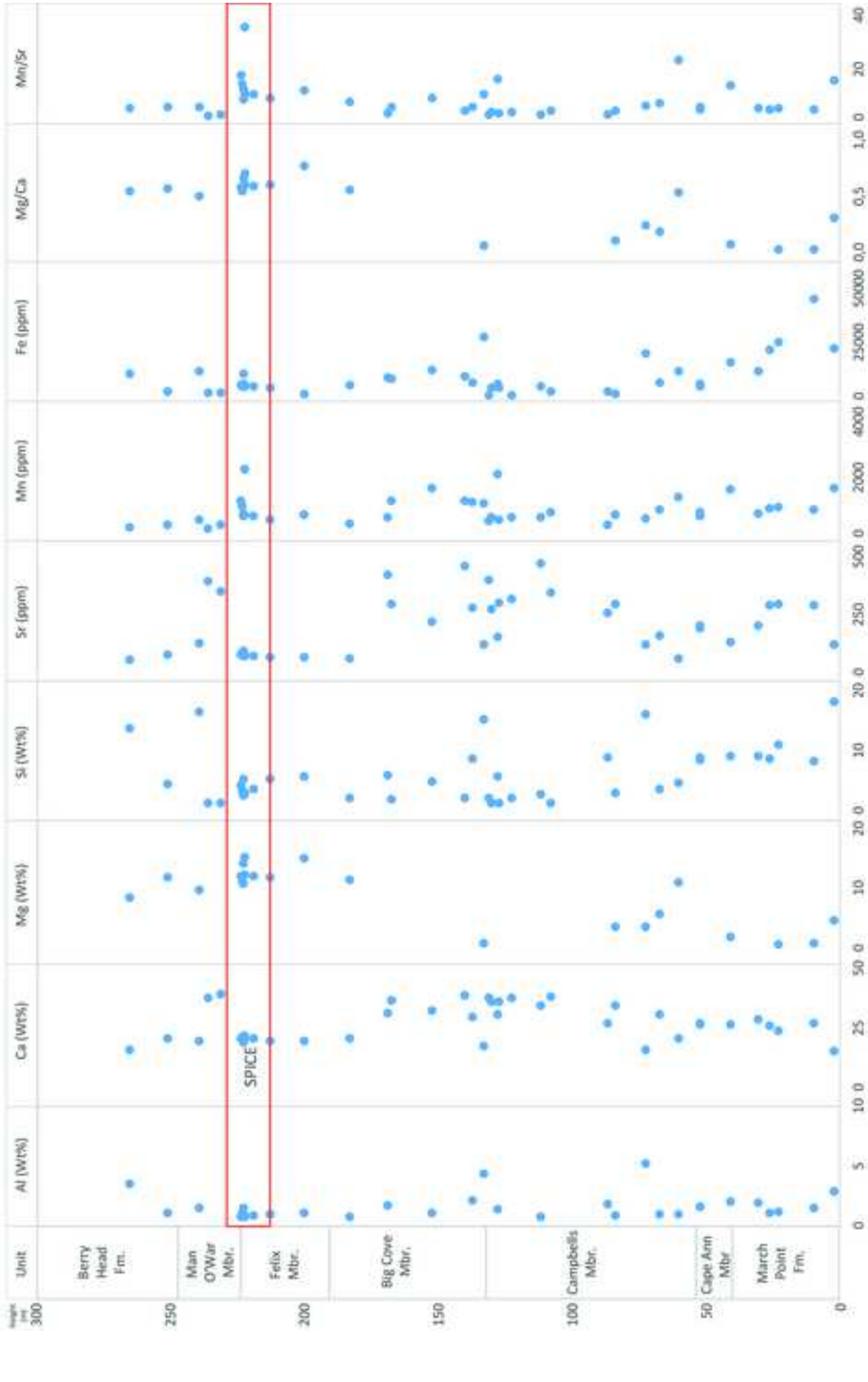

Figure 18

Click here to download high resolution image

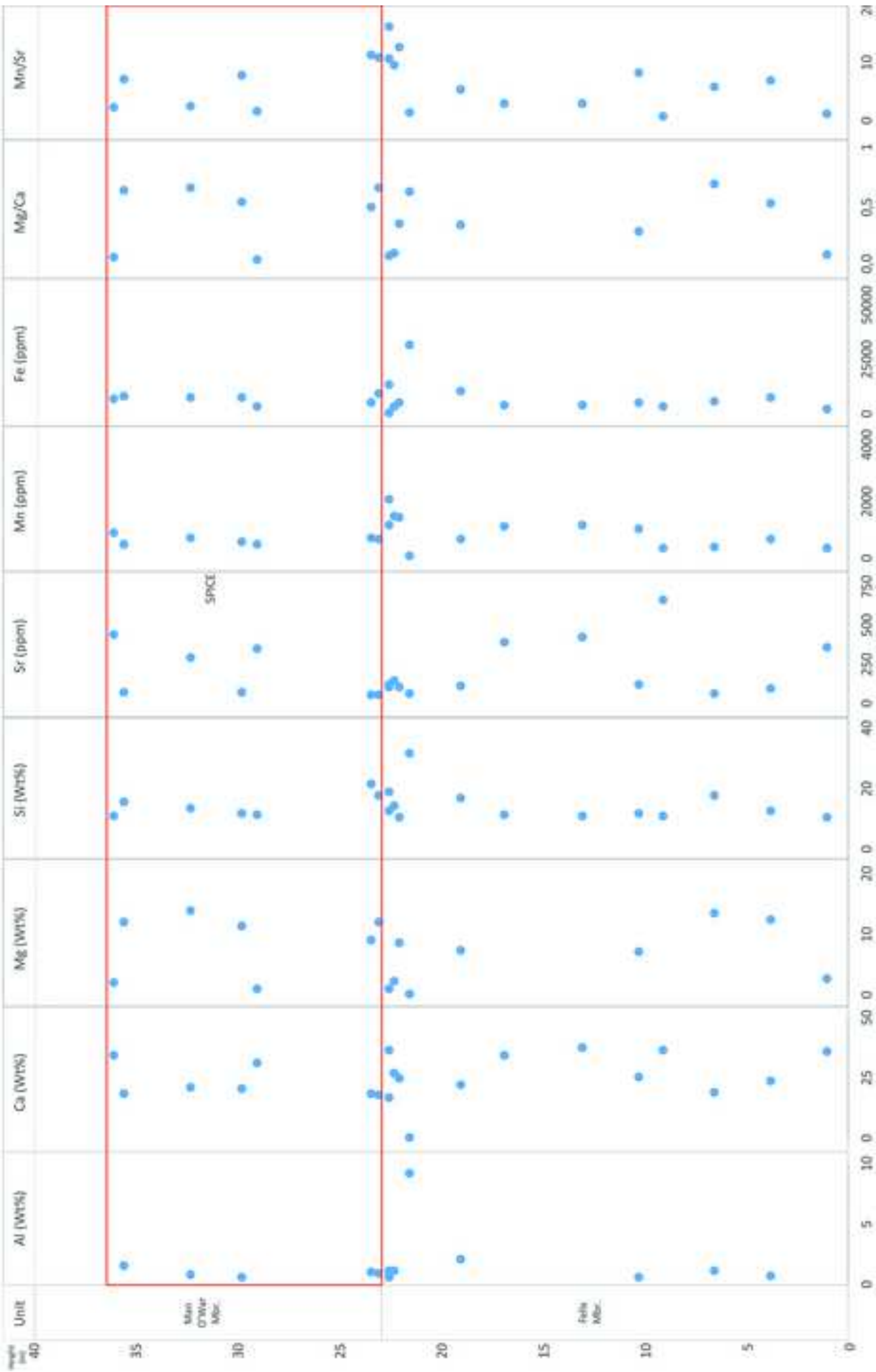

Figure 19
Click here to download high resolution image

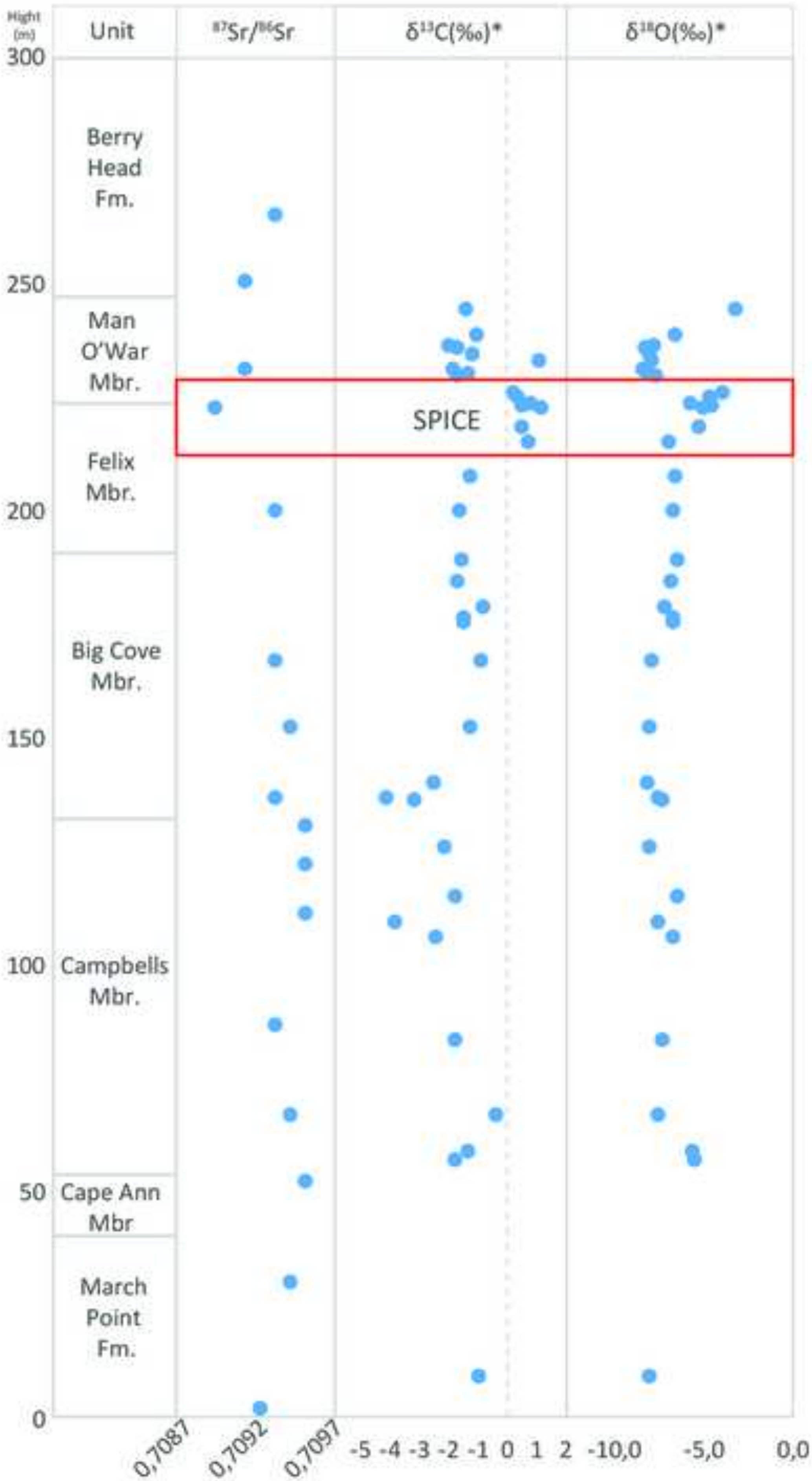

Figure 20
Click here to download high resolution image

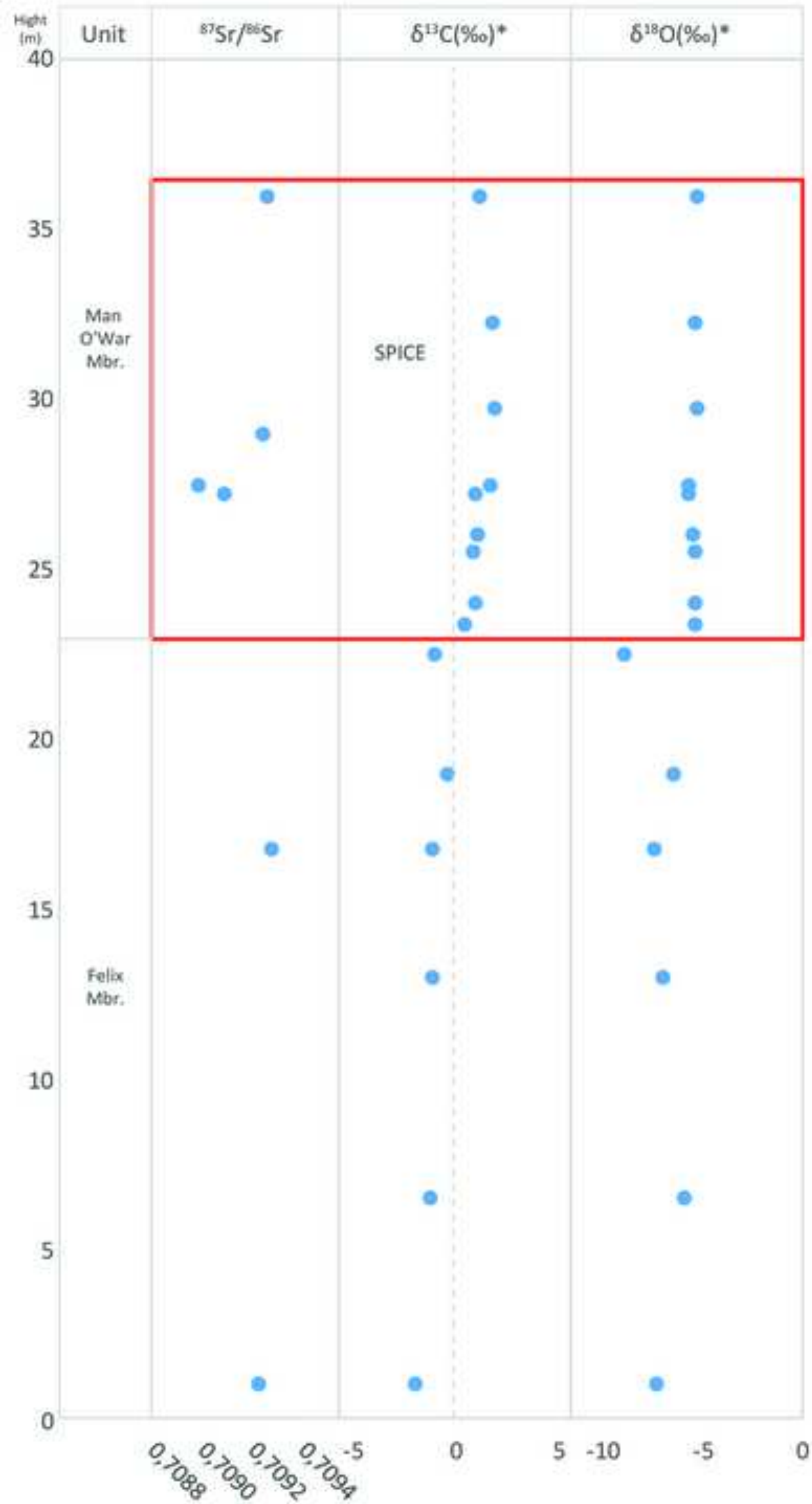

Figure 21
Click here to download high resolution image

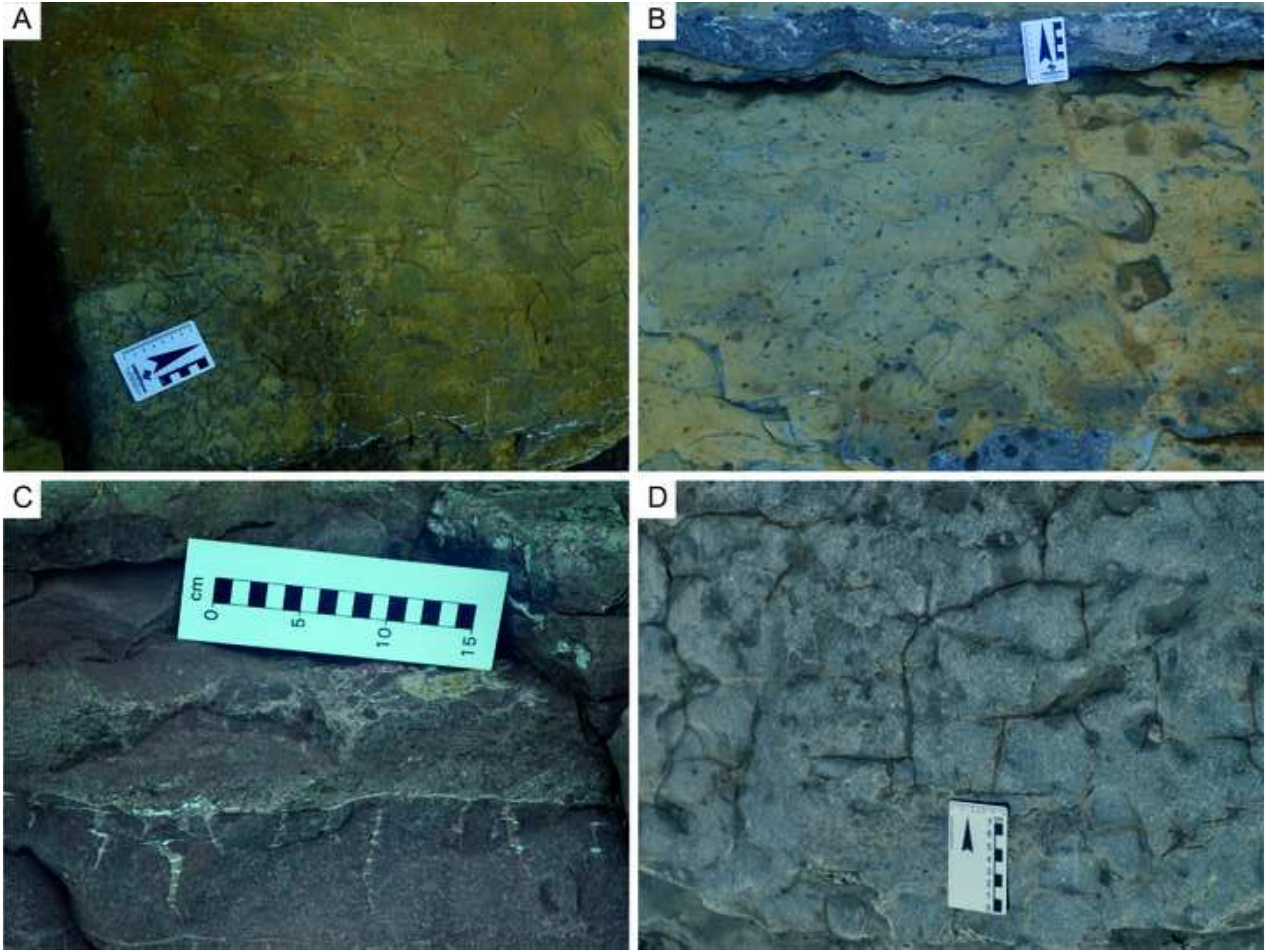

Figure 22
Click here to download high resolution image

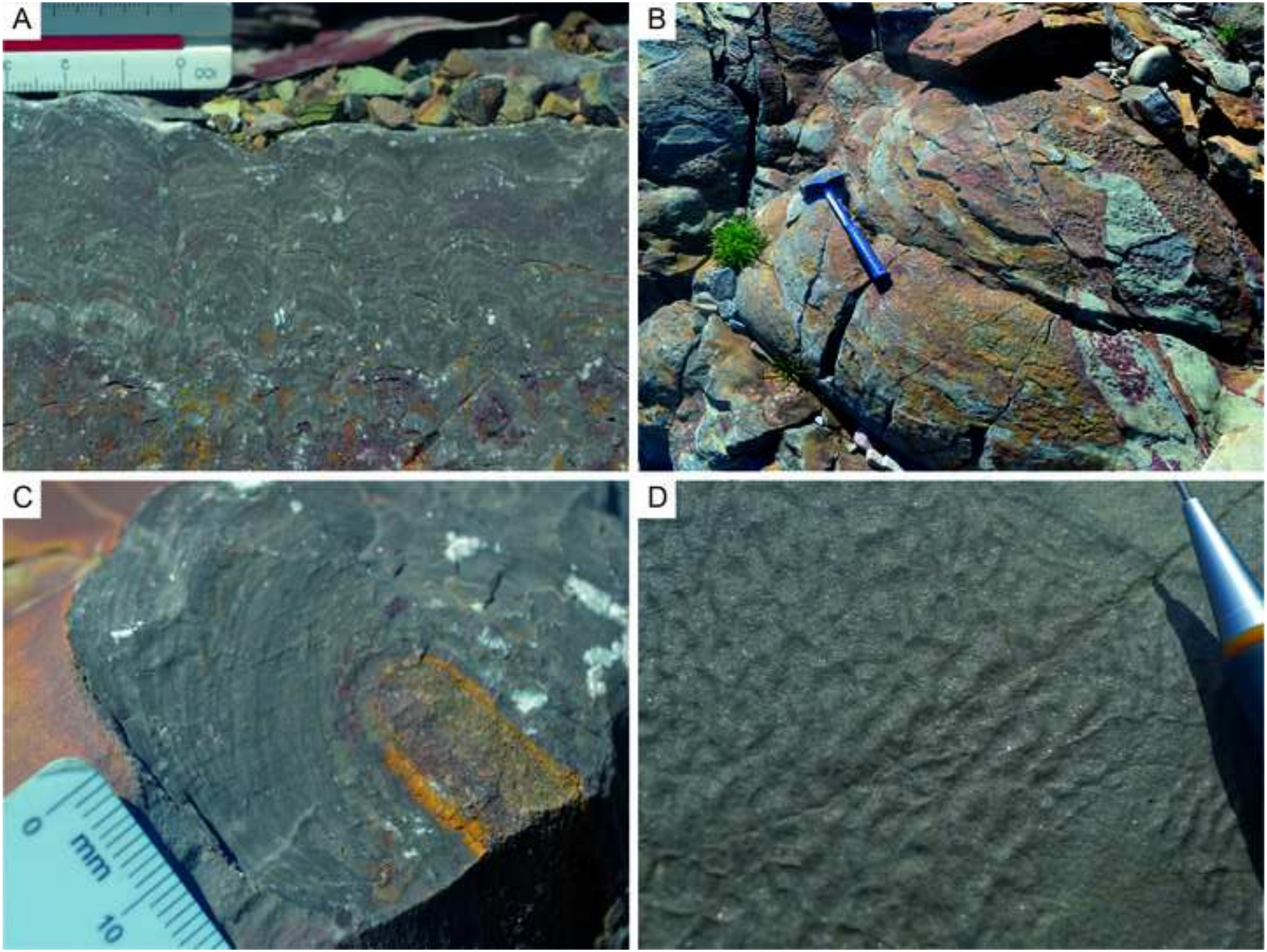

ARTIGO 3

DIAGENETIC PROCESSES AND PATTERNS IN CAMBRIAN CARBONATES FROM THE PORT AU PORT GROUP, NEWFOUNDLAND, CANADA

Artigo completo submetido ao periódico ***Facies***.

Submission ID: FACI-D-19-00064

Dear Miss Barili da Cunha,

Thank you for submitting your manuscript, Diagenetic Processes and Patterns in Cambrian Carbonates from the Port au Port Group, Newfoundland, Canada, to Facies.

The submission id is: FACI-D-19-00064
Please refer to this number in any future correspondence.

During the review process, you can keep track of the status of your manuscript by accessing the Editorial Manager Website.

Your username is: RosaliaBarili
If you forgot your password, you can click the 'Send Login Details' link on the EM Login page at https://www.editorialmanager.com/faci/

Should you require any further assistance please feel free to e-mail the Editorial Office by clicking on "Contact Us" in the menu bar at the top of the screen.

With kind regards,
Springer Journals Editorial Office
Facies

Facies

Diagenetic Processes and Patterns in Cambrian Carbonates from the Port au Port Group, Newfoundland, Canada

--Manuscript Draft--

Manuscript Number:	
Full Title:	Diagenetic Processes and Patterns in Cambrian Carbonates from the Port au Port Group, Newfoundland, Canada
Article Type:	Original Article
Keywords:	CAMBRIAN; DIAGENESIS; PORT AU PORT GROUP
Corresponding Author:	Rosalia Barili da Cunha, MSc Pontificia Universidade Catolica do Rio Grande do Sul BRAZIL
Corresponding Author Secondary Information:	
Corresponding Author's Institution:	Pontificia Universidade Catolica do Rio Grande do Sul
Corresponding Author's Secondary Institution:	
First Author:	Rosalia Barili da Cunha, MSc
First Author Secondary Information:	
Order of Authors:	Rosalia Barili da Cunha, MSc
	Argos Schrank, Master
	Joyce E. Neilson
	Luiz Fernando De Ros, Dr
Order of Authors Secondary Information:	
Funding Information:	Shell Brazil (-) — Miss Rosalia Barili da Cunha
Abstract:	The Port au Port Group is a mixed siliciclastic/carbonate sequence that marks the transition between Middle and Upper Cambrian, in western Newfoundland, Canada. This sequence is correlated to the Great North American Carbonate Bank formed during the evolution of the Iapetus Ocean in the surroundings of Laurentia. Petrographic analysis evidences early eodiagenesis occurings within marine phreatic conditions supported my extensive micritization and marine fibrous fringes. Calcite is the most abundant eodiagenetic constituent, occurring in different sorts of cement, related to phreatic meteoric zone. Microcrystalline dolomite also occurs as eodiagenetic process as result of mixing phreatic zones, where dissolution also occurs. With burial progression, mesodiagenesis starts, and dolomitization intensifies formatting blocky and saddle dolomite. The orogenic events that originated the Appalachians are also responsible by basin uplift and rock exposure, which telogianenetic products includes calcification of previous dolomites, dissolution and oxidation. Although extensive dolomitization, high strontium concentrations (up to 2000ppm) associated with the presence of fibrous fringes and preferential dissolution / replacement in bimineralic particles may be indicative of the original mineralogy of these rocks, requiring further studies.
Suggested Reviewers:	ANELIZE M. BAHNIUK anelize.bahniuk@ufpr.br EXPERTISE IN CARBONATE ROCKS
	RACHEL WOODS Rachel.Wood@ed.ac.uk EXPERTISE IN CARBONATE ROCKS
	ALCIDES SIAL

	sial@ufpe.br EXPERTISE IN CARBONATE ROCKS AND CHEMOSTRATIGRAPHY

Title: Diagenetic Processes and Patterns in Cambrian Carbonates from the Port au Port Group, Newfoundland, Canada

Author list

Barili, R.*, UFRGS/PUCRS, Porto Alegre, Brasil. Rosalia.barili@gmail.com; Rosalia.cunha@pucrs.br

Schrank, A. B. S., UFRGS, Porto Alegre, Brazil. argosssb@hotmail.com

Neilson, J. E., University of Aberdeen, Aberdeen. J.neilson@abdn.ac.uk

De Ros, L.F., UFRGS, Porto Alegre, Brazil. lfderos@inf.ufrgs.br

*Corresponding author

Abstract

The Port au Port Group is a mixed siliciclastic/carbonate sequence that marks the transition between Middle and Upper Cambrian, in western Newfoundland, Canada. This sequence is correlated to the Great North American Carbonate Bank formed during the evolution of the Iapetus Ocean in the surroundings of Laurentia. Petrographic analysis evidences early eodiagenesis occurings within marine phreatic conditions supported my extensive micritization and marine fibrous fringes. Calcite is the most abundant eodiagenetic constituent, occurring in different sorts of cement, related to phreatic meteoric zone. Microcrystalline dolomite also occurs as eodiagenetic process as result of mixing phreatic zones, where dissolution also occurs. With burial progression, mesodiagenesis starts, and dolomitization intensifies formatting blocky and saddle dolomite. The orogenic events that originated the Appalachians are also responsible by basin uplift and rock exposure, which telogianenetic products includes calcification of

previous dolomites, dissolution and oxidation. Although extensive dolomitization, high strontium concentrations (up to 2000ppm) associated with the presence of fibrous fringes and preferential dissolution / replacement in bimineralic particles may be indicative of the original mineralogy of these rocks, requiring further studies.

Keywords: CAMBRIAN, DIAGENESIS, PORT AU PORT GROUP

Acknowledgements

This work is part of the first author doctorate research, developed at do Rio Grande do Sul Federal University (UFRGS), Brazil, and partially funded by Shell. The authors gratefully acknowledge support from Shell Brasil through project BG05: UoA-UFRGS-SWB Sedimentary Systems, and the strategic importance of the Nacional Petroleum Agency (ANP) support, through its R&D levy regulation. We also would like to thank Dr. Alexander T. Brasier and Mr. John W. Still for the help during SEM/EDS analysis at the University of Aberdeen (UoA). The first author also acknowledge the Petroleum and Natural Resources Institute (IPR/PUCRS) colleagues for the support during the last few months, Prof. Marcia Boscato Gomes and Susan Drago, who helped with the Electron Microprobe analysis at UFRGS.

1. Introduction

The study of ancient carbonate rocks represents a considerable challenge, as their intense diagenesis normally erased their original fabrics and constituents. Deep burial, mesodiagenetic dolomitization and recrystallization can create barriers for petrographic and geochemical studies, destroying all evidence of original carbonate fabrics and mineralogy. Despite the difficulties brought by the diagenetic effects to the study of ancient carbonate rocks, remaining relict features may provide important clues about the ancient depositional and eodiagenetic environments.

The Port au Port Group corresponds to shallow-marine carbonate sediments deposited in an outer carbonate platform during the Cambrian (Williams 1976, 1979; Palmer and James 1979; Lavoie et al. 2012). Transgressive-regressive cycles identified in the group are correlated to the Cambrian Grand Cycles occurring throughout Laurentia (Chow 1985; Chow and James 1987a, b; Cowan and James 1993; Lavoie et al. 2012). The group is coeval with the SPICE, a strong positive carbon isotope excursion observed worldwide (Saltzman et al. 2000, 2004; Kouchinsky et al. 2008; Barili et al. 2018; Schmid et al. 2018) which may have occurred during an aragonite sea period (Neilson et al. 2016).

In this work, we present a study of the petrographic features of the Port au Port Group, integrating diagenetic processes, patterns and environments, and their connections to the depositional constituents and environments, where such reconstruction was possible. Additionally to the detailed petrographic characterization, Sr and Mg contents accessed through electron microprobe analysis, were used to investigate the probable original mineralogy of primary and early diagenetic constituents. This petrologic characterization, developed in combination with previous isotopic and facies studies

(Barili et al, 2019; in prep), aims to contribute to the understanding of a key period of global marine evolution.

1.1. Study area and geological background

The study area is located along the southern coast of the Port au Port Peninsula, western Newfoundland (Figure 1**Error! Reference source not found.**). Two key outcrop areas were studied. March Point comprises the most complete record of the Port au Port Group. Part of the Port au Port Group which shows the SPICE excursion outcrops at Felix Cove.

The Port au Port Group forms part of the autochthonous Cambrian-Ordovician sequence of the tectono-stratigraphic Humber zone of the northern Appalachian orogeny (Williams, 1976, 1979). It is interpreted as shallow-marine deposits from the outer part of a stable carbonate platform that surrounded the Iapetus Ocean (Williams 1976, 1979; Palmer and James 1979). These mixed carbonate-siliciclastic deposits record the gradual transition from Early Cambrian siliciclastic deposition to predominantly carbonate sedimentation in the Early Ordovician (Chow, 1985; Chow & James, 1987b; Cowan & James, 1993). The Group is composed of three formations, namely the March Point, Petit Jardin (with Cape Ann, Campbells, Big Cove, Felix and Man O'War Members) and Berry Head Formations.

Transgressive-regressive cycles are identified through the Port au Port Group (Figure 2), which are correlated to the Cambrian Grand Cycles occurring throughout Laurentia (Chow, 1985; Chow & James, 1987a, 1987b; Cowan and James 1993; Lavoie et al. 2012). The marine transgression at the beginning of the Grand Cycles resulted in a shallow subtidal environment, where ribbon limestones were deposited passing upward to into oolitic shoals of the upper half cycle (Cowan and James 1993). As sea level dropped at the top of the cycles, the environment returned to more restricted water circulation, although extensive evidence of subaerial exposure is absent (Chow 1985; Chow and James 1987a). Carbon isotope data for the Port au Port Group carbonates at Felix Cove show a strong positive $\delta^{13}C_{carb}$ excursion between the Felix and Man O'War Members (top of cycle B, Fig. 2), which has been interpreted as the SPICE (Saltzman et al. 2004; Barili et al. 2018).

2. Methodology

2.1. Petrography

The fieldwork was performed along March Point and Felix Cove, two main representative areas on the southern coast of the Port au Port Peninsula (Figure 1). Forty-five samples were selected from representative layers for petrographic characterization at March Point, and twenty samples were selected at Felix Cove. The samples were impregnated with blue epoxy resin for the preparation of polished thin sections. For identification of the carbonate species, the thin sections were stained with a solution of alizarin red S and potassium ferricyanide (Dickson, 1965). Quantitative and qualitative petrographic analysis was performed at the do Rio Grande do Sul Federal University (UFRGS).

2.2. SEM/BSE and Cathodoluminescence

The composition, habits, and paragenetic relations of diagenetic constituents were examined through scanning electron microscopy (SEM) with support of energy-dispersive X-ray spectrometry (EDS) analysis for compositional information of specific constituents, using a Carl Zeiss Gemini SEM 300 – high resolution Field Emission Scanning Electron Microscope (FESEM). Cathodoluminescence (CL) analyses were performed during SEM scanning, using a Centaurus CL detector, but also using a

Technosyn Mk III cold CL microscope, operated at c. 15 kV. Both, SEM and cold CL analysis were performed at the University of Aberdeen laboratories.

2.3. Electron microprobe

In order to identify the compositional variations in the ooids and riming interparticle cements, three selected polished thin sections were analyzed using wavelength dispersive spectrometry (WDS) in the Microprobe Laboratory of UFRGS, using a CAMECA SXFive electron microprobe.

3. Results

3.1. Petrography

3.1.1. Primary texture and composition

The analyzed rocks include oolitic grainstones (Figure **3**A), intraclastic and bioclastic floatstones (all carbonate rock classes *sensu* Embry III and Klovan 1971; Figure **3**B and 3C), intraclastic rudstones (Figure **3**D), wackestones, packstones, glauconite-siliciclastic and carbonate-siliciclastic hybrid arenites (*sensu* Zuffa 1980), quartzarenites (*sensu* Folk, 1968), and mudrocks. Their main primary constituents are described below.

The ooids show radial and concentric structures, commonly altered by micritization, recrystallization and dolomitization (Figure 3A and 3E). These are cases with internal radial structure and external non-concentric concentric envelopes, or with internal non-radial concentric structure with an external radial envelope. Evidence for an original bimineralic composition is indicated by selective dissolution or replacement of some envelopes. Radial envelopes seem to have been more dissolved or replaced, while concentric envelopes generally maintained their structure. Complete dissolution of ooids generated large oomoldic pores, which were commonly filled by well-developed calcite or dolomite crystals, commonly in optical continuity with the interparticle cement. Locally, prismatic calcite rims lined the oomoldic pores before their filling by coarse cement. Commonly micritized, dolomitized and/or recrystallized peloids, intraclasts, bioclasts (mainly of trilobites) are the most frequent ooid nuclei.

Carbonate peloids are generally micritized and dolomitized (Figure 3B) and are usually associated with microbial intraclasts. Oncoids show intraparticle dissolution filled by dolomite and locally displacive calcite that deformed their shape. Bioclasts are also commonly micritized, with trilobites and echinoderms (crinoids) being the most frequent (Figure **4**B and 4C). Brachiopods appear as fragments in the thin sections, and as whole shells in the field, mostly within lime mudstones, mudstones and shales.

Intraclasts appear in a range of lithologies. Microbial intraclasts are micritic, dolomitized and locally compacted to pseudomatrix (Figure 3B), being identified due to their characteristic clotted fabric. Grainstone intraclasts show varied texture and composition. Commonly these are a mixture of carbonate ooids, peloids and bioclasts with siliciclastic grains and glauconite peloids in subordinate concentrations, cemented by mosaic or microcrystalline calcite. Some intraclasts also show radial-prismatic cement or fibrous rims. Hybrid intraclasts are commonly glauconitic and composed by glauconite peloids and siliciclastic quartz sand. Mud intraclasts are frequent in the field and appear partially compacted to pseudomatrix, or replaced by calcite in siliciclastic and hybrid rocks.

Quartz grains are generally monocrystalline, but occasionally polycrystalline (Figure 4D). Microcline is the most common feldspar, but plagioclase is also present. In the carbonate rocks, quartz and feldspars occur as sub angular, smaller grains, while in sandstones these occur as well-rounded grains. Glauconite peloids were replaced by microcrystalline calcite/dolomite or compacted to pseudomatrix, occurring mainly in hybrid arenites, and, in in small amounts, in carbonate rocks. Other constituents include phosphatic brachiopods, phosphatic peloids, phosphatic intraclasts (siliciclastic sand cemented by phosphate), muscovite and glauconitized micas. Carbonaceous organic matter was also observed, usually associated with stylolites.

The hybrid arenites are composed of a mixture of glauconitic and siliciclastic grains with carbonate bioclasts and intraclasts. The siliciclastic sandstones are composed mainly by well-rounded quartz grains with small amounts of feldspar grains, and rare mud intraclasts and carbonate particles, and cemented by calcite.

3.1.2. Diagenetic processes and products

Several of the studied samples present partially dissolved/neomorphized fibrous rims covering the particles. The oolitic grainstones show well-developed fibrous rims (Figure 4E), while the hybrid arenites show only thin, incipient rims. Some samples display radial prismatic pore-filling cement covering the fibrous rims, which were locally fragmented and replaced by microcrystalline dolomite.

Micritization is a frequent early diagenetic feature in the analysed samples (Figure 3A, Figure **4**C). Calcite cementation appears in variable habits, including as radial-prismatic cement covering fibrous rims, mainly on ooids and trilobite bioclasts (Figure 4A, 4F, and 5A). These rims locally fill shelter porosity under trilobite bioclasts. Calcite also occurs as mosaic cement, filling oomoldic porosity (Figure 3A and Figure **5**A), and filling veins along rock fractures. Syntaxial calcite overgrowths are common on echinoderm bioclasts (Figure 4C). Locally radial-prismatic, followed by mosaic calcite was observed filling vugular porosity and displacing particles. Micro- to macrocrystalline, in places ferroan calcite also filled intercrystalline porosity and dolomite dissolution porosity (Figure 5B), rock fractures, and replaced directly blocky and saddle dolomite (Figure 5C). Microcrystalline calcite also replaced glauconite peloids. Compositional variation between ferroan and non-ferroan calcite is locally shown within the radial prismatic and mosaic cements (Figure 4E).

Dolomite occurs as one of the most frequent diagenetic products, especially in the intraclastic floatstones. Microcrystalline dolomite replaced the particles, partially preserving their internal structure, as well as the fibrous calcite rims and pseudomatrix generated by compaction of intraclasts. Blocky dolomite replaced the allochems and pseudomatrix, but also previous calcite cement (mosaic and radial-prismatic) and precipitated directly as a cement (Figure 5B and 5D). Locally, dolomite filled intraparticle porosity in dissolved ooids (Figure 3F, Figure **5**E and 5F), vugular and intraparticle porosity (Figure 4F, Figure **5**B and 5E). Dolomite is locally concentrated in stylolites. Saddle dolomite is also present, replacing calcite cement and filling porosity created by calcite and blocky dolomite dissolution.

Pseudomatrix was formed through the compaction of glauconite peloids and mud intraclasts in hybrid rocks, mud intraclasts in siliciclastic and carbonate rocks, and microbial intraclasts and peloids in carbonate rocks. Discontinuous K-feldspar and quartz overgrowths were observed in hybrid and siliciclastic rocks, and very scarce blocky quartz was observed in interparticle porosity and replacing calcite in hybrid rocks.

Partially oxidized pyrite is present in a variety of habits, including microcrystalline, macrocrystalline, framboidal and blocky, replacing carbonate particles and organic matter. Iron hydroxides/oxides, as well as pyrite, occur as microcrystalline aggregates replacing dolomite and filling dolomite dissolution porosity and intercrystalline porosity among dolomite crystals. In the field, dolomitized layers are generally pinkish, indicating late, telodiagenetic dolomite oxidation.

In general, porosity was obliterated by cementation and compaction. Just two thin sections presented any remaining visible porosity. In these cases, partial cementation by calcite rims and then dolomite was able to sustain the fabric and preserve the original interparticle porosity as well as some oomoldic porosity (Figure 5F). Porosity generated by partial dissolution of intraclasts and complete dissolution of ooids was totally filled by dolomite. Vugular porosity formed by particle and cement dissolution was also filled by calcite and dolomite (Figure 5A), mostly in the oolitic grainstones and intraclastic floatstones. Although for the intense diagenesis to which these rocks were subjected, the dissolved particles were recognized as ooids by the fibrous rims which marked the moldic porosity later filled by dolomite and calcite, and by the original shape of the grains.

3.2. SEM/BSE and Cathodoluminescence

Samples of oolitic grainstones of the Campbells Member were observed using SEM techniques with BSE and CL detectors (Figure 6). The gray scale in BSE images shows the dolomitization patterns, with the dark gray areas corresponding to dolomite. BSE images show the partial, selective dolomitization of external envelopes of the ooids and their fibrous rims. The CL patterns of dolomitized ooids, with irregular dull and bright luminescence areas, indicates different stages and environments of dolomitization.

3.3. Electron microprobe

The chemical composition of specific constituents of selected samples analyzed by electron microprobe commonly show high strontium concentrations, with the higher values corresponding to the fibrous rims (up to 2000 ppm – 0.20Wt%) and some ooid envelopes. The crinoid bioclasts and their syntaxial overgrowths contain near to 0 Wt% Sr, indicating an originally calcitic composition (Figure 7).

4. Discussion

4.1. Diagenetic pathways

Considering the main described diagenetic features, four main evolution pathways could be recognized in the Port au Port Group (PAP) carbonate rocks. Different diagenetic evolution patterns were defined for the oolitic grainstones, for grainstones and floatstones rich in carbonate peloids and microbial intraclasts, for bioclastic grainstones and floatstones, and for rudstones composed of carbonate sand intraclasts. These main diagenetic patterns are discussed below in relation to their eodiagenetic environments (cf. Longman 1980; James and Choquette 1983). These diagenetic pathways are summarized in Figure 8 and Figure **9**.

4.1.1. Oolitic grainstones

Grainstones predominantly of ooliths, with subordinate crinoid and trilobite bioclasts, microbial and oolitic intraclasts, show characteristically the diagenetic evolution represented in Figure 8. Micritization developed during very early diagenesis allowed the identification of particle shapes even after intense calcite/dolomite replacement. Micritization was probably developed under near stagnant marine phreatic conditions (Longman, 1980; James and Choquette, 1983). Chow (1985) and Chow and James (1987b) interpreted that micritization involved a stabilization of originally aragonitic particles to calcite, preventing their complete dissolution (Flügel, 1982). Fibrous isopachous rims were precipitated in the active marine phreatic zone (Longman, 1980; James and Choquette, 1983). Such fibrous rims are normally composed of calcite, high magnesium calcite (HMC) or aragonite (Flügel, 1982; James and Choquette, 1983; Tucker, 1985; 1993; 2001; Chow and James, 1987b). Their partial dissolution, dolomitization and recrystallization, renders it difficult to determine their original composition. However, the well-developed fibrous habit, and the high Sr content of the rims of some samples (Fig. 7) may indicate an originally aragonitic composition.

Dissolution was very selective in these grainstones, affecting only some ooid envelopes, or completely dissolving some others, leaving oomoldic pores. Porosity was preserved after total or partial dissolution and cementation by fibrous rims. The very heterogeneous dissolution of particles in the same sample, or even of different envelopes within a same ooid, indicates compositional variations in the original mineralogy. Originally calcitic particles or particles that were micritized, suffered little dissolution, while those with probably original aragonitic composition were completely dissolved. This process occurred within the meteoric phreatic dissolution zone (cf. Longman 1980; James and Choquette 1984).

Radial-prismatic pore-filling cement followed the fibrous rims partially replacing them, and displaying optical continuity with the ooids. This cement was precipitated within the active meteoric phreatic zone (Longman, 1980; James and Choquette, 1984). However, part of the prismatic habit may be due to recrystallization of the fibrous rims. Some of the radial-prismatic cementation occurred intraparticle after dissolution of the ooids. Calcite oomoldic and interparticle porosity filling also occurs as mosaic cement (Figure 8B), related to the active phreatic zone. Fractured and deformed ooids show evidence of mechanical compaction, likely related to limited cementation after ooid dissolution. Stylolites generated by chemical compaction are generally associated with the presence of organic matter.

Oolitic grainstones commonly show two stages of dolomitization. The first, which occurred probably during eodiagenesis due to mixing with meteoric waters (cf. Longman, 1980), microcrystalline dolomite extensively replaced carbonate allochems, partially preserving their internal structures. During the second, probably related to mesodiagenesis (Machel 2005), blocky and saddle dolomite replaced calcite cement and carbonate particles, and filled most remaining interparticle or intraparticle porosity. Pores remaining after late dolomite precipitation and fractures were filled by macrocrystalline, locally ferroan calcite. Telodiagenesis included partial dissolution of dolomite and its replacement by calcite (‘dedolomitization’; Sellwood et al. 1987) and iron oxides/hydroxides, which produce the characteristic pinkish color seen in the field.

4.1.2. Microbial intraclastic floatstones and grainstones

Floatstones and grainstones characterized by predominance of microbial intraclasts and carbonate peloids, with minor ooids, subordinate oolitic intraclasts and rare bioclasts show a characteristic diagenetic evolution (Figure 8). Their diagenesis also started with micritization, followed by fibrous rims and porosity from ooid dissolution later infilled. The main diagenetic process in these rocks was microcrystalline dolomitization, probably developed under eodiagenetic conditions (Longman, 1980; Machel, 2005) and consequent preservation of the original structure of the particles. The fibrous rims, also here commonly replaced by microcrystalline dolomite, preserved the particle outlines, allowing the identification of completely dissolved/filled ooids. The mechanical compaction of microbial intraclasts generated pseudomatrix, and chemical compaction formed stylolites.

During burial, blocky dolomite was precipitated as cement and replacing calcite cement and particles. Cementation is more significant in the intraclastic rocks with a higher content of ooids. The blocky dolomite cement was later dissolved and replaced by calcite, which filled the remnant porosity generated by calcite dissolution and the dolomite-dissolution intracrystalline porosity. Locally, a new phase of calcite dissolution created porosity later filled by saddle dolomite. Calcite veins formed after compaction and cementation cut the previous phases. Telodiagenetic iron oxides and hydroxides were formed within the remaining porosity and replacing dolomite (Figure 8).

4.1.3. Bioclastic grainstones and floatstones

Grainstones and floatstones essentially composed of trilobite and crinoid fragments, with subordinate ooids and rare intraclasts and brachiopod shells, commonly display the diagenetic evolution schematically represented in Figure 9. This paragenetic sequence also begins with micritization of the bioclasts, followed by precipitation of fibrous rims, later recrystallized. Radial-prismatic cement, precipitated on ooids and trilobite bioclasts, concomitant with syntaxial overgrowths on the crinoids. Mosaic calcite cementation filed the remaining porosity and was followed by blocky dolomite replacing previous cements and particles (Figure 9).

4.1.4. Intraclastic rudstones

Rudstones constituted of intraclasts of oolitic-peloidal-bioclastic grainstones cemented by calcite, show an abbreviated evolution (Figure 9). The diagenetic sequence is a simplification of that of the oolitic grainstones, beginning with micritization and fibrous rim formation, followed by radial-prismatic cementation. Local stylolitization is associated with organic matter. Dolomite replaced the particles and was later calcitized (Figure 9D).

The extensive early diagenesis by micritization and fibrous marine rim cementation was responsible for the formation of oolitic hardgrounds formed in the subtidal/shallow subtidal zone, especially in the shoal's mobile fringe, as well as of these intraclastic deposits ('flat pebble conglomerate'; Chow, 1985; Chow & James, 1992). Such early lithification occurred not only in carbonate, but also in hybrid deposits.

4.1.5. Dissolution

Locally, a paragenetic evolution characterized by more intense dissolution occurred both in the bioclastic grainstones and in the intraclastic-peloidal-floatstones. The sequence was initiated, as usual, by micritization and precipitation of fibrous rims. While the floatstones were compacted, the grainstones experienced partial to total dissolution, generating oomoldic porosity. Particles and fibrous rims were replaced by microcrystalline dolomite, and partially affected by a new dissolution event. Blocky dolomite cement filled the remaining porosity (interparticle, oomoldic, and intraparticle in intraclasts).

The diagenetic pathways presented have similarities, with intense early diagenesis within phreatic marine conditions associated with lower sedimentation rates, allowing hardgrounds and later intraclast formation observed throughout the group. Through subsidence and burial progression, but still within the eodiagenesis in the mixing phreatic zone allowed the formation of microcrystalline dolomite, and later evolved to mesodiagenesis evidenced by mechanical compaction and second dolomite formation. The exposure of the sequence, related to the orogeny events that originates the Appalachians (Williams 1976, 1979, 1995), is evidenced by the dolomite calcitization and oxidation of ferroan contend in dolomite, leading to the diagnostic pinkish color in the outcrops.

4.1.6. Evidence on the original mineralogy

Chow (1985) and Chow and James (1992) refer to bimineralic ooids, mainly in the upper Cambells Member, but also to the upper half of the Grand Cycles of the PAP. Such particles are characteristically partially dolomitized, with selectively replaced external envelopes, while internal envelopes maintain their calcitic mineralogy. Several dolomitized envelopes may occur in one specific particle, while others exhibit preserved, non-dolomitized concentric structures. Some samples contain completely dolomitized ooids together with calcitic ooids with well-preserved concentric structure.

Chow (1985) related the compositional differences in these bimineralic ooids to their radial, radial-concentric and concentric structure, attributing these differences to widespread chemical conditions, controlled by environmental conditions. In her model, the well preserved radial and radial concentric ooids would have a primary calcitic composition, while the envelopes that were either micritized or replaced by fine to medium calcite would be originally aragonitic (Chow 1985; Chow and James 1987b).

Other petrographic evidence of the primary mineralogy of the ooids is the occurrence of oomoldic porosity and partially dissolved ooids together with well-preserved particles. Very few samples exhibit any remaining preserved porosity. However, oomoldic pores are commonly filled by several euhedral crystals, or by a single large dolomite crystal, in cases after lining of these pores by prismatic calcite rims. Partially dissolved/recrystallized/filled ooids are also considered as indicative of HMC mineralogy, since aragonite is unstable under meteoric water and HMC is also prone to dissolution when interacting with unsaturated ($CaCO_3$) fluids (Flügel 1982; Tucker 1985, 1993, 2001; Tucker and Wright 1990).

Further evidence on the original mineralogy is indicated by the results of microprobe analyses, which show relatively high Sr levels in some ooids and associated fibrous rims (up to 2000ppm; 0.2 Wt%). These high Sr levels may be related to an original aragonite/HMC mineralogy (Assereto and Folk, 1980). In high-Mg calcite, higher Sr concentrations is allowed by disturbance of the atomic arrangement caused by the Mg^{2+} (Berner 1975; Zhang and Dawe 2000). Elevated Sr concentrations in HMC are reported to range between 600 and 1800ppm (Dickson, 2014), but Holocene abiotic HMC cements have lower Sr content than the maximum reported by Neilson et al. (2016) for fibrous cements from the Upper Cambrian of Oman’s Upper Cambrian, thought to have originally been composed of aragonite or HMC.

The presence of high amounts of Sr in these ancient fibrous cements presently suggests that they may have originally been composed of aragonite or HMC (Neilson et al. 2016). Heterogeneous oomoldic porosity, as well as the selective dissolution/recrystallization may also suggest an originally HMC/aragonite mineralogy for some of the ooids. However, this is only observed at the top of the Grand Cycles of the PAP, when the environment is likely to have been more restricted. These layers were further affected by extensive dolomitization, which is more accentuated in the Felix Member and Berry Head Formation.

The early fibrous cementation observed in PAP, was considered by Chow (1985) to have originally been originally aragonite or HMC. An original HMC composition of early cements, may still be recognized after neomorphism, especially if associated with microdolomite (Lohman and Meyers 1977; Longman 1980). The occurrence of microdolomite in the PAP is reported here within the oolitic grainstones of the Campbells Member (Figure 6), pointing to a possible HMC or aragonite composition. This and other evidence presented, reinforces the possibility that HMC/aragonite may have been precipitated from seawater as previously suggested for these rocks (Chow 1985; Chow and James 1987b) and for the SPICE layer (Neilson et al. 2016).

Considering the discussion above, the seawater composition during Middle to Upper Cambrian, previously believed as a calcite sea period (Hardie 1996; Stanley and Hardie 1998; Stanley et al. 2010), may in fact be related to a time of compositional changes. The SPICE coincides with a period with trilobite mass extinctions, possibly related to food chain disruption or anoxia, across Gondwana (Australia, Kazakhstan, and South China), and with a maximum regression, related to the Sauk II-III transition, within a major transgression trend in Laurentia (Cowan and James 1993; Saltzman et al. 2000, 2004; Lavoie et al. 2012; Neilson et al. 2016). Despite this coeval mass extinction worldwide and at the base of SPICE in Laurentia, it was also a time of life diversification (Palmer 1965; Saltzman et al. 2000), suggesting that while some organisms were disappearing due to environmental changes, including tectonism and seawater circulation and composition, others were spreading due favorable conditions.

5. Conclusions

Cambrian Port au Port Group rocks analyzed in two representative areas include oolitic grainstones, intraclastic and bioclastic floatstones, intraclastic rudstones, wackestones, packstones, glauconite-siliciclastic and carbonate-siliciclastic hybrid arenites, quartzarenites, and mudrocks. The effects of diagenesis in the Port au Port carbonate rocks can be synthetized in four main evolution pathways, according to their original composition and to the environment evolution. Early micritization contributed locally to stabilize particles originally composed of high-Mg calcite and/or aragonite. Fibrous rims were also precipitated very early, from seawater saturated with respect to HMC and/or aragonite.

Fine-crystalline dolomitization, which may have been formed in a mixing zone, preserved the fabrics of particles and early cements. Early dissolution, recrystallization and infilling of oomoldic porosity were generated within an active phreatic meteoric environment. Radial-prismatic, syntaxial overgrowths, mosaic and other calcite cements were precipitated in an active phreatic meteoric environment. Coarse blocky to saddle dolomite is the most frequent mesodiagenetic constituent, being more abundant.

Although these rocks have undergone extensive diagenesis, the presence of fibrous fringes with high Sr concentration and different degrees of dissolution/recrystallization of bimineralic ooids may be indicative of the original mineralogy. These features occur prior to and including the SPICE layer, suggesting a period of seawater chemistry prone to HMC/aragonite formation, therefore, requiring further investigation.

6. References

Assereto R, Folk RL (1980) Diagenetic fabrics of aragonite, calcite and dolomite in an ancient peritidal- spelean environment: Triassic Calcare Rosso, Lombardia, Italy. J Sediment Petrol 50:371–394

Barili R, Neilson JE, Brasier AT, et al (2018) Carbon isotopes, stratigraphy, and environmental change: the Middle–Upper Cambrian Positive Excursion (SPICE) in Port au Port Group, western Newfoundland, Canada. Can J Earth Sci 55:1209–1222. doi: 10.1139/cjes-2018-0025

Berner RA (1975) The role of magnesium in the crystal growth of calcite and aragonite from sea water. Geochim Cosmochim Acta 39:. doi: 10.1016/0016-7037(75)90102-7

Chow N (1985) Sedimentology and diagenesis of Middle and Upper Cambrian platform carbonates and siliciclastics, Port au Port Peninsula, western Newfoundland. Thesis (Unpublished) 458

Chow N, James NP (1992) Synsedimentary diagenesis of Cambrian peritidal carbonates: evidence from hardgrounds and surface paleokarst in the Port au Port Group, western Newfoundland. Bull Can Pet Geol 40:115–127

Chow N, James NP (1987a) Cambrian Grand Cycles : A northern Appalachian perspective. Geol Soc Am Bull 98:418–429. doi: 10.1130/0016-7606(1987)98<418

Chow N, James NP (1987b) Facies specific, calcitic and bimineralic ooids from Middle and Upper Cambrian platform carbonates, Western Newfoundland, Canada. J Sediment Petrol 57:907–921

Cowan CA, James NP (1993) The interactions of sea-level change, terrigenous-sediment influx, and carbonate productivity as controls on Upper Cambrian Grand Cycles of western Newfoundland, Canada. Geol Soc Am Bull 105:1576–1590. doi: 10.1130/0016-7606(1993)105<1576:TIOSLC>2.3.CO;2

Dickson JAD (1965) A modified staining technique for carbonates in thin section. Nature 205:587–587

Dickson JAD (2014) Marine Beachrocks. Carbonate Diagenesis Ltd.

Embry III AF, Klovan JE (1971) A late Devonian reef tract on northeastern Banks

Island, NWT. Bull Can Pet Geol 19:730–781

Flügel E (1982) Carbonate Diagenesis. In: Microfacies Analysis of Limestones. pp 64–104

Hardie LA (1996) Secular variation in seawater chemistry: An explanation for the coupled secular variation in the mineralogies of marine limestones and potash evaporites over the past 600 m.y. Geology 24:279–283. doi: 10.1130/0091-7613(1996)024<0279:SVISCA>2.3.CO;2

James NP, Choquette PW (1983) Diagenesis 6. Limestones — The Sea Floor Diagenetic Environment. Geosci Canada 10:162–179

James NP, Choquette PW (1984) Diagenesis 9. Limestones - The Meteoric Diagenetic Environment. Geosci Canada 11:161–194

Kouchinsky, Bengtson S, Gallet Y, et al (2008) The SPICE carbon isotope excursion in Siberia: a combined study of the upper Middle Cambrian–lowermost Ordovician Kulyumbe River section, northwestern Siberian Platform. Geol Mag 145:609–622. doi: 10.1017/S0016756808004913

Lavoie D, Desrochers A, Dix G, et al (2012) The great American carbonate bank in eastern Canada: An overview. In: Derby J, Fritz R, Longacre S, et al. (eds) AAPG Memoir 98 Great American Carbonate Bank. AAPG, pp 499–523

Lohman KC, Meyers WJ (1977) Microdolomite inclusions in cloudy prismatic calcites: A proposed criterion for former high-magnesium calcite. J Sediment Petrol 47:1078–1088

Longman MW (1980) Carbonate Diagenetic Textures from Nearsurface Diagenetic

Environments^. Am Assoc Pet Geol Bull 64:461–487

Machel HG (2005) Investigations of Burial Diagenesis in Carbonate Hydrocarbon Reservoir Rocks. Geosci Canada 32:103–128

Neilson JE, Brasier AT, North CP (2016) Primary aragonite and high-Mg calcite in the late Cambrian (Furongian). Potential evidence from marine carbonates in Oman. Terra Nov 28:306–315. doi: 10.1111/ter.12222

Palmer AR (1965) Trilobites of the Late Cambrian Pterocephaliid Biomere in the Great Basin, United States. United States Geol Surv Prof Pap 493:1–105

Palmer AR, James NP (1979) The Hawke Bay event: A circum- Iapetus regression near the lower middle Cambrian boundary. Virginia Polytech Inst State Univ Dep Geol Sci Mem 2:15–18

Saltzman MR, Cowan C a., Runkel AC, et al (2004) The Late Cambrian Spice (13C) Event and the Sauk II-SAUK III Regression: New Evidence from Laurentian Basins in Utah, Iowa, and Newfoundland. J Sediment Res 74:366–377. doi: 10.1306/120203740366

Saltzman MR, Ripperdan RL, Brasier MD, et al (2000) A global carbon isotope excursion (SPICE) during the Late Cambrian: Relation to trilobite extinctions, organic-matter burial and sea level. Palaeogeogr Palaeoclimatol Palaeoecol 162:211–223. doi: 10.1016/S0031-0182(00)00128-0

Schmid S, Smith PM, Woltering M (2018) A basin-wide record of the Late Cambrian Steptoean positive carbon isotope excursion (SPICE) in the Amadeus Basin, Australia. Palaeogeogr Palaeoclimatol Palaeoecol 508:116–128. doi: 10.1016/j.palaeo.2018.07.027

Sellwood BW, Scott J, James B, et al (1987) Regional significance of dedolomitization in Great Oolite reservoir facies of southern England. In: Brooks J, Glennie K (eds) Petroleum Geology of NorthWest Europe. Graham and Trotman, London, England, pp 129–137

Stanley SM, Hardie LA (1998) Secular oscillations in the carbonate mineralogy of reef-building and sediment-producing organisms driven by tectonically forced shifts in seawater chemistry. Palaeogeogr Palaeoclimatol Palaeoecol 144:3–19. doi: 10.1016/S0031-0182(98)00109-6

Stanley SM, Ries JB, Hardie L a. (2010) Increased Production of Calcite and Slower Growth for the Major Sediment-Producing Alga Halimeda as the Mg/Ca Ratio of Seawater is Lowered to a “Calcite Sea” Level. J Sediment Res 80:6–16. doi: 10.2110/jsr.2010.011

Tucker ME (1985) Calcitized aragonite ooids and cements from the Late Precambrian Biri Formation of southern Norway. Sediment Geol 43:67–84. doi: 10.1016/0037-0738(85)90055-7

Tucker ME (1993) Carbonate diagenesis in a sequence stratigraphic framework. In: Wright VP (ed) Sedimentology Review. Blackwell, Oxford, pp 51–72

Tucker ME (2001) Sedimentary Geology: An Introduction to the Origin of Sedimentary Rocks. Blackwell Science, Oxford

Tucker ME, Wright P (1990) Carbonate Sedimentology. John Wiley & Sons

Williams H (1976) Tectonic stratigraphic subdivision of the Appalachian Orogen. Geol Soc Am Abstr 8:300

Williams H (1979) Appalachian Orogen in Canada. Can J Earth Sci 16:792–807. doi: 10.1139/e79-070

Williams H (1995) Williams, Harold, ed. Geology of the Appalachian—Caledonian Orogen in Canada and Greenland. Geological Survey of Canada

Zhang Y, Dawe RA (2000) Influence of Mg2+ on the kinetics of calcite precipitation and calcite crystal morphology. Chem Geol 163:129–138. doi: 10.1016/S0009-2541(99)00097-2

Zuffa GG (1980) Hybrid Arenites: Their Composition and Classification. Sediment Geol 50:21–29

Figures captions

Figure 1. Study area in the Port au Port Peninsula. Location of the studied sections is shown by red rectangles (Barili et al. 2018).

Figure 2. Schematic stratigraphic log of the Port au Port Group (after Chow, 1985). Each of the Grand Cycles (A, B and C) consists of a lower shaley half-cycle mainly composed of parted limestone (interbedded shale and mudstone) and an upper carbonate half-cycle of oolitic grainstone / bioherms. Estimated Sauk II-III sequence limit is indicated (Chow and James 1987a; Saltzman et al. 2004)**.**

Figure 3. Photomicrographs of the main rock types and primary constituents. A) oolitic grainstone cemented by calcite, Uncrossed polarizers (//P). B) Intraclastic floatstone with peloids, ooids and microbial intraclasts locally compacted into pseudomatrix (//P). C) Bioclastic rudstone cemented by calcite(//P). D) Intraclastic Rudstone with large carbonate sand intraclasts (//P). E) Oolitic grainstone cemented by radial-prismatic cement displaying and preserved radial structure in some ooids while other are

completelly dissolved and porosity filled by calcite (crossed polarizers, XP). F) Pseudomorphically dolomitized ooid with selective envelope dissolution later filled by macrocrystalline calcite (pink staining) and clear dolomite (//P).

Figure 4. Photomicrographs of the main primary and diagenetic constituents. A) Intraclast with trilobite fragment surrounded by radial-prismatic calcite (//P). B) Trilobite and crinoid bioclasts (//P). C) Micitized crinoid bioclast with syntaxial calcite overgrowth (//P). D) Glauconite peloids mixed with quartz grains in hybrid arenite (XP). E) Detail of fibrous rims covering particles (stained pink) and pore-filling ferroan calcite cement (stained purple) (//P). F) Detail of pore-filling radial-prismatic cement covering fibrous rims.Intraparcle porosity from partial ooids dissolution filled by calcite and dolomite. (XP).

Figure 5. Photomicrographs of the main diagenetic constituents and porosity. A) Radial-prismatic calcite cement (stained pink) covering dolomitized particles and quartz grains, with late mosaic calcite filling vugular porosity. (XP). B) Dolomitized ooids and fibrous rims, with calcite (pink) locally filling intercrystalline porosity (//P). C) Blocky dolomite partially oxidized and replaced by calcite (pink) (//P). D) Dolomitized ooids and peloidal intraclasts cemented by blocky dolomite cement and intercrystalline calcite (XP). E) Porosity formed by dissolution of ooids filled by blocky and single-crystal dolomite. Pseudomatrix from compaction of microbial intraclasts (//P). F) Dolomitized oolitic grainstone with Original particle shapes visible due to micritization (//P).

Figure 6. BSE and CL images of oolitic grainstones from Campbells Member. A and B) BSE sample general view. C to F) Detail of images A and B (red rectangles). C and D) BSE images showing areas with calcite (brighter) and dolomite (darker). E and F) CL images from the same areas of C) and D), showing both dull and bright dolomite.

Figure 7. A) Sr x MgO % Electron microprobe results for Campbells Member. B) Detail of (A) evidencing the data distribution when MgO < 1%. C), D) and E) Photomicrographs of analyzed areas, showing ooids covered by isopachous fibrous rims. Scale bar indicated in the images.

Figure 8 Diagenetic pathways for oolitic grainstones and microbial intraclasts.

Figure 9 Diagenetic pathways for the bioclastic grainstones and for the intraclastic rudstones.

Figure 1

Click here to access/download;Figure;FIGURE 1-01.jpg

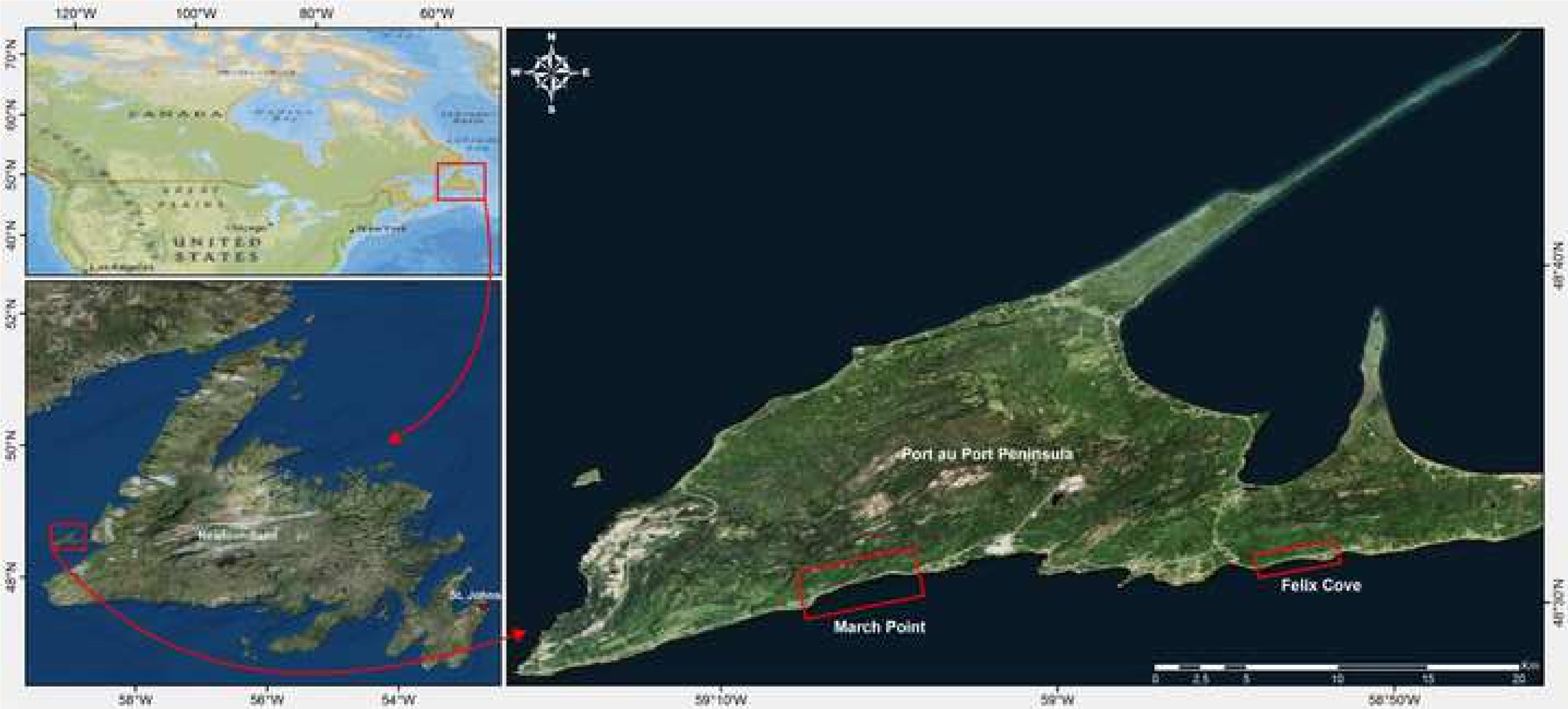

Figure 2

Click here to access/download;Figure;FIGURE 2-01.jpg

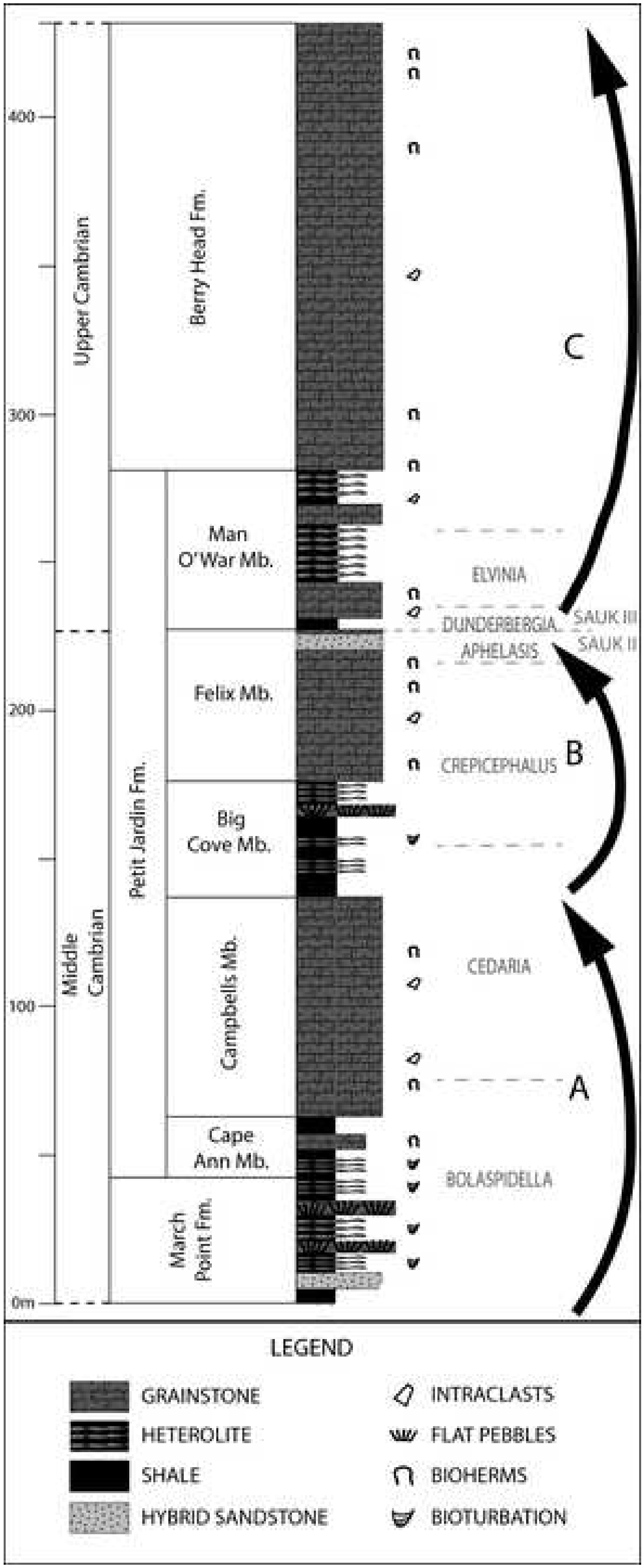

Figure 3 Click here to access/download;Figure;FIGURE 3.jpg

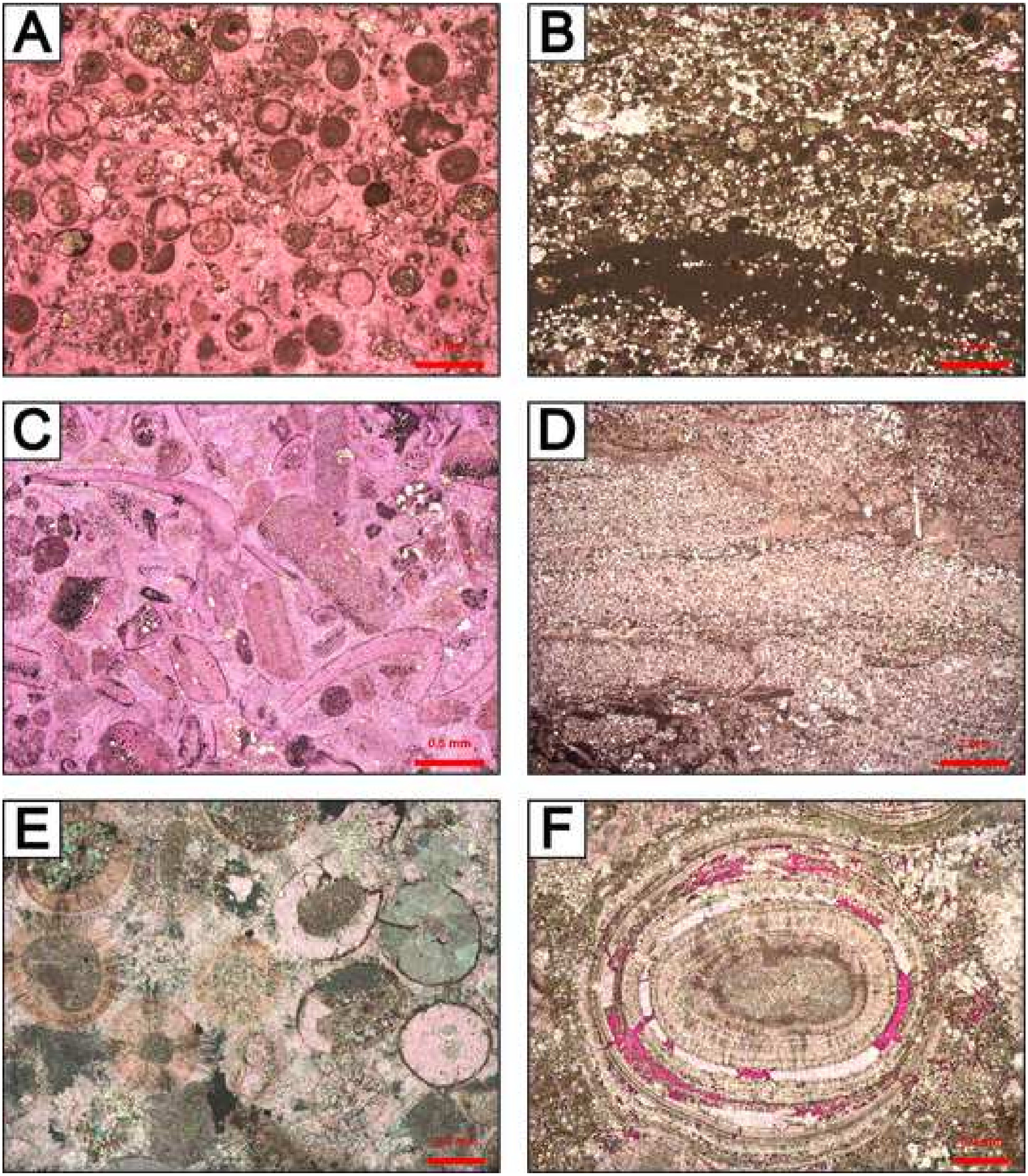

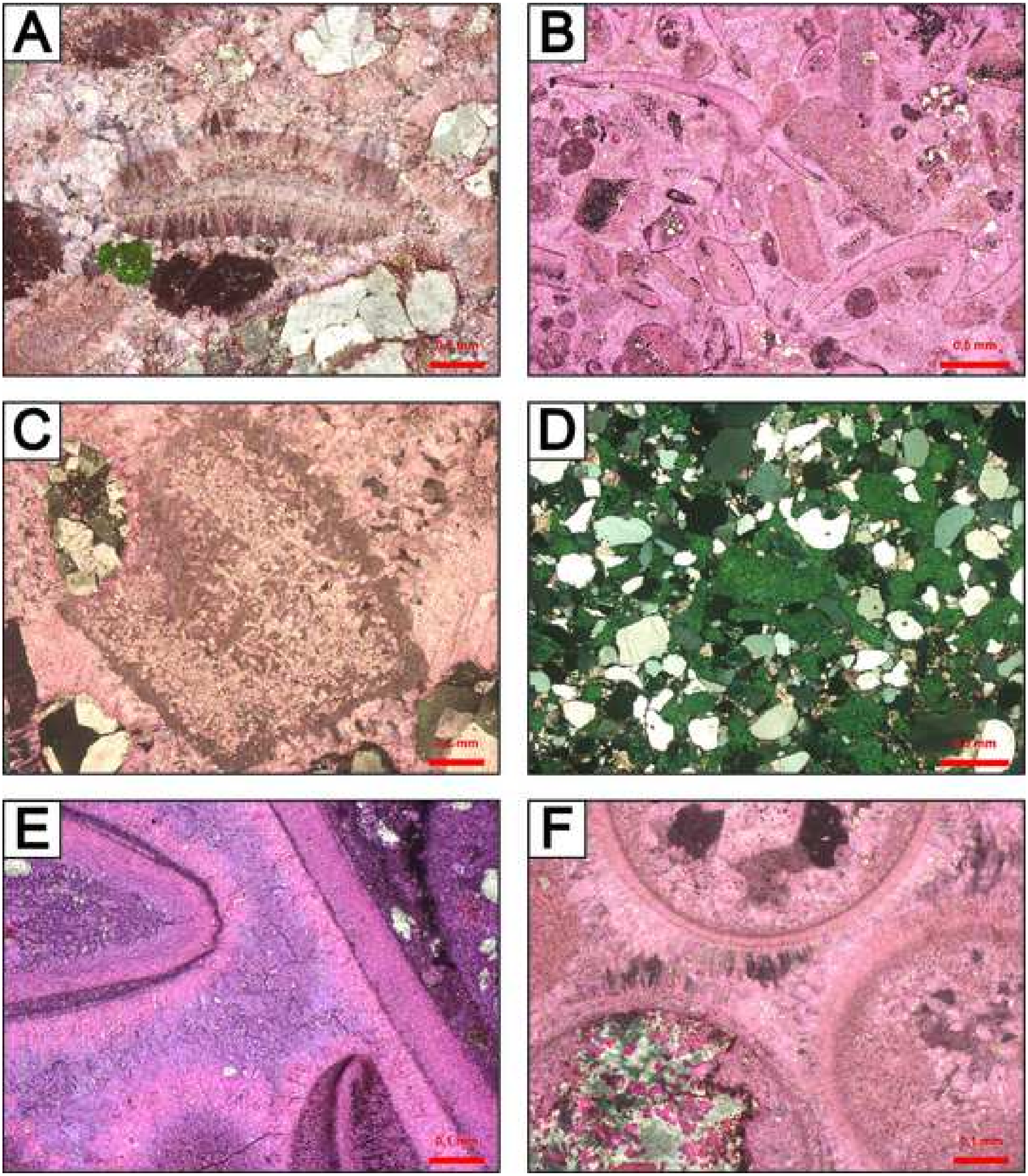
A
B
0.5 mm
C
D
E
F

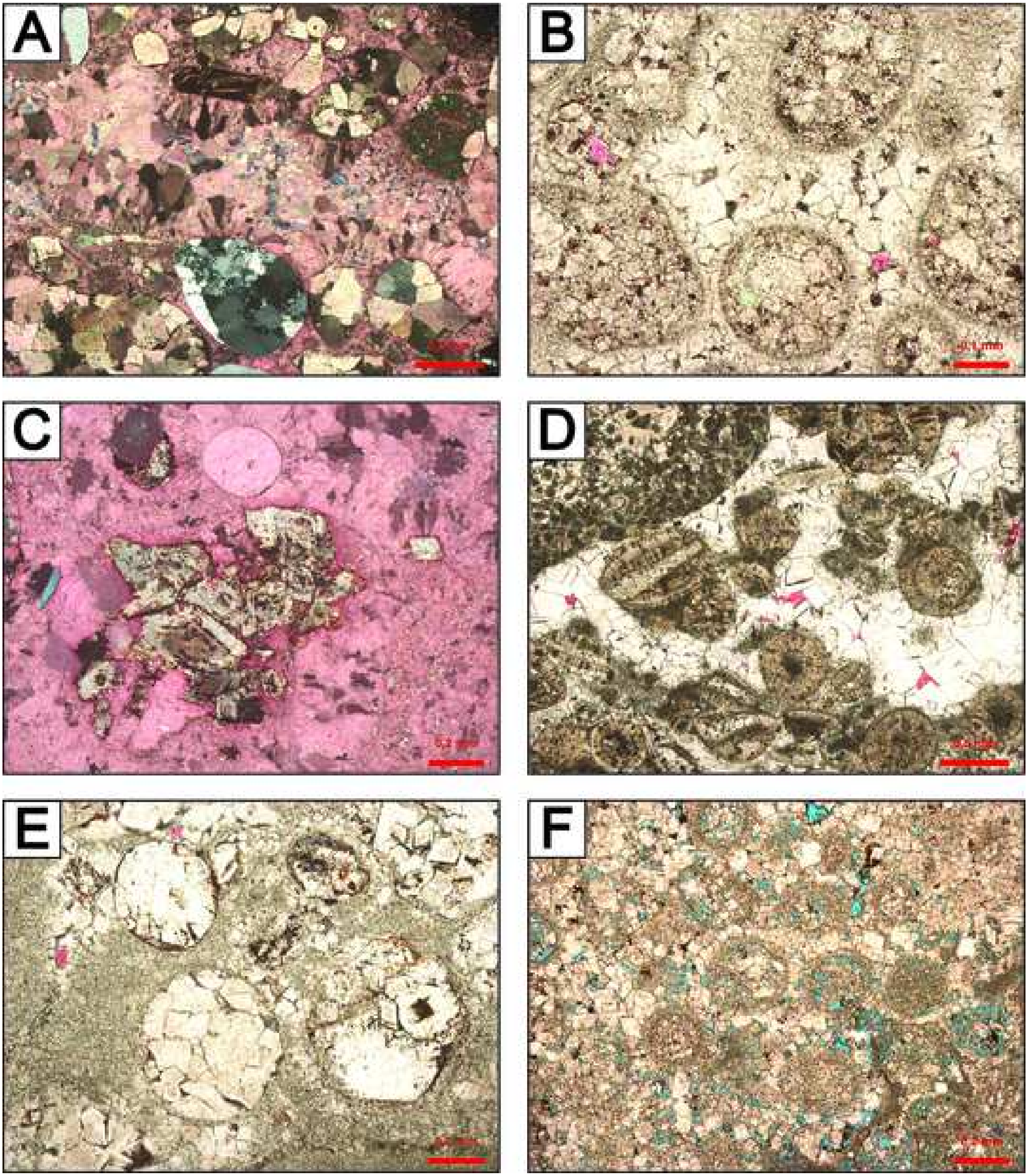
A
B
C
D
E
F

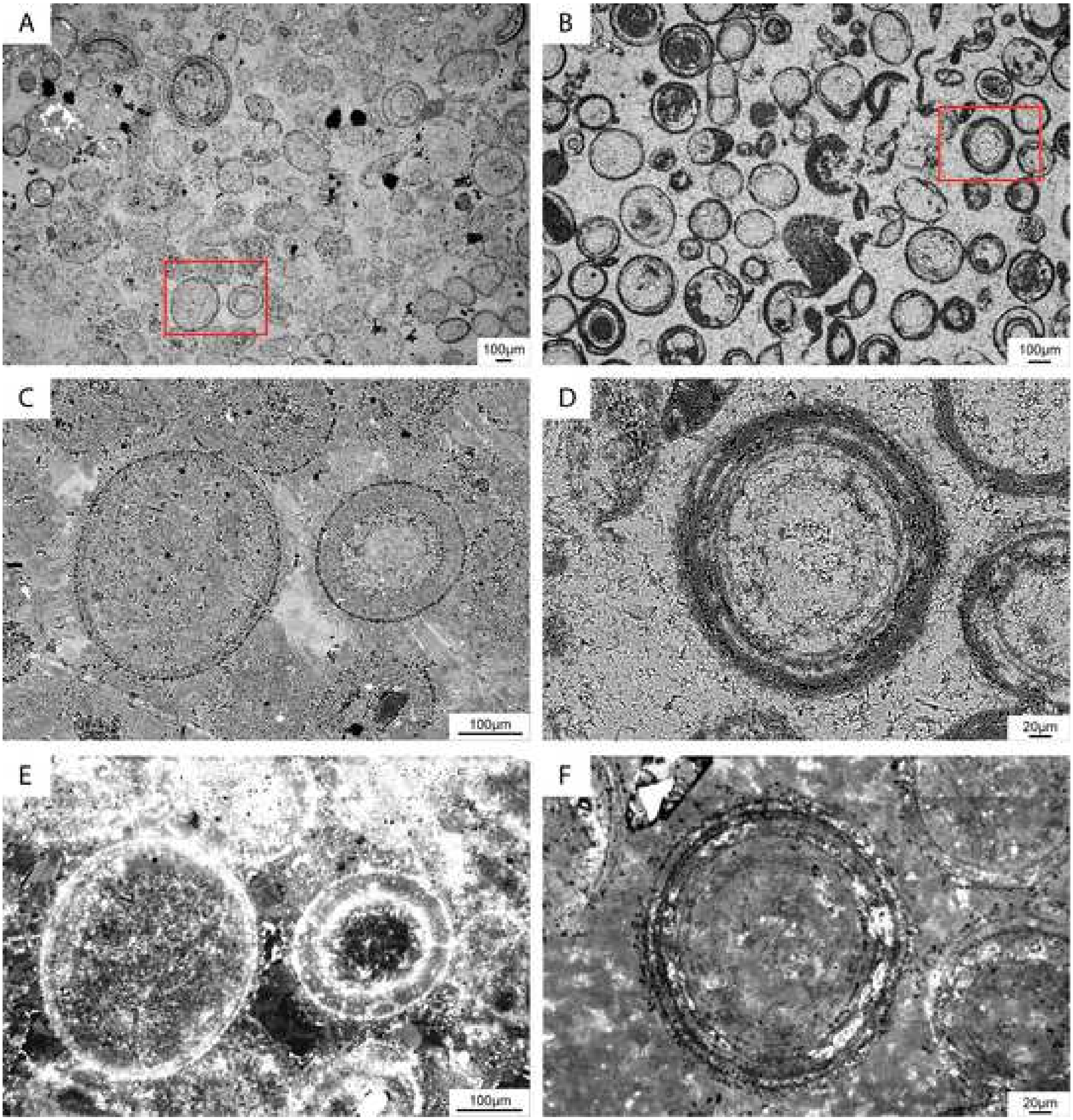
A
100μm
B
100μm
C
100μm
D
20μm
E
100μm
F
20μm

Figure

Click here to access/download;Figure;FIGURE 7.jpg

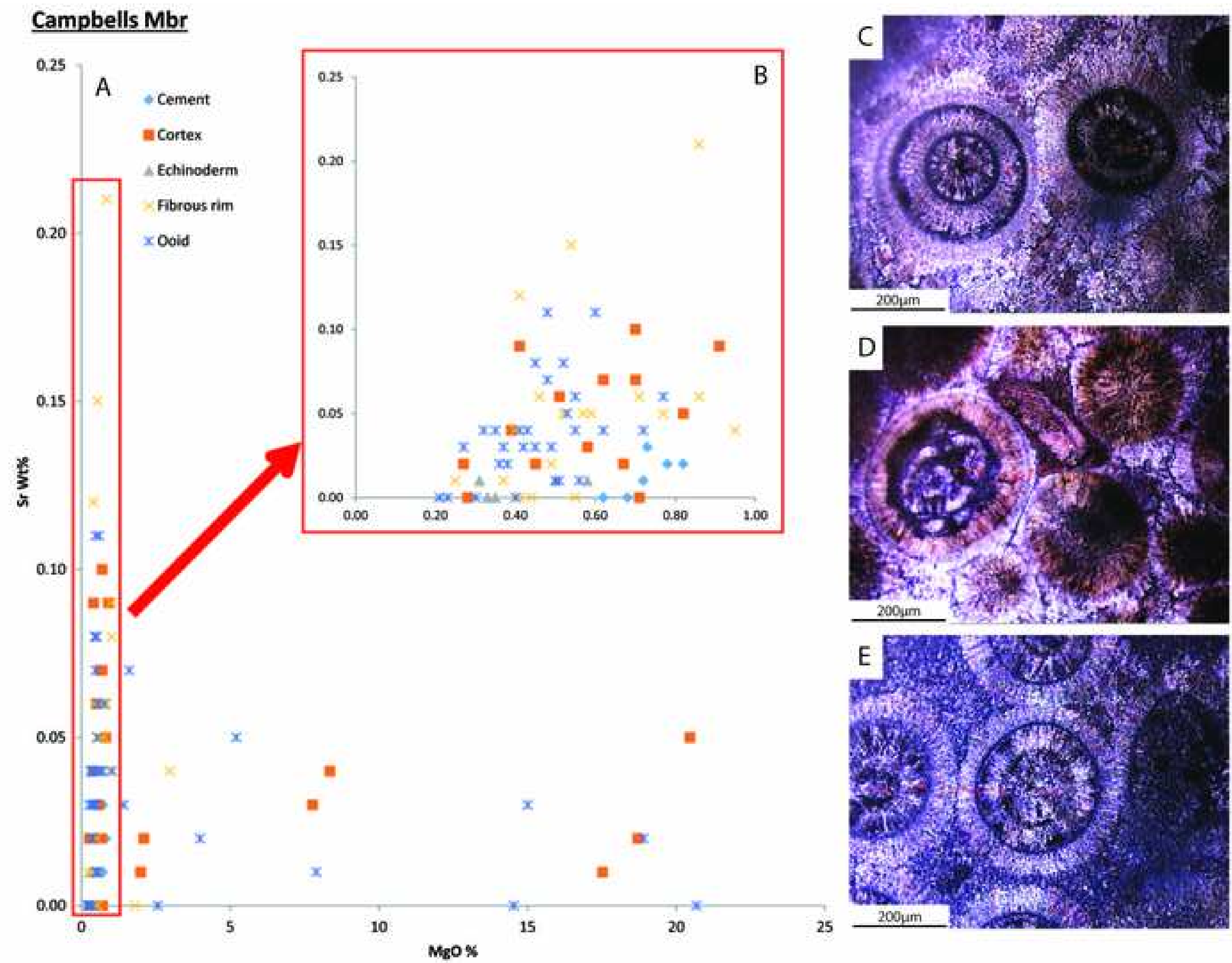

Figure 8

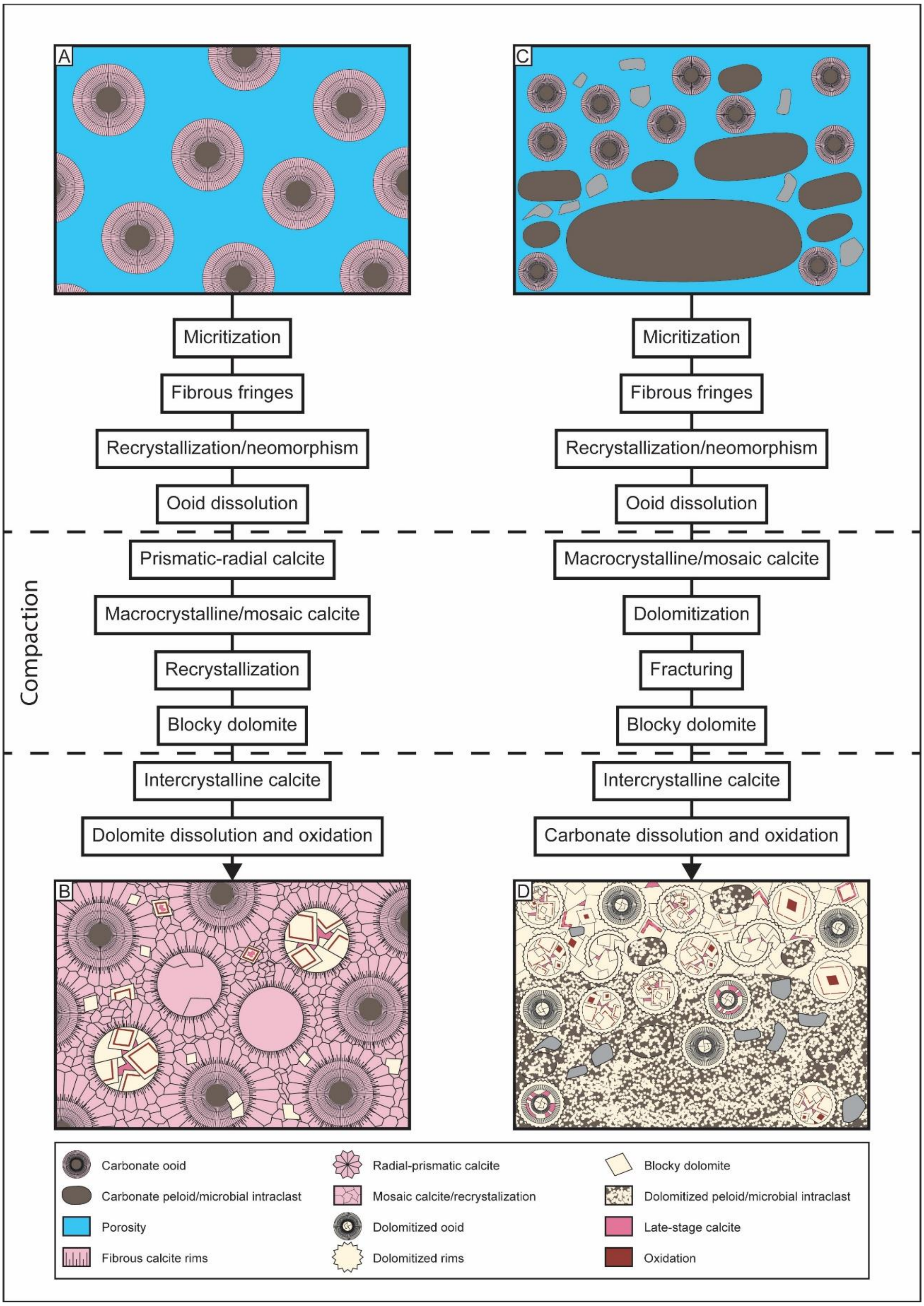
A
C
Micritization
Fibrous fringes
Recrystallization/neomorphism
Ooid dissolution
Compaction
Prismatic-radial calcite
Macrocrystalline/mosaic calcite
Recrystallization
Blocky dolomite
Intercrystalline calcite
Dolomite dissolution and oxidation
Micritization
Fibrous fringes
Recrystallization/neomorphism
Ooid dissolution
Macrocrystalline/mosaic calcite
Dolomitization
Fracturing
Blocky dolomite
Intercrystalline calcite
Carbonate dissolution and oxidation
B
D
Carbonate ooid
Carbonate peloid/microbial intraclast
Porosity
Fibrous calcite rims
Radial-prismatic calcite
Mosaic calcite/recrystallization
Dolomitized ooid
Dolomitized rims
Blocky dolomite
Dolomitized peloid/microbial intraclast
Late-stage calcite
Oxidation

Figure 9

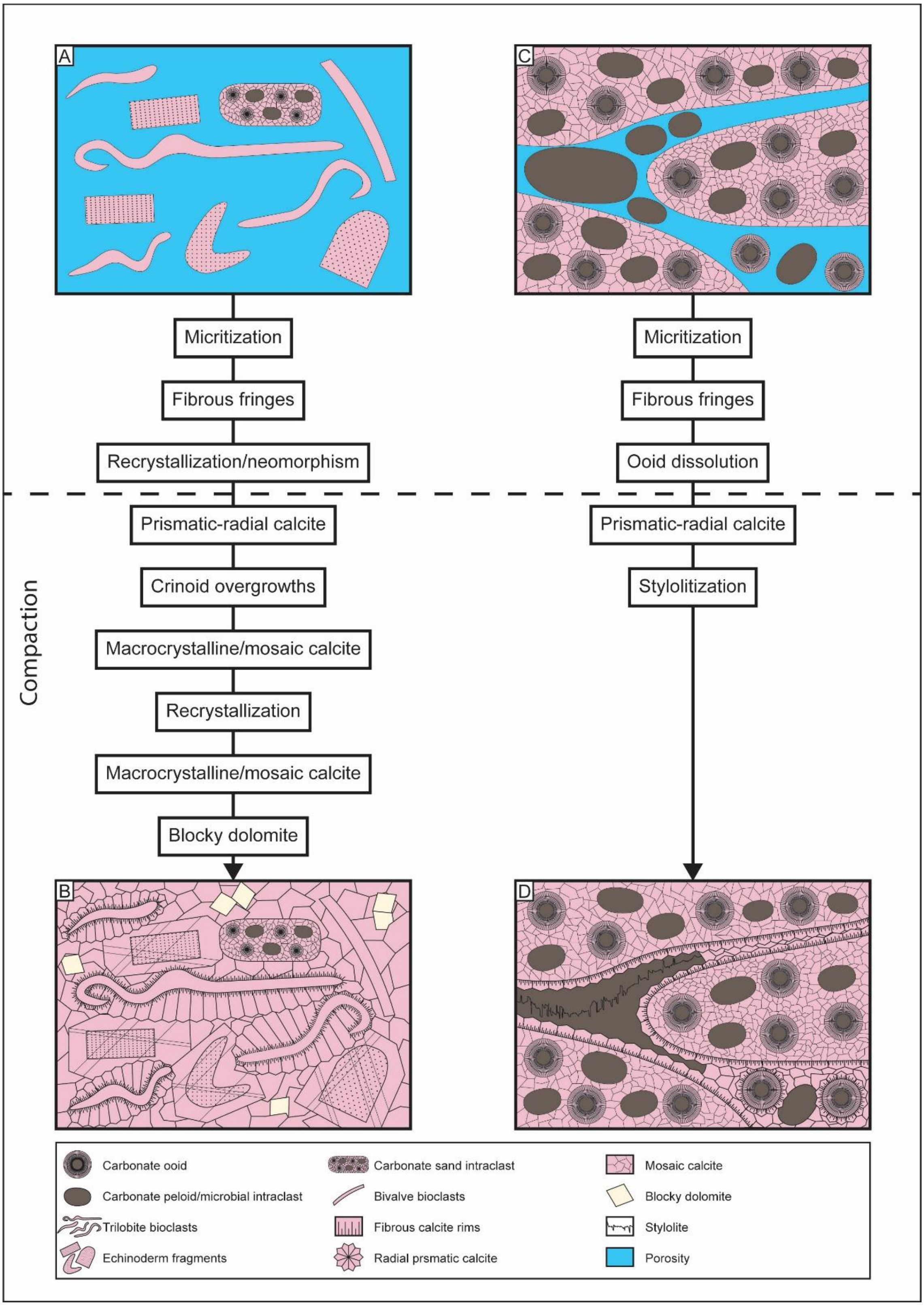

A
C
Micritization
Fibrous fringes
Recrystallization/neomorphism
Micritization
Fibrous fringes
Ooid dissolution
Compaction
Prismatic-radial calcite
Crinoid overgrowths
Macrocrystalline/mosaic calcite
Recrystallization
Macrocrystalline/mosaic calcite
Blocky dolomite
Prismatic-radial calcite
Stylolitization
B
D
Carbonate ooid
Carbonate sand intraclast
Mosaic calcite
Carbonate peloid/microbial intraclast
Bivalve bioclasts
Blocky dolomite
Trilobite bioclasts
Fibrous calcite rims
Stylolite
Echinoderm fragments
Radial prsmatic calcite
Porosity

PARTE III

Anexo A. TABELA DE FÁCIES

Tabela 1 Tabela de fácies do Grupo Port au Port. Classificação e códigos de fácies adaptadas de Dunham 1962, de Embry III & Klovan 1971 e de Miall 1978.

Facies	Cód. de fácies	Descrição	Espessura (m)	Interpretação	Foto de campo
Folhelho	Sh	Folhelho esverdeado a amarronzado, argiloso a síltico, micáceo.	0,5 to 3	Deposição por decantação abaixo do nível de onda normal, baixa energia.	
Mudstone / wackestone	M/W	*Mudstone* a *wackestone*, cinza escuro, maciço, com ocorrência de conchas de braquiópodes inteiras. Bioturbação pervasiva a moderada e gretas de sinerese, localmente preenchidas por oólitos cinza.	0,01 to 0,5	Deposição por decantação abaixo do nível de onda normal, baixa energia associados a argilas. Presença de biota marinha indica possível condição de mar aberto. Águas com oxigenação moderada a pervasiva.	

Heterolito	Ht	Intercalação mm a dcm de mudstone, wackestone e folhelho, cinza a preto, com acamamento flaser, wavy e lenticular. Gretas de sinerese e bioturbação fraca a moderada, preenchidas por oolitos	0,10 to 3	Deposição durante intervalos alternados de fluxo relativamente rápido e fluxo de baixa energia, associado com a presença de argila. Presença de biota marinha indica possível condição de mar aberto. Águas com oxigenação moderada a boa.	
Boundstone	B	Estromatólitos colunares, laminares ou arbustiformes, e trombolitos, cinza claros. Podem ocorrer isolados ou lateralmente conectados.	0,05 to 0,5	Calcificação de depósitos microbiais incluindo precipitação direta, e *trapping* e *binding* de partículas carbonáticas ou de grãos siliciclásticos. Ausência de bioclastos indica o desenvolvimento em uma posição protegida.	

Arenito hibrido	HS	Arenito híbrido, cinza escuro, fino, por quartzo e feldspato angulosos, pelóides de glauconita, e partículas carbonáticas (bioclastos e oólitos)	0,05 to 0,20	Fluxo hiperconcentrado ou retrabalhamento de sedimento devido à fluidização ou bioturbação intensa. Presença de biota marinha indica possível condição de mar aberto.	
Arenito quartzoso	Sm	Arenito, cinza a amarelado, maciço, bem selecionado, composto por quartzo, e feldspato subordinado, cimentados por calcita.	0,10 to 0,50	Fluxo hiperconcentrado ou retrabalhamento de sedimento devido à fluidização ou bioturbação intensa.	

Grainstone	G	Grainstone oolítico / bioclástico, amarronzado a rosado, com estratificação cruzada tipo *herringbone*, e/ou incipiente / tangencial presença de estilolitos associado a presença de lama ou matéria orgânica. Localmente, intraclastos lamosos e oolíticos ocorrem na porção basal dos sets, apresentando contato erosivo com a camada sotoposta.	0,10 to 10 (variando entre sets de 0,10 to 0,75 m)	Fluxo bidirecional (mare) com desenvolvimento de dunas de areias carbonáticas, fluxo de regime inferior, formação de oólitos e retrabalhamento de bioclastos em condições de alta energia.	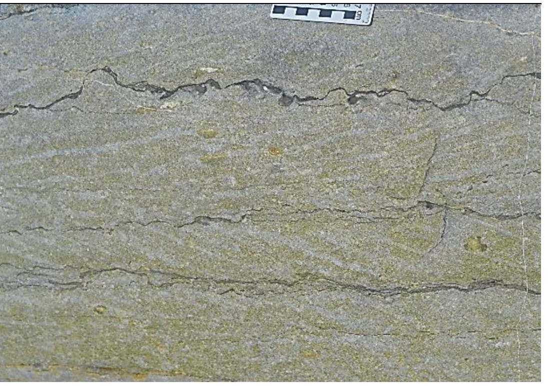
Flat Pebble Conglomerate	FPC	Conglomerado, acinzentado a amarelado, composto por intraclastos de *mudstone* retrabalhados e imbricados, com arestas arredondadas e tamanho variando entre <1 a 20 cm.	0,05 to 0,50	Retrabalhamento de mudstones causado pela ação de tempestades.	

Anexo B. PERFIL ESTRATIGRÁFICO COMPLETO

Felix Cove section

March Point section

Anexo C. REGISTRO FOTOMICROGRÁFICO DOS CONSTITUINTES PRIMÁRIOS E DIAGENÉTICOS

Foto 1 Grainstone oolítico intraclástico. Oólitos radiais e concêntricos, parcialmente micritizados, cimentados por franjas prismáticas radiais e mosaico de calcita. Polarizadores descruzados (//P).

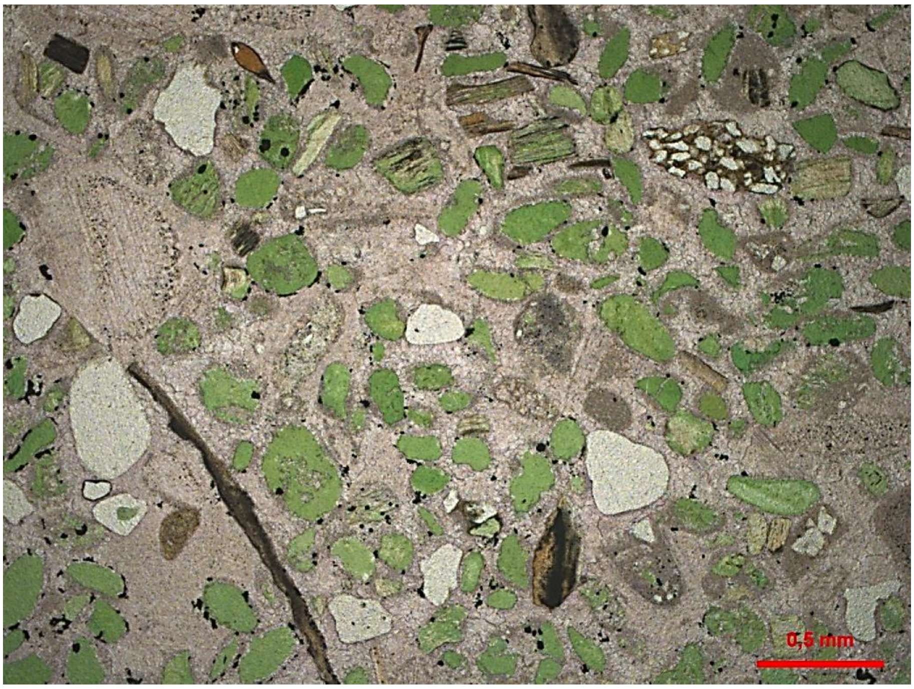

Foto 2. Arenito híbrido, composto por bioclastos (crinóides e braquiópodes), pelóides de glauconita, grãos de quartzo, cimentado por mosaico de calcita. (//P).

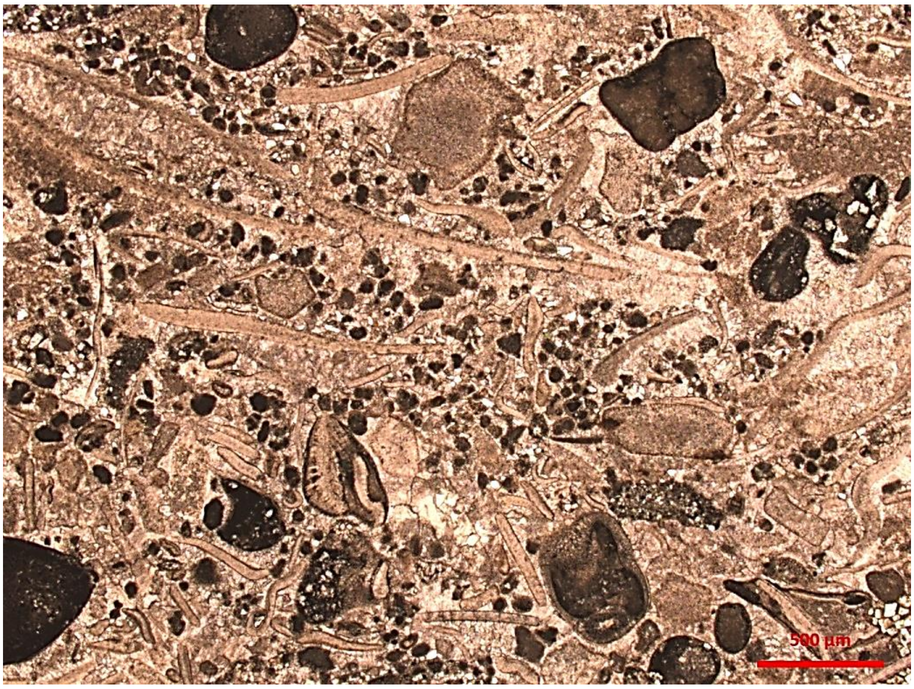

Foto 3. Grainstone bioclástico-peloidal com intraclastos microbiais. Bioclastos e pelóides com diferentes graus de micritização, cimentados por calcita. (//P).

Foto 4. Detalhe de oólito radial. Partículas com intensa micritização, cimentadas por franjas fibrosas e cimento calcítico espático. Polarizadores cruzados (XP).

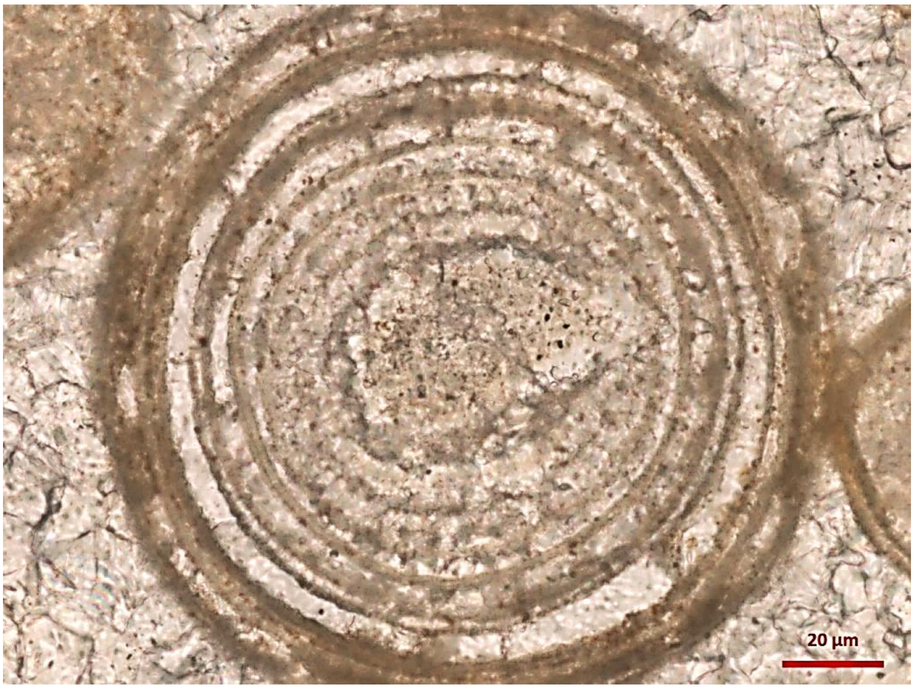

Foto 5. Detalhe de oólito com envelopes parte micritizados, parte recristalizados. (//P).

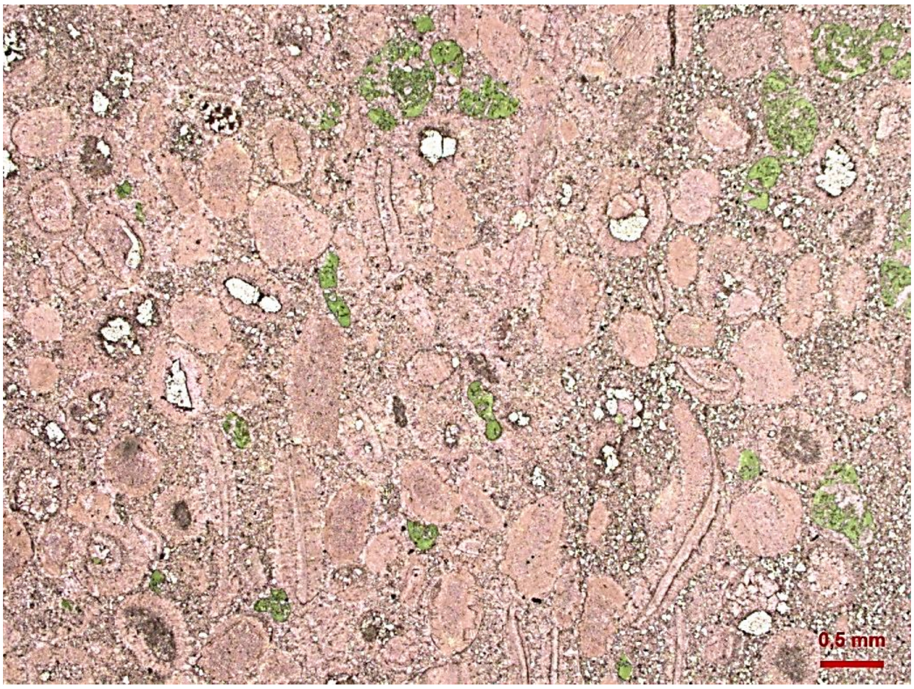

Foto 6. Arenito híbrido composto por bioclastos, oólitos e pelóides de glauconita. Calcitização parcial dos pelóides de glauconita, e dolomitização de alguns núcleos de oólitos (branco). (//P).

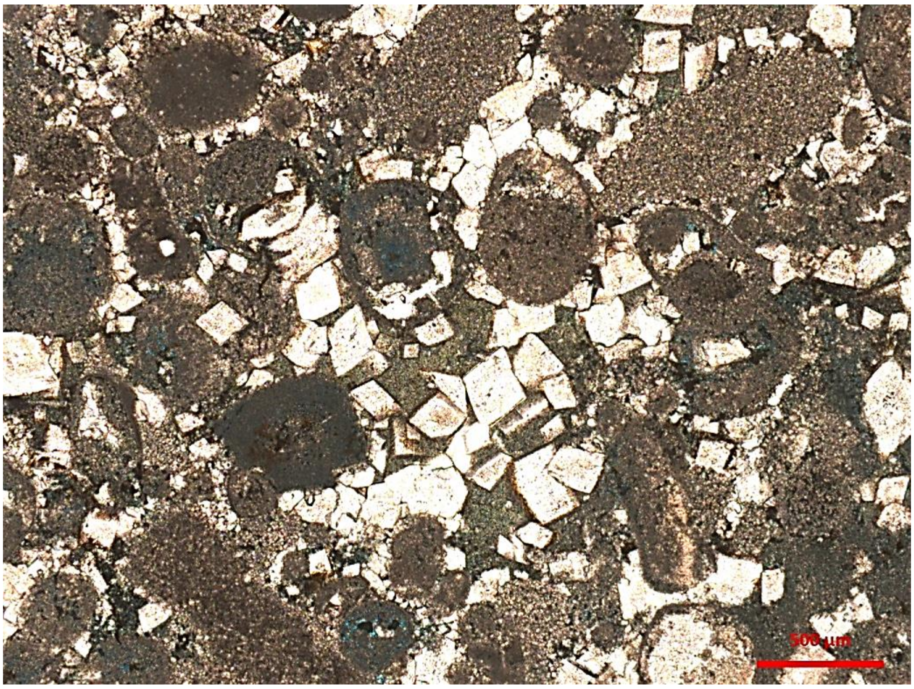

Foto 7. Grainstone oolítico-peloidal-bioclástico com intensa micritização, com partículas cimentadas e parcialmente substituídas por dolomita blocosa. (//P).

Foto 8. Detalhe de estilolito com matéria orgânica. Também é possível verificar intensa micritização e dolomitização parcial dos bioclastos. (//P).

Foto 9. Doloespatito com feições fantasmas de oólitos. (//P).

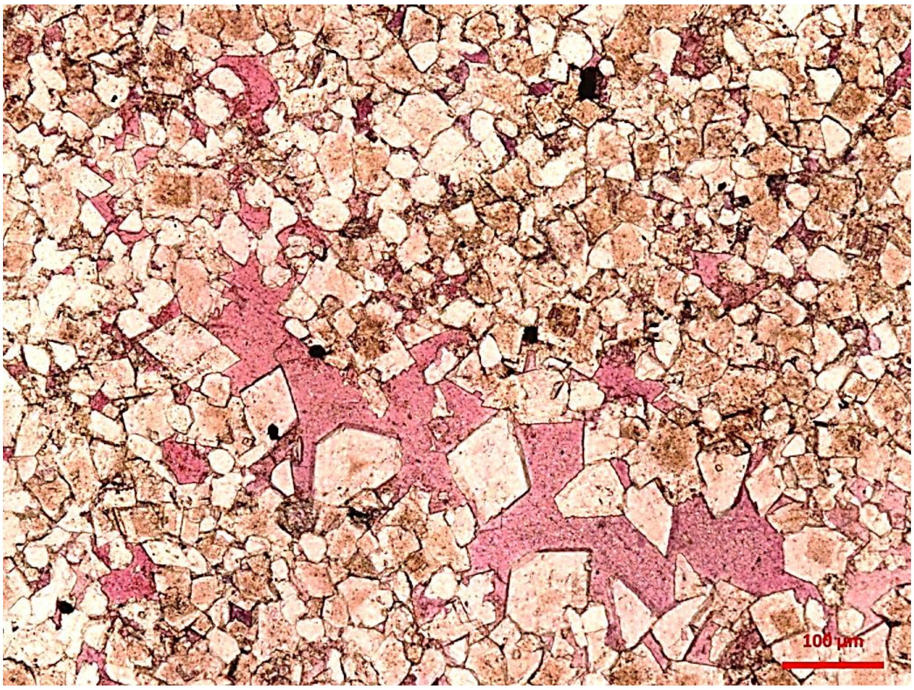

Foto 10. Doloespatito com dolomita em sela, parcialmente substituída por calcita macrocristalina (tingida de rosa). (//P).

Anexo D. TABELAS DE RESULTADOS GEOQUÍMICOS E ISOTÓPICOS

Tabela 2 Resultados geoquímicos e isotópicos para o Grupo Port au Port no afloramento de March Point.

Altura (m)	Al (Wt%)	Ca (Wt%)	Mg (Wt%)	Si (Wt%)	Sr (ppm)	Mn (ppm)	Fe (ppm)	Mg/Ca	Mn/Sr	Sr/Ca	$^{87}Sr/^{86}Sr$	$\delta^{13}C$(‰)*	$\delta^{18}O$(‰)*
36,00	<LOD	34,09	2,20	1,93	440,94	896,31	7017,02	0,06	2,03	0,00001	0,7092	+1,10	-5,30
35,50	1,57	18,52	12,04	6,71	67,24	482,10	8188,89	0,65	7,17	0,00004	-	-	-
32,25	0,86	21,06	14,07	4,35	290,51	711,22	7497,89	0,67	2,45	0,00002	-	+1,70	-5,46
29,75	0,66	20,72	11,38	2,88	70,12	562,14	7088,37	0,55	8,02	0,00001	-	+1,83	-5,34
29,00	<LOD	31,08	1,15	2,22	353,75	476,09	3388,02	0,04	1,35	0,00001	0,7092	-	-
27,50	-	-	-	-	-	-	-	-	-	-	0,7089	+1,59	-5,76
27,25	-	-	-	-	-	-	-	-	-	-	*0,7091*	+0,90	-5,70
26,00	-	-	-	-	-	-	-	-	-	-	-	+1,02	-5,57
25,50	-	-	-	-	-	-	-	-	-	-	-	+0,80	-5,40
24,00	-	-	-	-	-	-	-	-	-	-	-	+0,90	-5,40
23,40	1,09	18,46	9,17	12,32	58,62	683,20	4816,95	0,50	11,65	0,00007	-	+0,40	-5,40
23,00	0,88	18,05	12,04	8,86	56,70	634,18	9057,78	0,67	11,18	0,00005	-	-	-
22,50	0,62	16,98	1,15	18,82	102,70	1130,44	12995,62	0,07	11,01	0,00011	-	-1,10	-9,00
22,50	1,14	36,62	<LOD	3,48	120,90	2055,92	126,52	-	17,00	0,00001	-	-	-
22,25	1,15	26,99	2,33	5,32	147,73	1467,61	3410,50	0,09	9,93	0,00002	-	-	-
22,00	<LOD	24,95	8,79	1,63	107,49	1409,58	5014,38	0,35	13,11	0,00001	-	-	-
21,50	9,21	0,39	0,25	31,74	60,54	78,89	31239,31	0,64	1,30	0,00805	-	-	-
19,00	2,13	21,93	7,42	8,00	116,11	627,17	10189,58	0,34	5,40	0,00004	-	-0,50	-6,50
16,80	<LOD	34,40	<LOD	2,25	393,99	1112,43	3729,13	-	2,82	0,00001	0,7093	-1,20	-7,50
13,00	<LOD	37,53	<LOD	1,71	421,78	1167,46	3668,53	-	2,77	0,00000	-	-1,20	-7,00
10,25	0,61	25,07	7,28	2,56	119,95	1020,38	4726,05	0,29	8,51	0,00001	-	-	-
9,00	<LOD	36,51	<LOD	1,75	661,33	348,03	3513,13	0,00	0,53	0,00000	-	-	-
6,50	1,19	19,00	13,55	8,60	62,45	369,04	5352,55	0,71	5,91	0,00005	-	-1,30	-5,90
3,75	0,72	23,51	12,61	3,54	95,99	668,19	7165,58	0,54	6,96	0,00002	-	-	-
1,00	<LOD	36,12	2,85	1,46	357,58	345,03	2164,35	0,08	0,96	0,00000	0,7092	-2,00	-7,30

Devio Padrão,	0,29	0,04	0,25	0,60	0,00	0,00	0,05		
Reprodutibilidade %	4,46	2,05	18,44	3,89	0,77	4,62	0,85	0,1	0,1

Tabela 3 Resultados geoquímicos e isotópicos para o Grupo Port au Port no afloramento de Felix Cove.

Altura(m)	Al (Wt%)	Ca (Wt%)	Mg (Wt%)	Si (Wt%)	Sr (ppm)	Mn (ppm)	Fe (ppm)	Mg/Ca	Mn/Sr	Sr/Ca	$^{87}Sr/^{86}Sr$	$\delta^{13}C$(‰)*	$\delta^{18}O$(‰)*
265,5	3,45	15,53	8,41	13,59	54,79	188,94	10391,90	0,54	3,45	0,00009	0,7093	-	-
251	1,01	20,80	11,90	4,22	74,91	279,99	2110,59	0,57	3,74	0,00002	0,7091	-	-
244,50	-	-	-	-	-	-	-	-	-	-	-	-1,38	-3,32
239,25	1,44	19,60	9,83	16,33	122,82	483,10	11510,99	0,50	3,93	0,00008	-	-1,07	-6,57
236,75	-	-	-	-	-	-	-	-	-	-	-	-2,01	-7,86
236,00	<LOD	37,31	<LOD	1,11	392,07	148,92	-1302,40	-	0,38	0	-	-1,73	-8,32
235,00	-	-	-	-	-	-	-	-	-	-	-	-1,19	-8,08
233,50	-	-	-	-	-	-	-	-	-	-	-	-1,05	-7,95
231,50	<LOD	39,08	<LOD	1,12	349,91	278,99	-1277,97	-	0,80	0	0,7091	-1,83	-8,47
230,75	-	-	-	-	-	-	-	-	-	-	-	-1,35	-8,18
230,00	-	-	-	-	-	-	-	-	-	-	-	-1,74	-7,73
226,25	-	-	-	-	-	-	-	-	-	-	-	-0,18	-4,04
225,50	-	-	-	-	-	-	-	-	-	-	-	-0,31	-4,75
223,75	-	-	-	-	-	-	-	-	-	-	-	0,79	-5,76
223,60	0,77	20,59	12,04	4,16	75,87	1162,45	5122,87	0,59	15,32	0,00002	-	0,52	-4,58
223,30	0,99	20,41	11,24	3,31	80,66	973,36	4174,81	0,55	12,07	0,00002	-	-	-
222,75	0,77	21,42	14,17	2,50	92,16	625,17	5763,05	0,66	6,78	0,00001	0,7089	1,13	-5,08
222,60	1,45	18,85	10,86	5,08	68,20	712,22	10541,43	0,58	10,44	0,00003	-	-	-
222,50	0,81	20,43	12,23	2,85	76,83	656,19	4986,03	0,60	8,54	0,00001	-	-	-
222,25	0,69	21,87	15,39	2,62	68,20	2272,04	4317,51	0,70	33,31	0,00001	-	-	-
218,75	0,83	20,40	12,09	3,52	71,08	598,16	4650,79	0,59	8,42	0,00002	-	-0,46	-5,27
215,50	-	-	-	-	-	-	-	-	-	-	-	-0,68	-6,93
213,00	0,97	19,71	11,81	5,24	66,29	464,09	4093,69	0,60	7,00	0,00003	-	-	-

208,00	-	-	-	-	-	-	-	-	-	-	-	-1,29	-6,66
200,25	1,03	19,75	15,16	5,50	65,33	635,18	1094,12	0,77	9,72	0,00003	0,7093	-1,61	-6,76
189,50	-	-	-	-	-	-	-	-	-	-	-	-1,53	-6,56
184,50	-	-	-	-	-	-	-	-	-	-	-	-1,72	-6,87
183,00	0,73	20,48	11,53	1,97	56,70	312,01	4743,64	0,56	5,50	0,00001	-	-	-
179,00	-	-	-	-	-	-	-	-	-	-	-	-0,84	-7,19
176,50	-	-	-	-	-	-	-	-	-	-	-	-1,49	-6,72
175,50	-	-	-	-	-	-	-	-	-	-	-	-1,49	-6,72
168,75	1,73	31,22	<LOD	5,74	419,86	575,15	8273,92	-	1,37	0,00002	-	-	-
167,25	<LOD	36,20	<LOD	1,89	296,25	1161,45	8231,90	-	3,92	0,00001	0,7093	-0,9	-7,94
152,25	1,03	32,42	<LOD	4,76	217,68	1586,68	12111,10	-	7,29	0,00001	0,7094	-1,29	-8
140,25	-	-	-	-	-	-	-	-	-	-	-	-2,54	-8,19
139,75	<LOD	38,49	<LOD	1,98	459,15	1129,44	9212,20	-	2,46	0,00001	-	-	-
137	2,08	29,81	<LOD	8,49	279,97	1090,42	6072,87	-	3,89	0,00003	0,7093	-4,16	-7,57
136,25	-	-	-	-	-	-	-	-	-	-	-	-3,18	-7,38
133,00	4,30	17,27	0,96	15,23	120,90	1043,39	27396,27	0,06	8,63	0,00009	-	-	-
130,75	<LOD	37,26	<LOD	1,90	399,74	432,07	562,43	-	1,08	0,00001	0,7095	-	-
130,00	<LOD	35,99	<LOD	1,21	272,30	578,15	3779,95	-	2,12	0	-	-	-
127,50	1,31	30,63	<LOD	5,52	149,65	2087,94	5462,99	-	13,95	0,00002	-	-	-
127,25	<LOD	35,82	<LOD	1,20	300,09	448,08	3630,41	-	1,49	0	-	-	-
126,00	-	-	-	-	-	-	-	-	-	-	-	-2,16	-8,01
122,25	<LOD	37,52	<LOD	2,00	314,46	562,14	-538,09	-	1,79	0,00001	0,7095	-	-
115,25	-	-	-	-	-	-	-	-	-	-	-	-1,77	-6,55
111,5	0,72	34,23	<LOD	2,68	466,81	546,13	4474,87	-	1,17	0,00001	0,7095	-	-
109,50	-	-	-	-	-	-	-	-	-	-	-	-3,84	-7,62
108,00	<LOD	38,30	<LOD	1,22	344,16	742,23	2132,10	-	2,16	0	-	-	-
106,00	-	-	-	-	-	-	-	-	-	-	-	-2,46	-6,74
86,50	1,75	26,86	<LOD	8,67	255,05	303,00	2271,86	-	1,19	0,00003	0,7093	-	-
83,5	0,85	34,25	3,55	2,87	294,34	632,18	742,27	0,10	2,15	0,00001	-	-1,8	-7,37
72,5	5,18	15,53	3,74	15,97	120,90	525,12	19480,51	0,24	4,34	0,0001	-	-	-
67	0,97	30,39	5,68	3,54	158,27	819,27	6376,84	0,19	5,18	0,00001	0,7094	-0,41	-7,63

60,00	0,94	20,46	10,96	4,57	60,54	1276,51	11395,66	0,54	21,09	0,00002	-	-	-
59,00	-	-	-	-	-	-	-	-	-	-	-	-1,32	-5,7
56,75	-	-	-	-	-	-	-	-	-	-	-	-1,79	-5,51
52,00	1,59	26,83	<LOD	8,73	202,35	617,17	4578,47	-	3,05	0,00003	0,7095	-	-
52,00	1,60	26,14	<LOD	8,28	187,98	742,23	5569,53	-	3,95	0,00003	-	-	-
40,75	1,97	26,51	1,90	9,07	131,44	1541,65	15301,25	0,07	11,73	0,00003	-	-	-
30,00	1,91	28,32	<LOD	9,04	200,43	683,20	11276,42	-	3,41	0,00003	0,7094	-	-
26,00	1,04	25,73	<LOD	8,64	289,55	859,30	21174,30	-	2,97	0,00003	-	-	-
22,75	1,10	23,69	0,68	10,98	292,42	924,33	25227,48	0,03	3,16	0,00005	-	-	-
9,25	1,45	26,88	0,82	8,10	289,55	831,28	44898,13	0,03	2,87	0,00003	-	-0,96	-8,09
2,00	2,80	15,43	4,73	18,21	118,03	1595,68	22289,49	0,31	13,52	0,00012	0,7092	-	-
Devio Padrão,	0,29	0,04	0,25	0,60	0,00	0,00	0,05						
Reprodutibilidade%	4,46	2,05	18,44	3,89	0,77	4,62	0,85						

Anexo E. TRABALHOS APRESENTADOS EM EVENTOS CIENTÍFICOS NACIONAIS E INTERNACIONAIS

SIMPÓSIO INTERNACIONAL DA TRANSIÇÃO EDIACARANO – CAMBRIANO (ISECT, 2017)

Stable isotopic signature from a Cambro-Ordovician carbonate sequence on western Newfoundland, CA

Barili, R.[1,*], Neilson, J.[2], Brasier, A.[3], Goldberg, K.[4], De Ros, L.F.[5], Leng, M. [6]

1, 5 Universidade Federal do Rio Grande do Sul, Porto Alegre, Brasil.
2, 3 University of Aberdeen, Aberdeen, Scotland, U.K.
4 Kansas State University, Manhattan, Kansas, USA.
6 NERC Isotope Geosciences Laboratory, British Geological Survey, Nottingham, U.K.
*Rosalia.barili@gmail.com.

The Port au Port Group, western Newfoundland, is interpreted as a shallow marine record from the outer part of a stable carbonate platform that surrounded the Iapetus Ocean. These mixed deposits mark the gradual transition from siliciclastic deposition in the lower Cambrian to carbonate sedimentation in the lower Ordovician. Asymmetric shallowing-upward grand cycles are easily identified across the group. Each grand cycle consists of a lower ribbon, half-cycle, that includes mainly parted limestones, with shale, mudstone and subordinate wackestone, and represents subtidal deposits; and a upper oolitic half-cycle that may include ooid grainstones, packstones and laminated carbonates. The latter does not show a predictable stacking pattern as result of vertical and lateral accretion, related to subtidal, intertidal and supratidal deposits respectively. Stromatolites and thrombolites, as meter scale biostrome and bioherms, occur through both ribbon and oolitic half-cycles. Carbonates from the Felix and Man O' War Members of the Petit Jardin Formation, are believed to show an isotopic signature that indicates a strong carbon excursion related to the Steptoean Carbon Isotope Excursion (SPICE). This worldwide excursion of up to +5‰, has been shown to be coeval with the major Sauk II – III regression in Laurentia. Regarding the occurrence of the SPICE in the Port au Port Group, this work aims to better understand this event and its relationship with local and/or global depositional controls. Therefore, systematic sampling and logging has been carried out along the southern coast of the Port-au-Port peninsula at various localities from March Point to Felix Cove. Petrographic, cathodoluminescence and stable isotope analysis ($\delta^{13}C_{org}$, $\delta^{13}C_{carb}$ and $\delta^{18}O$) have been carried out. Preliminary $\delta^{13}C_{org}$ results from the March Point section show a range from -30‰ to -21,3‰ with the highest values around the boundary between the Felix and Man O'War Members, consistent with a temporal variation in organic productivity. These results are similar to previous publications that indicate the development of a positive carbon isotope excursion (CIE) in organic rich mudstones that can also be related to the SPICE.

49º Congresso Brasileiro de Geologia
20 a 24 de agosto de 2018 – Rio de Janeiro

INFLUÊNCIA PALEOAMBIENTAL E DIAGENÉTICA SOBRE A ASSINATURA ISOTÓPICA ($\delta^{13}C$) DE CARBONATOS CAMBRIANOS EM NEWFOUNDLAND, CANADÁ

Barili, R.[1]; De Ros, L.F.[1]; Neilson, J.[2]; Goldberg, K.[3]; Brasier, A.[2]; Bardola, T.P.[1].
[1]Universidade Federal do Rio Grande do Sul; Aberdeen University, Escócia; [3] Kansas State University, USA

RESUMO: O Grupo Port au Port, oeste de Newfoundland (Terra Nova), Canadá, é uma sucessão carbonática cambriana, composta por três ciclos transgressivos-regressivos de carbonatos lamosos e folhelhos na base e grainstones oolíticos no topo. Um influxo de sedimentos siliciclásticos coincide com valores positivos da razão isotópica de carbono ($\delta^{13}C_{VPDB}$) nos carbonatos marinhos. Esta excursão, que apresenta magnitude de até + 5 ‰ em sucessões carbonáticas do Cambriano Superior de diversas localidades, incluindo China, Kazaquistão e Omã, é denominada SPICE (*Steptoean Positive Isotope Carbon Excursion*). No cráton Norte Americano (Laurentia), esta excursão indica o limite entre as sequências Sauk II e Sauk III, marcado pelo influxo de sedimentos siliciclásticos durante a máxima regressão. A espessura e a magnitude da excursão variam de ~200 m e + 5 ‰ em Nevada e Utah (EUA), e ~20 m e +2 ‰ em Newfoundland. Novos dados de $\delta^{13}C$, $\delta^{18}O$, $\delta^{13}C_{org}$ e de petrografia do Grupo Port au Port nas localidades de March Point e de Felix Cove devem auxiliar no entendimento da dinâmica e das condições paleoambientais da geração da SPICE. O arcabouço estratigráfico e as características dos depósitos siliciclásticos variam ligeiramente entre estas duas localidades. Em March Point, uma camada de ~1 m de espessura de quartzarenito fino, moderadamente selecionado e compactado ocorre ligeiramente acima do pico da excursão. Em Felix Cove, uma camada quartzarenito bem selecionado e arredondado com ~0,25 m de espessura ocorre junto com a inflexão positiva do $\delta^{13}C$. A análise petrográfica preliminar indica uma forte influência da diagênese, com extensa dolomitização nas camadas imediatamente sotopostas e sobrepostas à excursão, principalmente em March Point. Os valores de $\delta^{13}C$ da excursão em Felix Cove chegam a +1,8 ‰ (um pouco inferiores aos da literatura, +2,2‰) em um intervalo de ~20 m de espessura , enquanto que na localidade de March Point os valores de $\delta^{13}C$ chegaram a +1,1 ‰ em ~5 m. As razões isotópicas de carbono na matéria orgânica (δ13Corg) confirmam a excursão positiva, variando entre -30 e -22 ‰, apesar do comportamento ser diferente do observado para os valores de δ13C dos carbonatos. Os valores de isótopos de oxigênio ($\delta^{18}O_{VPDB}$) variam entre -9.0 e -5,4 ‰ em Felix Cove, e entre -8,5 e -4,5‰ em March Point, sem clara correlação com os valores de $\delta^{13}C$. Análises de isótopos de estrôncio (Sr^{87}/Sr^{86}) em execução deverão auxiliar na análise das variações do nível relativo do mar, desde que avaliações preliminares indicam uma influência da paleogeografia na acumulação dos carbonatos. Por outro lado, processos diagenéticos podem ter influenciado nas diferenças de magnitude da excursão positiva de carbono observada nas rochas carbonáticas cambrianas de Newfoundland.

PALAVRAS-CHAVE: CARBONATOS, CAMBRIANO, ISÓTOPOS